THE MOLECULAR MECHANISMS OF ANTIBIOTIC RESISTANCE IN AQUATIC PATHOGENS

EDITED BY: Xiangmin Lin, Patrícia Poeta, Bo Peng and Xiao-Peng Xiong
PUBLISHED IN: Frontiers in Cellular and Infection Microbiology

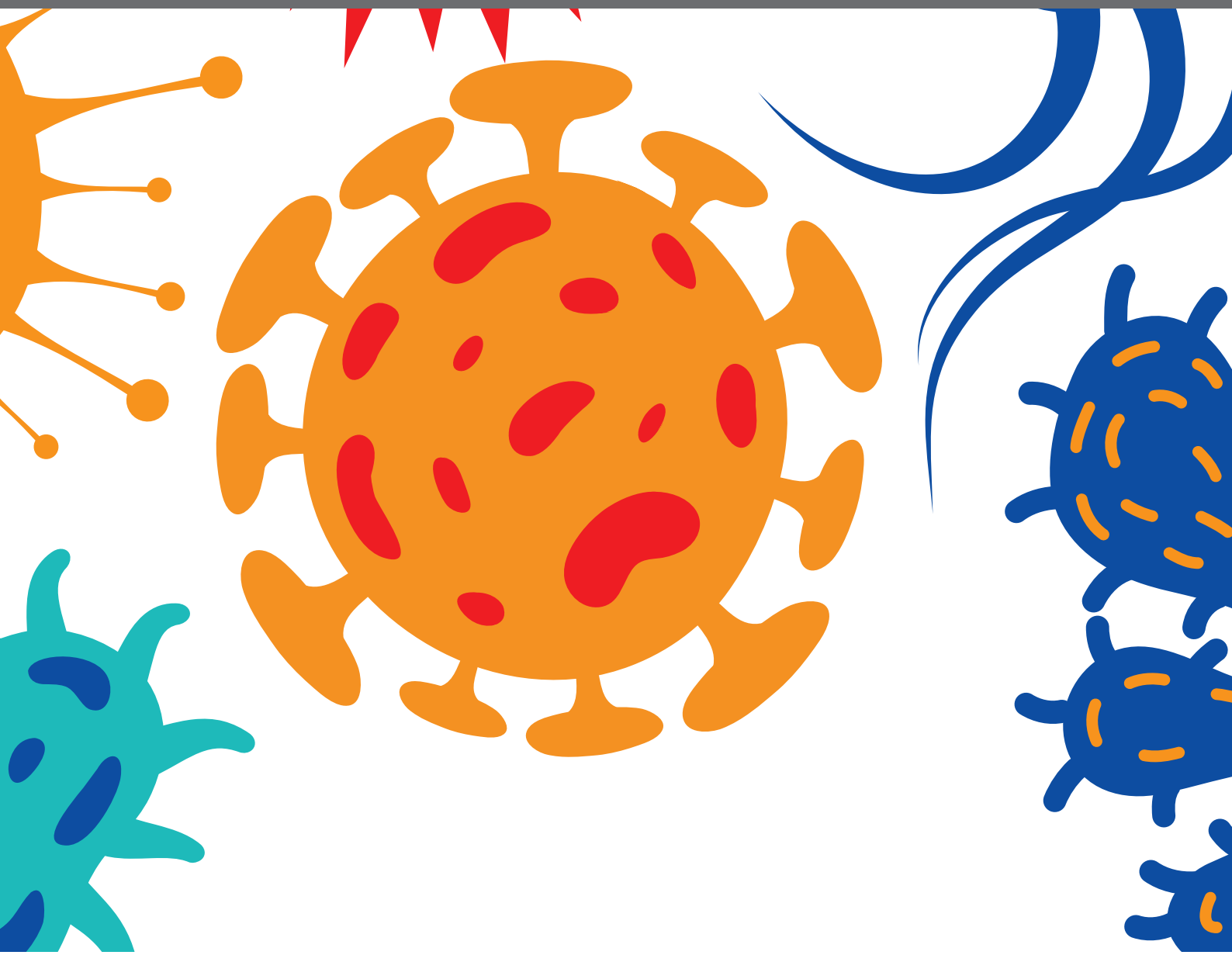

frontiers Research Topics

frontiers

ISSN 1664-8714
ISBN 978-2-88966-169-5
DOI 10.3389/978-2-88966-169-5

About Frontiers

Frontiers is more than just an open-access publisher of scholarly articles: it is a pioneering approach to the world of academia, radically improving the way scholarly research is managed. The grand vision of Frontiers is a world where all people have an equal opportunity to seek, share and generate knowledge. Frontiers provides immediate and permanent online open access to all its publications, but this alone is not enough to realize our grand goals.

Frontiers Journal Series

The Frontiers Journal Series is a multi-tier and interdisciplinary set of open-access, online journals, promising a paradigm shift from the current review, selection and dissemination processes in academic publishing. All Frontiers journals are driven by researchers for researchers; therefore, they constitute a service to the scholarly community. At the same time, the Frontiers Journal Series operates on a revolutionary invention, the tiered publishing system, initially addressing specific communities of scholars, and gradually climbing up to broader public understanding, thus serving the interests of the lay society, too.

Dedication to Quality

Each Frontiers article is a landmark of the highest quality, thanks to genuinely collaborative interactions between authors and review editors, who include some of the world's best academicians. Research must be certified by peers before entering a stream of knowledge that may eventually reach the public - and shape society; therefore, Frontiers only applies the most rigorous and unbiased reviews.
Frontiers revolutionizes research publishing by freely delivering the most outstanding research, evaluated with no bias from both the academic and social point of view. By applying the most advanced information technologies, Frontiers is catapulting scholarly publishing into a new generation.

What are Frontiers Research Topics?

Frontiers Research Topics are very popular trademarks of the Frontiers Journals Series: they are collections of at least ten articles, all centered on a particular subject. With their unique mix of varied contributions from Original Research to Review Articles, Frontiers Research Topics unify the most influential researchers, the latest key findings and historical advances in a hot research area! Find out more on how to host your own Frontiers Research Topic or contribute to one as an author by contacting the Frontiers Editorial Office: researchtopics@frontiersin.org

THE MOLECULAR MECHANISMS OF ANTIBIOTIC RESISTANCE IN AQUATIC PATHOGENS

Topic Editors:
Xiangmin Lin, Fujian Agriculture and Forestry University, China
Patrícia Poeta, University of Trás-os-Montes and Alto Douro, Portugal
Bo Peng, Sun Yat-sen University, China
Xiao-Peng Xiong, Sanford Burnham Institute for Medical Research, United States

Citation: Lin, X., Poeta, P., Peng, B., Xiong, X.-P., eds. (2020). The Molecular Mechanisms of Antibiotic Resistance in Aquatic Pathogens.
Lausanne: Frontiers Media SA. doi: 10.3389/978-2-88966-169-5

Table of Contents

frontiers in Cellular and Infection Microbiology

EDITORIAL
published: 24 September 2020
doi: 10.3389/fcimb.2020.586460

Editorial: The Molecular Mechanisms of Antibiotic Resistance in Aquatic Pathogens

Xiangmin Lin[1]*, *Patrícia Poeta*[2] *and Bo Peng*[3]

[1] School of Life Sciences, Fujian Agriculture and Forestry University, Fuzhou, China, [2] Microbiology and Antibiotic Resistance Team (MicroART), Department of Veterinary Sciences, University of Trás-os-Montes and Alto Douro (UTAD), Vila Real, Portugal, [3] School of Life Sciences, Sun Yat-sen University, Guangzhou, China

Keywords: aquatic pathogens, antibiotic resistance, mechanisms, multidrug resistance, prevention strategies

Editorial on the Research Topic

The Molecular Mechanisms of Antibiotic Resistance in Aquatic Pathogens

Bacterial antibiotic resistance has become a formidable problem in the treatment of infectious diseases worldwide. The molecular mechanisms of antibiotic resistance remain elusive, especially for aquatic pathogens. Antibiotic resistance and virulence determinants in environmental/aquatic bacterial pathogens are the subject of five research articles published in this Research Topic. Mishra et al. have investigated the influence of outer membrane proteins (OMPs) on the antibiotic resistance profile and virulence factors of *Enterobacter* isolated from aquatic environments and clinical settings. The environmental *Enterobacter* isolates lack OmpC, are unable to invade host cells, and induce low amounts of reactive oxygen species (ROS) production by neutrophils. In contrast, a clinical *Enterobacter* isolate described possesses OmpF, has better invasive and adhesive capabilities, and stimulates a higher amount of ROS production. Furthermore, some clinical *Enterobacter* isolates which have the *ompA* gene also have the strong capacity to form biofilms. Taking a different angle, Abdelhamed et al. and Opazo-Capurro et al. have sequenced the whole genomes of the *Edwardsiella piscicida* MS 18-99 strain possessing a 117.4 kb conjugative plasmid pEPMS-1899, and *Acinetobacter radioresistens* A154 harboring several plasmids, respectively. The genome analysis revealed that several antimicrobial resistance genes/elements confer resistance to various antibiotics, such as *tetA&R*, *strA&B*, *sul2,* and *floR* in MS 18-99, *arsA* and *arsD* on pEPMS-1899, and *tetB*, *strA*, *strB*, *aph(3′)-Vla*, *aac(3)-IIa*, *blaSCO-1*, *blaTEM-1B,* and *blaPER-2* in *A. radioresistens*. A study by Montso et al. describes the presence of genes such as *shiga toxins* (*stx*) and *bundle-forming pili* (*bfpA*) that are related to virulence determinants and antibiotic resistance in atypical enteropathogenic *Escherichia coli* (aEPEC) O177, the first reported occurrence of the aEPEC O177 strain in South African cattle. Tekedar et al. have characterized genome sequences of *Aeromonas veronii* MS 17-88 strains isolated from channel catfish to uncover the mechanism of multidrug resistance. This strain has several antimicrobial resistance genes/elements such as *tet(34)*, *tet(35)*, *tet(E)*, *tetR*, *mcr-7.1,* and *floR*. These five studies have all contributed further evidence of the abundance and prevalence of antibiotic resistance genes in different bacterial genomes.

Proteins are the fundamental and vital material of life. Ribosome rescue is a mechanism to maintain protein synthesis when mistakes or stalling occur. Quality control of protein synthesis is part of this process, which requires transfer-messenger RNA (tmRNA) and small protein B (SmpB). In this Research Topic, there are three articles from Prof. Liu's group describing the involvement of tmRNA and SmpB in the antibiotic resistance and persistence development of *A. veronii*. The transcriptomic data presented reveal the downregulation of protein secretion systems, such as the type VI secretion system (T6SS) and type IV pilus assembly, in the SmpB deficient strain.

OPEN ACCESS

Edited and reviewed by:
John S. Gunn,
The Research Institute at Nationwide Children's Hospital, United States

***Correspondence:**
Xiangmin Lin
xiangmin@fafu.edu.cn

Specialty section:
This article was submitted to Molecular Bacterial Pathogenesis, a section of the journal Frontiers in Cellular and Infection Microbiology

Received: *23 July 2020*
Accepted: *20 August 2020*
Published: *24 September 2020*

Citation:
Lin X, Poeta P and Peng B (2020) Editorial: The Molecular Mechanisms of Antibiotic Resistance in Aquatic Pathogens. Front. Cell. Infect. Microbiol. 10:586460. doi: 10.3389/fcimb.2020.586460

This downregulation attenuated the production of virulence factors and the colonization ability of *A. veronii*. However, the alternative rescue factor A (AvrA) acts as a substitute for virulence compensation. The decreased level of *avrA* expression increases the expression level of iron-sulfur protein activator *iscR*, resulting in an increase in bacterial antioxidant ability through enhancement of the synthesis of the iron-sulfur protein and assembly of iron-sulfur clusters (Santos et al., 2014). SmpB deficiency showed attenuated virulence and enhanced tolerance to oxidative stress. In another study, the deletion of the *smpB* gene in *A. veronii* enhanced the expression of enzymes related to adenosine metabolism, which leads to increases in the products such as adenosine AMP, cAMP and deoxyadenosine. By comparison, the deletion of *ssrA* (tmRNA) upregulated the expression of guanosine metabolism and hypoxanthine synthesis, eventually increasing the levels of the metabolic product xanthine, which in turn downregulated the genes related to the efflux pump such as *acrA* and *acrB*. With the *ssrA* and *smpB* genes deleted, the minimal inhibitory concentration of trimethoprim against *A. veronii* was lower. Therefore, this study demonstrates the effect of SmpB and tmRNA on different branches of purine metabolism and tolerance to trimethoprim (Wang et al.). A study by Yu et al. showed that the deletion of *ssrA* (tmRNA) increased the capacity of *A. veronii* to form persister cells. Moreover, Δ*ssrA* significantly raised the intercellular levels of N-acetylglucosamine production, promoting NaCl osmotic stress tolerance. To confirm this, the authors exogenously added N-acetylglucosamine to the medium and observed resistance to osmotic pressure and higher persistence to cefotaxime in *A. veronii*. Overall, these three research articles suggest that the trans-translation system might be an effective target in the treatment of *A. veronii* and other multidrug resistant aquatic bacterial pathogens.

Enhancing the efficiency of traditional antibiotics is a vital strategy for combatting the antibiotic resistance in bacterial pathogens. A study by Sun et al. has revealed that indole and its derivative 2,5-methylindole potentiate the killing efficacy of tobramycin against persister cells of *Staphylococcus aureus*. Furthermore, combinations of indole and its derivatives with aminoglycoside antibiotics were effective in inhibiting the growth of many Gram-positive bacterial pathogens such as *Streptococcus pyogenes* and *Enterococcus faecalis*. Finally, Zhou et al. have studied the role of the type III secretion system (T3SS) on the pathogenicity of *Vibrio alginolyticus*. Swarming motility is inhibited in the T3SS mutant strain *tyeA* and its virulence toward zebrafish is also reduced. Further, the *tyeA* mutant strain is extremely susceptible to cefoperazone, minocycline, amikacin, and gentamicin. The effects of a live attenuated vaccine made from the mutant strain on the survival of zebrafish was tested. The data presented show that the survival of zebrafish infected with mutant was enhanced compared to the control infected with the wild-type strain. Both of these approaches may pave the way for the development of an effective treatment strategy to combat antibiotic resistance in bacterial pathogens.

AUTHOR CONTRIBUTIONS

XL and PP wrote the manuscript. BP revised and approved the final version of the manuscript. All authors conceived the outline of the manuscript.

ACKNOWLEDGMENTS

This work was sponsored by grants from NSFC projects (Nos. 31670129). We thank Dr. Xiaopeng Xiong for suggesting on the manuscript.

REFERENCES

Santos, J. A., Alonso-García, N., Macedo-Ribeiro, S., and Pereira, P. J.B. (2014). The unique regulation of iron-sulfur cluster biogenesis in a Gram-positive bacterium. *Proc. Natl. Acad. Sci. U.S.A.* 111, 2251–2260. doi: 10.1073/pnas.1322728111

Conflict of Interest: The authors declare that the research was conducted in the absence of any commercial or financial relationships that could be construed as a potential conflict of interest.

frontiers in Cellular and Infection Microbiology

ORIGINAL RESEARCH
published: 08 May 2019
doi: 10.3389/fcimb.2019.00142

Small RNA AvrA Regulates IscR to Increase the Stress Tolerances in SmpB Deficiency of *Aeromonas veronii*

Dan Wang, Hong Li, Xiang Ma, Yanqiong Tang, Hongqian Tang, Xinwen Hu and Zhu Liu**

Key Laboratory of Tropical Biological Resources of Ministry of Education, School of Life and Pharmaceutical Sciences, Hainan University, Haikou, China

The superbacteria *Aeromonas veronii* displays not only a strong pathogenicity but also the resistance to nine kinds of antibiotics, resulting in the economic losses and health hazards. Small Protein B (SmpB) plays an important role in protein quality control, virulence, and stress reactions. Transcriptomic data revealed that expressions of the type IV pilus assembly and type VI secretion system (T6SS) proteins were downregulated in SmpB deficiency, indicating that the virulence of *A. veronii* might be attenuated. Although SmpB deletion decreased colonization in the mouse spleen and liver, LD50 of the *smpB* mutant was not altered as expected, compared with the wild type. Further, the transcriptomic and quantitative RT-PCR analyses showed that the combination of the downregulated AvrA and the upregulated iron-sulfur protein activator IscR, mediated the oxidative tolerance in *smpB* deletion. Next a reporter plasmid was constructed in which the promoter of *iscR* was applied to control the expression of the enhanced green fluorescent protein (eGFP) gene. When the reporter plasmid was co-expressed with the AvrA expression into *E. coli*, the relative fluorescence intensity was decreased significantly, suggesting that AvrA bound to *iscR* mRNA by base pairing, which in turn relieved the inhibition of *iscR* and intensified the downstream iron-sulfur proteins. Collectively, the *smpB* mutant exhibited an attenuated virulence in mice and enhanced tolerances to oxidative stress. This study demonstrates the complexity of gene regulation networks mediated by sRNA in systems biology, and also reflects the strong adaptability of superbacteria *A. veronii* in the process of evolution.

Keywords: oxidative, stress, iron deficiency, iron/sulfur clusters, virulence

OPEN ACCESS

Edited by:
Xiangmin Lin,
Fujian Agriculture and Forestry University, China

Reviewed by:
Shengkang Li,
Shantou University, China
Zhihong Xie,
Yantai Institute of Coastal Zone Research (CAS), China

****Correspondence:***
Xinwen Hu
huxinwen@hainu.edu.cn
Zhu Liu
zhuliu@hainu.edu.cn

Specialty section:
This article was submitted to Molecular Bacterial Pathogenesis, a section of the journal Frontiers in Cellular and Infection Microbiology

Received: *14 March 2019*
Accepted: *17 April 2019*
Published: *08 May 2019*

Citation:
Wang D, Li H, Ma X, Tang Y, Tang H, Hu X and Liu Z (2019) Small RNA AvrA Regulates IscR to Increase the Stress Tolerances in SmpB Deficiency of Aeromonas veronii. Front. Cell. Infect. Microbiol. 9:142. doi: 10.3389/fcimb.2019.00142

INTRODUCTION

With the application of antimicrobial drugs, a wide range of mechanisms have evolved for bacteria to combat the huge selection pressures of antibacterial agents. Superbacteria have accumulated in a long evolutionary history, while the abuse of antibiotics has accelerated its formation. The superbacterium *Aeromonas veronii* (*A. veronii*) has been isolated, which has displayed not only a strong pathogenicity but also the resistance to nine kinds of antibiotics (Liu et al., 2016, 2018). As *A. veronii* infects fish, it causes fish canker and perforated disease, eventually resulting in economic losses. Furthermore, *A. veronii* increases human diseases such as neonatal sepsis, diarrhea and

dysentery (Aguilera-Arreola et al., 2007). In view of the wide array of infections to the host and a strong tolerance to antibiotics, *A. veronii* is worth researching further, as a model strain.

Proteins are the material basis of life. If there is a mistake in the protein synthesis process, ribosome rescue should occur in order to maintain life. Trans-translation which is composed of small protein B(SmpB) and transfer-message RNA (tmRNA) is the predominant form of ribosome rescue (Himeno et al., 2014). The malfunction of trans-translation exhibits more sensitivity to virulence and tolerance in most pathogens such as *Mycobacterium tuberculosis*, *Legionella pneumophila*, and *Neisseria gonorrhoeae* (Keiler, 2008, 2015). However, the alternative pathways have evolved to compensate for the deficiency of trans-translation. For example, the alternative rescue factor A (ArfA) acts to release the stocked mRNA in Proteobacteria and mycobacteria, and the alternative rescue factor B (ArfB) appears in 34% of bacteria (Kurita et al., 2014; Huter et al., 2017; Fiedler et al., 2018). Therefore, superbacteria might have alternate ways for SmpB defects, while no reports indicate that other functions of SmpB are maintained by small RNA (sRNA).

In this study, the transcriptome analysis was compared between wild type and *smpB* knockout strains, showing that the expressions of the pilus and virulence protein were downregulated after *smpB* deletion. However, the capacities of oxidative stress and iron were increased by sRNA downregulation in *smpB* knockout. Non-coding sRNA modulates bacterial metabolism and stress by base pairing with target genes and reacts faster than transcription factor regulation (Durand et al., 2015; Oliva et al., 2015). Here a sRNA designated as AvrA was revealed to negatively regulate the expression of IscR (iron-sulfur cluster assembly transcriptional regulator) IscR governs iron hemostasis as a global regulator during growth and stress responses (Aguilera-Arreola et al., 2007), which exhibits a resistance to oxidants (Mandin et al., 2016), and represses iron-sulfur metabolism under iron starvation (Haines et al., 2015; Carrier et al., 2017). The overproduction of IscR favored the tolerance under the nutrient deficiency and oxidative, iron-limited and membrane stresses when *smpB* was knocked out and followed by AvrA downregulation.

Survival under detrimental stresses is preliminary when pathogens are infected to the host and escape from macrophage recognition in the immune system (Mandin et al., 2016). And then the bacteria are transported to tissues using blood and lymph as channels, eventually causing tissue damage. Iron metabolism is of vital importance to bacteria. The proteins composed of iron/sulfur clusters participate in multiple cellular processes, such as gene expression, DNA repair, RNA modification, central metabolism and respiration (Roche et al., 2013). Iron sulfur proteins also relate to oxidoreductase which is involved in the basic metabolism of bacteria (Xu and Moller, 2008; Ilbert and Bonnefoy, 2013). So, overexpression of IscR is vital for bacteria to survive in adverse conditions.

In summary, SmpB plays an important role in protein quality control, virulence, gene transcription, and antibiotic and stress reaction (Liang and Deutscher, 2010; Li et al., 2013; Mu et al., 2013; Mraheil et al., 2017). Unlike *Salmonella Typhimurium*, the virulence of the *A. veronii* Δ*smpB* strain did not become avirulent but maintained a strong pathogenicity. Loss of function caused by smpB deletion can be compensated through different pathways. For instance, some bacteria employ ArfA and ArfB to rescue stalled ribosomes when *smpB* is deficient (Keiler, 2015; Liu et al., 2016; Huter et al., 2017). Additionally, sRNA AvrA releases the trapped IscR promotor to activate the expression of iron sulfur proteins, remedying the iron deficiency after *smpB* destruction. In the evolutionary history of bacteria, it offers additional evidence for the formation of superbacteria.

TABLE 1 | Strains and vector used in this paper.

Strains or plasmids	Traits	Sources
E. coli DH5α	Gene cloning strain	This lab
E. coli Felden	Gene cloning strain	This lab (Liu et al., 2018)
E. coli WM3064	Gene cloning strain	This lab (Liu et al., 2018)
Aeromonas veronii	Wild type strain	This lab (Liu et al., 2018)
smpB mutant	*smpB* deletion mutant	This lab
smpB complement	*smpB* complement strain	This lab
avrA mutant	*avrA* deletion mutant	This paper
avrA complement	*avrA* complement	This paper
pUC19	Report vector	This lab (Liu et al., 2016)
PRE112	Gene cloning vector	This lab (Liu et al., 2016)
PBBR1MCS-2	Gene cloning vector	This lab (Liu et al., 2018)
pDH114	Report vector	This lab (Liu et al., 2016)
pRE112-*avrA*del	avrA deletion vector	This paper
pBBR-*avrA*	avrA expression pBBR1MCS-2 vector	This paper
p*avrA*	avrA expression pUC19 vector	This paper
pavrAmutP1	P1 site mutation on p*avrA*	This paper
Φ (piscR-eGFP)	fusion vector including the promoter of iscR and eGFP	This paper
Φ (piscR mutP1-eGFP)	P1 site mutation on Φ(piscR-eGFP)	This paper
Φ (piscRmutP2-eGFP)	P2 site mutation on Φ(piscR-eGFP)	This paper

MATERIALS AND METHODS

Plasmids

The plasmids and primers are listed in **Tables 1**, **2**, respectively.

For the construction of plasmid p*iscR*-eGFP, the 200 bp-DNA fragments containing the promoter of *iscR* was amplified from the genomic DNA of *A. veronii* with primers pro*iscR*_F/pro*iscR*_R. In the meantime, the 750 bp-encoding region of eGFP was amplified from a plasmid pDH114 with primer eGFP_F/eGFP_R. The fusion was produced using the above two fragments as the templates by overlapping the PCR with primers F_PiscR/eGFP_R and by insertion into the backbone of the plasmid pUC19 to construct the Φ(p*iscR*-eGFP) vector. The plasmid p*avrA* was constructed in a similar manner using the primers pro*avrA*_F and pro*avrA*_R. To

TABLE 2 | Primers used in vector construction and real-time qPCR.

Names of primers	Sequences (5′ –3′)	Usage
SP 1_F	ATGGTCGCAGAGCTTGTC	Strain validation
SP 1_R	CAGCACAATAGAACACCAGAC	Strain validation
*avrA*_F1	TCTTAGATCCAGGTACCTGGTCCAGCAACAGATCTCCGAT	avrA knockout
avrA_R1	ATTATTGTCCATTGCATTGGCCGGAGTGTTAATCATGGTG	avrA knockout
avrA_F2	ATTCCTGTCCATTGCATTGGTTGTATGTCGCCCCTAAAGG	avrA knockout
avrA_R2	CTGCAGAACCAGAGCTCTGGAGCGGGACAAACTGTTCG	avrA knockout
avrA_F0	TCTCCAGGCAAATACGCTCG	avrA knockout
avrA_R0	GAGTTCAGGCTGGTCGACTG	avrA knockout
mtarP1:	CGAGATGGATGGGGTAGACGCAGACAACATGCATCCACTTGCGG	Site mutation of p1
mtarP1cr	CCGCAAGTGGATGCATGTTGTCTGCGTCTACCCCATCCATCTCG	Site mutation of p1
mtarP2:	GACGGTCTCAACATGCATCCAGAACGCGATGATCCGCTCCCGATCGC	Site mutation of p2
mtarP2cr:	GCGATCGGGAGCGGATCATCGCGTTCTGGATGCATGTTGAGACCGTC	Site mutation of p2
11665F	GGTCTTGCCTACGTGCTTGA	Real-time PCR
11665R	CACACTCGCCTTTGGCATTG	Real-time PCR
11670F	AGCTGCAATTGAAGATCAGCG	Real-time PCR
11670R	TGTGTTCTTGATGCCAGCCG	Real-time PCR
11675F	AACGTGTTCCGGGTAACCTC	Real-time PCR
11675R	CGACCGATGGAGTCACGAAT	Real-time PCR
11680F	CGCAAACATGGTCTGGTGAG	Real-time PCR
11680R	CGGCCAAGGTAATATCCCCG	Real-time PCR
pro*iscR*_F	ACGCGTCGACGCGGTATTCTGACCTCGGTG	Fusion vector
pro*iscR*_R	CTCGCCCTTGCTCACCATCAGTCTCATGTGCCTTACCG	Fusion vector
eGFP_F	CGGTAAGGCACATGAGACTGATGGTGAGCAAGGGCGAG	Fusion vector
eGFP_R	TCGCGGATCCTTACTTGTACAGCTCGTCCA	Fusion vector
pUC19_F	AATGCAGCTGGCACGACAGG	Fusion vector
pUC19_R	CCATTCAGGCTGCGCAACTG	Fusion vector
pro*avrA*_F	CGGGGTACCCAGTCGTTGCTCCATGGCGG	Fusion vector
pro*avrA*_R	CCGGAATCCGGTCGCCAACTTCTACATCT	Fusion vector
pro*avrA* comF	CGGGGTACCAAACAGTAGCCAGGGACCGAG	Fusion vector
pro*avrA* comR	GGCCGGAATTCGCCTTTATCGCCGATCTGC	Fusion vector
pBBR1MCS-2 F	GGCACCCCAGGCTTTACACT	Complement plasmid validation
pBBR1MCS-2 R	GATGTGCTGCAAGGCGATTAAG	Complement plasmid validation

construct the gene knockout strain of Δ*avrA*, the flanking sequences of Δ*avrA* were amplified and inserted into the plasmid pRE112, resulting in the gene knockout vector pRE112-*avrA*del. The complementary plasmid pBBR-*avrA* was applied to express the extra AvrA using plasmid pBBR1MCS-2 as the backbone.

Strains and Culture Conditions

The strains used are listed in **Table 1**. The derivative *A. veronii* strains were picked from frozen stocks and cultured at 30°C in Luria-Bertani (LB) broth or M9 medium with aeration. The Antibiotics included 50 μg/mL ampicillin, 25 μg/mL chloramphenicol, 50 μg/mL kanamycin. The *E. Coli* Felden strain was chosen for the expression of eGFP and sRNA (Liu et al., 2015). *E. Coli* WM3064 was selected for gene knockout by homologous recombination, which is capable of growth at 37°C in LB broth with 0.3 mM diaminopimelic acid (DAP).

The plasmid pRE112-*avrA*KO was transformed into the competent *E. coli* WM3064 and delivered into *A. veronii* by conjugation (Liu et al., 2016). The *A. veronii* Δ*avrA* was screened on LB agar supplemented with 6% sucrose and ampicillin and was further checked by sequencing.

The plasmid pBBR-*avrA* was transformed into the competent *E. coli* WM3064, and mobilized into the Δ*avrA* strain by conjugation, resulting in complementary *A. veronii* Δ*avrA*::*avrA*.

RNA Sequencing and Bioinformatics Analysis

Strains were grown in a 10 mL M9 medium containing 50 μg/mL ampicillin at 30°C, 150 rpm for 20 h. The cells were collected and lysed. RNA samples were extracted by phenol-chloroform. The concentration and quality of RNA was detected by the Agilent 2100 Bio analyzer. The samples were treated with DNase I to eliminate double-stranded and single-stranded

DNA, followed by the depletion of rRNA with the Ribo-Zero Magnetic Kit. First-strand cDNA was generated using a random primer reverse transcription, followed by a second-strand cDNA synthesis. The end of the synthesized cDNA was subjected to repair and adenylate. The adapters were ligated to the ends of these 3′-adenylated cDNA fragments. The cDNA fragments were enriched by PCR amplification with a PCR Primer Cocktail, and the purified products were sequenced on the Hiseq Xten (Illumina, San Diego, CA, USA) using the gel-free protocol. Libraries were sequenced as 100 bp paired-end reads to a minimum target depth of 2G clean data per sample. The software HISAT (V2.0.1-beta) was used for

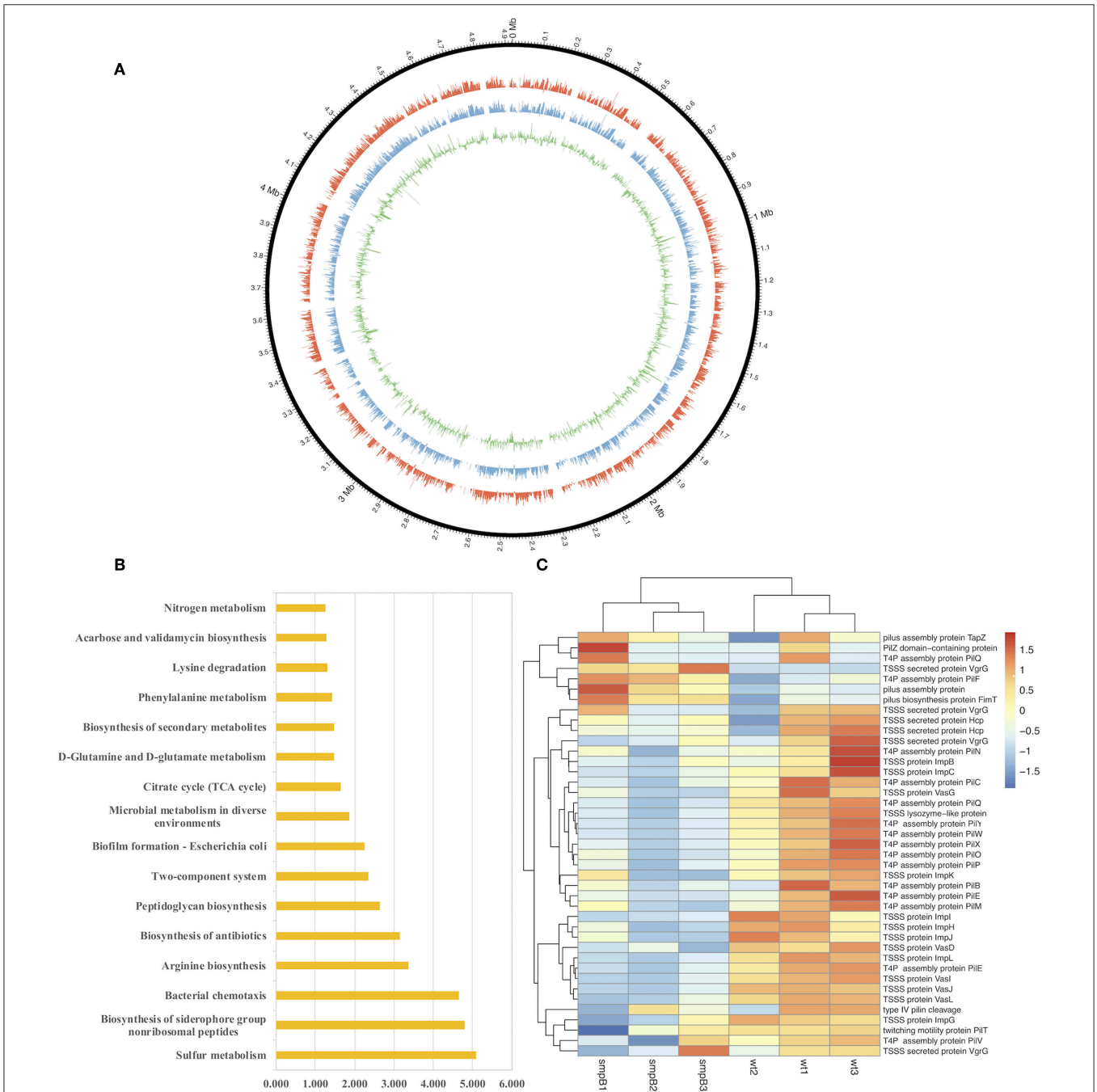

FIGURE 1 | Transcriptomic analysis between wild type and *smpB* knockout. **(A)** Circos diagram of read distribution and gene expression. From inside, green (fold change of gene expression between Δ*smpB* and wild type), blue (mRNA expression of wild type *A. veronii* by rpkm), red (mRNA expression of Δ*smpB* by rpkm), black (reads distribution on the reference genome NZ_CP012504.1). **(B)** Pathways affected by *smpB*. The horizontal and vertical axes represented as –log(*p*) value and the pathway names ($p < 0.05$). **(C)** Heat map representing the expressions of type IV pilus assembly, type VI secretion system and outer membrane genes.

the reference genome alignment, and CPC (coding potential calculator) was used to characterize the translation possibility of new transcripts. To identify the differential expression between wild type and Δ*smpB*, Bowtie 2(v2.2.5) was used to analyze the mRNA expression. Fragments per kilobase of transcript per million fragments sequenced (FPKM) were used to normalize the gene expression levels. For each gene, the *p*-value was evaluated, and Benjamini-Hochberg false discovery rate (FDR) was applied for the correction. The differential expressions of the transcripts were estimated by the virtue of ≥1 absolute log2 -fold change and < 0.001 FDR adjusted *p*-value. These results were sorted by GO categories using Perl scripts. The GO and KEGG pathway enrichments of differential uni-genes were analyzed. The hypergeometric test was used to compare differential expression genes in the pathway with the entire genome background. Pathways with a $p \leq 0.05$ were considered as significant. GEO accession number **GSE120603**.

LD50 Test in Mice

The derivative of *A. veronii* was streaked onto M9 medium and grown for 18–20 h at 30°C. The cells were re-suspended in sterile PBS. ICR mice (male, 6–8 weeks old) were infected by intraperitoneal injection with 10^3–10^7 CFU/g of each strain ($n = 8$) and monitored daily for weight loss and signs of illness. The animals were euthanized if they accorded with alternate endpoint criteria including the loss of mobility. The 50% lethal dose was calculated by linear regression (Torii et al., 2015).

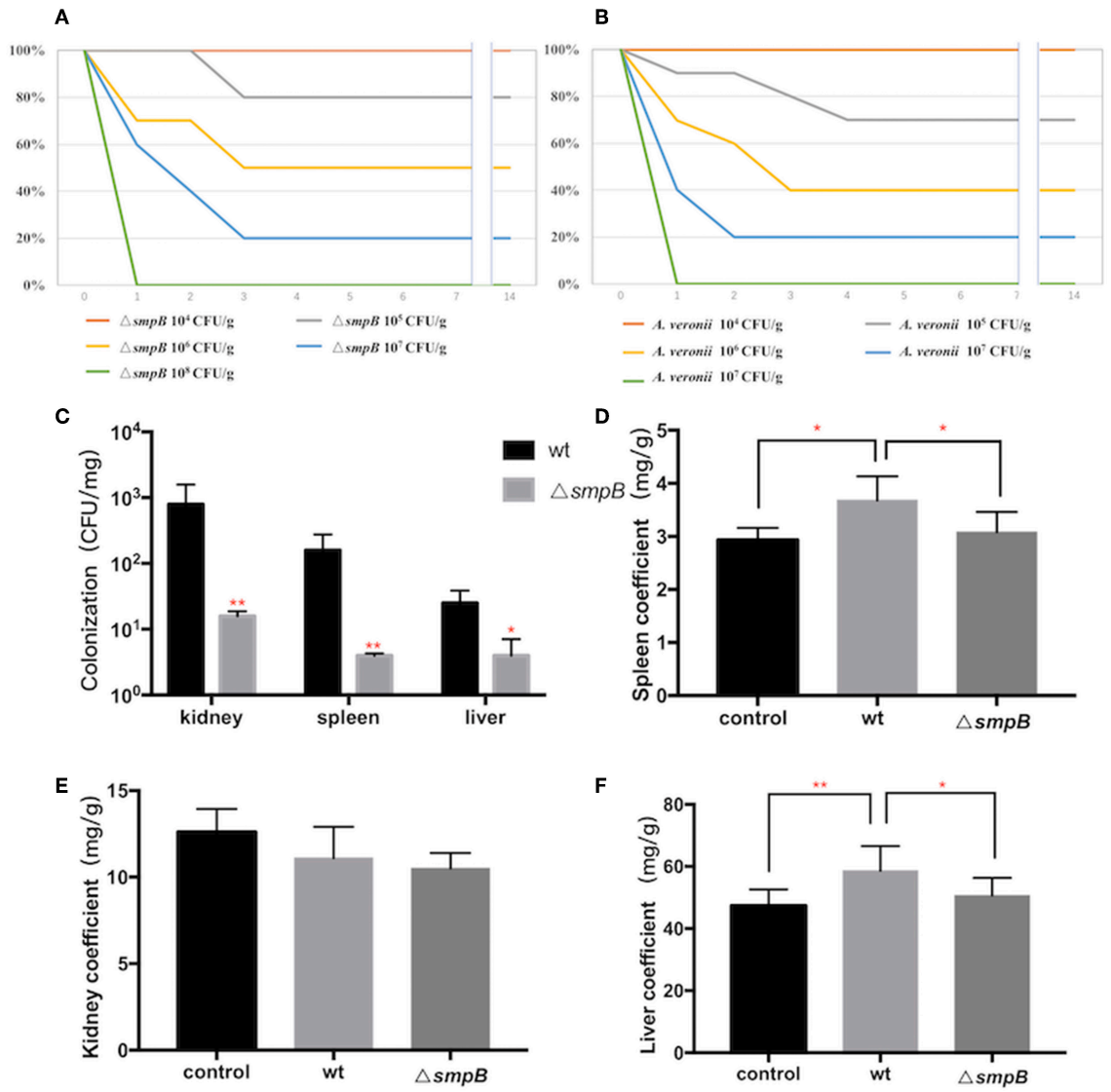

FIGURE 2 | SmpB deletion decreases the colonization in host tissue. **(A)** Survival rate of mice treated by wild type *A. veronii*. **(B)** Survival rate of mice treated by Δ*smpB* strain. **(C)** Colonization of wild type and Δ*smpB* in spleen, kidney, and liver of ICR mice. **(D)** Spleen coefficient (mg/g). **(E)** Kidney coefficient (mg/g). **(F)** Liver coefficient (mg/g). Error bars were shown as SD. $^{**}p < 0.01$, $^{*}p < 0.05$, following by one-way ANOVA, independent *t*-tests.

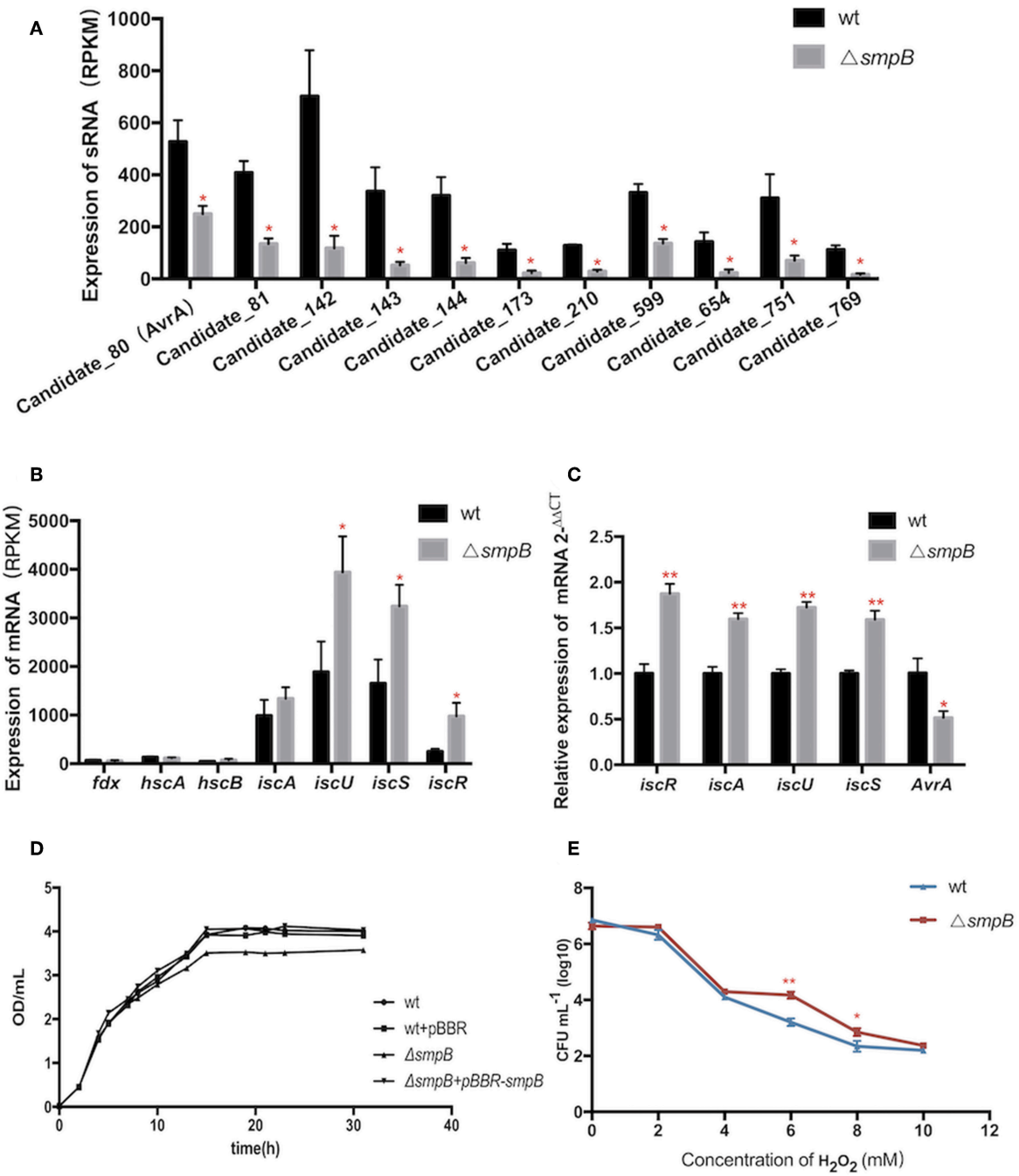

FIGURE 3 | The AvrA downregulation and IscR upregulation mediate the oxidative tolerance of Δ*smpB*. **(A)** Transcriptomic comparisons of 11 sRNA between wild type and Δ*smpB*. **(B)** Transcriptomic comparisons of *iscR* operon genes between wild type and Δ*smpB*. **(C)** Realtime qPCR detection of *iscR* operon and AvrA. **(D)** The growth curves of the derivative *A. veronii*. **(E)** The survivals of Δ*smpB* and wild type in H_2O_2 concentrations ranging from 0 to 10 mM. $^{**}p < 0.01$, $^{*}p < 0.05$, following by one-way ANOVA, independent *t*-tests.

Organ Coefficient

The coefficient of organs was calculated from the ratio of organ weight and body weight of the same mouse. The change of coefficient was used to characterize the degree of injury by contrasting the pathological with the normal tissue (Zhang et al., 2014).

All animal experiments were approved by the Committee of the Ethics on Animal Care and Experiments at Hainan

TABLE 3 | sRNAs and Pathways effected in Δ*smpB*.

Candidate sRNA	Metabolic pathways Involved
Candidate_80(AvrA)	Iron-sulfur cluster assembly
Candidate_81	Cellular homeostasis
Candidate_142	Ubiquitylation process
Candidate_143	Coenzyme biosynthetic process
Candidate_144	Intrinsic component of membrane
Candidate_173	Amino acid metabolism
Candidate_210	Purine ribonucleotide catabolic process
Candidate_599	Wide pore channel activity
Candidate_654	Energy metabolism
Candidate_751	Energy metabolism
Candidate_769	Aerobic respiration

University, and were carried out in accordance with the university guidelines.

Measurement of Growth Curve

The condition of iron deficiency was equipped with LB medium containing 200 mM dipyridyl. M9 medium was considered as the nutrient limited condition. The strains were cultured at logarithmic phase, and then inoculated into 50 ml media at an initial OD_{600} of 0.05. The ODs were monitored with a spectrophotometer (INESA 970CRT, Shanghai, China) at regular intervals.

Survival Under Oxidative Stress

The derivative of *A. veronii* was grown until to the OD_{600} value of 0.6 in the LB broth appended with 200 mM dipyridyl and subsequently challenged with 0–10 mM H_2O_2. The cultures were continuously incubated at 30°C with shaking for 10 min, and the survival colonies were counted on the LB agar plate with 50 μg/mL ampicillin.

Real-Time PCR Experiment

The wild type and mutant strains of *A. veronii* were grown in LB and M9 supplemented with 50 μg/mL ampicillin at 30°C till to stationary stage. The total amount of RNA was extracted for relative expression analysis of the genes, including *smpB*, the predicted targets of AvrA (t15190, t21425, t18380, t22295, t14250), Fe/S cluster assembly regulation factor (*iscR*) and its regulated targets *iscA*, *iscU*, *iscS*.

Florescent Measurement

The cells conferring eGFP expression were suspended in PBS buffer, and loaded to a 96 well microtiter plate (Greiner BIOONE, Nurnberg, Germany). The fluorescent intensity was measured at 488 nm excitation and 540 nm emission wavelengths with a fluorescence microplate reader (Infinite® 200 PRO, Tecan, Shanghai, China). The relative fluorescence was calculated as the total fluorescence divided by OD_{600} value.

Statistical Analysis

Statistical data were analyzed using the statistical Package for the Social Science (SPSS) version 20.0 (SPSS, Chicago, IL, United States) and GraphPad Prism version 6.0 (GraphPad, San Diego, CA, United States). The results were presented as mean values of three independent experiments with standard deviation (SD) using one-way analysis of variance (ANOVA). $P < 0.05$ or 0.01 were represented as significant or extremely significant.

RESULTS

Transcriptomic Analysis

To determine the differences in pathways and gene expressions between wild type and *smpB* knockout (Δ*smpB*) in the M9 medium, the transcriptome assembly of *A. veronii* was generated from 91.17 million paired-end RNA-seq reads using Illumina Xten technology and a total of 22,055 transcripts were mapped by genome NZ_CP012504.1 (**Figure 1A**). Sixteen pathways were significantly affected by SmpB knockout, including sulfur metabolism, biosynthesis of siderophore group non-ribosomal peptides, bacterial chemotaxis, arginine and peptidoglycan biosynthesis, and microbial metabolism in a diverse environment (**Figure 1B**). Among them, 21 and 20 genes were downregulated, respectively in the type IV pilus assembly and the type VI secretion system at the stationary phase (**Figure 1C**). The type IV pili are ubiquitously expressed on the surface of many Gram-negative bacteria and are important virulence factors that facilitate host-pathogen interactions and persistence of infection. T6SS is the molecular machine, which transports the virulence effectors from the interior cytoplasm or cytosol into an adjacent target cell across the cellular envelope. The downregulated pilus and secretion system proteins revealed that toxicity might be attenuated in Δ*smpB*.

SmpB Deletion Decreases the Colonization in Host Tissue

To compare the virulence between wild type and Δ*smpB*, Institute of Cancer Research (ICR) mice were divided into 10 groups with 10^4–10^8 CFU/g bacterial infection. The survival rate of ICR mice revealed that the virulence of the wild type was no different compared with the *smpB* deletion (**Figures 2A,B**).

After the mice were intraperitoneally injected with 5×10^5 CFU/g bacterial strains, the liver, spleen and kidneys were collected, and tissue suspension was cultured on LB plates supplemented with ampicillin. The wild type was colonized significantly more than Δ*smpB* in the kidney, liver, and spleen (**Figure 2C**), and the results agreed with the downregulated expressions of the type IV pilus assembly proteins (**Figure 1C**). Organ coefficient is a common toxicology indicator of ratio of organ and body weight reflecting animal damage (Zhang et al., 2014). In our study, the coefficients of spleen and liver infected by the wild type were 3.68 ± 0.45 and 58.65 ± 7.94 mg/g, which were significantly higher than the control group (2.93 ± 0.23 and 47.38 ± 5.27 mg/g) and Δ*smpB* group (3.08 ± 0.38 and 50.65 ± 5.62 mg/g) (**Figures 2D,E**), while little difference was observed in the kidney (**Figure 2E**). Next the organ coefficient was evaluated for the visceral injury between the treatment and the control group. The coefficients of the spleen and liver infected by the wild type were significantly higher than the control group and Δ*smpB* group (**Figures 2D–F**), while little difference was

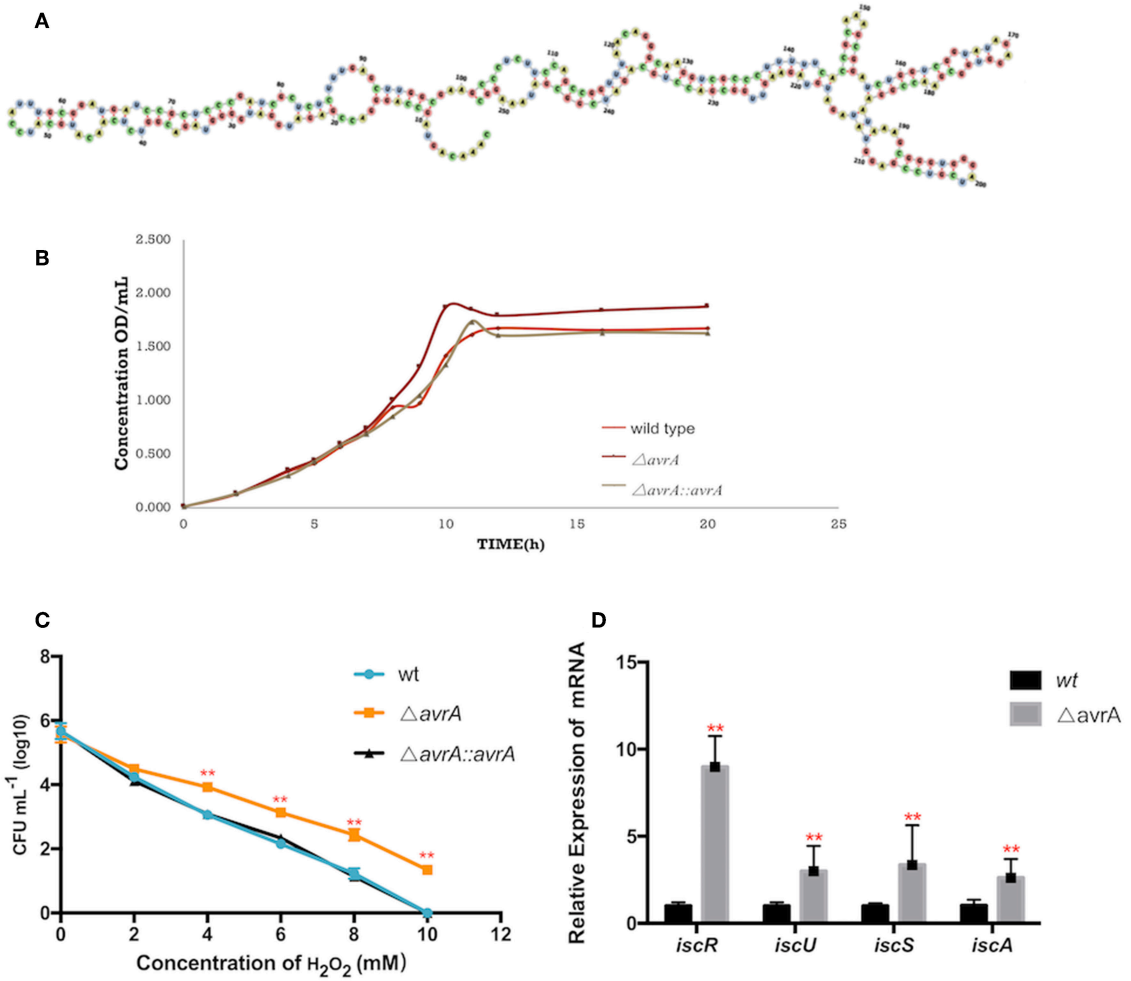

FIGURE 4 | AvrA increases the tolerances to oxidative stress and iron deficiency. **(A)** The secondary structure prediction of AvrA by software RNAfold. **(B)** Growth curves of wild type, Δ*avrA* and the complemented strain in iron deficiency treatment. **(C)** The survivals of wild type, Δ*avrA* and the complemented strain under H_2O_2 stress in the concentrations ranging from 0 to 10 mM **(D)** Relative expression of *iscR* operon at stationary phage in iron deficiency treating with DIP. $^{**}p < 0.01$, following by one-way ANOVA, independent *t*-tests.

observed in the kidney (**Figure 2E**). This also suggested that the virulence of wild type *A. veronii* was not affected by *smpB* deletion. Consistently, the acute LD50 for Δ*smpB* strain in mice was calculated as 5×10^5 CFU/g, which was close to that of 10^6 CFU/g for the wild type. Because of the contradiction between the decreased pathogenicity and unvaried lethality, we speculated that the bacterial resistance had enhanced in the host.

The Combination of the Downregulated AvrA and Upregulated IscR Mediates the Oxidative Tolerance in smpB Deletion

Expressions of transcripts were compared between the wild type and *smpB* mutant in the transcriptomic data. A total of 466 non-coding transcripts were defined as sRNA, including 50–500 nt. Among them, 11 sRNAs were analyzed to express specifically between the wild type and Δ*smpB* at the stationary stage in the M9 medium (**Figure 3A**). There were 62 differentially expressed target genes of the 11 sRNAs involved in stress response pathways, pathogenesis, and also the regulations of metabolism, transport, quorum sensing (**Supplementary Table 1**). The pathways were associated with the synthesis of cell membrane, protein translocation, ATPase, Fe/S protein assembly and energy metabolism (**Table 3**). The candidate_80 sRNA, designated as AvrA (*Aeromonas veronii* non-coding RNA A) was potentially associated with the target gene *iscR* in Fe/S assembly. After *smpB* was knocked out, AvrA expression declined (**Figure 3A**) resulting in the increased expression of the predicted targets *isc* operon genes which encoded iron-sulfur proteins (**Figure 3B**). The similar tendency of AvrA and its target genes was also turned out by Real-time PCR (**Figure 3C**).

To evaluate whether *smpB* mutation lived better in stress conditions than the wild type, the iron deficiency condition was performed to mimic the host environment

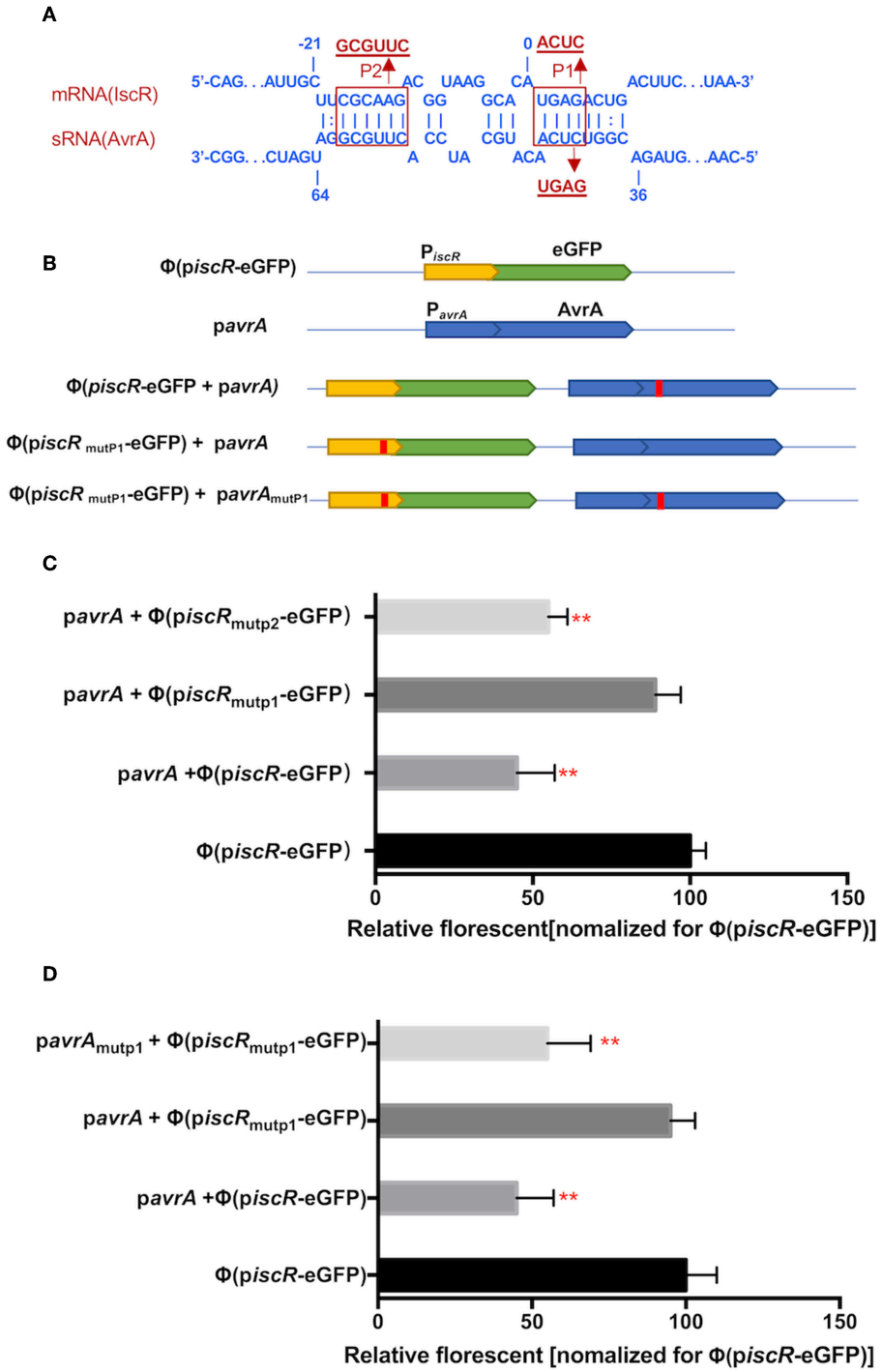

FIGURE 5 | AvrA interacts with *iscR* mRNA by base pairing. **(A)** Predicted interaction between AvrA and *iscR* mRNA by the RNAplex program. **(B)** Basic architecture of the plasmid constructs. **(C,D)** The relative florescence was measured at 488 nm excitation and 520 nm emission lights after the corresponding constructs were co-transformed in *E. coli* strain. $^{**}p < 0.01$, following by one-way ANOVA, independent *t*-tests.

and the tolerance to hydrogen peroxide oxidation (H_2O_2) was tested. The *smpB* mutation exhibited a slow growth compared with the wild type and the complementary strain (**Figure 3D**). The Δ*smpB* survived better than the wild type when the H_2O_2 concentration ranged from 6 to 10 mM, revealing that Δ*smpB* was endowed

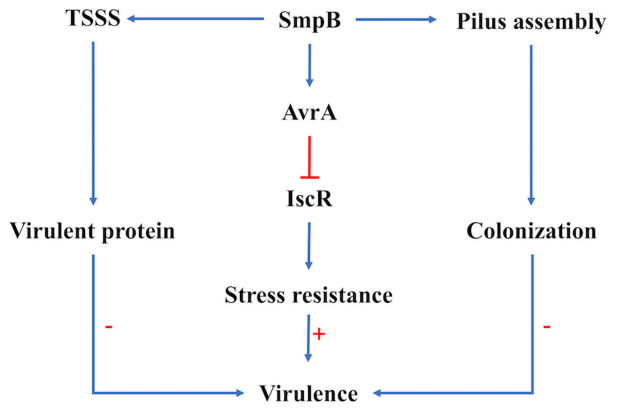

FIGURE 6 | Regulation of SmpB in virulence regulation. The virulence of *A. veronii* was affected by the expression of virulent proteins the ability of host colonization and the resistance to adversity. Type VI secretion system and pilus assembly were affected on the transcription and translation level by SmpB regulation directly. The sRNA AvrA functioned the stress resistance directly, which was mediated by SmpB indirectly. The arrows in blue showed the positive regulation, and the line in red showed repression. The symbol "+", "–" indicated upregulation and downregulation, respectively.

with a stronger capability of growth under adverse conditions (**Figure 3E**).

AvrA Deletion Increases the Tolerances to Iron Deficiency and Oxidative Stress by Upregulating Iron-Sulfur Gene Expression

AvrA was a non-coding RNA of 253nt, and its secondary structure was predicted by the software RNAfold (http://rna.tbi.univie.ac.at/cgi-bin/RNAWebSuite/RNAfold.cgi) (**Figure 4A**). The growth results demonstrated that the AvrA deletion presented a better ability to grow under dipyridyl (DIP)-chelated iron deficiency state (**Figure 4B**). Also, the oxidation resistance of Δ*avrA* was evaluated under 0–10 mM H_2O_2 in comparison with the wild type and the complemented strains, showing that the antioxidation capacity was enhanced after AvrA knockout (**Figure 4C**). Realtime qPCR results showed that the transcriptional expressions of the iron-sulfur genes *iscR*, *iscU, iscS, and iscA* were significantly increased (**Figure 4D**).

AvrA Binds and Downregulates iscR mRNA by Base Pairing

The potential interaction site was predicted between AvrA and the *iscR* promotor using the RNAplex program. Interestingly, the base-pairing region encompassed the ribosome binding site and the start codon AUG of *iscR,* and the binding site spanned from C_{37} to A_{63} of 5′-end AvrA (**Figure 5A**). Two mutations, P1 (from A_2 to C_5, ACUC) and P2 (from C_{-18} to G_{-13}, GCGUUC), were introduced in the *iscR* promoter (*piscR*) and fused with the enhanced green fluorescent protein (eGFP) to produce Φ(p*iscR* $_{mutP1}$-eGFP) and Φ(p$iscR_{mutP2}$-eGFP), respectively (**Figures 5A,B**). When AvrA was co-expressed with Φ(p*iscR*-eGFP), the fluorescence was repressed, suggesting that AvrA could interact with the promotor of *iscR* by base pairing (**Figure 5C**). Furthermore, the fluorescence recovered when AvrA was co-transformed with Φ(p$iscR_{mutP1}$-eGFP), revealing that P1 was the exact site for interaction (**Figure 5C**). Next, a mutation named p$avrA_{mutP1}$ was introduced in the AvrA expression plasmid p*avrA* to match Φ (p*iscR* $_{mutP1}$-eGFP), resulting in fluorescent repression. Conversely the mutated p$avrA_{mutP1}$ did not reduce the fluorescence when co-expressed with the wild type Φ(*iscR*-eGFP) (**Figure 5D**). The results concluded that AvrA repressed the expression of *iscR* by base pairing with the *iscR* translation initiation region P1.

DISCUSSION

SmpB is not only the key component of the trans-translation system, but also plays an important role as a transcription regulator in the global regulation of bacteria (Liu et al., 2016). In our study, the *smpB* deletion affected the transcriptional expression of the genes related to the bacterial growth, metabolism and protein secretion in multiple metabolic pathways in *A. veronii*. Previously Type II, III, and VI secretion systems were reported in multiple strains of *Aeromonas* bacteria, which function by exporting bacterial virulence proteins and by infecting host cells (Suarez et al., 2009; Journet and Cascales, 2016). The gene expression of the Type III secretion system had extremely low abundance, while those of Type VI performed higher in the transcriptome**.** Most of all, virulence-related genes which mediated the pili assembly (type IV pilus) and protein secretion (type VI secretion system, TSSS) were totally downregulated (**Figure 1**). Previously, the type VI secretion system was identified to function as the virulence factor in *Vibrio hollisae* and *Aeromonas hydrophila* (Russell et al., 2014). The colonization of wild type *A. veronii* was significantly higher than that of Δ*smpB*. However, the survival rates of the infected mice showed no significant differences between the wild type and Δ*smpB* strain. Previously the *smpB* deletion mutant of *Listeria monocytogenes* and *Salmonella Typhimurium* were avirulent and deficient in the intramacrophage survival (Kivisaar, 2003; Mraheil et al., 2017) The results were inconsistent with past reports, indicating that there are other pathways maintaining the virulence in *A. veronii smpB* mutants. Subsequently, sRNA AvrA was revealed as an alternative for virulence compensation. The downregulation of AvrA affected the expression of IscR in Δ*smpB A. veronii*. In case of iron deficiency, IscR enhanced iron-sulfur cluster assembly and iron sulfur protein synthesis (Santos et al., 2014), and amended the antioxidant ability of *A. veronii*.

When bacteria infect the host, they are subjected to stressful conditions such as strong oxidization, deficient nutrition and metal ion. The harsh conditions cause starvation, accumulation of secondary metabolites, decreased fidelity of DNA replication and the reduction in DNA repair activity which are similarly encountered during the stationary stage (De Biase et al., 1999; Kivisaar, 2003). Most sRNAs are expressed as important regulators in the process of gene regulation under adverse stress (Michaux et al., 2014; Amin et al., 2016; Holmqvist and Wagner, 2017). The sRNA AvrA was uncovered to function by base pairing with its target gene *iscR*. IscR regulated a set of genes involved in iron-sulfur cluster assembly in adversity like iron deficiency and

oxidative stress (**Figure 6**). However, the transcription factors associated with oxidative stress, including Fur (ferric uptake regulation protein), OxyR (hydrogen peroxide-inducible genes activator), SoxR (hydrogen peroxide-inducible genes activator) were insignificantly expressed by comparing Δ*smpB* strains the with wild type strains (**Supplementary Table 2**). The mutation of *smpB* resulted in the downregulation of sRNA AvrA, which leads to the upregulation of *iscR* expression and the enhancement of the adverse resistance. Combined with the attenuated virulence and the increased survival in adversity in Δ*smpB*, the strains performed a similar lethality in mice compared with the wild type. Virulence is a trait that has been selected in evolutionary history (Rafaluk et al., 2015; Gerstein and Nielsen, 2017). Therefore, the survival viability in the macrophage and the tolerance to adverse environments caused by *smpB* mutation compensates for the loss of function in virulence, causing *A. veronii* to evolve as a superbug.

DATA AVAILABILITY

The raw data supporting the conclusions of this manuscript will be made available by the authors, without undue reservation, to any qualified researcher.

AUTHOR CONTRIBUTIONS

ZL, XM, and DW contributed the conception and design of the study. DW, HL, YT, HT, and ZL performed the statistical analysis. DW, HL, XH, and ZL drafted the manuscript. All authors contributed to manuscript revision, read and approved the submitted version.

FUNDING

This work was supported by grants from the Hainan Natural Science Foundation Nos. 317015 (to YT) and 319QN161 (to HL), and the Science and Technology Program of Hainan Province ZDYF2017020 (to ZL).This work was also partially supported by grants from the National Natural Science Foundation of China Nos. 31560021, 31772887 (to ZL), and 31860676 (to YT).

SUPPLEMENTARY MATERIAL

The Supplementary Material for this article can be found online at: https://www.frontiersin.org/articles/10.3389/fcimb.2019.00142/full#supplementary-material

REFERENCES

Aguilera-Arreola, M. G., Hernandez-Rodriguez, C., Zuniga, G., Figueras, M. J., Garduno, R. A., and Castro-Escarpulli, G. (2007). Virulence potential and genetic diversity of *Aeromonas caviae*, *Aeromonas veronii*, and *Aeromonas hydrophila* clinical isolates from Mexico and Spain: a comparative study. *Can. J. Microbiol.* 53, 877–887. doi: 10.1139/W07-051

Amin, S. V., Roberts, J. T., Patterson, D. G., Coley, A. B., Allred, J. A., Denner, J. M., et al. (2016). Novel small RNA (sRNA) landscape of the starvation-stress response transcriptome of *Salmonella enterica* serovar typhimurium. *RNA Biol.* 13, 331–342. doi: 10.1080/15476286.2016.1144010

Carrier, M.-C., Bourassa, J.-S., and Massé, E. (2017). Cellular homeostasis: a small RNA at the crossroads of iron and photosynthesis. *Curr. Biol.* 27, R380–R383. doi: 10.1016/j.cub.2017.04.003

De Biase, D., Tramonti, A., and Bossa, F., and Visca, P. (1999). The response to stationary-phase stress conditions in *Escherichia coli* : role and regulation of the glutamic acid decarboxylase system.. *Mol. Microbiol.* 32, 1198–1211.

Durand, S., Tomasini, A., Braun, F., Condon, C., and Romby, P. (2015). sRNA and mRNA turnover in gram-positive bacteria. *FEMS Microbiol. Rev.* 39, 316–330. doi: 10.1093/femsre/fuv007

Fiedler, M. R. M., Cairns, T. C., Koch, O., Kubisch, C., and Meyer, V. (2018). Conditional expression of the small GTPase ArfA impacts secretion, morphology, growth, and actin ring position in *Aspergillus niger*. *Front. Microbiol.* 9:878. doi: 10.3389/fmicb.2018.00878

Gerstein, A. C., and Nielsen, K. (2017). It's not all about us: evolution and maintenance of *Cryptococcus* virulence requires selection outside the human host. *Yeast* 34, 143–154. doi: 10.1002/yea.3222

Haines, S., Arnaud-Barbe, N., Poncet, D., Reverchon, S., Wawrzyniak, J., Nasser, W., et al. (2015). IscR regulates synthesis of colonization factor antigen I fimbriae in response to iron starvation in enterotoxigenic *Escherichia coli*. *J. Bacteriol.* 197, 2896–2907. doi: 10.1128/JB.00214-15

Himeno, H., Kurita, D., and Muto, A. (2014). tmRNA-mediated trans-translation as the major ribosome rescue system in a bacterial cell. *Front. Genet.* 5:66. doi: 10.3389/fgene.2014.00066

Holmqvist, E., and Wagner, E. G. H. (2017). Impact of bacterial sRNAs in stress responses. *Biochem. Soc. Trans.* 45, 1203–1212. doi: 10.1042/BST20160363

Huter, P., Muller, C., Arenz, S., Beckert, B., and Wilson, D. N. (2017). Structural basis for ribosome rescue in bacteria. *Trends Biochem. Sci.* 42, 669–680. doi: 10.1016/j.tibs.2017.05.009

Ilbert, M., and Bonnefoy, V. (2013). Insight into the evolution of the iron oxidation pathways. *Biochim. Biophys. Acta* 1827, 161–175. doi: 10.1016/j.bbabio.2012.10.001

Journet, L., and Cascales, E. (2016). The type VI secretion system in *Escherichia coli* and related species. *EcoSal Plus* 7:20. doi: 10.1128/ecosalplus.ESP-0009-2015

Keiler, K. C. (2008). Biology of trans-translation. *Annu. Rev. Microbiol.* 62, 133–151. doi: 10.1146/annurev.micro.62.081307.162948

Keiler, K. C. (2015). Mechanisms of ribosome rescue in bacteria. *Nat. Rev. Microbiol.* 13, 285–297. doi: 10.1038/nrmicro3438

Kivisaar, M. (2003). Stationary phase mutagenesis: mechanisms that accelerate adaptation of microbial populations under environmental stress. *Environ. Microbiol.* 5, 814–827. doi: 10.1046/j.1462-2920.2003.00488.x

Kurita, D., Miller, M. R., Muto, A., Buskirk, A. R., and Himeno, H. (2014). Rejection of tmRNA·SmpB after GTP hydrolysis by EF-Tu on ribosomes stalled on intact mRNA. *RNA* 20, 1706–1714. doi: 10.1261/rna.045773.114

Li, J., Ji, L., Shi, W., Xie, J., and Zhang, Y. (2013). Trans-translation mediates tolerance to multiple antibiotics and stresses in *Escherichia coli*. *J. Antimicrobial Chemother.* 68, 2477–2481. doi: 10.1093/jac/dkt231

Liang, W., and Deutscher, M. P. (2010). A novel mechanism for ribonuclease regulation: transfer-messenger RNA (tmRNA) and its associated protein SmpB regulate the stability of RNase R. *J. Biol. Chem.* 285, 29054–29058. doi: 10.1074/jbc.C110.168641

Liu, P., Chen, Y., Wang, D., Tang, Y., Tang, H., Song, H., et al. (2016). Genetic selection of peptide aptamers that interact and inhibit both small protein B and alternative ribosome-rescue factor A of *Aeromonas veronii* C4. *Front. Microbiol.* 7:1228. doi: 10.3389/fmicb.2016.01228

Liu, Z., Hu, K., Tang, Y., Li, H., Tang, H., Hu, X., et al. (2018). SmpB down-regulates proton-motive force for the persister tolerance to aminoglycosides in *Aeromonas veronii*. *Biochem. Biophys. Res. Commun.* 507, 407–413. doi: 10.1016/j.bbrc.2018.11.052

Liu, Z., Liu, P., Liu, S., Song, H., Tang, H., and Hu, X. (2015). Small protein B upregulates sensor kinase bvgS expression in *Aeromonas veronii*. *Front. Microbiol.* 6:579. doi: 10.3389/fmicb.2015.00579

Mandin, P., Chareyre, S., and Barras, F. (2016). A regulatory circuit composed of a transcription factor, IscR, and a regulatory RNA, RyhB, controls Fe-S cluster delivery. *mBio* 7:e00966-16. doi: 10.1128/mBio.00966-16

Michaux, C., Verneuil, N., and Hartke, A., and Giard, J.-C. (2014). Physiological roles of small RNA molecules. *Microbiology* 160(Pt. 6), 1007–1019. doi: 10.1099/mic.0.076208-0

Mraheil, M. A., Frantz, R., Teubner, L., Wendt, H., Linne, U., Wingerath, J., et al. (2017). Requirement of the RNA-binding protein SmpB during intracellular growth of *Listeria monocytogenes*. *Int. J. Med. Microbiol.* 307, 166–173. doi: 10.1016/j.ijmm.2017.01.007

Mu, X., Huan, H., Xu, H., Gao, Q., Xiong, L., Gao, R., et al. (2013). The transfer-messenger RNA-small protein B system plays a role in avian pathogenic *Escherichia coli* pathogenicity. *J. Bacteriol.* 195, 5064–5071. doi: 10.1128/JB.00628-13

Oliva, G., Sahr, T., and Buchrieser, C. (2015). Small RNAs, 5′ UTR elements and RNA-binding proteins in intracellular bacteria: impact on metabolism and virulence. *FEMS Microbiol. Rev.* 39, 331–349. doi: 10.1093/femsre/fuv022

Rafaluk, C., Gildenhard, M., Mitschke, A., Telschow, A., Schulenburg, H., and Joop, G. (2015). Rapid evolution of virulence leading to host extinction under host-parasite coevolution. *BMC Evol. Biol.* 15:112. doi: 10.1186/s12862-015-0407-0

Roche, B., Aussel, L., Ezraty, B., Mandin, P., Py, B., and Barras, F. (2013). Iron/sulfur proteins biogenesis in prokaryotes: formation, regulation and diversity. *Biochim. Biophys. Acta* 1827, 455–469. doi: 10.1016/j.bbabio.2012.12.010

Russell, A. B., Wexler, A. G., Harding, B. N., Whitney, J. C., Bohn, A. J., Goo, Y. A., et al. (2014). A type VI secretion-related pathway in bacteroidetes mediates interbacterial antagonism. *Cell Host Microbe* 16, 227–236. doi: 10.1016/j.chom.2014.07.007

Santos, J. A., Alonso-Garcia, N., Macedo-Ribeiro, S., and Pereira, P. J. (2014). The unique regulation of iron-sulfur cluster biogenesis in a Gram-positive bacterium. *Proc. Natl. Acad. Sci. U S A.* 111, E2251–E2260. doi: 10.1073/pnas.1322728111

Suarez, G., Sierra, J. C., Erova, T. E., Sha, J., Horneman, A. J., and Chopra, A. K. (2009). A type VI secretion system effector protein, VgrG1, from *Aeromonas hydrophila* that induces host cell toxicity by ADP ribosylation of actin. *J. Bacteriol.* 192, 155–168. doi: 10.1128/jb.01260-09

Torii, Y., Goto, Y., Nakahira, S., Kozaki, S., Kaji, R., and Ginnaga, A. (2015). Comparison of Systemic toxicity between botulinum toxin subtypes A1 and A2 in mice and rats. *Basic Clin. Pharmacol. Toxicol.* 116, 524–528. doi: 10.1111/bcpt.12351

Xu, X. M., and Moller, S. G. (2008). Iron-sulfur cluster biogenesis systems and their crosstalk. *Chembiochem* 9, 2355–2362. doi: 10.1002/cbic.200800384

Zhang, R., Zhang, L., Jiang, D., Zheng, K., Cui, Y., Li, M., et al. (2014). Mouse organ coefficient and abnormal sperm rate analysis with exposure to tap water and source water in Nanjing reach of Yangtze River. *Ecotoxicology* 23, 641–646. doi: 10.1007/s10646-014-1228-4

Conflict of Interest Statement: The authors declare that the research was conducted in the absence of any commercial or financial relationships that could be construed as a potential conflict of interest.

frontiers in Cellular and Infection Microbiology

BRIEF RESEARCH REPORT
published: 13 September 2019
doi: 10.3389/fcimb.2019.00328

Genetic Features of Antarctic *Acinetobacter radioresistens* Strain A154 Harboring Multiple Antibiotic-Resistance Genes

Andrés Opazo-Capurro[1,2], *Paul G. Higgins*[3,4], *Julia Wille*[3,4], *Harald Seifert*[3,4], *Camila Cigarroa*[1], *Paulina González-Muñoz*[1,2,5], *Mario Quezada-Aguiluz*[1,2], *Mariana Domínguez-Yévenes*[1,2], *Helia Bello-Toledo*[1,2], *Luis Vergara*[5] *and Gerardo González-Rocha*[1,2]*

[1] *Laboratorio de Investigación en Agentes Antibacterianos (LIAA), Departamento de Microbiología, Facultad de Ciencias Biológicas, Universidad de Concepción, Concepción, Chile,* [2] *Millennium Nucleus for Collaborative Research on Bacterial Resistance (MICROB-R), Santiago, Chile,* [3] *Institute for Medical Microbiology, Immunology and Hygiene, University of Cologne, Cologne, Germany,* [4] *German Center for Infection Research (DZIF), Partner Site Bonn-Cologne, Cologne, Germany,* [5] *Departamento de Ciencias Biológicas y Químicas, Facultad de Medicina y Ciencia, Universidad San Sebastián, Concepción, Chile*

OPEN ACCESS

Edited by:
Xiangmin Lin, Fujian Agriculture and Forestry University, China

Reviewed by:
Hossam Abdelhamed, Mississippi State University, United States
José Alejandro Di Conza, University of Buenos Aires, Argentina

***Correspondence:**
Gerardo González-Rocha
ggonzal@udec.cl

Specialty section:
This article was submitted to Molecular Bacterial Pathogenesis, a section of the journal Frontiers in Cellular and Infection Microbiology

Received: *14 June 2019*
Accepted: *02 September 2019*
Published: *13 September 2019*

Citation:
Opazo-Capurro A, Higgins PG, Wille J, Seifert H, Cigarroa C, González-Muñoz P, Quezada-Aguiluz M, Domínguez-Yévenes M, Bello-Toledo H, Vergara L and González-Rocha G (2019) Genetic Features of Antarctic Acinetobacter radioresistens Strain A154 Harboring Multiple Antibiotic-Resistance Genes. Front. Cell. Infect. Microbiol. 9:328. doi: 10.3389/fcimb.2019.00328

While antibiotic-resistant bacteria have been detected in extreme environments, including Antarctica, to date there are no reports of *Acinetobacter* species isolated from this region. Here, we characterized by whole-genome sequencing (WGS) the genetic content of a single antibiotic-resistant *Acinetobacter* spp. isolate (A154) collected in Antarctica. The isolate was recovered in 2013 from soil samples at Fildes Peninsula, Antarctica, and was identified by detection of the intrinsic OXA-23 gene, and confirmed by Tetra Correlation Search (TCS) and WGS. The antibiotic susceptibility profile was determined by disc diffusion, E-test, and broth microdilution methods. From WGS data, the acquired resistome and insertion sequence (IS) content were identified by *in silico* analyses. Plasmids were studied by the alkaline lysis method followed by pulsed-field gel electrophoresis and conventional PCR. The A154 isolate was identified as *A. radioresistens* by WGS analysis and displayed >99.9 of similarity by TCS in relation with the databases. Moreover, it was resistant to ampicillin, ceftriaxone, ceftazidime, cefepime, cefotaxime, streptomycin, and kanamycin. Likewise, in addition to the intrinsic $bla_{\text{OXA-23-like}}$ gene, A154 harbored the plasmid-encoded antibiotic-resistance genes $bla_{\text{PER-2}}$, *tet(B)*, *aph(3′)-VIa*, *strA*, and *strB*, as well as a large diversity of ISs. This is the first report of antibiotic-resistant *A. radioresistens* in Antarctica. Our findings show the presence of several resistance genes which could be either intrinsic or acquired in the region.

Keywords: antibiotic-resistance genes, *Acinetobacter*, Antarctica, whole-genome sequencing, resistance plasmid, ecotoxicology

INTRODUCTION

Antarctica possesses one of the most extreme environmental conditions on earth, where low temperatures, high levels of UV radiation, and low water availability, limit the growth of living organisms, including bacteria (Convey et al., 2008). In these ecosystems, diverse survival strategies to ward off competing microorganisms are present, including the production of antibiotics by environmental microbiota (Aronson et al., 2011). Lately, it has been determined that antibiotic production and resistance have ancient origins in nature, ranging from 2 billion years to 40 million years (Dcosta et al., 2011). In this sense, several antibiotic resistance genes (ARGs) have been identified in uncontaminated soil in Antarctica, confirming that this continent possesses a natural microbial community associated with a local resistome (Van Goethem et al., 2018). Although this natural phenomenon is old, the high use of antibiotics in human practice, as well as the rise of anthropic activity around the globe, have favored to increase the selection and dissemination of antibiotic resistant bacteria and antibiotic resistance determinants (Rabbia et al., 2016).

Although Antarctica has been historically considered as a pristine unexplored continent, the anthropogenic activity has been increasing recently, which could potentially have an impact on the resistome of the natural bacterial community (Rabbia et al., 2016). It has been demonstrated that the presence of military bases, scientific programs, and tourism, promotes the dissemination of ARGs possibly due to the introduction of human-related microorganisms (Hernandez and González-Acuña, 2016). For instance, we recently found that *Escherichia coli* isolates collected from seawater and waste-water treatment plants located in the Antarctic Treaty area showed resistance to β-lactams, aminoglycosides, tetracycline, and trimethoprim-sulphonamide, which is probably associated with discharged of inefficiently treated water emanating from waste-water plants (Rabbia et al., 2016).

Acinetobacter radioresistens is able to survive extreme levels of oxidative stress, desiccation, and irradiation (Touchon et al., 2014; Sacher et al., 2018) and has primarily been isolated from environmental sources (i.e., cotton, water, and soil), and has also been identified as part of the human skin microbiota of healthy people (Seifert et al., 1997), as well as from fecal samples from chickens (Ngaiganam et al., 2019). Few studies on the presence of ARGs in *A. radioresistens* are published, and the species is considered largely susceptible to antibiotics.

A. radioresistens isolate A154 was collected from a soil sample in Antarctica in 2013. Interestingly, it displayed an unusual resistance pattern to diverse antibiotics, including β-lactams and aminoglycosides. Hence, to further understand the genetic features of the Antarctic A154 isolate containing multiple ARGs, we report its genome sequence.

MATERIALS AND METHODS

Bacterial Source

Acinetobacter spp. isolate A154 was recovered from ornitogenic soil (superficial layer) in Ardley Island (−62°12′60.00″S −58°55′59.99″W) in Fildes Peninsula, Antarctica, during a scientific expedition in 2013. Specifically, the isolate was recovered in a soil sample from a lagoon shore. Fildes Peninsula is located on King George Island and holds the largest number of scientific research bases in the Antarctic Treaty Area (Rabbia et al., 2016). The isolate was grown on trypticase soy agar incubated overnight at 30°C.

PCR Experiments

Total DNA was extracted by the boiling water method and utilized as template for preliminary species identification by the detection of the intrinsic chromosomally-encoded $bla_{\mathrm{OXA-23-like}}$ gene.

Susceptibility Testing

Susceptibility testing were performed by disc diffusion following the CLSI recommendations, for ampicillin (AMP, 10 μg), cefotaxime (CTX, 30 μg), ceftriaxone (CRO, 30 μg), ceftazidime (CAZ, 30 μg), cefepime (FEP, 30 μg), imipenem (IPM, 10 μg), meropenem (MEM, 10 μg), gentamicin (GEN, 10 μg), amikacin (AMK, 30 μg), kanamycin (KAN, 30 μg), streptomycin (STR, 10 μg), tetracycline (TET, 30 μg), and ciprofloxacin (CIP, 5 μg) (Clinical Laboratory Standards Institute, 2017). Minimum inhibitory concentrations (MICs) were determined by E-test and broth microdilution for AMP, CTX, IPM, MEM, GEN, AMK, and KAN (Clinical Laboratory Standards Institute, 2017).

Whole-Genome Sequencing

Total DNA for whole-genome sequencing (WGS) was extracted using the Wizard® Genomic DNA Purification kit (Promega, USA) following the manufacturer's protocol. DNA concentration and integrity were verified using a Take3 plate (BioTek Instruments). WGS was performed by the Illumina MiSeq platform (2 × 250 bp paired end reads) with libraries prepared by the NexteraXT kit (Illumina).

In silico Genome Analyses

De novo assembly was performed by using the SPades software version 3.9 available at the CGE server (https://cge.cbs.dtu.dk/services/SPAdes/), utilizing default values (Nurk et al., 2013). Species identification was carried out by the SpeciesFinder service, version 1.3 (https://cge.cbs.dtu.dk/services/SpeciesFinder/), which is based on the *16S rRNA* sequence. Genome annotation was accomplished using the NCBI Prokaryotic Genome Annotation Pipeline (PGAP) web-service (http://www.ncbi.nlm.nih.gov/genome/annotation_prok).
Moreover, the draft genome was analyzed by the Comprehensive Genome Analysis service (https://www.patricbrc.org/app/ComprehensiveGenomeAnalysis), which incorporates the RAST tool kit (RASTtk). The genetic contexts of the contigs in which plasmid-encoded ARGs were detected, were plotted using the Artemis software, version 18.0.2 (Carver et al., 2012).

In order to establish the taxonomic relatedness of A154, we used the Tetra Correlation Search (TCS), which allows to compare the draft genome of this isolate against the genomes reference database GenomesDB (http://jspecies.ribohost.com/jspeciesws/#genomesdb), which contains >30.000 whole and

draft genomes with pre-calculated overall genome relatedness indices (Richter et al., 2015). In addition, we determined the acquired resistome, insertion sequences (ISs) content and toxin-antitoxin (TA) systems through ResFinder (https://cge.cbs.dtu.dk/services/ResFinder/), RASTtk and Pathosystems Resource Integration Center (PATRIC) platforms. Plasmid replicons were searched using the PlasmidFinder tool (Carattoli et al., 2014) and the PATRIC platform. The genome of the isolate A154 was deposited at DDBJ/EMBL/GenBank under the accession number PXJD00000000.1.

Molecular Typing

Additionally, from WGS data we extracted the seven alleles according to the Pasteur MLST scheme which were submitted to the PubMLST database (https://pubmlst.org/) in order to assign a specific sequence type (ST).

Plasmids Studies

Plasmids were isolated by the alkaline lysis method according to a standard protocol (Kado and Liu, 1981). Afterwards, DNA concentration of the plasmids extracts were measured by spectrophotometry (BioTek Instruments) and chromosomal contamination was evaluated by detecting the *16S rDNA* gene, which is chromosomally encoded. After, ARGs previously detected in total DNA were screened using the pure DNA plasmids extracts. Moreover, we performed mating and plasmid curing experiments (Trevors, 1986; Leungtongkam et al., 2018).

RESULTS AND DISCUSSION

The A154 isolate was identified as *A. radioresistens* according to its *16S rRNA* sequence, and displayed >99.9 of similarity by TCS with the genome of *A. radioresistens* strain SK82 (NCBI: txid596318), thus confirming that A154 belongs to this species. Additionally, it was resistant to AMP, CRO, CTX, CAZ, FEP, KAN, and STR, intermediate to GEN, and susceptible to IMP, MEM, CIP, TET, and AMK. MICs values of AMP, CAZ, CTX, FEP, GEN, and KAN were >128, >128, 128, 32, 8, and 128 μg/mL, respectively (**Table 1**).

From *in silico* analyses, we determined that the WGS data generated resulted in 205 contigs and a N_{50} contig size of 131,303 bp. Moreover, A154 genome comprised 3,448,645 bp with an average GC content of 41.5%, 3,444 coding sequences (CDS), 64 transfer RNA (tRNA) genes, and 8 ribosomal RNA (rRNA) genes.

From RASTtk results, we determined that the resistome of A154 was comprised of aminoglycoside modifying enzymes (AMEs) encoded by *aph(3′)-VIa*, *aac(3)-IIa*, *strA* (*aph(3″)-Ia*), and *strB* (*aph(6)-Id*), as well as the β-lactamase genes $bla_{\mathrm{OXA-23-like}}$ (intrinsic to this species), $bla_{\mathrm{TEM-1B}}$, $bla_{\mathrm{SCO-1}}$ and $bla_{\mathrm{PER-2}}$, and the tetracycline-resistance gene *tet(B)* (**Table 1**). ARGs positions on the genome of A154 are shown in **Figure 1**. Interestingly, the $bla_{\mathrm{OXA-23-like}}$ allele identified in A154 did not match with any variant from the database, sharing a 98.18% identity with $bla_{\mathrm{OXA-565}}$ (accession number KY883665). SCO-1 encodes for a RTG-type carbenicillinase identified in *Escherichia coli* and *Acinetobacter* spp. (Papagiannitsis et al., 2007; Poirel et al., 2007). To the author's knowledge, the single report of this enzyme in *Acinetobacter* genus occurred in isolates collected in Argentina (Poirel et al., 2007); thus its presence could be associated to isolates from South America and nearby regions. According to Van Goethem et al. (2018), resistance determinants present in environmental soil, especially from extreme and remote ecosystems, are still underrepresented, thus our findings represent the very first description of *A. radioresistens* resistant to multiple antibiotics in this area.

Importantly, *A. radioresistens* has been rarely associated with human infections and the species is normally highly susceptible to antibiotics. In this sense, Visca et al. described a community-acquired bacteraemia caused by this species, but the isolate was susceptible to cephalosporins and aminoglycosides (Visca et al., 2001). Similarly, Poirel et al. published a study that included five *A. radioresistens* isolates that were fully susceptible to all antibiotics tested, including penicillins and carbapenems, despite the detection of $bla_{\mathrm{OXA-23-like}}$ gene (Poirel et al., 2008). On the other hand, Higgins *et al.* identified two carbapenem-resistant *A. radioresistens* isolates that were recovered from the same patient 17 days apart, which were also resistant to fluoroquinolones (Higgins et al., 2013). Additionally, two *A. radioresistens* isolates collected from companion animal infections, which harbored $bla_{\mathrm{IMP-1}}$, *sul1*, *aadA1*, and *aac(6)-31*, were resistant to carbapenems and fluoroquinolones (Kimura et al., 2017), but despite the presence of AMEs, the isolates were susceptible to GEN and AMK.

Our findings show that the isolate A154 was resistant to β-lactams, except carbapenems, which could be explained by the presence of the $bla_{\mathrm{TEM-1B}}$, $bla_{\mathrm{PER-2}}$, and $bla_{\mathrm{SCO-1}}$ genes. Interestingly, PER-2 corresponds to an extended-spectrum β-lactamase (Pasteran et al., 2006; Gutkind et al., 2012), while TEM-1B and SCO-1 are class A narrow-spectrum β-lactamases (Poirel et al., 2007), which could be mediating the resistance displayed against β-lactams, such as cephalosporins (Gutkind et al., 2012). These findings are particularly interesting since although β-lactamase genes are common components of the soil resistome, they are not highly abundant. Accordingly, a study of soil samples from the Mackay Glacier in Antarctica showed a very low β-lactamase abundance (Van Goethem et al., 2018). The same study also demonstrated that β-lactamase genes are more common in soil samples from regions that are more likely to have been exposed to human activity (Van Goethem et al., 2018), representing a possible source of selective pressure.

Importantly, A154 was resistant to KAN and STR, and intermediate to GEN. Although the isolate was classified as AMK susceptible, the MIC value (16 μg/mL) was only one dilution below the CLSI breakpoint for intermediate (32 μg/mL). This particular phenotype is mainly explained by the activity the APH(3′)-VIa enzyme, which was originally described in *A. baumannii* and confers resistance to AMK and KAN (Ramirez and Tolmasky, 2010). Additionally, other AME genes detected were *strA* and *strB* which confer resistance to STR (Ramirez and Tolmasky, 2010), in concordance with the observed phenotype. We also identified the *aac(3)-IIa* gene, which is related to resistance to GEN and tobramycin (TOB) (Ramirez and Tolmasky, 2010). Similarly, the identified resistome included the *tet(B)* gene, however, the isolate was susceptible to tetracycline. These inconsistencies suggest that *A. radioresistens* might need a complementary mechanism

TABLE 1 | Antibiotic susceptibilities and genetic features of isolate A154 from Antarctica.

MIC (ug/mL)						Main genetic features	
AMP	**CAZ**	**CTX**	**FEP**	**GEN**	**KAN**	**ARGs**	**ST**
>128	>128	128	32	8	128	bla_{TEM-1B}; bla_{SCO-1}, *aac(3)-IIa*, bla_{PER-2} (pl); *aph(3″)-VIa* (pl); *strA* (pl); *strB* (pl); *tet(B)* (pl)	1207

MIC, minimum inhibitory concentration; AMP, ampicillin; CAZ, ceftazidime; CTX, cefotaxime; FEP, cefepime; GEN, gentamicin; KAN, kanamycin; ARGs, antibiotic-resistance genes; ST, sequence-type; pl, plasmid-encoded.

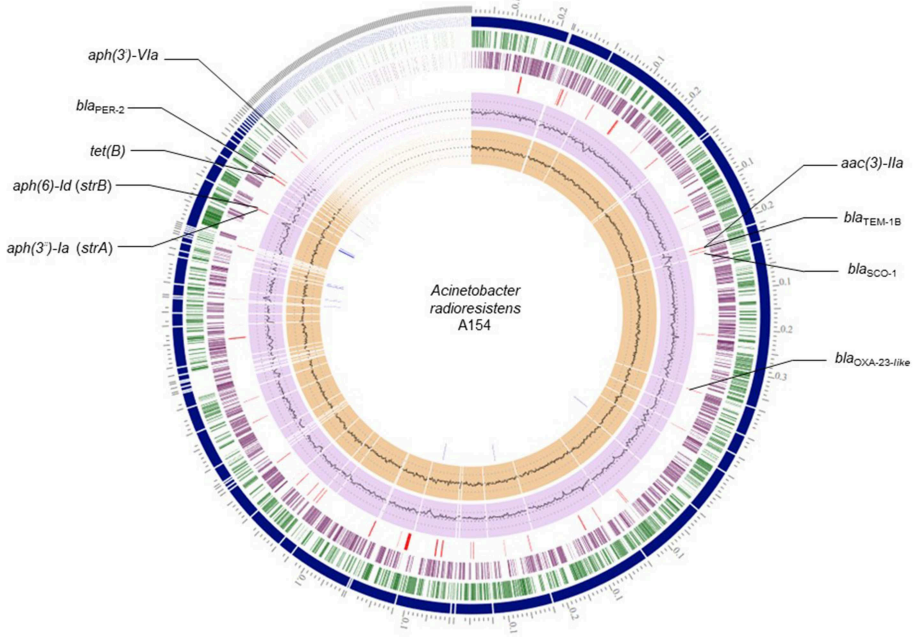

FIGURE 1 | Circular representation of A154 draft genome. Circles from the outermost are as follows: contigs; forward CDS; reverse CDS; GC content; GC skew. Red lines: antibiotic-resistance genes; blue lines: transposase genes.

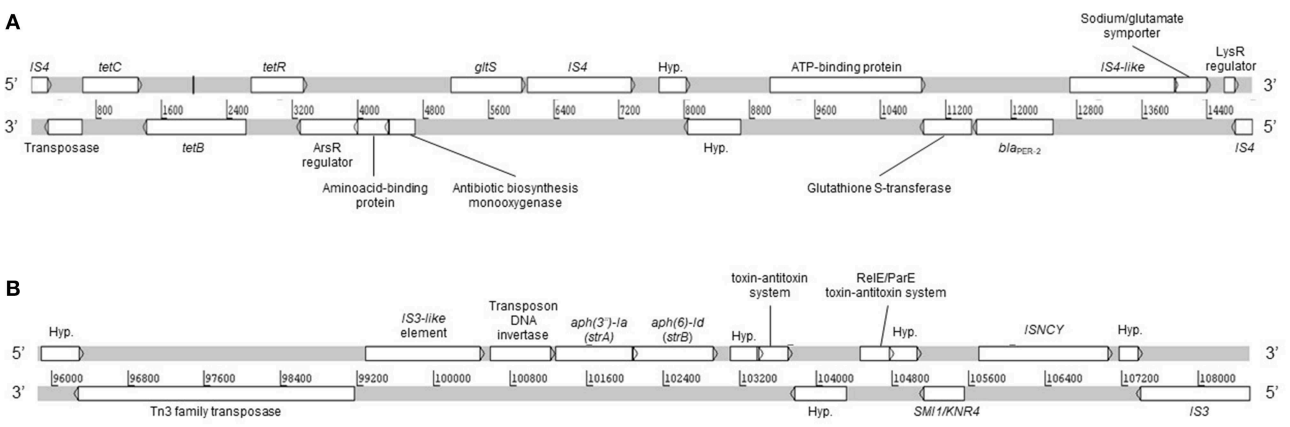

FIGURE 2 | Linear map of A154 contigs 35 **(A)** and 10 **(B)**. DNA strands sense and anti-sense are represented. Hyp., hypothetical protein. The linear representation was generated by using Artemis software.

of aminoglycosides/tetracycline resistance or to regulate the expression of ARGs to develop the resistance phenotype. This assumption is reaffirmed by the presence of the intrinsic $bla_{OXA-23-like}$ gene in carbapenem-susceptible *A. radioresistens*, which when present in *A. baumannii*, confers resistance to carbapenems (Evans and Amyes, 2014), when over-expressed (Higgins et al., 2013). Therefore, expression experiments of the ARGs are required in order to understand the potential influence of these determinants on the resistance level to antimicrobials in the species described.

On the other hand, A154 was assigned to the ST1207 in PubMLST (https://pubmlst.org/), which corresponds to a novel ST. This is a novel lineage which corresponds to a singleton, since is not associated to any described ST of the database. Accordingly, it is important to analyze a larger collection of isolates from regions with and without human influence in order to determine whether this ST is endemic/prevalent to this area or it was introduced. This is particularly important since we have previously determined that antibiotic-resistant *E. coli* isolates in Antarctica are more frequent in regions with a significant anthropic influence (Rabbia et al., 2016). In the case of A154, it was collected from the same region of the study mentioned above, thus the local microbiome and resistome are probably affected by human activity. However, since the soil from which the isolate was recovered corresponded to surface soil, which is determined by the influence of organic matter from animals, it is possible that it could be carried by migrating birds (Segawa et al., 2013), which might be playing an important role in the genetic contamination of this region.

Moreover, no plasmid replicons were detected by PlasmidFinder and PATRIC. However, we detected a large plasmid of ca. 280 kb which was not detected *in silico* from WGS (data not shown). Moreover, the plasmid could not be transferred by conjugation and neither cured by temperature. The latter could be explained by the presence of the type II toxin-antitoxin systems RelB/DinJ (accession number PSD36295.1) and RelE/ParE (accession number PSD36025.1), which were detected from WGS. Interestingly, the RelE/ParE genes were located adjacent to *strA* and *strB* genes (**Figure 2**), which suggests that both are contained in the same plasmid. The toxin-antitoxin systems are defined as plasmid maintenance systems present in almost all free-living bacteria (Kang et al., 2018), which could confer stability against curing agents. Conjugation experiments under different conditions should be performed in order to determine the ability of the plasmid to be mobilized.

Remarkably, a large diversity of IS-family transposases was found on the genomes of A154. Specifically, its IS content was composed by fifteen copies of IS/IS1182 transposase, twelve of IS6, 11 of IS30, eight of IS4, four of ISL3, two each of IS3-like and IS5-like, and a single copy each of IS982, IS200/IS605, ISNCY, IS481, and IS1. IS-elements are capable of mobilizing and controlling the expression of ARGs, among other functions, therefore the isolate has an important potential to acquire/disseminate and over-express resistance determinants (Siguier et al., 2014). Notably, the bla_{PER-2}; *aph(3′)-VIa*; *strA*; *strB*; *tet(B)* were identified in the plasmid extract obtained from alkaline lysis, and are also located in the same region of the genome in which diverse ISs were also located (**Figure 1**). This suggests that they could has been incorporated by A154 by horizontal-gene transfer mediated by plasmids and/or IS-elements. As shown in **Figure 2**, the plasmid-encoded ARGs were located in different contigs from WGS, in which also several IS-elements were located, reaffirming the potential role of these mobile-genetic elements in their mobilization. The contig in which *aph(3′)-VIa* is located, was not represented since it was contained in a short contig, which harbored only two genes.

An important limitation of our study is the Illumina platform generates short reads, making it difficult to determine the entire sequence and structure of the plasmid contained by A154 (Roosaare et al., 2018). In consequence, the use of this sequencing technology to predict plasmids (i.e., by PlasmidFinder) is limited, being only possible to search for the incompatibility groups detected in the genome which are deposited on the databases. A potential solution for this problem, is to isolate the plasmid and sequence it or use new sequencing technologies, such as Oxford Nanopore Technology (ONT) (Lemon et al., 2017).

In conclusion, our results represent the first description of *A. radioresistens* in Antarctica containing several ARGs, in an isolate recovered from a region under both human and animal influences, thus these factors could be contributing to the introduction of ARGs in Antarctica. These findings contribute to better understand the knowledge of the biology of *Acinetobacter* as well as to add more data about the content of ARGs in the region.

DATA AVAILABILITY

The raw data supporting the conclusions of this manuscript will be made available by the authors, without undue reservation, to any qualified researcher.

AUTHOR CONTRIBUTIONS

AO-C, PG-M, PH, and JW contributed to the acquisition, analysis, and interpretation of the data. AO-C, CC, PG-M, and MQ-A made important contributions to the design of the work. HS, MD-Y, HB-T, LV, and GG-R provided approval for publication of the content and contributed drafting the work and critically revisiting the manuscript.

FUNDING

This work was funded by the post-doctoral project N°3150286 from The National Fund for Scientific and Technological Development (FONDECYT) and the Chilean Antarctic Institute (INACH) project number RT_06_12.

ACKNOWLEDGMENTS

The authors highly appreciate the support from the Chilean National Commission for Scientific and Technological Research (CONICYT), the Chilean Antarctic Institute (INACH), and the Millennium Science Initiative of the Ministry of Economy, Development and Tourism, Chile.

REFERENCES

Aronson, R. B., Thatje, S., Mcclintock, J. B., and Hughes, K. A. (2011). Anthropogenic impacts on marine ecosystems in Antarctica. *Ann. N. Y. Acad. Sci.* 1223, 82–107. doi: 10.1111/j.1749-6632.2010.05926.x

Carattoli, A., Zankari, E., Garciá-Fernández, A., Larsen, M. V., Lund, O., Villa, L., et al. (2014). *In silico* detection and typing of plasmids using plasmidfinder and plasmid multilocus sequence typing. *Antimicrob. Agents Chemother.* 58, 3895–3903. doi: 10.1128/AAC.02412-14

Carver, T., Harris, S. R., Berriman, M., Parkhill, J., and McQuillan, J. A. (2012). Artemis: An integrated platform for visualization and analysis of high-throughput sequence-based experimental data. *Bioinformatics* 28, 464–469. doi: 10.1093/bioinformatics/btr703

Clinical and Laboratory Standards Institute (2017). *CLSI. Performance Standards for Antimicrobial Susceptibility Testing. 27th Edn. CLSI supplement M100*. Wayne, PA: Clinical and Laboratory Standards Institute.

Convey, P., Gibson, J. A. E., Hillenbrand, C. D., Hodgson, D. A., Pugh, P. J. A., Smellie, J. L., et al. (2008). Antarctic terrestrial life–challenging the history of the frozen continent? *Biol. Rev.* 83, 103–117. doi: 10.1111/j.1469-185X.2008.00034.x

Dcosta, V. M., King, C. E., Kalan, L., Morar, M., Sung, W. W. L., Schwarz, C., et al. (2011). Antibiotic resistance is ancient. *Nature* 477, 457–461. doi: 10.1038/nature10388

Evans, B. A., and Amyes, S. G. B. (2014). OXA β-lactamases. *Clin. Microbiol. Rev.* 27, 241–263. doi: 10.1128/CMR.00117-13

Gutkind, O. G., Di Conza, J., Power, P., and Radice, M. (2012). β-lactamase-mediated resistance: a biochemical, epidemiological and genetic overview. *Curr. Pharm. Des.* 19, 164–208. doi: 10.2174/13816128130202

Hernandez, J., and González-Acuña, D. (2016). Anthropogenic antibiotic resistance genes mobilization to the polar regions. *Infect. Ecol. Epidemiol.* 12:32112. doi: 10.3402/iee.v6.32112

Higgins, P. G., Zander, E., and Seifert, H. (2013). Identification of a novel insertion sequence element associated with carbapenem resistance and the development of fluoroquinolone resistance in *Acinetobacter radioresistens*. *J. Antimicrob. Chemother.* 68, 720–722. doi: 10.1093/jac/dks446

Kado, C., and Liu, S. (1981). Rapid procedure for detection and isolation of large and small plasmids. *J. Bacteriol.* 145, 1365–1373.

Kang, S. M., Kim, D. H., Jin, C., and Lee, B. J. (2018). A systematic overview of type II and III toxin-antitoxin systems with a focus on druggability. *Toxins (Basel)* 10:E515. doi: 10.3390/toxins10120515

Kimura, Y., Miyamoto, T., Aoki, K., Ishii, Y., Harada, K., Watarai, M., et al. (2017). Analysis of IMP-1 type metallo-β-lactamase-producing *Acinetobacter radioresistens* isolated from companion animals. *J. Infect. Chemother.* 23, 655–657. doi: 10.1016/j.jiac.2017.03.011

Lemon, J. K., Khil, P. P., Frank, K. M., and Dekker, J. P. (2017). Rapid nanopore sequencing of plasmids and resistance gene detection in clinical isolates. *J. Clin. Microbiol.* 55, 3530–3543. doi: 10.1128/JCM.01069-17

Leungtongkam, U., Thummeepak, R., Tasanapak, K., and Sitthisak, S. (2018). Acquisition and transfer of antibiotic resistance genes in association with conjugative plasmid or class 1 integrons of *Acinetobacter baumannii*. *PLoS ONE* 13:e0208468. doi: 10.1371/journal.pone.0208468

Ngaiganam, E. P., Rolain, J.-M., and Diene, S. M. (2019). Detection of a new variant of OXA-23 carbapenemase in *Acinetobacter radioresistens* isolates from urban animals in Marseille, France. *J. Glob. Antimicrob. Resist.* 16, 178–180. doi: 10.1016/j.jgar.2019.01.021

Nurk, S., Bankevich, A., Antipov, D., Gurevich, A. A., Korobeynikov, A., Lapidus, A., et al. (2013). Assembling single-cell genomes and mini-metagenomes from chimeric MDA products. *J. Comput. Biol.* 20, 714–737. doi: 10.1089/cmb.2013.0084

Papagiannitsis, C. C., Loli, A., Tzouvelekis, L. S., Tzelepi, E., Arlet, G., and Miriagou, V. (2007). SCO-1, a novel plasmid-mediated class A β-lactamase with carbenicillinase characteristics from *Escherichia coli*. *Antimicrob. Agents Chemother.* 51, 2185–2188. doi: 10.1128/AAC.01439-06

Pasteran, F., Rapoport, M., Petroni, A., Faccone, D., Corso, A., Galas, M., et al. (2006). Emergence of PER-2 and VEB-1a in *Acinetobacter baumannii* strains in the Americas. *Antimicrob. Agents Chemother.* 50, 3222–3224. doi: 10.1128/AAC.00284-06

Poirel, L., Corvec, S., Rapoport, M., Mugnier, P., Petroni, A., Pasteran, F., et al. (2007). Identification of the novel narrow-spectrum β-lactamase SCO-1 in *Acinetobacter* spp. from Argentina. *Antimicrob. Agents Chemother.* 51, 2179–2184. doi: 10.1128/AAC.01600-06

Poirel, L., Figueiredo, S., Cattoir, V., Carattoli, A., and Nordmann, P. (2008). *Acinetobacter radioresistens* as a silent source of carbapenem resistance for *Acinetobacter* spp. *Antimicrob. Agents Chemother.* 52, 1252–1256. doi: 10.1128/AAC.01304-07

Rabbia, V., Bello-Toledo, H., Jiménez, S., Quezada, M., Domínguez, M., Vergara, L., et al. (2016). Antibiotic resistance in *Escherichia coli* strains isolated from Antarctic bird feces, water from inside a wastewater treatment plant, and seawater samples collected in the Antarctic Treaty area. *Polar Sci.* 10, 123–131. doi: 10.1016/j.polar.2016.04.002

Ramirez, M. S., and Tolmasky, M. E. (2010). Aminoglucoside modifing enzymes. *Drug Resist. Updat.* 13, 151–171. doi: 10.1016/j.drup.2010.08.003

Richter, M., Rosselló-Móra, R., Oliver Glöckner, F., and Peplies, J. (2015). JSpeciesWS: A web server for prokaryotic species circumscription based on pairwise genome comparison. *Bioinformatics* 32, 929–931. doi: 10.1093/bioinformatics/btv681

Roosaare, M., Puustusmaa, M., Möls, M., Vaher, M., and Remm, M. (2018). PlasmidSeeker: identification of known plasmids from bacterial whole genome sequencing reads. *PeerJ* 6:e4588. doi: 10.7717/peerj.4588

Sacher, J. C., Yee, E., Szymanski, C. M., and Miller, W. G. (2018). Complete genome sequence of *Acinetobacter radioresistens* strain LH6, a multidrug-resistant bacteriophage-propagating strain. *Microbiol. Resour. Announc.* 7:e00929-18. doi: 10.1128/MRA.01317-18

Segawa, T., Takeuchi, N., Rivera, A., Yamada, A., Yoshimura, Y., Barcaza, G., et al. (2013). Distribution of antibiotic resistance genes in glacier environments. *Environ. Microbiol. Rep.* 5, 127–134. doi: 10.1111/1758-2229.12011

Seifert, H., Dijkshoorn, L., Gerner-Smidt, P., Pelzer, N., Tjernberg, I., and Vaneechoutte, M. (1997). Distribution of *Acinetobacter* species on human skin: Comparison of phenotypic and genotypic identification methods. *J. Clin. Microbiol.* 35, 2819–2825. doi: 10.1128/CMR.00064-16

Siguier, P., Gourbeyre, E., and Chandler, M. (2014). Bacterial insertion sequences: their genomic impact and diversity. *FEMS Microbiol. Rev.* 38, 865–891. doi: 10.1111/1574-6976.12067

Touchon, M., Cury, J., Yoon, E. J., Krizova, L., Cerqueira, G. C., Murphy, C., et al. (2014). The genomic diversification of the whole *Acinetobacter* genus: origins, mechanisms, and consequences. *Genome Biol. Evol.* 6, 2866–2882. doi: 10.1093/gbe/evu225

Trevors, J. T. (1986). Plasmid curing. *FEMS Microbiol. Rev.* 32, 149–157.

Van Goethem, M. W., Van Pierneef, R., Bezuidt, O. K. I., Peer, Y., Van De, Cowan, D. A., and Makhalanyane, T. P. (2018). A reservoir of 'historical' antibiotic resistance genes in remote pristine Antarctic soils. *Microbiome* 6:40. doi: 10.1186/s40168-018-0424-5

Visca, P., Petrucca, A., De Mori, P., Festa, A., Boumis, E., Antinori, A., et al. (2001). Community-acquired *Acinetobacter radioresistens* bacteremia in an HIV-positive patient. *Emerg. Infect. Dis.* 7, 1032–1035. doi: 10.3201/eid0706.010621

Conflict of Interest Statement: The authors declare that the research was conducted in the absence of any commercial or financial relationships that could be construed as a potential conflict of interest.

frontiers in Cellular and Infection Microbiology

ORIGINAL RESEARCH
published: 24 September 2019
doi: 10.3389/fcimb.2019.00333

The First Isolation and Molecular Characterization of Shiga Toxin-Producing Virulent Multi-Drug Resistant Atypical Enteropathogenic *Escherichia coli* O177 Serogroup From South African Cattle

Peter Kotsoana Montso[1], *Victor Mlambo*[2] *and Collins Njie Ateba*[1]*

[1] Bacteriophage Therapy and Phage Bio-control Laboratory, Department of Microbiology, Faculty of Natural and Agricultural Sciences, North-West University, Mmabatho, South Africa, [2] Faculty of Agriculture and Natural Sciences School of Agricultural Sciences, University of Mpumalanga, Nelspruit, South Africa

OPEN ACCESS

Edited by:
Patrícia Poeta, University of Trás-os-Montes and Alto Douro, Portugal

Reviewed by:
Indranil Samanta, West Bengal University of Animal and Fishery Sciences, India
Farhad Safarpoor Dehkordi, University of Tehran, Iran

***Correspondence:**
Collins Njie Ateba
collins.ateba@nwu.ac.za

Specialty section:
This article was submitted to Molecular Bacterial Pathogenesis, a section of the journal Frontiers in Cellular and Infection Microbiology

Received: *17 June 2019*
Accepted: *10 September 2019*
Published: *24 September 2019*

Citation:
Montso PK, Mlambo V and Ateba CN (2019) The First Isolation and Molecular Characterization of Shiga Toxin-Producing Virulent Multi-Drug Resistant Atypical Enteropathogenic Escherichia coli O177 Serogroup From South African Cattle. Front. Cell. Infect. Microbiol. 9:333. doi: 10.3389/fcimb.2019.00333

Atypical enteropathogenic *E. coli* (aEPEC) is a group of diarrhoeagenic *Escherichia coli* with high diversity of serogroups, which lack the bundle-forming pili (BFP) and genes encoding for shiga toxins. The aim of this study was to isolate, identify and determine virulence and antibiotic resistance profiles of aEPEC O177 strains from cattle feces. A total of 780 samples were collected from beef and dairy cattle and analyzed for the presence of *E. coli* O177. One thousand two hundred and seventy-two (1272) presumptive isolates were obtained and 915 were confirmed as *E. coli* species. Three hundred and seventy-six isolates were positively confirmed as *E. coli* O177 through amplification of *rmlB* and *wzy* gene sequences using multiplex PCR. None of these isolates harbored *bfpA* gene. A larger proportion (12.74%) of the isolates harbored *hlyA* gene while 11.20, 9.07, 7.25, 2.60, and 0.63% possessed stx_2, stx_1, *eaeA*, stx_{2a}, and stx_{2d}, respectively. Most of *E. coli* O177 isolates carried stx_2/*hlyA* (9.74%). Furthermore, 7.40% of the isolates harbored stx_1/stx_2 while 7.09% possessed stx_1/stx_2/*hlyA* genes. Only one isolate harbored stx_1/stx_2/*hly*/*eaeA*/stx_{2a}/stx_{2d} while 5.11% of the isolates harbored all the four major virulence genes stx_1/stx_2/*hlyA*/*eaeA*, simultaneously. Further analysis revealed that the isolates displayed varied antimicrobial resistance to erythromycin (63.84%), ampicillin (21.54%), tetracycline (13.37%), streptomycin (17.01%), kanamycin (2.42%), chloramphenicol (1.97%), and norfloxacin (1.40%). Moreover, 20.7% of the isolates exhibited different phenotypic multi-drug resistance patterns. All 73 isolates harbored at least one antimicrobial resistance gene. The *aadA*, *streA*, *streB*, *erm,* and *tetA* resistance genes were detected separately and/or concurrently. In conclusion, our findings indicate that environmental isolates of aEPEC

O177 strains obtained from cattle in South Africa harbored virulence and antimicrobial resistance gene determinants similar to those reported in other shiga-toxin producing *E. coli* strains and suggest that these determinants may contribute to the virulence of the isolates.

Keywords: atypical enteropathogenic *E. coli* (aEPEC), bundle-forming pili (BFP), *E. coli* O177, virulence factors, antimicrobial resistance, shiga-toxins, diarrhoeagenic *E. coli*

INTRODUCTION

Enteropathogenic *E. coli* (EPEC) is a group of diarrhoeagenic *E. coli* that is reported to cause high morbidity and mortality in humans, especially in immune-compromised subjects, elderly individuals and young children. EPEC are characterized by the presence of intimin (*eae*) genes coupled with the absence of the *stx* genes (Martins et al., 2016; Alonso et al., 2017). The *eae* gene is responsible for attaching and effacing (A/E) lesions on the intestinal epithelial cell of the host (Kaper et al., 2004; Martins et al., 2016; Malik et al., 2017). Based on the presence or absence of the EPEC adherence factor (EAF) plasmid, EPEC is subdivided into two groups that include typical Enteropathogenic *E. coli* (tEPEC) and atypical Enteropathogenic *E. coli* (aEPEC) (Trabulsi et al., 2002; Alonso et al., 2017). The tEPEC strains possess EAF plasmid, which encodes a bundle forming pili (*bfp*A) while aEPEC strains lack the *bfpA* gene (Canizalez-Roman et al., 2013; Malik et al., 2017). It is on these bases that the virulence potentials of aEPEC is poorly understood and highly questioned. Despite the fact that tEPEC have been most often associated disease complications in humans, it is only recently that aEPEC been reported to cause diseases in both animals and humans (Malik et al., 2017). This may account for the reason why previous studies that have been documented worldwide and in the study area have focused on EHEC, especially *E. coli* O157 and non-O157 strains that received great attention due to its high pathogenicity (Ateba and Bezuidenhout, 2008; Ateba and Mbewe, 2011; Iwu et al., 2016; Jajarmi et al., 2017; Toro et al., 2018). The findings of most of these studies were in agreement with previous reports indicating that EHEC strains possessed *stx*, stx_2, *hlyA,* and *eaeA* gene determinants that enhance their potential to cause infections such as diarrhea, hemorrhagic colitis (HC) and hemolytic uremic syndrome (HUS) in humans (Farrokh et al., 2013). However, to the best of our knowledge there is currently no report on the occurrence of EPEC, and aEPEC in particular among South African food-producing animals. This therefore creates a knowledge gap on the virulence profiles of aEPEC strains in the area. Despite the fact that aEPEC strains were known to be less pathogenic when compared to EHEC counterparts, data from some recent studies have revealed the presence of virulence determinants in aEPEC strains thus making them to start receiving attention as pathogens of severe clinical significance in humans (Beutin et al., 2005; Bibbal et al., 2017) as well as in food-producing animals, especially sheep and wildlife (Otero et al., 2013; Álvarez-Suárez et al., 2016; Martins et al., 2016). In this study, we expand our previous investigations on aEPEC in the area by determining the occurrence of aEPEC O177 strains in cattle and also provide an overview of the putative virulence and antimicrobial resistance profiles of the isolates. This was motivated from the fact that cattle are the primary reservoir of both EHEC (stx^+) and aEPEC (stx^-) strains, thus providing opportunities for horizontal transfer of virulence and antibiotic resistant genes between species and/or strains living in the same ecological niches (Bibbal et al., 2017).

MATERIALS AND METHODS

Samples Collection and Isolation of *E. coli* O177 Serogroup

A total of 780 cattle fecal samples were collected from eight commercial dairy and beef cattle farms in the North West Province, South Africa. Ethical clearance was obtained from the North West University Research Ethics Committee prior to the commencement of the study. Sampling was done between January 2017 and July 2017. The selection of the farms was based on the production system; either intensive, semi-intensive, and/or extensive farming system in the study area. The selection of all the three systems was based on the fact their management system is different. Furthermore, this was to avoid biasness in terms of selecting the farms. Ethical procedures such as restraining the animals using proper facilities and equipment were enforced during the collection of the samples. Fecal samples were collected directly from the rectum of individual animals using sterile arm-length gloves and in order to avoid duplication of sampling, the cattle were looked in their respective handling pens immediately after collection. Samples were placed in sterile sample collection bottles, labeled appropriately and immediately transported on ice to the Antimicrobial Resistance and Phage Biocontrol Laboratory (AREPHABREG), in the Department of Microbiology, North-West University for microbial analysis. Data on antibiotic type and treatment history were collected for the purpose of understanding antibiotic exposure histories of isolates from the study population.

Approximately, 2 g of fecal samples were dissolved in 10 mL of 10% (w/v) saline solution and homogenized. Aliquots of 5 μL were transferred into 10 mL buffered peptone water (Oxoid Ltd., Basingstok, Hampshire, UK). Ten-fold serial dilutions were prepared and aliquots of 100 μL from each dilution was spread-plated on Rainbow agarO157 plates (Kase et al., 2015) obtained from Biolog Inc., USA. The plates were incubated aerobically at 37°C for 24 h. Colonies with purple and pink colors were randomly picked and purified by streaking on sorbitol MacConkey agar (Merck, S.A) supplemented with 1 mg/L potassium tellurite (Merck, SA) and incubated aerobically at 37°C for 24 h. Pure isolates were preserved in 20 % (v/v) glycerol (Merck, SA) and stored at −80°C for future use.

Genomic DNA Extraction From Presumptive Isolates

Overnight culture for each sample was prepared and genomic DNA was extracted from the cultures using the Zymo Research Genomic DNA^{TM}-Tissue MiniPrep Kit (Biolab, South Africa) following the manufacturer's instructions. DNA concentration and purity was determined using the NanoDrop Lite 1,000 spectrophotometer (model: Thermo Fisher Scientific, USA) and the DNA was stored at −80°C until further analysis by PCR.

Identification of *E. coli* O177 Serogroup Using Multiplex PCR Assay

A singleplex PCR assay targeting the *uidA E. coli* O177-specific gene sequence was performed using a previous protocol (Anbazhagan et al., 2011). *Escherichia coli* O177 serogroup-specific primer pairs were designed using the Primer3 software (this study), based on *rmlB* and *wzy* gene sequences that encode for dTDP-glucose 4, 6-dehydratase, and O-antigen polymerase, respectively (Ye et al., 2012). The specificity of the PCR primers was tested using National Center for Biotechnology Information/Primer-Basic Alignment Search Tool (NCBI/Primer-BLAST) (https://www.ncbi.nlm.nih.gov/tools/primer-blast/). The oligonucleotides were synthesized and supplied by Inqaba Biotechnical Industry Ltd., Pretoria, South Africa. The newly developed multiplex PCR protocol was empirically validated for its specificity, sensitivity reproducibility, and robustness. PCR assays was performed to amplify *rmlB* and *wzy* gene fragments and the primer sequences, targeted genes, amplicon sizes as well as the PCR conditions are listed in **Table 1**. The PCR reactions constituted 12.5 μL of 2X DreamTaq Green Master Mix, 0.5 μM of each primer and 1 μL of template DNA. The volume of the reaction mixture was adjusted to 25 μL with RNase-nuclease free PCR water. A non-DNA template (nuclease-free water) reaction tube served as a negative control while a DNA sample from *E. coli* O177 (isolated during the preliminary study) was used as positive control. All the PCR reagents used were Fermentas USA products supplied by Inqaba Biotec Industry Ltd., Sunnyside, Pretoria, South Africa. Amplifications were performed using DNA thermal cycler (model- Bio-Rad C1000 Touch^{TM} Thermal Cycler, Singapore). All the PCR products were held at 4°C until gel electrophoresis.

Detection of Virulence Genes in *E. coli* O177 Isolates

E. coli O177 isolates were subjected to a *bfp* gene PCR analysis in order to screen for characters of aEPEC strains. A highly virulent environmental *E. coli* O157:H7 isolate (*bfp*$^{+}$) previously isolated from our research group (AREPHABREG) was used as positive control. The positive control *E. coli* O157:H7 possessed the stx_1, stx_2, *eaeA,* and *hlyA* genes. In addition, DNA extracted from an *E. coli* (ATCC 98222) that is a non-pathogenic strain was included in each PCR run as a negative control. Isolates that were positive for the *bfp* gene were further screened for the presence of an array of STEC virulence genes that included *eaeA*, *hlyA*, stx_1, stx_2, and stx_2 variants (stx_{2a}, stx_{2b}, stx_{2c}, stx_{2d}, stx_{2e}, stx_{2f}, stx_{2g}) using previously described protocols (Paton and Paton, 1998; He et al., 2012). Primer sequences, target genes, amplicon sizes as well as PCR cycling conditions for the different genes are listed in **Table 1**. All the PCR reactions were prepared as 25 μL standard volumes comprising 12.5 μL of 2X DreamTaq Green Master Mix, 0.5 μM of each primer, 1 μL of template DNA and RNase-nuclease free PCR water. Amplifications were performed using DNA thermal cycler (model- Bio-Rad C1000 Touch^{TM} Thermal Cycler, Singapore). All the PCR products were held at 4°C until they were separated by electrophoresis.

Antimicrobial Susceptibility Test

The antimicrobial susceptibility profile of the isolates was determined using the Kirby-Bauer disc diffusion technique (Bauer et al., 1966), making use of antibiotic discs obtained from Mast Diagnostics, UK. The antibiotics using in this study comprised Ampicillin (AMP), 10 μg; Chloramphenicol (C), 30 μg; Erythromycin (E), 15 μg; Kanamycin (K), 30 μg; Norfloxacin (NOR), 10 μg; Streptomycin (S), 10 μg and Tetracycline (TE), 30 μg. Some of these antimicrobial agents were selected due to the fact that they are widely used as prophylactics in both beef and dairy cattle farming in South Africa. Plates were incubated aerobically at 37°C for 24 h and antibiotic growth inhibition zone diameter data were compared with standard reference values in order to classify the isolates as sensitive, intermediate resistance or resistant to a particular antibiotic (Clinical Laboratory Standards Institute, 2016). *Escherichia coli* ATCC 25922 was used as a reference for quality control in antimicrobial susceptibility test.

Detection of Genetic Determinants for Antibiotic Resistance Genes by PCR

All confirmed *E. coli* O177 isolates that were resistant to three or more antibiotics were designated multi-drug resistant isolates and were screened for the presence of the *tetA*, *tetW, aadA*, *strA*, *strB*, *ampC*, *cmlA*, *ermB,* and *kan* antibiotic resistance determinants. Primer sequences, target genes, amplicon sizes as well as PCR cycling conditions for the different genes are listed in **Table 2**. All the PCR reactions were prepared as 25 μL standard volumes comprising 12.5 μL of 2X DreamTaq Green Master Mix, 0.5 μM of each primer, 1 μL of template DNA and RNase-nuclease free PCR water. Amplifications were performed using DNA thermal cycler (model- Bio-Rad C1000 Touch^{TM} Thermal Cycler, Singapore). All the PCR products were kept at 4°C and later resolved by electrophoresis.

Agarose Gel Electrophoresis

All PCR amplicons were resolved by electrophoresis on a 2% (w/v) agarose gel containing 0.001 μg/mL ethidium bromide. A 100 bp DNA molecular weight DNA marker (Fermentas, USA) was included in each gel and used to confirm the sizes of the amplicons. A ChemiDoc Imaging System (Bio-Rad ChemiDoc^{TM} MP Imaging System, UK) was used to capture the images using Gene Snap software, version 6.0022.

Sequence Analysis

The amplified *rmlB* and *wzy* gene fragments were sequenced by Inqaba Biotec, Pretoria, South Africa, and sequences

TABLE 1 | Oligonucleotide primers used for amplification of the various targeted genes in *E. coli* O177 serogroup.

Primers	Sequence	Target genes	Amplicon size (bp)	PCR conditions	PCR volume (25 μL)	References
I-IDENTIFICATION						
UidA-F	CTGGTATCAGCGCGAAGTCT	*uidA*	600	95°C, 10 min(1x); 95°C, 45 s; 59°C, 30 s; 72°C, 90 s (35x); 72°C for 10 min (1x)	12.5 μL of 2X DreamTaq Green Master Mix, 11 μL of nuclease free water, 0.5 μL of each primer and 1 μL of template DNA	Anbazhagan et al., 2011
UidA-R	AGCGGGTAGATATCACACTC					
RmlB-F	CGCGGATTTTTGCTCTGCAT	*rmB*	645	95°C, 3 min (1x); 94°C, 30 s; 55°C, 30 s; 72°C, 60 s (30x); 72°C for 5 min (1x)	12.5 μL of 2X DreamTaq Green Master Mix, 11 μL of nuclease free water, 1 μL (0.5 μL of each) primer and 1 μL of template DNA	This study
RmlB-R	CAGTAATTGCGAGCCGCTTC					
Wzy-F	GGTCAGGAGCATGGAGCATT	*wzy*	457			
Wzy-R	AATCCATCCGGTGTATCGGC					
II-VIRULENCE GENES						
Bfp-F	AAT GGT GCT TGC GCT TGC TGC	*bfp*	324	95°C, 3 min (1x); 94°C, 60 s; 64°C, 60 s; 72°C, 2 min (35x); 72°C for 10 min (1x)	12.5 μL of 2X DreamTaq Green Master Mix, 11 μL of nuclease free water, 0.5 μL of each primer ad	Ghanbarpour et al., 2017
Bfp-R	GCC GCT TTATCC AAC CTG GTA					
EaeA-F	GACCCGGCACAAGCATAAGC	*eaeA*	384	95°C, 10 min (1x); 95°C, 60 s; 62°C, 2 min; 72°C, 90 s (35x), 72°C, 5 min (1x)	1 μL of template A	Paton and Paton, 1998
EaeA-R	CCACCTGCAGCAACAAGAGG					
HlyA-F	GCATCATCAAGCGTACGTTCC	*hlyA*	534	95°C, 10 min (1x); 95°C, 60 s; 64°C, 2 min; 72°C, 90 s (35x), 72°C, 5 min (1x)		
HlyA-R	AATGAGCCAAGCTGGTTAAGCT					
Stx1-F	ATAAATCGCCATTCGTTGACTAC	stx_1	180	95°C, 10 min (1x); 95°C, 60 s; 62°C, 2 min; 72°C, 90 s (35x), 72°C, 5 min (1x)		
Stx1-R	AGAACGCCCACTGAGATCATC					
Stx2-F	GGCACTGTCTGAAACTGCTCC	stx_2	255			
Stx2-R	TCGCCAGTTATCTGACATTCT					
Stx2a-F	AGATATCGACCCCTCTTGAA	stx_{2a}	969	94°C, 5 min (1x); 94°C, 45 s; 60°C, 45 s; 72°C, 90 s (25x); 72°C, 7 min (1x)	12.5 μL of 2X DreamTaq Green Master Mix, 11 μL of nuclease free water, 0.5 μL of each primer and 1 μL of template DNA	He et al., 2012
Stx2a-R	GTCAACCTTCACTGTAAATG					
Stx2-G2-F	TATACGATGACACCGGAAGAAG	stx_{2b}	300	94°C, 5 min (1x); 94°C, 45 s; 65°C, 30 s; 72°C, 60 s (25x); 72°C for 5 min (1x)		
Stx2-G2-R	CCTGCGATTCAGAAAAGCAGC					
Stx2/2c	TTTTATATACAACGGGTA	stx_{2c}	163	94°C, 5 min (1x); 94°C, 45 s; 51°C, 30 s; 72°C, 60 s (30x); 72°C, 5 min (1x)		
Stx2-G1-R	GGCCACTTTTACTGTGAATGTA					
Stx2d-act	CTTTATATACAACGGGTG	stx_{2d}	359	94°C, 5 min (1x); 94°C, 60 s; 50°C, 60 s; 72°C, 60 s (25x); 72°C, 5 min (1x)		
CKS2	CTGAATTGTGACACAGATTAC					
Stx2-G4-F	CAGGAAGTTATATTTCCGTAGG	stx_{2e}	911	94°C, 5 min (1x); 94°C, 30 s; 55°C, 30 s; 72°C, 60 s (25x); 72°C, 5 min (1x)		
Stx2-G4-R	GTATTCTCTTCCTGACACCTTC					
Stx2-G3-F	TTTACTGTGGATTTCTCTTCGC	stx_{2f}	875	94°C, 5 min (1x); 94°C, 30 s; 61°C, 30 s; 72°C, 60 s (25x); 72°C for 5 min (1x)		
Stx2-G3-R	TCAGTAAGATCCTGAGGCTTG					
209-F	GTTATATTTCTGTGGATATC	stx_{2g}	573	94°C, 5 min (1x); 94°C, 45 s; 55°C, 60 s; 72°C, 60 s (25x); 72°C for 7 min (1x)		
781-R	GAATAACCGCTACAGTA					

were subjected to a Blast Search Tool (https://blast.ncbi.nlm.nih.gov/Blast.cgi) in order to confirm the identities of the isolates (Altschul et al., 1997). Nucleotide sequence data were further deposited into GenBank using the BankIt NCBI web-based sequence submission tool (https://www.ncbi.nlm.nih.gov/genbank/) in order to obtain their accession numbers.

Statistical Analysis

Measured parameters were tested for normality using the NORMAL option in the Proc Univariate statement prior to analysis of variance. Data on the proportions of samples positive for *E. coli* O177 serogroup were analyzed for effect of farming system using the general linear models (GLM) procedures of SAS

TABLE 2 | Oligonucleotide primers used for amplification of the various targeted antibiotic resistance genes in *E. coli* O177 serogroup.

Primers	Sequence	Target genes	Amplicon size (bp)	PCR conditions	PCR volume (25 μL)	References
AadA-F	GTGGATGGCGGCCTGAAGCC	*aadA*	525	95°C, 3 min (1x); 94°C, 30 s; 55°C, 30 s; 72°C, 60 s (35x), 72°C, 5 min (1x)	12.5 μL of 2X DreamTaq Green Master Mix, 11 μL of nuclease free water, 0.5 μL of each primer and 1 μL of template DNA	Srinivasan et al., 2007
AadA-R	AATGCCCAGTCGGCAGCG					
StrA-F	CCTGGTGATAACGGCAATTC	*strA*	549			
StrA-R	CCAATCGCAGATAGAAGGC					
StrB-F	ATCGTCAAGGGATTGAAACC	*strB*	509			
StrB-R	GGATCGTAGAACATATTGGC					
CmlA-F	CCGCCACGGTGTTGTTGTTATC	*cmlA*	698			
CmlA-R	CACCTTGCCTGCCCATCATTAG					
AmpC-F	CATATGCTTAATCAGTGAGG CACCT	*ampC*	850	95°C, 3 min (1x); 95°C, 60 s; 59°C, 60 s; 72°C, 2 min (35x), 72°C, 10 min (1x)	12.5 μL of 2X DreamTaq Green Master Mix, 11 μL of nuclease free water, 0.5 μL of each primer and 1 μL of template DNA	Samra et al., 2009
AmpC-R	GAATTCAGTATTCAACATTTCC GTGTCG					
Kan-F	CATATGAGAAAAACTCATCGA GCATC	*kan*	810			
Kan-R	GAATTCAGCCATATTCAACGGGAA					
TetA-F	GCTACATCCTGCTTGCCTTC	*tet(A)*	210	95°C, 3 min (1x); 94°C, 30 s; 58°C, 30 s; 72°C, 60 s (35x); 72°C, 5 min (1x)	12.5 μL of 2X DreamTaq Green Master Mix, 11 μL of nuclease free water, 0.5 μL of each primer and 1 μL of template DNA	Bergeron et al., 2015
TetA-R	CATAGATCGCCGTGAAGAGG					
TetW-F	GAGAGCCTGCTATATGCC AGC	*tet(W)*	168			
TetW-R	GGGCGTATCCACAATGTTAAC					
ErmB-F	GATACCGTTTACGAA ATTGG	*ermB*	364	95°C, 60 s; 94°C, 15 s; 56°C, 30 s; 72°C, 60 s (40x) 72°C, 5 min	12.5 μL of 2X DreamTaq Green Master Mix, 11 μL of nuclease free water, 0.5 μL of each primer and 1 μL of template DNA	
ErmB-R	GAATCGAGACTTGAGTGTGC					

(2010) according to the following statistical model:

$$Y_{ij} = \mu + F_i + E_{ij}$$

where, Y_{ij}, response variable, μ, overall mean, F_i, farming system (intensive, semi-intensive and extensive) effect and E_{ij}, random error associated with observation *ij*, assumed to be normally and independently distributed. Data on number of isolates carrying virulent genes, number of antibiotic resistant isolates, number of isolates carrying antibiotic resistance genes, and number of multidrug resistant isolates were square root-transformed before statistical analysis using the GLM procedures (SAS, 2010). For all statistical tests, significance was declared at $p < 0.05$.

RESULTS

Identification of *E. coli* O177 Serogroup Using Multiplex PCR Analysis

A total of 780 cattle fecal samples were analyzed for the presence of *E. coli* O177 using Rainbow agarO157 and a total of 1,272 non-repetitive presumptive isolates were obtained. Amplification of the *uid*A *E. coli* genus-specific gene sequence revealed that a large proportion (915; 71.93%) of the isolates were successfully identified as *E. coli* isolates. All the 915 *E. coli* isolates were further screened for the presence of *E. coli* O177 serogroup specific *rmlB* and *wzy* gene fragments using multiplex PCR analysis. Out of 915 isolates screened, 376 (41.09%) were identified as *E. coli* O177 serogroup and **Figure 1** indicates a 2% (w/v) agarose gel of representative *rmlB* and *wzy* gene fragments amplified in the study. No significant ($p > 0.05$) differences were observed on the occurrence of *E. coli* O177 serogroup across intensive, semi-intensive, and extensive animal production systems. The occurrence of *E. coli* O177 serogroup was 33.3 ± 14.43, 33.3 ± 14.43, and 50.0 ± 14.18% in intensive semi-intensive extensive farming systems, respectively.

Detection of Virulence Genotypes in *E. coli* O177 Isolates

A total of 376 atypical *E. coli* O177 isolates that were positively confirmed by PCR were screened for the presence of five virulence genes; *bfpA*, *eaeA*, *hlyA*, stx_1, and stx_2, using PCR analysis. None of the isolates possessed the *bfpA* gene fragment and thus were classified as aEPEC strains. On the contrary, all the other four virulence genes (*eaeA*, *hlyA*, stx_1, and stx_2) were successfully detected in this study. Generally, 350 isolates harbored these virulence genes. There were significant differences ($p < 0.001$) in terms of occurrence of various virulence genes in *E. coli* O177 isolates. The *hlyA* (12.74%) and stx_2 (11.20%) were the most commonly detected genes ($p < 0.001$), followed by stx_1 (9.07%), and *eaeA* (7.25%), **Figure 2**. Two stx_2 subtypes namely; the stx_{2a} and stx_{2d}, were detected among the isolates. A few of the isolates (2.60%) harbored stx_{2a}, while 0.63%

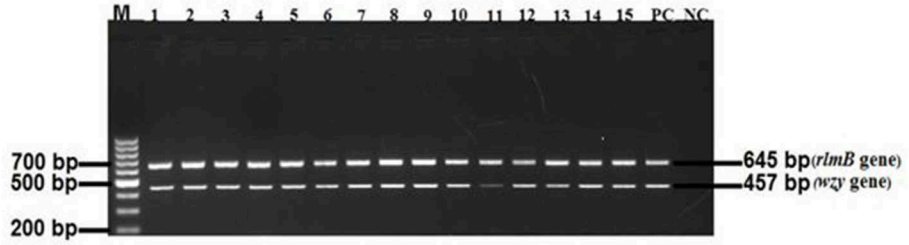

FIGURE 1 | A 2% agarose gel image of the *rmlB* (645 bp) and *wzy* (457 bp) gene fragments amplified from *E. coli* O177 isolates. Lane M = 100 bp molecular marker; Lanes 1–15 = *rmlB* and *wzy* gene fragments, respectively, that were amplified from *E. coli* O177 isolates; Lane PC = *rmlB* and *wzy* gene fragments amplified from *E. coli* O177 serotype; Lane NC = negative control sample with DNA from *E. coli* O157:H7 environmental isolate.

possessed stx_{2d}gene. Some of the isolates carried a combination of the genes detected. The majority (9.74%) of the isolates carried a combination of *hlyA*/stx_2 while 7.40, 7.09, 6.80, and 5.55% possessed stx_1/stx_2, stx_1/stx_2/*hlyA*, *hlyA*/*eaeA,* and stx_2/*hlyA*/*eaeA*, respectively ($p < 0.001$). There was no difference ($p > 0.05$) between the occurrences of stx_1/*eaeA* (6.35%) and stx_1/stx_2/*hlyA*/*eaeA* (5.11%) in *E. coli* O177 isolates. Only one isolate possessed stx_1/stx_2/stx_{2a}/stx_{2d}/*hlyA*/*eaeA*. Despite the fact that none of the isolates possessed the stx_2 subtypes stx_{2b}, stx_{2c}, stx_{2e}, stx_{2f}, and stx_{2g}, the virulence gene profiles of these aEPEC strains especially the isolate with the stx_2 subtypes was a cause for concern.

Antimicrobial Resistance Profiles

Antimicrobial susceptibility tests of the 376 isolates revealed varied antimicrobial resistance profiles against all the seven antibiotics tested. Most of the *E. coli* O177 isolates were resistant to erythromycin (63.84%) compared to other antibiotics ($p < 0.001$), **Figure 3**. No difference ($p > 0.05$) was observed in *E. coli* O177 resistance to ampicillin (21.54%), tetracycline (13.37%), streptomycin (17.01%), kanamycin (2.42%), chloramphenicol (1.97%), and norfloxacin (1.40%). The isolates showed resistance to at least two antibiotics tested. Most of the isolates (20.74%) exhibited high level of resistance to three or more antibiotics, **Figure 4** ($p < 0.001$).

Proportion of Isolates With Antimicrobial Resistance Genes

A total of 73 *E. coli* O177 isolates harbored either one or more different antimicrobial resistance genes investigated, however, only five of the ten genes were detected in the isolates. Resistance genes associated with streptomycin and erythromycin were the most frequently detected. Genes *aadA* (22.86%), *strA* (19.85%), *strB* (19.38%) *ermB* (19.68%), and *tetA* (18.23%) were detected. However, there was no significant differences in the occurrence of these genes in *E. coli* O177 isolates. No isolates possessed the *tetW* gene. Some isolates harbored a combination of three or more antibiotic resistance genes. Most (24%) of the isolates carried a combination of the *aadA*, *strA,* and *strB* genes while a smaller proportion 11% isolates possessed all the five antimicrobial resistance genes (*aadA*/*strA*/*strB*/*ermB*/*tetA*) ($p < 0.05$).

Sequence Identifier and Accession Numbers

Sequence data analysis of the *rmlB* and *wzy* gene fragments amplified from chromosomal DNA of isolates revealed a high percentage similarity (97%) sequence homology to *E. coli* serogroup O177. The nucleotide sequences for Seq1, Seq2, and Seq3 were assigned GenBank Accession numbers; MH389799, MH389800, and MH389801, respectively.

DISCUSSION

In this study, the occurrence of aEPEC, *E. coli* O177 serogroup in cattle was investigated. Although the virulence profiles of aEPEC strains is poorly understood, recent reports suggest increased incidence of human infections caused by aEPEC strains worldwide (Ingle et al., 2016; Martins et al., 2016). Cattle are primary reservoir of *E. coli* species and contaminated meat as well as their associated food products have been implicated in foodborne infections in humans (Ateba and Mbewe, 2011). Studies have reported the occurrence of aEPEC strain in food-producing animals, foods of animal origin and farm environments (Horcajo et al., 2012; Otero et al., 2013; Ghanbarpour et al., 2017). *Escherichia coli* was successfully isolated from cattle feces using Rainbow agar O157. The identities of the isolates were confirmed as *E. coli* through amplification of *uidA* gene fragments. The r*mlB* and *wzy* O-antigen gene clusters specific for *E. coli* O177 were successfully amplified through Multiplex PCR analysis. The PCR assay was highly specific and reproducible for the detection of *E. coli* O177 serogroup from cattle feces. The occurrence of *E. coli* O177 in cattle was higher (41.09 %) in this study when compared to a previous report which detected this serogroup in ovine (Martins et al., 2016). Despite this, there were no significant ($p > 0.05$) differences on the occurrence of *E. coli* O177 serogroup across all the three farming systems.

Given the fact that aEPEC strains are known to lack medically important virulence factors, their ability to cause diseases particularly in humans is not yet well-understood (Ingle et al., 2016). Previous reports indicated that aEPEC strains do not harbor *stx* and *bfpA* genes. However, recent reports have revealed that aEPEC strains especially those from ruminants, harbor

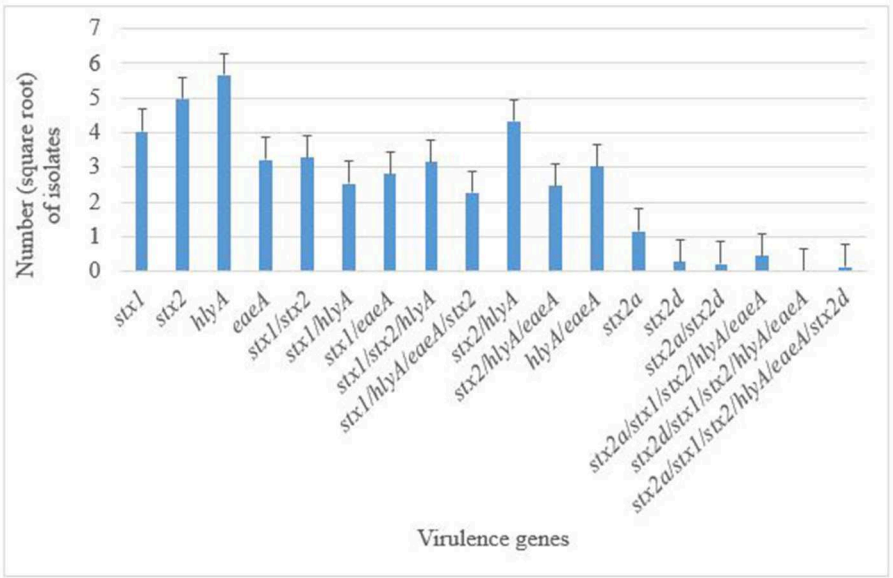

FIGURE 2 | Distribution of virulence genes in *E. coli* O177 serogroup isolated from cattle feces. The bars indicate the standard error ($p < 0.05$).

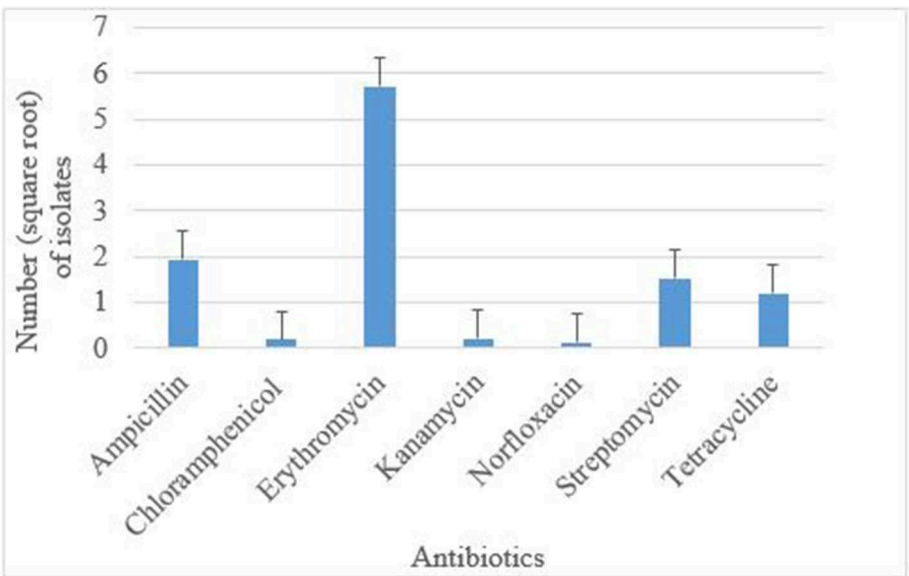

FIGURE 3 | Antibiotic resistance pattern of *E. coli* O177 serogroup isolated from cattle feces. The bars indicate the standard error ($p < 0.05$).

virulence gene profiles similar to those of the EHEC strains (Horcajo et al., 2012). In addition, some studies have reported that aEPEC strains may represent LEE-positive Shiga toxin-producing *E. coli* (STEC) that have lost the toxin-encoding prophage, or tEPEC that have lost the genes for BFP indicating the potential to have evolved from other pathogenic *E. coli* strains (Tennant et al., 2009). A motivation was the fact that previous studies conducted in the study area revealed a large proportion of virulent EHEC strains (Ateba and Bezuidenhout, 2008; Ateba and Mbewe, 2011, 2013, 2014). Despite the fact that we were unable at this stage to determine if aEPEC isolated from humans in South African cattle fall into either of these categories, an assessment of the *bfpA* and other primary STEC virulence genes (*eaeA*, *hlyA*, stx_1, stx_2, and stx_2 variants) was performed. Data of the shiga toxin subtypes among non-O157 STEC serogroups in cattle may provide an indication of the potential health risks these aEPEC isolates may cause humans. The *bfpA* gene was not detected in all the *E. coli* isolates analyzed and thus confirmed that the isolates

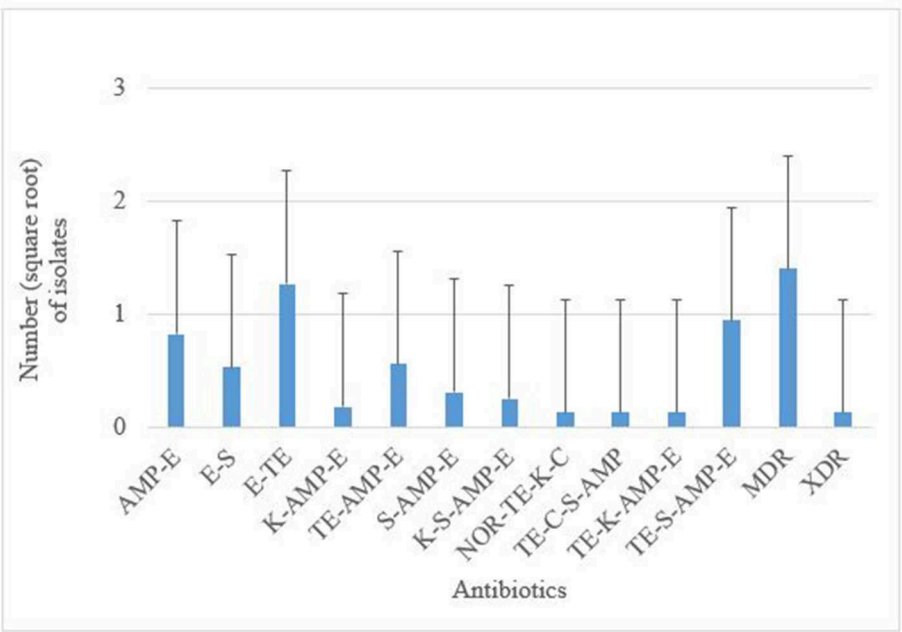

FIGURE 4 | AMP, ampicillin; C, chloramphenicol; E, erythromycin; K, kanamycin; NOR, norfloxacin; TE, tetracycline; S, streptomycin; MDR, multidrug-resistant; XDR, extensively drug-resistant. Multiple resistance patterns of *E. coli* O177 serogroup obtained from cattle feces. The bars indicate the standard error ($p < 0.05$).

belonged to aEPEC group, emerging diarrheagenic pathogens in both developing and developed countries (Ingle et al., 2016; González et al., 2017).

All the major virulence genes (stx_1, stx_2, *hlyA,* and *eaeA*) were detected in this study. Similar findings were reported by Momtaz et al. (2013a) and Momtaz et al. (2013b). Generally, the majority of *E. coli* O177 isolates possessed virulence genes. The *hlyA* was the most frequently detected virulence gene in this study. These results are similar to those reported in other studies (Ateba and Bezuidenhout, 2008; Ateba and Mbewe, 2011; Momtaz et al., 2013c), which described high prevalence of *hlyA* gene in *E. coli* O157 isolated from cattle, beef, vegetable and water intended for human consumption. The high prevalence of *hlyA* gene may be attributed to the fact that *hlyA* is a plasmid encoded gene and as a result, it may be transferred between strains of the same species (Ateba and Mbewe, 2011). The *hlyA* gene encodes α-hemolysin, a toxin that lyses mammalian erythrocytes (Toro et al., 2018).

Another observation was that the *E. coli* O177 isolates possessed *stx* genes. These genes are considered as primary virulence genes in shiga toxin-producing *E. coli* and their presence in aEPEC strains, especially *E. coli* O177 serogroup raises a serious public health concern. The stx_2 was the most prevalent gene detected in STEC/EHEC (Ateba and Mbewe, 2011; Rantsiou et al., 2012). Despite the fact that low frequency of stx_2 gene was observed in this study, the occurrence of this gene was significantly higher than stx_1 ($p < 0.001$). This observation was similar to the findings of the previous studies (Beutin et al., 2005; Jajarmi et al., 2017; Toro et al., 2018). Interestingly, stx_2 positive isolates also harbored stx_{2a} and stx_{2d} gene subtypes. However, the other stx_2 subtypes were not detected. Despite this, the presence of stx_2, stx_{2a}, and stx_{2d} genes in *E. coli* O177 serogroup is a serious concern. Strains harboring these genes have been implicated in hemolytic colitis and hemorrhagic uremic syndrome infections in humans (Farrokh et al., 2013). It is also reported that a strain harboring stx_2 gene is more virulent than a strain carrying either stx_1 or both stx_1 and stx_2 (Farrokh et al., 2013; Toro et al., 2018). Moreover, stx_{2a} and stx_{2d} subtypes are associated with severe HC and HUS infections in human (Farrokh et al., 2013; Cha et al., 2018). Therefore, the presence of stx_2gene and its subtypes in *E. coli* O177 may increase the spectrum of infections in humans and thus creating a public health concern.

The stx_1 and *eaeA* genes were also detected but at low levels compared to *hlyA* and stx_2 gene fragments. This was in contrast with the previous studies, which reported high occurrence of stx_1 and *eaeA* genes in *E. coli* isolated from poultry meat and humans (Momtaz et al., 2013b; Hemmatinezhad et al., 2015). Despite low detection of these genes, especially *E. coli* O177 serogroup, these findings cannot be overemphasized. The strain carrying stx_1 may cause diarrhea in immunocompromised individuals (Farrokh et al., 2013). In addition, the *eaeA* gene encodes for the outer membrane which mediates adherence between the STEC and/or EPEC and intestinal epithelial cells (Kaper et al., 2004; Farrokh et al., 2013). Although *eaeA* was detected in this study, this gene was not detected in some isolates. This was surprising because all the isolates were negative for *bfpA* gene and thus classified as aEPEC strains. These results differ significantly with other studies where the *eaeA* gene has been detected in aEPEC strains (Trabulsi et al., 2002; Beutin et al.,

2005; Otero et al., 2013; Martins et al., 2016; Ghanbarpour et al., 2017; González et al., 2017). The possible explanation for this observation could be that the isolates may have lost the gene during sub-culturing process (Karch et al., 1992). Given that the strains carrying *eaeA* gene are considered potentially pathogenic, absence of this gene in some of the isolates in this study should not be underestimated. The *eaeA*-negative isolates may use other genes such as *saa*, *aidA*, *agn43*, *ehaA,* or *iha* to adhere to the epithelial cell of the host (Toro et al., 2018). However, the presence of these genes was not investigated in this study.

The co-expression of stx_1, stx_2, *hlyA,* and *eaeA* genes may increase the pathogenicity of *E. coli* strains (Jajarmi et al., 2017). It was observed that *E. coli* O177 isolates possessed combinations of virulence genes. There were twelve different combinations of virulence genes detected in this study. The most frequently detected combinations were stx_2/*hlyA* (9.74 %), stx_1/stx_2 (7.40%), stx_1/stx_2/*hlyA* (7.09%), and *hlyA*/*eaeA* (6.80%). Only 5.11% of the isolates harbored all the four genes (*eaeA*/*hlyA*/stx_1/stx_2). It was also remarkable that one isolate possessed all the virulence (stx_1/stx_2/*hlyA*/*eaeA*) genes and two stx_2 (stx_{2a} and stx_{2d} genes) subtypes. Simultaneous detection of these virulence genes in *E. coli* O177 serogroup in cattle pose a public health concern. Furthermore, these findings are similar to those reported in *E. coli* O26 in a previous study (Jajarmi et al., 2017; Ranjbar et al., 2017). The combinations of virulence genes in this study are higher than those reported by the previous studies (Ateba and Mbewe, 2011; Jajarmi et al., 2017; Toro et al., 2018). However, there was low occurrence of combination of stx_2 subtypes as compared to a previous study (Jajarmi et al., 2017).

Antimicrobial agents primarily play a vital role in the lives of both humans and animals worldwide (Hudson et al., 2017). South Africa, is one of the countries where the usage of antimicrobial agents in animal production is very high (Hudson et al., 2017). In addition, the overuse of antimicrobial agents in food-producing animals, often without either professional consultation or supervision, has resulted in the emergence of antimicrobial resistant bacteria and antibiotic resistant genes in human and animal pathogens (Qiao et al., 2017). Moreover, previous investigations in the study area revealed the presence of antimicrobial resistant gene determinants in *E. coli* O157 isolated from cattle, beef, pig, pork, vegetables, and water intended for human consumption (Ateba and Bezuidenhout, 2008). Despite this, farmers continue to use antimicrobial agents to maximize production and this presents severe public health challenges.

In this study, *E. coli* O177 isolates revealed phenotypic resistance against all the seven classes of antimicrobial agents tested. In contrary to the previous study which reported high prevalence of resistance against ampicillin (100%), gentamicine (100%), and tetracycline (96.87%) Ranjbar et al. (2018), this study revealed resistance against erythromycin (63.84%), ampicillin (21.54%), tetracycline (13.37%), streptomycin (17.01%), and kanamycine (2.42%). These disparities could be attributed to geographical location and the sample type. Furthermore, 20.74% of the isolates were resistant to at least three and antimicrobial agents tested. These results were similarly to those reported in the previous study (Ranjbar et al., 2017). Antimicrobial resistance genes encoding for three antibiotics (erythromycin, streptomycin, and tetracycline) were detected. It has been reported that antibiotic resistance is common among *E. coli* isolates obtained from animals and food of animal origin due to frequent use of antibiotics in animals (Ryu et al., 2012). Generally, all isolates harbored antibiotic resistance genes. It is also worth mentioning that the same isolates harbored STEC virulence genes and previous studies have shown that isolates with similar genetic determinants may pose severe complications in humans (Ateba and Bezuidenhout, 2008; Hemeg, 2018). The occurrence of antibiotic resistance genes detected in this study was higher as compared to the previous study (Ryu et al., 2012). This could be due to the relatively higher usage of antimicrobial agents in the intensive livestock farming system where the isolates were obtained.

Antibiotic resistance genes associated with some of the antibiotics tested in this study were detected. The aadA*, strA,* and *strB* were the most frequently detected genes. However, there were significant differences among all the genes. Most of the isolates possessed *aadA* (22.86%), *strA* (19.85%), and *strB* (19.38%) genes that code for resistance to streptomycin and similar observations have been reported in other studies (Srinivasan et al., 2007; Shahrani et al., 2014; Bibbal et al., 2017). Despite the fact that *tet* genes are commonly found in *E. coli* from cattle due to the high usage of tetracycline in dairy and feedlot cattle, the occurrence of *tet* resistance genes in *E. coli* O177 isolates was low. Only the *tetA* gene was detected individually or in combination with other genes. However, in a previous report (Olowe et al., 2013), the proportion of *tet*A (43.8%) was higher than *tetB* (32.0%) and a combination of both *tetA* and *tetB* (4.4%) among clinical *E. coli* isolates. In addition, Ranjbar et al. (2018) reported *tetA* (76.56%), *tetB* (20.31%), *cat1* (18.75%) and *cmlA* (1.50%) in *E. coli* O157 and non-O157 serogroups from milk. Another study reported high detection of *tetA* and *tetB* in *E. coli* isolated from urinary infection patients, ruminants and donkey raw milk (Momtaz et al., 2012, 2013c). Similar to a previous report (Olowe et al., 2013), none of the isolates in this study harbored the *tetW*, *amp*, *cml*A, and *kan* genes.

In conclusion, to the best of our knowledge this is the first study to report the occurrence of *E. coli* O177 strain in cattle, especially in South Africa. In this study, the search for virulence determinants in aEPEC clearly revealed that a majority of strains harbored DNA sequences that encode known virulence-associated determinants of other pathogenic *E. coli* such as O157 and non-O157 strains. In addition, *E. coli* O177 strains from this study displayed high levels of resistance to aminoglycoside antibiotic group thus have the potential to pose a public health concern to humans. Indeed, the fact that all aEPEC strains in this study expressed a variety of tEPEC virulence determinants supports the case for continued efforts to conduct a large scale study designed to determine the phylogenetic homology among aEPEC isolates from different sources. Furthermore, whole genome sequencing of *E. coli* O177 is required in

order to understand the complete pathogenic determinants of this serogroup.

DATA AVAILABILITY STATEMENT

The datasets generated for this study can be found in the NCBI.

AUTHOR CONTRIBUTIONS

VM and CA contributed to project conception and contributed reagents, materials, and analysis tools. PM, VM, and CA designed the experiments. PM performed the experiments. All authors contributed to manuscript revision and read and approved the submitted version.

FUNDING

This research was supported financially by the National Research Foundation (Grant No. 112543) and the North-West University Postgraduate Bursary.

ACKNOWLEDGMENTS

The authors wish to thank Mr. BJ Morapedi and Dr. A Kumar for their assistance with this project.

REFERENCES

Alonso, C. A., Mora, A., Díaz, D., Blanco, M., González-Barrio, D., Ruiz-Fons, F., et al. (2017). Occurrence and characterization of *stx* and/or *eae*-apositive *Escherichia coli* isolated from wildlife, including a typical EPEC strain from a wild boar. *Vet. Microbiol.* 207, 69–73. doi: 10.1016/j.vetmic.2017.05.028

Altschul, S. F., Madden, T. L., Schäffer, A. A., Zhang, J., Zhang, Z., Miller, W., et al. (1997). Gapped BLAST and PSI-BLAST: a new generation of protein database search programs. *Nucleic Acids Res.* 25, 3389–3402. doi: 10.1093/nar/25.17.3389

Álvarez-Suárez, M. E., Otero, A., García-López, M. L., Dahbi, G., Blanco, M., Mora, A., et al. (2016). Genetic characterization of Shiga toxin-producing *Escherichia coli* (STEC) and atypical enteropathogenic *Escherichia coli* (EPEC) isolates from goat's milk and goat farm environment. *Int. J. Food Microbiol.* 236, 148–154. doi: 10.1016/j.ijfoodmicro.2016.07.035

Anbazhagan, D., Mui, W. S., Mansor, M., Yan, G. O., Yusof, M. Y., and Sekaran, S. D. (2011). Development of conventional and real-time multiplex PCR assays for the detection of nosocomial pathogens. *Braz. J. Microbiol.* 42, 448–458. doi: 10.1590/S1517-83822011000200006

Ateba, C. N., and Bezuidenhout, C. C. (2008). Characterisation of *Escherichia coli* O157strains from humans, cattle, and pigs in the North-West Province, South Africa. *Int. J. Food Microbiol.* 128, 181–188. doi: 10.1016/j.ijfoodmicro.2008.08.011

Ateba, C. N., and Mbewe, M. (2011). Detection of *Escherichia coli* O157: H7 virulence genes in isolates from beef, pork, water, human, and animal species in the northwest province, South Africa: public health implications. *Res. Microbiol.* 162, 240–248. doi: 10.1016/j.resmic.2010.11.008

Ateba, C. N., and Mbewe, M. (2013). Determination of the genetic similarities of fingerprints from *Escherichia coli* O157:H7 isolated from different sources in the North West Province, South Africa using ISR, BOXAIR, and REP-PCR analysis. *Microbiol. Res.* 168, 438–446. doi: 10.1016/j.micres.2013.02.003

Ateba, C. N., and Mbewe, M. (2014). Genotypic characterization of *Escherichia coli O*157:H7isolates from different sources in the north-west province, South Africa, using enterobacterial repetitive intergenic consensus PCR analysis. *Int. J Mol. Sci.* 15, 9735–9747. doi: 10.3390/ijms15069735

Bauer, A. W., Kirby, W. M., Sherris, J. C., and Turck, M. (1966). Antibiotic susceptibility testing by a standardized single disk method. *Am. J. Clin. Pathol.* 45, 493–496. doi: 10.1093/ajcp/45.4_ts.493

Bergeron, S., Boopathy, R., Nathaniel, R., Corbin, A., and LaFleur, G. (2015). Presence of antibiotic resistant bacteria and antibiotic resistance genes in raw source water and treated drinking water. *Int. Biodeter. Biodegrad.* 102, 370–374. doi: 10.1016/j.ibiod.2015.04.017

Beutin, L., Kong, Q., Feng, L., Wang, Q., Krause, G., Leomil, L., et al. (2005). Development of PCR assays targeting the genes involved in synthesis and assembly of the new *Escherichia coli* O174 and O177 O antigens. *J. Clin. Microbiol.* 43, 5143–5149. doi: 10.1128/JCM.43.10.5143-5149.2005

Bibbal, D., Um, M. M., Kérourédan, M., Dupouy, V., Toutain, P. L., Bousquet-Mélou, A., et al. (2017). Mixing of Shiga toxin-producing and enteropathogenic *Escherichia coli* in a wastewater treatment plant receiving city and slaughterhouse wastewater. *Int. J. Hyg. Environ. Health* 221, 355–363. doi: 10.1016/j.ijheh.2017.12.009

Canizalez-Roman, A., Gonzalez-Nuñez, E., Vidal, J. E., Flores-Villaseñor, H., and León-Sicairos, N. (2013). Prevalence and antibiotic resistance profiles of diarrheagenic *Escherichia coli* strains isolated from food items in northwestern Mexico. *Int. J. Food Microbiol.* 164, 36–45. doi: 10.1016/j.ijfoodmicro.2013.03.020

Cha, W., Fratamico, P. M., Ruth, L. E., Bowman, A. S., Nolting, J. M., Manning, S. D., et al. (2018). Prevalence and characteristics of Shiga toxin-producing *Escherichia coli* in finishing pigs: Implications on public health. *Int. J. Food Microbiol.* 264, 8–15. doi: 10.1016/j.ijfoodmicro.2017.10.017

Clinical and Laboratory Standards Institute (2016). *Performance Standards for Antimicrobial Susceptibility Testing, 26th Edn*. CLSI supplement M100S. Wayne, PA: Clinical and Laboratory Standards Institute.

Farrokh, C., Jordan, K., Auvray, F., Glass, K., Oppegaard, H., Raynaud, S., et al. (2013). Review of Shiga-toxin-producing *Escherichia coli* (STEC) and their significance in dairy production. *Int. J. Food Microbiol.* 162, 190–212. doi: 10.1016/j.ijfoodmicro.2012.08.008

Ghanbarpour, R., Askari, N., Ghorbanpour, M., Tahamtan, Y., Mashayekhi, K., Afsharipour, N., et al. (2017). Genotypic analysis of virulence genes and antimicrobial profile of diarrhoeagenic *Escherichia coli* isolated from diseased lambs in Iran. *Trop. Anim. Health Prod.* 49, 591–597. doi: 10.1007/s11250-017-1234-7

González, J., Cadona, J. S., Sanz, M., Bustamante, A. V., and Sanso, A. M. (2017). Molecular characterization of diarrheagenic *Escherichia coli* isolated from vegetables in Argentina. *Int. J. Food Microbiol.* 261, 57–61. doi: 10.1016/j.ijfoodmicro.2017.09.021

He, X., Quiñones, B., Mcmahon, S., and Mandrell, R. E. (2012). A single-step purification and molecular characterization of functional Shiga-toxin 2 variants from pathogenic *Escherichia coli*. *Toxins* 4, 487–504. doi: 10.3390/toxins4070487

Hemeg, H. A. (2018). Molecular characterization of antibiotic resistant *Escherichia coli* isolates recovered from food samples and outpatient Clinics, AKA. *Saudi J. of Biol. Sci.* 25, 928–931. doi: 10.1016/j.sjbs.2018.01.016

Hemmatinezhad, B., Khamesipour, F., Mohammadi, M., Safarpoor Dehkordi, F., and Mashak, Z. (2015). Microbiological investigation of O-serogroups, virulence factors and antimicrobial resistance properties of shiga toxin-producing *Escherichia coli* isolated from ostrich, turkey and quail meats. *J. Food Safety* 35, 491–500. doi: 10.1111/jfs.12199

Horcajo, P., Domínguez-Bernal, G., de La Fuente, R., Ruiz-Santa-Quiteria, J. A., Blanco, J. E., Blanco, M., et al. (2012). Comparison of ruminant and human attaching and effacing *Escherichia coli* (AEEC) strains. *Vet. Microbiol.* 155, 341–348. doi: 10.1016/j.vetmic.2011.08.034

Hudson, J. A., Frewer, L. J., Jones, G., Brereton, P. A., Whittingham, M. J., and Stewart, G. (2017). The agri-food chain and antimicrobial resistance: a review. *Trends Food Sci. Techn.* 69, 131–147. doi: 10.1016/j.tifs.2017.09.007

Ingle, D. J., Tauschek, M., Edwards, D. J., Hocking, D. M., Pickard, D. J., Azzopardi, K. I., et al. (2016). Evolution of atypical enteropathogenic *E. coli*

by repeated acquisition of LEE pathogenicity island variants. *Nat Microbiol.* 1:15010. doi: 10.1038/nmicrobiol.2015.10

Iwu, C. J., Iweriebor, B. C., Obi, L. C., and Okoh, A. I. (2016). Occurrence of non-O157 Shiga toxin-producing *Escherichia coli* in two commercial swine farms in the Eastern Cape Province, South Africa. *Comp. Immunol. Microbiol. Infect. Dis.* 44, 48–53. doi: 10.1016/j.cimid.2015.12.004

Jajarmi, M., Fooladi, A. A., Badouei, M. A., and Ahmadi, A. (2017). Virulence genes, Shiga toxin subtypes, major O-serogroups, and phylogenetic background of Shiga toxin-producing *Escherichia coli* strains isolated from cattle in Iran. *Microb. Pathog.* 109, 274–279. doi: 10.1016/j.micpath.2017.05.041

Kaper, J. B., Nataro, J. P., and Mobley, H. L. (2004). Pathogenic *Escherichia coli*. *Nature Rev. Microbiol.* 2, 123–140. doi: 10.1038/nrmicro818

Karch, H., Meyer, T., Rüssmann, H., and Heesemann, J. (1992). Frequent loss of Shiga-like toxin genes in clinical isolates of *Escherichia coli* upon subcultivation. *Infect. Immun.* 60, 3464–3467.

Kase, J. A., Maounounen-Laasri, A., Son, I., Lin, A., and Hammack, T. S. (2015). Comparison of eight different agars for the recovery of clinically relevant non-O157 Shiga toxin-producing *Escherichia coli* from baby spinach, cilantro, alfalfa sprouts and raw milk. *Food Microbiol.* 46, 280–287. doi: 10.1016/j.fm.2014.08.020

Malik, A., Nagy, B., Kugler, R., and Szmolka, A. (2017). Pathogenic potential and virulence genotypes of intestinal and faecal isolates of porcine post-weaning enteropathogenic *Escherichia coli*. *Res. Vet. Sci.* 115, 102–108. doi: 10.1016/j.rvsc.2017.02.002

Martins, F. H., Guth, B. E., Piazza, R. M., Elias, W. P., Leão, S. C., Marzoa, J., et al. (2016). Lambs are an important source of atypical enteropathogenic *Escherichia coli* in southern Brazil. *Vet. Microbiol.* 196, 72–77. doi: 10.1016/j.vetmic.2016.10.009

Momtaz, H., Dehkordi, F., Hosseini, M. J., Sarshar, M., and Heidari, M. (2013b). Serogroups, virulence genes and antibiotic resistance in Shiga toxin-producing *Escherichia coli* isolated from diarrheic and non-diarrheic pediatric patients in Iran. *Gut pathogens* 5:39. doi: 10.1186/1757-4749-5-39

Momtaz, H., Dehkordi, F. S., Rahimi, E., Ezadi, H., and Arab, R. (2013a). Incidence of Shiga toxin-producing *Escherichia coli* serogroups in ruminant's meat. *Meat Sci.* 95, 381–388. doi: 10.1016/j.meatsci.2013.04.051

Momtaz, H., Farzan, R., Rahimi, E., Safarpoor Dehkordi, F., and Souod, N. (2012). Molecular characterization of Shiga toxin-producing *Escherichia coli* isolated from ruminant and donkey raw milk samples and traditional dairy products in Iran. *Sci. World J.* 2012:231342. doi: 10.1100/2012/231342

Momtaz, H., Karimian, A., Madani, M., Dehkordi, F., Ranjbar, R., Sarshar, M., et al. (2013c). Uropathogenic *Escherichia coli* in Iran: serogroup distributions, virulence factors and antimicrobial resistance properties. *Ann. Clin. Microbiol. Antimicrob.* 12:8. doi: 10.1186/1476-0711-12-8

Olowe, O. A., Idris, O. J., and Taiwo, S. S. (2013). Prevalence of TET genes mediating tetracycline resistance in *Escherichia coli* clinical isolates in Osun State, Nigeria. *Eur. J. Microbiol. Immunol.* 3, 135–140. doi: 10.1556/EuJMI.3.2013.2.7

Otero, V., Rodríguez-Calleja, J.-M., Otero, A., García-López, M.-L., and Santos, J. A. (2013). Genetic characterization of atypical enteropathogenic *Escherichia coli* isolates from ewes' milk, sheep farm environments, and humans by multilocus sequence typing and pulsed-field gel electrophoresis. *Appl. Environ. Microbiol.* 79, 5864–5869. doi: 10.1128/AEM.01809-13

Paton, A. W., and Paton, J. C. (1998). Detection and characterization of shiga toxigenic *Escherichia coli* by using multiplex PCR assays for stx1, stx2, eaeA, enterohemorrhagic *E. coli* hlyA, rfbO111, and rfbO157. *J. Clin. Microbiol.* 36, 598–602.

Qiao, M., Ying, G. G., Singer, A. C., and Zhu, Y. G. (2017). Review of antibiotic resistance in China and its environment. *Environ. Int.* 110, 160–172. doi: 10.1016/j.envint.2017.10.016

Ranjbar, R., Dehkordi, F. S., Shahreza, M. H., and Rahimi, E. (2018). Prevalence, identification of virulence factors, O-serogroups and antibiotic resistance properties of Shiga-toxin producing *Escherichia coli* strains isolated from raw milk and traditional dairy products. *Antimicrob. Resist. Infect. Control* 7:53. doi: 10.1186/s13756-018-0345-x

Ranjbar, R., Masoudimanesh, M., Dehkordi, F. S., Jonaidi-Jafari, N., and Rahimi, E. (2017). Shiga (Vero)-toxin producing *Escherichia coli* isolated from the hospital foods; virulence factors, o-serogroups and antimicrobial resistance properties. *Antimicrob. Resist. Infect. Control* 6:4. doi: 10.1186/s13756-016-0163-y

Rantsiou, K., Alessandria, V., and Cocolin, L. (2012). Prevalence of Shiga toxin-producing *Escherichia coli* in food products of animal origin as determined by molecular methods. *Int. J. Food Microbiol.* 154, 37–43. doi: 10.1016/j.ijfoodmicro.2011.12.010

Ryu, S. H., Lee, J. H., Park, S. H., Song, M. O., Park, S. H., Jung, H. W., et al. (2012). Antimicrobial resistance profiles among *Escherichia coli* strains isolated from commercial and cooked foods. *Int. J. Food Microbiol.* 159, 263–266. doi: 10.1016/j.ijfoodmicro.2012.09.001

Samra, Z. Q., Naseem, M., Khan, S. J., Nadia, D., and Athar, M. A. (2009). PCR targeting of antibiotic resistant bacteria in public drinking water of Lahore metropolitan, Pakistan. *BioMed. Environ. Sci.* 22, 458–463. doi: 10.1016/S0895-3988(10)60002-5

SAS (2010). *Users Guide: Statistics*. Version 9.4. Cary, NC: SAS Institute.

Shahrani, M., Dehkordi, F. S., and Momtaz, H. (2014). Characterization of *Escherichia coli* virulence genes, pathotypes and antibiotic resistance properties in diarrheic calves in Iran. *Biol. Res.* 47:28. doi: 10.1186/0717-6287-47-28

Srinivasan, V., Gillespie, B. E., Lewis, M. J., Nguyen, L. T., Headrick, S. I., Schukken, Y. H., et al. (2007). Phenotypic and genotypic antimicrobial resistance patterns of *Escherichia coli* isolated from dairy cows with mastitis. *Vet. Microbiol.* 124, 319–328. doi: 10.1016/j.vetmic.2007.04.040

Tennant, S. M., Tauschek, M., Azzopardi, K., Bigham, A., Bennett-Wood, V., Hartland, E. L., et al. (2009). Characterisation of atypical enteropathogenic *E. coli* strains of clinical origin. *BMC Microbiol.* 9:117. doi: 10.1186/1471-2180-9-117

Toro, M., Rivera, D., Jiménez, M. F., Díaz, L., Navarrete, P., and Reyes-Jara, A. (2018). Isolation and characterization of non-O157 Shiga toxin-producing *Escherichia coli* (STEC) isolated from retail ground beef in Santiago, Chile. *Food Microbiol.* 75, 55–60. doi: 10.1016/j.fm.2017.10.015

Trabulsi, L. R., Keller, R., and Gomes, T. A. (2002). Typical and atypical Enteropathogenic *Escherichia coli*. *Emerg. Infect. Dis.* 8, 508–513. doi: 10.3201/eid0805.010385

Ye, J., Coulouris, G., Zaretskaya, I., Cutcutache, I., Rozen, S., and Madden, T. L. (2012). Primer-BLAST: a tool to design target-specific primers for polymerase chain reaction. *BMC Bioinformat.* 13:134. doi: 10.1186/1471-2105-13-134

Conflict of Interest: The authors declare that the research was conducted in the absence of any commercial or financial relationships that could be construed as a potential conflict of interest.

frontiers in Cellular and Infection Microbiology

ORIGINAL RESEARCH
published: 27 November 2019
doi: 10.3389/fcimb.2019.00404

Characterization of a Novel Conjugative Plasmid in *Edwardsiella piscicida* Strain MS-18-199

Hossam Abdelhamed[1]*, *Reshma Ramachandran*[1], *Ozan Ozdemir*[1], *Geoffrey Waldbieser*[2] *and Mark L. Lawrence*[1]

[1] College of Veterinary Medicine, Mississippi State University, Mississippi State, MS, United States, [2] Warmwater Aquaculture Research Unit, Thad Cochran National Warmwater Aquaculture Center (USDA-ARS), Stoneville, MS, United States

Edwardsiella piscicida is a pathogenic bacterium responsible for significant losses in important wild and cultured fish species. *E. piscicida* strain MS-18-199 recovered from a diseased hybrid catfish from East Mississippi and showed resistance to florfenicol, chloramphenicol, oxytetracycline, doxycycline, erythromycin, tetracycline, azitromycin, spectinomycin, sulfonamide, and bacitracin. To explore the mechanisms of resistance in *E. piscicida* strain MS-18-199, genomic DNA was extracted and subjected to whole genome sequencing (WGS) using a combination of long (Oxford Nanopore) and short (Illumina) reads. The genome of strain MS-18-199 revealed a novel plasmid named pEPMS-18199. The 117,448 bp plasmid contains several antimicrobial resistance (AMR) elements/genes, including florfenicol efflux pump (*floR*), tetracycline efflux pump (*tetA*), tetracycline repressor protein (*tetR*), sulfonamide resistance (*sul2*), aminoglycoside O-phosphotransferase *aph(6)*-Id (*strB*), and aminoglycoside O-phosphotransferase *aph(3)*-Ib (*strA*). Two genes, *arsA* and *arsD*, that encode protein components related to transport/resistance to arsenic were also found in pEPMS-18199. In addition, pEPMS-18199 carried twelve conjugative transfer genes (*tra*), eight transposases and insertion elements, two plasmid stability proteins, two replication proteins, and three partitioning proteins (*par* system). Results from mobilization and stability experiments revealed that pEPMS-18199 is highly stable in the host cell and could be transferred to *Escherichia coli* and *Edwardsiella ictaluri* by conjugation. To our knowledge, this is the first detection of a multidrug resistance (MDR) conjugative plasmid in *E. piscicida* in the United States. Careful tracking of this plasmid in the aquaculture system is warranted. Knowledge regarding the molecular mechanisms of AMR in aquaculture is important for antimicrobial stewardship.

Keywords: antimicrobial resistance, mobile genetic element, *Edwardsiella*, aquaculture, genome sequence

OPEN ACCESS

Edited by:
Xiao-Peng Xiong, Sanford-Burnham Institute for Medical Research, United States

Reviewed by:
Zhijie Xia, Sanford Burnham Prebys Medical Discovery Institute, United States
Jingting Yu, Salk Institute for Biological Studies, United States

***Correspondence:**
Hossam Abdelhamed
abdelhamed@cvm.msstate.edu

Specialty section:
This article was submitted to Molecular Bacterial Pathogenesis, a section of the journal Frontiers in Cellular and Infection Microbiology

Received: *31 July 2019*
Accepted: *12 November 2019*
Published: *27 November 2019*

Citation:
Abdelhamed H, Ramachandran R, Ozdemir O, Waldbieser G and Lawrence ML (2019) Characterization of a Novel Conjugative Plasmid in Edwardsiella piscicida Strain MS-18-199. Front. Cell. Infect. Microbiol. 9:404. doi: 10.3389/fcimb.2019.00404

INTRODUCTION

Edwardsiella piscicida, a member of family *Enterobacteriaceae*, is a motile Gram negative and facultative anaerobic bacterium (Ewing et al., 1965). The description of *E. piscicida* (previously identified as *Edwardsiella tarda*) resulted from a reclassification of diverse isolates obtained from diseased fish (Abayneh et al., 2013). Besides its importance as a pathogen of aquatic species, *E. piscicida* has been isolated from a wide range of hosts (including birds, reptiles, and humans)

from a broad geographical range and ecological niches (Camus et al., 2016; Buján et al., 2018b). At present, *E. piscicida* is the etiologic agent of edwardsiellosis and is responsible for high mortality rates in several fish species (more than 20 fish species as hosts) (Abayneh et al., 2013; Camus et al., 2016; Loch et al., 2017; Buján et al., 2018b). Common clinical signs associated with edwardsiellosis include exophthalmia, abdominal distension, skin hemorrhages, mild to moderate dermal ulcerations, discolorations on the fish surface, and erratic swimming (Buján et al., 2018b).

Commercial production of channel catfish (*Ictalurus punctatus*) and channel catfish × blue catfish (*I. furcatus*) hybrids dominates aquaculture in the United States accounting for $360 million in 2018, and the majority of production occurs in Mississippi (USDA, 2019). Loss to disease and feed cost are the major factors that influence profitable catfish aquaculture (Wagner et al., 2002). Approximately 45% of inventory losses on catfish farms are attributable to infectious diseases, of which 60% are associated with single or mixed bacterial infections (Hawke and Khoo, 2004). *Edwardsiella* species continue to be the bacterial pathogen of primary concern in catfish aquaculture in the southeastern United States (Hawke et al., 1981, 2013). There is a trend toward increased incidence and prevalence of *E. piscicida* septicemia in US catfish aquaculture (Griffin et al., 2019). The recent reclassification and review of archival data indicated that *E. piscicida* is more problematic in catfish aquaculture than *E. tarda* (Buján et al., 2018b; Griffin et al., 2019). Moreover, recent genotypic analysis of bacterial isolates historically classified as *E. tarda* concluded that many isolates previously classified as *E. tarda* actually belong to the species *E. piscicida* (Reichley et al., 2017; Buján et al., 2018a).

Because no definite vaccine is available, antimicrobial (AM) medicated-feeds are the current available strategy to control the bacterial diseases caused by *E. piscicida* and other fish pathogens (Reichley et al., 2017; Buján et al., 2018b). Terramycin (oxytetracycline), Romet-30 (sulfadimethoxine-ormetoprim), and Aquaflor (florfenicol) are three AM agents approved by the FDA for use in medicated-feed to control bacterial infections in cultured fish (Bowker et al., 2010). Although AM use is highly restricted and strongly regulated in the United States aquaculture, a multidrug resistant (MDR) strain of *E. piscicida* strain MS-18-199 (unpublished data) has been recovered from moribund hybrid catfish submitted to Aquatic Diagnostic Laboratories at College of Veterinary Medicine Mississippi State University (CVM/MSU). The mechanisms that drive resistance in this isolate is unclear. Here, we describe the genetic feature of a large conjugative plasmid identified in *E. piscicida*. Moreover, we evaluated plasmid mobility and stability. Characterizing a plasmid carrying resistance determinants, especially in clinical isolates, will increase our understanding of the flow of resistance.

MATERIALS AND METHODS

Bacterial Isolates and Growth Condition

Edwardsiella piscicida strain MS-18-199 was isolated from moribund hybrid catfish clinical case presented to the Fish Diagnostic Laboratory at CVM/MSU. The diseased fish exhibited large ulceration on the dorsal head with bone erosion and scant yellow ascites. The internal examination of catfish revealed moderate granulomatous hepatitis. The initial presumptive diagnosis based on clinical signs was *E. piscicida* infection. Pure colonies with identical morphology were isolated from posterior kidney on Mueller Hinton agar (Becton, Dickinson and Company, Franklin Lakes, NJ, USA) supplemented with 5% defibrinated sheep blood (HemoStat Laboratories, Dixon, CA, USA) at 30°C. A stock culture was stored at −80°C in 20% glycerol. The isolate was confirmed phenotypically as *E. piscicida* infection. The API 20E profile of *E. piscicida* strain MS-18-199 is present in **Supplementary Table 1**. *Escherichia coli* J53Az^r (resistant to sodium azide) (Martinez-Martinez et al., 1998), *E. ictaluri* 93-146 with pAK*gfplux1* (ampicillin resistant) (Karsi and Lawrence, 2007), and *Aeromonas hydrophila* ML09-119 (ampicillin resistant) (Tekedar et al., 2013b) were used as a recipient for conjugation. *Edwardsiella* species were cultured in brain heart infusion (BHI) media (Difco, Sparks, MD, USA) and incubated at 30°C with orbital shaking (250 rpm). *E. coli* and *A. hydrophila* strains were cultured in Luria–Bertani (LB) agar and broth (Becton Dickinson) at 30°C and 37°C, respectively.

Antimicrobial Susceptibility

The susceptibilities of *E. piscicida* strain MS-18-199 to 23 AMs were determined using Kirby-Bauer disk diffusion assays according to CDC guidelines, as described by the Clinical and Laboratory Standards Institute (CLSI) (CLSI, 2010). The tested AMs included: florfenicol FFC30 (30 μg); doxycycline D30 (30 μg); erythromycin E15 (15 μg); oxytetracycline T30 (30 μg); gentamicin GM10 (10 μg); nalidixic acid NA30 (30 μg); chloramphenicol C30 (30 μg); sulfamethoxazole (25 μg); trimethoprim-sulfamethoxazole (1.25 and 23.75 μg); tetracycline TE30 (30 μg); azitromycin AZM15 (15 μg); ceftriaxone CRO30 (30 μg); amoxicillin/clavulanic acid AMC30 (30 μg); ciprofloxacin CIP5 (5 μg); streptomycin S10 (10 μg); spectinomycin SPT100 (100 μg); ampicillin AM10 (10 μg); cefpodoxime CPD10 (10 μg); ceftiofur XNL30 (30 μg); penicillin P10 (10 μg); enrofloxacin ENO 5 (5 μg); bacitracin B10 (10 μg); and novobiocin NB30 (30 μg). Bacterial strains were reported as susceptible, intermediate, or resistant based on inhibition zone size as published in the CLSI standard (CLSI, 2010).

DNA Isolation

A single colony of *E. piscicida* strain MS-18-199 was grown overnight at 30°C in BHI. Overnight culture was pelleted by centrifugation, and genomic DNA (gDNA) isolated using standard ethanol precipitation following phenol: chloroform: isoamyl alcohol (24:25:1 v/v; AppliChem) treatment, as previously described (Psifidi et al., 2010; Green and Sambrook, 2017). The quality of extracted gDNA was assessed using an Agilent 2100 Bioanalyzer (High sensitivity DNA chip), and a Nanodrop spectrophotometer. Genomic DNA with an ultraviolet absorbance 260/280 of ∼ 1.8 and absorbance 260/230 of 2.0–2.2 was used for library preparation.

Whole Genome Sequence of *E. piscicida* Strain MS-18-199

The genome of *E. piscicida* strain MS-18-199 was sequenced using long and short read technologies. Long reads were produced on a GridION sequencer (Oxford Nanopore Technologies, Oxford, UK) from 400 ng genomic DNA using the RAD004 kit on a v9.4.1 flow cell. The nanopore sequences were filtered to an average quality of 10 (90% accuracy) with 100 bp cropped from each end and minimum length of 700 bp (De Coster et al., 2018) to produce 2.4 Gb of sequence from 185,481 reads ranging from 700 bp to 191 kb (average length 13.4 kb). A genomic DNA library was prepared using the Nextera XT DNA kit (Illumina Inc., San Diego, CA, USA) and 150 bp paired reads were sequenced on the Illumina MiSeq4000 Platform (Novogene Corporation, Sacramento, CA). The Illumina sequence was filtered using Trimmomatic v0.38 (Bolger et al., 2014) using the parameters "LEADING:30 TRAILING:30 SLIDINGWINDOW:4:30 MINLEN:50" to produce 1.6 Gb sequence in 5.5 M paired reads.

Genome Assembly

The nanopore sequence was assembled *de novo* [Canu v1.7; Koren et al., 2017] into two contigs of 3.9 Mb and 230 kb. The linear contigs were manually trimmed at the sequence overlap within the putative circular genome and plasmid, then sequence from the 3′ end of each contig (1 Mb and 100 kb, respectively) was cut and moved to the 5′ end of each respective contig. The filtered nanopore reads were mapped to these contigs and visualized using the IGV viewer (Robinson et al., 2011) to validate the sequence contiguity and therefore the circular nature of the genome and plasmid. The consensus sequences were corrected using four iterations of Nanopolish v.10.2 (Loman et al., 2015) using the filtered Nanopore sequences, then corrected with two iterations of Pilon v1.2.2 (Walker et al., 2014) using the filtered Illumina reads.

Genome Annotation and Function Analysis of Strain MS-18-199

The assembled genome was submitted to the National Center for Biotechnology Information (NCBI) database (http://www.ncbi.nlm.nih.gov/) prokaryotic genome annotation pipeline. Antimicrobial resistance (AMR) genes were automatically annotated as resistance genes at the NCBI. Each annotated resistant protein was searched against NCBI database using the best match from a blastn search (NCBI BLAST v2.2.27+). Further confirmation was performed by blast search against the Antibiotic Resistance Database (ARDB) (http://ardb.cbcb.umd.edu/) (Balabanov et al., 2012) and Comprehensive Antibiotic Resistance Database (CARD) (https://card.mcmaster.ca/) (McArthur et al., 2013). The NCBI BLAST results were used to confirm the annotation of insertion sequence, replication, and conjugative proteins. Gene function was predicted using the Gene Rapid Annotation Subsystem Technology (RAST) server (http://rast.nmpdr.org/) (Overbeek et al., 2014).

Conjugation Experiment

Plasmid mobility was evaluated by conjugation experiments on filter paper placed on agar plates as previously described (Abdelhamed et al., 2018a). *E. piscicida* strain MS-18-199 was used as a donor strain, and *E. coli* J53, *E. ictaluri*, and *A. hydrophila* ML09-119 were used as recipient strains. Briefly, overnight cultures of donor and recipient cells were diluted and incubated at 30°C with shaking until they reached logarithmic phase. Bacteria were harvested by centrifugation at 12,000 rpm, mixed into 1:1 ratio, placed onto filter paper on agar plate, and incubated at 30°C overnight. After mating, bacteria were collected, washed, diluted, and plated on BHI plates containing sodium azide (100 μg/ml) or ampicillin (100 μg/ml) for counter selection, and florfenicol (30 μg/ml) and tetracycline (30 μg/ml) to select for resistance. The transconjugant colonies were counted and the mobilization efficiency was estimated as the number of transconjugants CFU (colony-forming unit) per recipient CFU (Zeng et al., 2015). The resistance phenotypes of the transconjugant colonies were evaluated using the disc diffusion assay as described in the above section. Further confirmation of plasmid carriage in the transconjugant colonies was performed by PCR amplification of florfenicol resistance using FlorR_F (CTGATGGCTCCTTTCGACAT) and FlorR_R (AGACGACT GGCGACTTATCG) primers.

Plasmid Stability Assays

A stability test of the plasmid in *E. piscicida* strain MS-18-199 was conducted as previously described (Moleres et al., 2015). Briefly, a single colony of *E. piscicida* strain MS-18-199 harboring the plasmid was inoculated in BHI without antibiotic and grown overnight at 30°C. This culture was passaged by serial 1:100 dilutions in 5 ml BHI on consecutive days for up to 20 days. In each subculture step, bacteria were plated on BHI agar, and the proportion of plasmid-containing cells was deduced by replica inoculation of 100 colonies on BHI broth and BHI broth containing florfenicol. The number of colonies carrying the plasmid was calculated as the percentage of florfenicol-resistant colonies in every subculture/total number of colonies replicated each subculture (Moleres et al., 2015).

Plasmid Copy Number

Plasmid copy numbers in *E. piscicida* strain MS-18-199 were determined using quantitative real-time PCR (qRT-PCR) as previously described (Botts et al., 2017). Briefly, total genomic DNA (gDNA) was extracted from early stationary phase cells using the Genomic DNA Mini Kit (IBI Scientific), as per manufacturer's instructions. The gDNA was quantified then serially diluted two-fold and used as the qRT-PCR template. qRT-PCR was performed in triplicate using SYBR Green Real-time PCR master mix (Roche Diagnostic GmbH, Mannheim, Germany). Chromosomal and plasmid DNA were quantified using primers targeting L-asparaginase 1 gene of *E. piscicida* strain MS-18-199 (locus tag: EVK84_00005; FP: ACCGATACCATGGCGTTTAC; RP: CCAGATAGAGGGCG TTTAACAG), which exists on the chromosome as a single copy, and the single-copy *floR* gene encoded on the plasmid

TABLE 1 | Antibiotic resistance patterns of *Edwardsiella piscicida* strain MS-18-199.

Antimicrobial agents	Disk content (μg)	Diameter of inhibition zone (mm)	Sensitivity
Florfenicol FFC30	30	0	R
Doxycycline D30	30	0	R
Erythromycin E15	15	0	R
Oxytetracycline T30	30	0	R
Gentamicin GM10	10	26	S
Nalidixic acid NA30	30	37	S
Chloramphenicol C30	30	0	R
Sulfamethoxazole	25	0	R
Sulphamethoxazole trimethoprim SXT	25	26	S
Tetracycline TE30	30	0	R
Azitromycin AZM15	15	0	R
Ceftriaxone CRO30	30	35	S
Amoxicillin/clavulanic acid AMC30	30	27	S
Ciprofloxacin CIP5	5	40	S
Streptomycin S10	10	24	S
Spectinomycin SPT100	100	0	R
Ampicillin AM10	10	27	S
Cefpodoxime CPD10	10	23	S
Ceftiofur XNL30	30	35	S
Penicillin P10	10	21	S
Enrofloxacin ENO 5	15	38	S
Bacitracin B10	10	0	R
Novobiocin NB30	30	18	S

(locus tag: EVK84_18305; FP: TGATCGTGACAACCCGTTTC; RP: GATGAAGGTGAGGAATGACGG).

RESULTS

Resistance Phenotypes of *E. piscicida* Strain MS-18-199

The susceptibility pattern of *E. piscicida* strain MS-18-199 to 23 AM agents are shown in **Table 1**. Strain MS-18-199 was resistant to florfenicol, chloramphenicol, oxytetracycline, doxycycline, erythromycin, tetracycline, azitromycin, spectinomycin, sulfamethoxazole, and bacitracin.

Basic Data of *E. piscicida* Strain MS-18-199 Genome

We conducted whole genome sequencing and assembly to gain further insight on the molecular mechanism of resistance of *E. piscicida* strain MS-18-199. The genome of strain MS-18-199 consisted of one circular chromosome and one circular plasmid, and both sequences have been submitted to GenBank under accession numbers CP035668.1 and CP035669.1, respectively. The 3,905,600 bp genome contained 59.47% GC content and 3,758 genes, including 3,631 coding sequences (CDS), 83 pseudogenes, and 127 RNAs [including 25 rRNAs (9, 8, and 8 for 5S, 16S, and 23S, respectively), 97 tRNAs, and 5 ncRNAs]. The complete genome of *E. piscicida* strain MS-18-199 shared 99.40% average nucleotide identity (ANI) with *Edwardsiella piscicida* C07-08 (Tekedar et al., 2013a), and 99.35% with *Edwardsiella piscicida* isolate S11-285 (Reichley et al., 2016).

Identification of pEPMS-18199 Plasmid in *E. piscicida* Strain MS-18-199

A circular plasmid was identified from the assembly of long sequencing reads from *E. piscicida* strain MS-18-199. The plasmid pEPMS-18199 is 117,448 bp with an average 47.34% GC content, ∼12% lower than the genome. Genome annotation revealed 124 open reading frames (ORFs), of which five were associated with plasmid DNA replication and partition, 12 with DNA transfer, 13 with DNA-restriction and site-specific DNA methylation, eight with family transposase, eight with antimicrobial resistance, and 44 with unknown function "hypothetical protein" (**Figure 1A**). A BLASTN search revealed pEPMS-18199 was nearly identical (99.97 % identity, ANI 99.94%, and 95% coverage) to 127,046 bp plasmid ET080813 (CP006665.1) isolated from *E. anguillarum* in China (Shao et al., 2015).

Six AMR genes were identified in the pEPMS-18199 sequence, including major facilitator superfamily (MFS) antibiotic efflux pump (*floR*), tetracycline repressor protein (*tetR*), tetracycline resistance protein class A (*tetA*), sulfonamide-resistant dihydropteroate synthase (*sul2*), aminoglycoside O-phosphotransferase *aph(6)*-Id, and aminoglycoside O-phosphotransferase *aph(3″)*-Ib (*strA*) (**Table 2**). Two genes corresponding to proteins predicted to be involved in arsenic resistance were also identified in the pEPMS-18199 sequence; arsenite efflux transporter metallochaperone *arsD* and arsenical pump-driving ATPase *arsA*. All the AMR genes were clustered in one region between 9,052 and 28,696 of pEPMS-18199. This region was flanked upstream and downstream with transposable elements (**Figure 1B**).

The pEPMS-18199 plasmid contains twelve conjugative transfer genes clustered in two regions, designated as Tra1 and Tra2. The Tra1 region is located between sequence coordinates 40,209 and 47,900 and consists of three proteins (TraFHG). The Tra2 region is located between 72,240 and 98,771, and consists of nine proteins (TraI, TraL, TraKBVA, and TraCWU). The pEPMS-18199 plasmid encodes eight transposases and insertion sequences belonging to Tn3-like element TnAs1 family transposase, IS6-like element IS26 family transposase, IS91-like element ISVsa3 family transposase, IS110 family transposase, two Tn3 family transposase, IS6-like element IS26 family transposase, and IS5-like element ISKpn26 family transposase. The plasmid also harbors plasmid stability protein (ParM/StbA family protein) and two plasmid replication proteins. Furthermore, the pEPMS-18199 plasmid encodes additional maintenance proteins including three chromosome partitioning proteins (ParB, ParA, and ParB/RepB family protein).

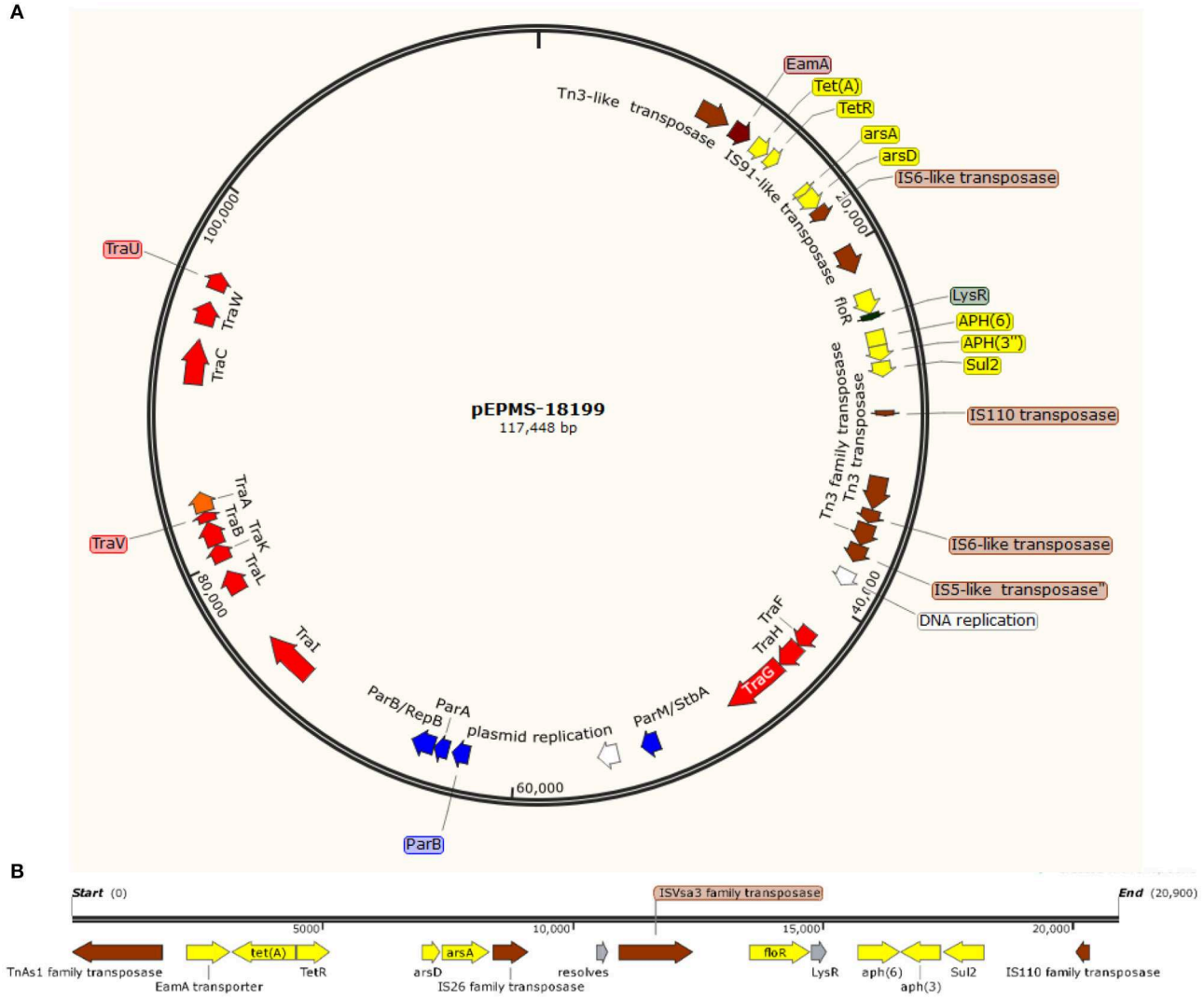

FIGURE 1 | (A) Circular genetic map of the pEPMS-18199 plasmid from *Edwardsiella piscicida* strain MS-18-199. The pEPMS-18199 plasmid carries antibiotic resistance (yellow), transposons and insertion sequences (brown), maintenance/stability protein and partitioning proteins (par system) (blue), DNA replication (white), and conjugative transfer genes (red). **(B)** Antimicrobial resistant cassette regions in pEPMS-18199 plasmid.

General Annotation for pEPMS-18199 Plasmid and *E. piscicida* Strain MS-18-199 Genome

The genomic features of pEPMS-18199 plasmid annotated using RAST revealed that pEPMS-18199 contains 13 proteins encoding for membrane transport, one protein encoding for nucleosides and nucleotides, one protein encoding for protein metabolism, four proteins encoding DNA metabolism, one protein encoding respiration, and three proteins encoding stress response (**Figure 2A**).

The genomic features of chromosome annotated using RAST revealed that *E. piscicida* strain MS-18-199 genome contains 3,551 coding sequences and 497 subsystems (**Figure 2B**). The most represented subsystem features are cofactors, vitamins, prosthetic croups, pigments (294 genes), cell wall and capsule (191), virulence, disease and defense (72), potassium metabolism (30), phages, prophages, transposable elements, plasmids (43), iron acquisition and metabolism (46), membrane transport (99), RNA metabolism (230), nucleosides and nucleotides (113), protein metabolism (277) fatty acids, lipids, and isoprenoids (121), amino acids and derivatives (359), phosphorus metabolism (33), and carbohydrates (384).

Mobilization and Stability of the pEPMS-18199 Plasmid

Successful conjugation mating experiments indicated that the pEPMS-18199 plasmid was capable of being transferred from *E. piscicida* to *E. coli* and *E. ictaluri* with an average efficiency of 6.86×10^{-5} and 6.13×10^{-5} CFU/recipient, respectively. Furthermore, *E. coli* and *E. ictaluri* transconjugants showed the

TABLE 2 | Predicted AMR elements in pEPMS-18199 plasmid using CARD.

ARO Term	AMR gene family	Resistance mechanism	% Identity of matching region	% Length of reference sequence
tetR	Major facilitator superfamily (MFS) antibiotic efflux pump	Tetracycline antibiotic, glycylcycline	52.74	108.17
sul2	Sulfonamide resistant sul	Sulfonamide antibiotic, sulfone antibiotic	100.0	100.00
tet(A)	Major facilitator superfamily (MFS) antibiotic efflux pump	Tetracycline antibiotic	79.39	100.76
floR	Major facilitator superfamily (MFS) antibiotic efflux pump	Phenicol antibiotic	98.76	100.00
APH(3″)-Ib	APH(3″)	Aminoglycoside antibiotic	99.63	100.00
APH(6)-Id	APH(6)	Aminoglycoside antibiotic	99.64	100.00

same pattern of resistance as donor strain. Also, PCRs confirmed the presence of plasmid in transconjugants. Conversely, pEPMS-18199 could not be transferred from *E. piscicida* to *A. hydrophila*.

The stability of pEPMS-18199 plasmid was assessed by inoculating and propagating *E. piscicida* in the absence of antibiotic selection. Following 20 serial subcultures without any antibiotic pressure, no colony (among 100 colonies each subculture) had lost the plasmid as indicated by no change in the AMR profiles of the cultures and was further confirmed by PCR.

Plasmid Copy Number

Plasmid copy number was determined for pEPMS-18199 in strain MS-18-199 using qRT-PCR by comparing plasmid abundance with that of gDNA. Our result suggests that only a single copy of pEPMS-18199 was carried in strain MS-18-199. Following qRT-PCR, cycle threshold (Ct) values obtained for the *floR* gene representing the pEPMS-18199 were similar to that of the L-asparaginase 1 gene representing the strain MS-18-199 chromosome (**Figure 3**).

DISCUSSION

As in other areas of animal production, selection pressures created by antimicrobial (AMs) usage represent a major concern in the aquatic environment. Selection pressure could favor the amplification of resistant bacterial strains and resistance genes. Several studies have documented development of resistant bacteria in and around fish farms in different types of aquaculture production systems (Schmidt et al., 2000; Petersen et al., 2002; Miranda et al., 2003; Alcaide et al., 2005; Furushita et al., 2005; Sapkota et al., 2008). However, little information is available about the molecular basis of resistance. Therefore, the goal of this study was to characterize the genomic feature of the pEPMS-18199 plasmid identified in *E. piscicida* MS-18-199. This in fact will provide an insight into the molecular mechanism of resistance in *E. piscicida* in the aquatic environments. Also, we evaluated the mobility and stability of this plasmid.

The genome sequence of *E. piscicida* strain MS-18-199 demonstrated a MDR-plasmid that is highly similar to a plasmid isolated from *E. anguillarum* ET080813 (CP006665.1) from China (Shao et al., 2015), sharing almost identical backbones (proteins coding for conjugal transfer, replication, stability, and maintenance). The plasmid replication database and Pfam database were used to identify incompatibility group and origin of replication of the pEPMS-18199 plasmid. However, pEPMS-18199 cannot be assigned to any of the historical incompatibility groups. This may be because the incompatibility group includes only plasmids with high nucleotide identity (Shintani et al., 2015).

Six AMR elements were found in the pEPMS-18199 plasmid known to confer resistance to tetracyclines, phenicol compounds, sulfonamides, and aminoglycosides. Resistance of the host strain to these AMs is attributed to the resistance genes located in the pEPMS-18199 plasmid. In previous studies by our group and other investigators, an IncA/C plasmid-mediated carrying of *floR, sul2,* and *tetA* genes was detected in *E. ictaluri* isolated from catfish in the southeastern United States (Welch et al., 2009; Abdelhamed et al., 2018c) as well as *Yersinia ruckeri* and *Aeromonas salmonicida* isolates from salmonids (McIntosh et al., 2008; Lafrentz et al., 2011). In another study, two plasmids harboring *floR*, *tetA*, and *sul2* resistance genes were reported in a *Plesiomonas shigelloides* strain isolated from catfish in the United States (Abdelhamed et al., 2018b). The similarity of resistance phenotypes and genotypes among *E. piscicida, E. ictaluri,* and *P. shigelloides* isolated from catfish farms suggest the circulation of these resistance elements/genes in catfish ponds and other aquatic environments.

Tetracyclines are among the approved AMs for use on catfish farms. In the present study, the pEPMS-18199 plasmid was found to carry *tetR* family transcriptional repressor and *tetA* tetracycline efflux pump. In fish farm-associated bacteria, tetracycline resistance was found to be mainly due to acquisition of *tet* determinants rather than due to mutation of chromosomal genes (Rhodes et al., 2000). A *tetA* gene has been previously identified in Gram-negative bacteria from fish farms from a number of geographic locations, including in the United States (Miranda et al., 2013). For example, a *tetA* gene located on Inc*K*-plasmid was found in *E. ictaluri* isolates obtained from diseased freshwater catfish (*Pangasianodon hypophthalmus)* in Vietnam (Dung et al., 2009). In another study, the *tetA* gene was located in a smaller plasmid in an *Aeromonas salmonicida* isolate (Schmidt et al., 2001). In general, these findings indicate that *tetA* is main *tet* determinant genes among different plasmids in different fish farm-associated bacteria. However, further explanation on the spread of tetracycline resistance determinants is warranted.

Florfenicol, a chloramphenicol derivative, is effective against a number of important bacterial fish pathogens

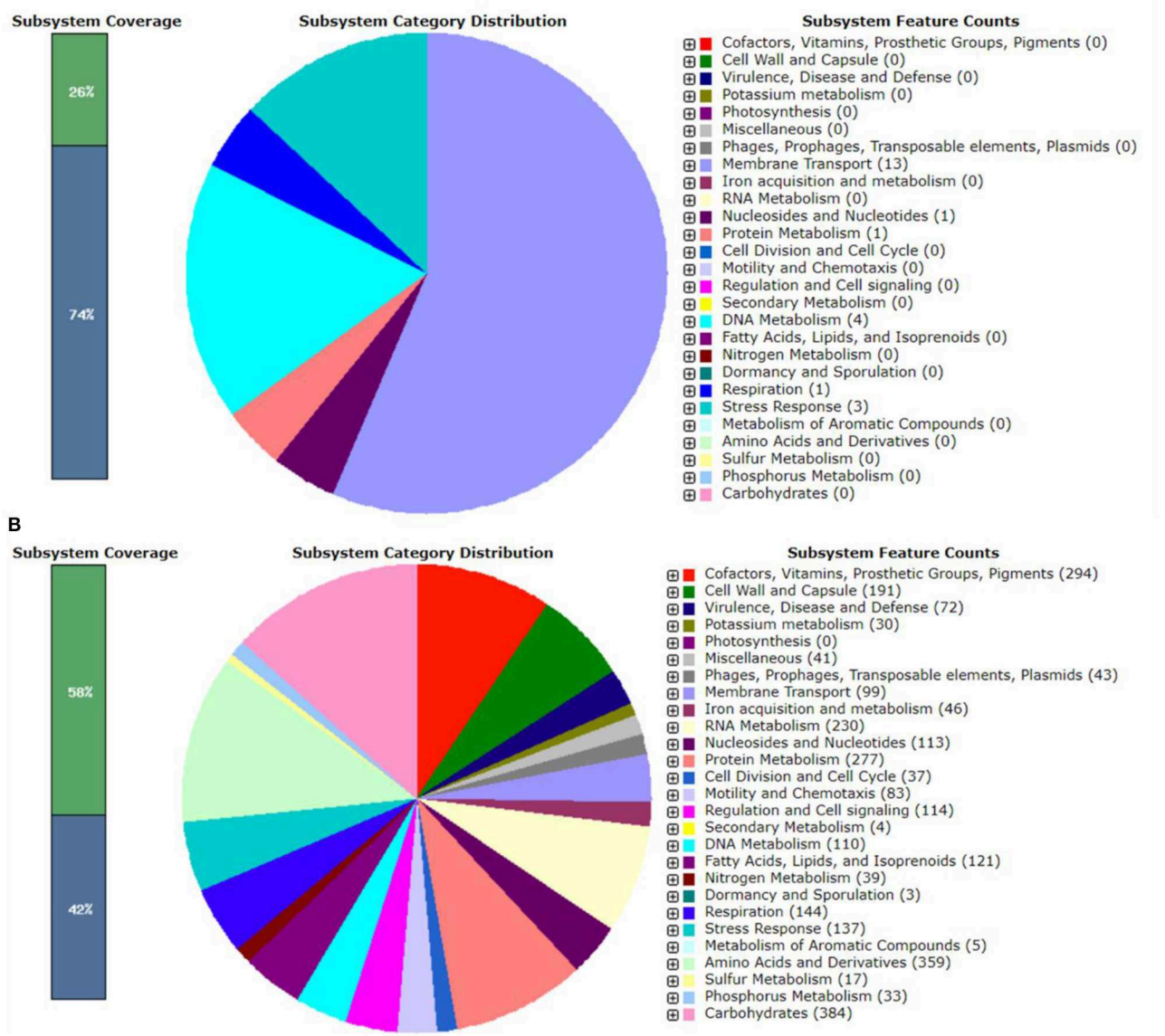

FIGURE 2 | RAST annotation summary of **(A)** pEPMS-18199 plasmid and **(B)** *Edwardsiella piscicida* strain MS-18-199. The RAST annotation robot assigns names and functions to protein-coding genes via their subsystem technology. The green color represents features that are found in RAST subsystem. The blue color represents features not assigned to a subsystem.

(Gaunt et al., 2010). In the present study, plasmid pEPMS-18199 was found to carry the *floR* gene, which confers resistance to florfenicol and chloramphenicol. The *floR* gene belongs to a major facilitator superfamily and codes for efflux proteins that export florfenicol out of the cell (Schwarz et al., 2004). RNA methyltransferases and specific hydrolases are other mechanisms of resistance to florfenicol (Schwarz et al., 2004; Long et al., 2006). However, most previous studies on florfenicol-resistant bacterial strains isolated from fish farms reported occurrence of the *floR* gene (Miranda et al., 2013).

In the current study, the *sul2* gene, encoding sulfonamide-resistant dihydropteroate synthase, was also found in the pEPMS-18199 plasmid. The *sul1* and *sul2* genes are predominant forms of *sul* genes in Gram-negative bacteria (Rådström et al., 1991). In the present study, the *sul2* gene found was 816 bases in length and was highly similar to *sul2* present in *Acinetobacter baumannii* and *E. coli*. The *sul1* gene is usually found in plasmids flanked by the insertion element (Rådström et al., 1991). The *sul2* was flanked downstream with IS110 family transposase and flanked upstream with two aminoglycoside resistance genes, *aph(3″)-Ib* and *aph(6)-Id*, which confer resistance to streptomycin, a broad

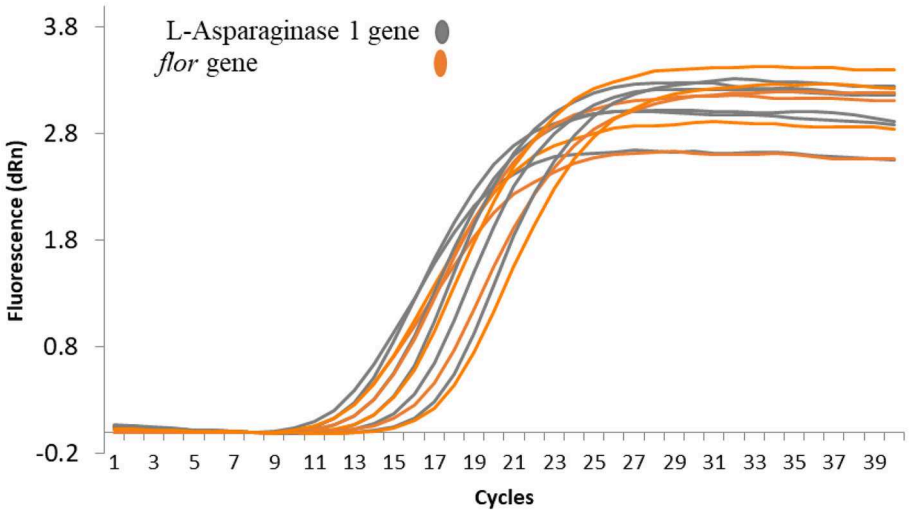

FIGURE 3 | qRT-PCR amplification plots showing the relative plasmid copy number of pEPMS-18199 in *E. piscicida* strain MS-18-199. The cycle threshold (Ct) values obtained for the *floR* gene were similar to the L-asparaginase 1 gene indicating only a single copy of the plasmid is carried by the strain MS-18-199. Orange color represent *floR* gene carried by pEPMS-18199 and gray color represent L-asparaginase 1 gene located in *E. piscicida* chromosome.

spectrum aminoglycoside (van Treeck et al., 1981; Enne et al., 2004). The *aph(3″)-Ib* gene is also denominated as *strA* and *aph(6)-Id* as *strB* (Ramirez and Tolmasky, 2010). Furthermore, the cluster of *sul2, strB,* and *strA* is commonly found in plasmids isolated from both Gram-positive and Gram-negative bacteria, such as *Aeromonas bestiarum* and *Salmonella* enterica serotype Typhimurium (Daly et al., 2005; Gordon et al., 2008). Interestingly, strain MS-18-199 was found to be susceptible to trimethoprim-sulphonamide combination (SXT), possibly because of the absence of the *dhfr1* gene encoding resistance to trimethoprim in pEPMS-18199 plasmid. The combination of trimethoprim-sulphonamide is approved for use in catfish farms for treating bacterial infections.

The relationship between metal resistance (tolerance) and antibiotic resistance is well recognized (Knapp et al., 2017), but few studies have been reported in fish (McIntosh et al., 2008). The resistance to arsenic is conferred by the presence of *ars* operon, which consists of five genes *arsR, arsD, arsA, arsB,* and *arsC,* located on either the plasmid or chromosome (Qin et al., 2006). In the present study, we demonstrated two genes on pEPMS-18199 that encode proteins that confer resistance to arsenic: *arsD* and *arsA*. The *arsD* is 363bp in length and *arsA* is 969 bp in length. *arsD*/*arsA* regions are flanked downstream with IS6-like element IS26 family transposase. Arsenic and other heavy metals are characterized by long persistent in the environment and may accumulate in soil, water, and sediments from agricultural or industrial practices (Wu et al., 2018).

Plasmid-mediated AMR is often carried through mobile elements, such as transposons (Gordon et al., 2008) and/or integrons (Kummerer, 2004). In the present study, pEPMS-18199 contains eight transposable elements. The *tetA*/*tetR* gene is associated with a Tn3-like element, TnAs1 family transposase, whereas *floR, aph(3″)-Ib*, *aph(3″)-Ib*, and *sul2* are flanked by IS91-like element, ISVsa3 family transposase. Transposons play key roles in horizontal gene transfer and recombination events. Thus, facilitate spread of resistant elements among bacterial isolates and species (Roberts, 1994). In addition, another factor for consideration is that the resistance cassette present in pEPMS-18199 carrying the transposon*s* gene is likely to be able to be mobilized by itself to other bacteria.

There are two Tra regions that encode components of the type IV secretion system in pEPMS-18199. Data from conjugation experiments demonstrated that pEPMS-18199 can mobilize to *E. coli* and *E. ictaluri*, however, it could not be mobilized to an *A. hydrophila* host, probably due to inability of *A. hydrophila* to recognize the plasmid origin of replication/transfer. *Edwardsiella* and *E. coli* are members of the *Enterobacteriaceae,* but *A. hydrophila* is member of family *Aeromonadaceae.* Therefore, the successful self-mobilization indicates that pEPMS-18199 is capable of transfer among *Enterobacteriaceae* members. In addition to *tra* regions, pEPMS-18199 also carries a DNA relaxase required for initiating plasmid DNA transfer during conjugation by cleaving a specific site at the origin of replication (Smillie et al., 2010). The results from conjugation experiment support the role of Tra regions in plasmid transfer by conjugation. Together, these data suggest the promotion of active transfer of pEPMS-18199 among bacterial strains (Cascales and Christie, 2003).

The plasmid stability experiment indicated that the *E. piscicida* host did not lose pEPMS-18199 following subculture without antibiotic pressure. pEPMS-18199 carries a partition system (*par*) involved in segregating plasmids to daughter cells during cell division (Baxter and Funnell, 2014; Brooks and Hwang, 2017). In fact, partition mechanisms are known to be responsible for the

positioning of plasmids inside the cell as well as are the most important determinant for the stable maintenance of low-copy-number plasmids (Baxter and Funnell, 2014). Besides the partition system, the sequence of pEPMS-18199 revealed three plasmid addiction proteins, including restriction endonuclease subunit M, endonuclease, and DNA cytosine methyltransferase. Plasmid addiction systems help ensure that plasmids remain established in the bacterial population even in the absence of selection pressure by preventing the survival of plasmid-free cells due to selective killing (Tschäpe, 1994; Kroll et al., 2010). Plasmid partition proteins and addiction systems likely contribute to stable maintenance and persistence of pEPMS-18199 in host cells. The stability of pEPMS-18199 suggests that, in addition to providing the host with antibiotic resistance, this naturally occurring plasmid may also confer other advantages to the host under certain environment conditions.

To our knowledge, this study describes for the first time a high molecular weight conjugative plasmid carrying AMR genes in an *E. piscicida* isolate in the United States. The presence of *tetA/tetR, floR,* and *sul2* resistance genes on plasmid pEPMS-18199 mediate resistance to the three AMs approved for use in U.S. aquaculture. Interestingly, the frequency rate of MDR *E. piscicida* isolates is still low, resistant phenotypes was detected in 6.4% (3 out of 47) of the isolates among cases submitted to CVM/MSU Aquatic Research and Diagnostic Laboratory, Thad Cochran National Warmwater Aquaculture Center at Stoneville (unpublished data from 2018 annual case summary). Besides conferring the host strain with an AMR phenotype, pEPMS-18199 may also confer other advantages to the host. Careful and prudent use of antimicrobials in aquaculture production could help to reduce the persistence and propagation of such plasmid. Also, conducting AM sensitivity assays before antimicrobial therapy is strongly recommended.

DATA AVAILABILITY STATEMENT

The datasets generated for this manuscript can be found in GenBank under accession numbers CP035668.1 and CP035669.1

AUTHOR CONTRIBUTIONS

HA and ML designed the experiment. HA, RR, OO, and GW performed the experiment. HA wrote the draft. All authors read and review the manuscript.

FUNDING

Salary support to HA was provided by the Center for Biomedical Research Excellence in Pathogen–Host Interactions, National Institute of General Medical Sciences, and National Institutes of Health awarded grant number P20GM103646-07. This project was funded by College of Veterinary Medicine and by USDA-ARS SCA no. 58-6066-7081 titled MS Center for Food Safety and Post-Harvest Technology, MS Agricultural and Forestry Experiment Station.

ACKNOWLEDGMENTS

We thank the Aquatic Diagnostic Laboratory at the College of Veterinary Medicine for providing *Edwardsiella piscicida* strain MS-18-199. We also thank Mark A. Arick II and Chuan-Yu Hsu for providing assistance with Illumina sequencing.

SUPPLEMENTARY MATERIAL

The Supplementary Material for this article can be found online at: https://www.frontiersin.org/articles/10.3389/fcimb.2019.00404/full#supplementary-material

REFERENCES

Abayneh, T., Colquhoun, D. J., and Sorum, H. (2013). *Edwardsiella piscicida* sp. nov., a novel species pathogenic to fish. *J. Appl. Microbiol.* 114, 644–654. doi: 10.1111/jam.12080

Abdelhamed, H., Lawrence, M. L., and Karsi, A. (2018a). Development and characterization of a novel live attenuated vaccine against enteric septicemia of catfish. *Front. Microbiol.* 9:1819. doi: 10.3389/fmicb.2018.01819

Abdelhamed, H., Ozdemir, O., Tekedar, H. C., Arick, M. A. II, Hsu, C. Y., Karsi, A., and Lawrence, M. L. (2018b). Complete genome sequence of multidrug-resistant *Plesiomonas shigelloides* strain MS-17-188. *Genome Announc.* 6:e00477-18. doi: 10.1128/genomeA.00387-18

Abdelhamed, H., Tekedar, H. C., Ozdemir, O., Hsu, C. Y., Arick, M. A. II, Karsi, A., and Lawrence, M. L. (2018c). Complete genome sequence of multidrug-resistant *Edwardsiella ictaluri* strain MS-17-156. *Genome Announc.* 6:e00477-18. doi: 10.1128/genomeA.00477-18

Alcaide, E., Blasco, M. D., and Esteve, C. (2005). Occurrence of drug-resistant bacteria in two European eel farms. *Appl. Environ. Microbiol.* 71, 3348–3350. doi: 10.1128/AEM.71.6.3348-3350.2005

Balabanov, V. P., Pustovoit, K. S., and Zavil'gel'skii, G. B. (2012). [Comparative analysis of antirestriction activity of R64 ArdA and ArdB proteins]. *Mol. Biol.* 46, 269–275. doi: 10.1134/S0026893312010025

Baxter, J. C., and Funnell, B. E. (2014). Plasmid Partition Mechanisms. *Microbiol. Spectrum* 2:PLAS-0023-2014. doi: 10.1128/microbiolspec.PLAS-0023-2014

Bolger, A. M., Lohse, M., and Usadel, B. (2014). Trimmomatic: a flexible trimmer for Illumina sequence data. *Bioinformatics* 30, 2114–2120. doi: 10.1093/bioinformatics/btu170

Botts, R. T., Apffel, B. A., Walters, C. J., Davidson, K. E., Echols, R. S., Geiger, M. R., et al. (2017). Characterization of four multidrug resistance plasmids captured from the sediments of an Urban Coastal Wetland. *Front. Microbiol.* 8:1922. doi: 10.3389/fmicb.2017.01922

Bowker, J. D., Ostland, V. E., Carty, D., and Bowman, M. P. (2010). Effectiveness of aquaflor (50% florfenicol) to control mortality associated with Streptococcus iniae in freshwater-reared subadult sunshine bass. *J. Aquat. Anim. Health* 22, 254–265. doi: 10.1577/H09-010.1

Brooks, A. C., and Hwang, L. C. (2017). Reconstitutions of plasmid partition systems and their mechanisms. *Plasmid* 91, 37–41. doi: 10.1016/j.plasmid.2017.03.004

Buján, N., Balboa, S. L., Romalde, J. E., Toranzo, A., and Magariños, B. (2018a). Population genetic and evolution analysis of controversial genus Edwardsiella by multilocus sequence typing. *Mol. Phylogenet. Evol.* 127, 513–521. doi: 10.1016/j.ympev.2018.05.006

Buján, N., Toranzo, A. E., and Magarinos, B. (2018b). *Edwardsiella piscicida*: a significant bacterial pathogen of cultured fish. *Dis. Aquat. Organ* 131, 59–71. doi: 10.3354/dao03281

Camus, A., Dill, J., McDermott, A., Hatcher, N., and Griffin, M. (2016). *Edwardsiella piscicida*-associated septicaemia in a blotched fantail stingray Taeniura meyeni (Mueller & Henle). *J. Fish Dis.* 39, 1125–1131. doi: 10.1111/jfd.12435

Cascales, E., and Christie, P. J. (2003). The versatile bacterial type IV secretion systems. *Nat. Rev. Microbiol.* 1, 137–149. doi: 10.1038/nrmicro753

CLSI (2010). *Performance Standards for Antimicrobial Susceptibility* Testing. CLSI document M100-S20. Wayne, PA: Clinical and Laboratory Standards Institute.

Daly, M., Villa, L., Pezzella, C., Fanning, S., and Carattoli, A. (2005). Comparison of multidrug resistance gene regions between two geographically unrelated Salmonella serotypes. *J. Antimicrob. Chemother.* 55, 558–561. doi: 10.1093/jac/dki015

De Coster, W., D'Hert, S., Schultz, D. T., Cruts, M., and Van Broeckhoven, C. (2018). NanoPack: visualizing and processing long-read sequencing data. *Bioinformatics* 34, 2666–2669. doi: 10.1093/bioinformatics/bty149

Dung, T. T., Haesebrouck, F., Sorgeloos, P., Tuan, N. A., Pasmans, F., Smet, A., et al. (2009). IncK plasmid-mediated tetracycline resistance in *Edwardsiella ictaluri* isolates from diseased freshwater catfish in Vietnam. *Aquaculture* 295, 157–159. doi: 10.1016/j.aquaculture.2009.07.010

Enne, V. I., Bennett, P. M., Livermore, D. M., and Hall, L. M. (2004). Enhancement of host fitness by the sul2-coding plasmid p9123 in the absence of selective pressure. *J. Antimicrob. Chemother.* 53, 958–963. doi: 10.1093/jac/dkh217

Ewing, W. H., Mcwhorter, A. C., Escobar, M. R., and Lubin, A. H. (1965). Edwardsiella, a new genus of Enterobacteriaceae based on a new species, *E. tarda*. *Int. J. Syst. Evol. Microbiol.* 15, 33–38. doi: 10.1099/00207713-15-1-33

Furushita, M., Okamoto, A., Maeda, T., Ohta, M., and Shiba, T. (2005). Isolation of multidrug-resistant *Stenotrophomonas maltophilia* from cultured yellowtail (*Seriola quinqueradiata*) from a marine fish farm. *Appl. Environ. Microbiol.* 71, 5598–5600. doi: 10.1128/AEM.71.9.5598-5600.2005

Gaunt, P. S., Gao, D., Sun, F., and Endris, R. (2010). Efficacy of florfenicol for control of mortality caused by Flavobacterium columnare infection in channel catfish. *J. Aquat. Anim. Health* 22, 115–122. doi: 10.1577/H09-057.1

Gordon, L., Cloeckaert, A., Doublet, B., Schwarz, S., Bouju-Albert, A., Ganiere, J. P., et al. (2008). Complete sequence of the floR-carrying multiresistance plasmid pAB5S9 from freshwater *Aeromonas bestiarum*. *J. Antimicrob. Chemother.* 62, 65–71. doi: 10.1093/jac/dkn166

Green, M. R., and Sambrook, J. (2017). *Isolation of High-Molecular-Weight DNA Using Organic Solvents. Cold Spring Harbor Protocols*. Cold Spring Harbor, NY: Cold Spring Harbor Laboratory Press. doi: 10.1101/pdb.prot093450.

Griffin, M. J., Reichley, S. R., Baumgartner, W. A., Aarattuthodiyil, S., Ware, C., Steadman, J. M., et al. (2019). Emergence of *Edwardsiella piscicida* in Farmed Channel ♀, *Ictalurus punctatus* × Blue ♂, *Ictalurus furcatus*, Hybrid Catfish Cultured in Mississippi. *J. World Aquac. Soc.* 50, 420–432. doi: 10.1111/jwas.12533

Hawke, J. P., Kent, M., Rogge, M., Baumgartner, W., Wiles, J., Shelley, J., et al. (2013). Edwardsiellosis caused by *Edwardsiella ictaluri* in laboratory populations of Zebrafish Danio rerio. *J. Aquat. Anim. Health* 25, 171–183. doi: 10.1080/08997659.2013.782226

Hawke, J. P., and Khoo, L. H. (2004). "Infectious diseases," in *Bio-logy and Culture of Channel Catfish*, eds I. C. S. Tucker and J. A. Hargreaves (Amsterdam: Elsevier), 387–443.

Hawke, J. P., McWhorter, A. C., Steigerwalt, A.G., and Brenner, D. J. (1981). *Edwardsiella ictaluri* sp. nov., the causative agent of enteric septicemia of catfish. *Int. J. Syst. Evol. Microbiol.* 31, 396–400. doi: 10.1099/00207713-31-4-396

Karsi, A., and Lawrence, M. L. (2007). Broad host range fluorescence and bioluminescence expression vectors for Gram-negative bacteria. *Plasmid* 57, 286–295. doi: 10.1016/j.plasmid.2006.11.002

Knapp, C. W., Callan, A. C., Aitken, B., Shearn, R., Koenders, A., and Hinwood, A. (2017). Relationship between antibiotic resistance genes and metals in residential soil samples from Western Australia. *Environ. Sci. Pollut. Res. Int.* 24, 2484–2494. doi: 10.1007/s11356-016-7997-y

Koren, S., Walenz, B. P., Berlin, K., Miller, J. R., Bergman, N. H., and Phillippy, A. M. (2017). Canu: scalable and accurate long-read assembly via adaptive k-mer weighting and repeat separation. *Genome Res.* 27, 722–736. doi: 10.1101/gr.215087.116

Kroll, J., Klinter, S., Schneider, C., Voss, I., and Steinbuchel, A. (2010). Plasmid addiction systems: perspectives and applications in biotechnology. *Microbial Biotechnol.* 3, 634–657. doi: 10.1111/j.1751-7915.2010.00170.x

Kummerer, K. (2004). Resistance in the environment. *J. Antimicrob. Chemother.* 54, 311–320. doi: 10.1093/jac/dkh325

Lafrentz, B. R., Welch, T. J., Shoemaker, C. A., Drennan, J. D., and Klesius, P. H. (2011). Modified live *Edwardsiella ictaluri* vaccine, AQUAVAC-ESC, lacks multidrug resistance plasmids. *J. Aquat. Anim. Health* 23, 195–199. doi: 10.1080/08997659.2011.642093

Loch, T. P., Hawke, J. P., Reichley, S. R., Faisal, M., Del Piero, F., and Griffin, M. J. (2017). Outbreaks of edwardsiellosis caused by *Edwardsiella piscicida* and *Edwardsiella tarda* in farmed barramundi (Lates calcarifer). *Aquaculture* 481, 202–210. doi: 10.1016/j.aquaculture.2017.09.005

Loman, N. J., Quick, J., and Simpson, J. T. (2015). A complete bacterial genome assembled de novo using only nanopore sequencing data. *Nature. Methods* 12:733. doi: 10.1038/nmeth.3444

Long, K. S., Poehlsgaard, J., Kehrenberg, C., Schwarz, S., and Vester, B. (2006). The Cfr rRNA methyltransferase confers resistance to Phenicols, Lincosamides, Oxazolidinones, Pleuromutilins, and Streptogramin A antibiotics. *Antimicrob. Agents Chemother.* 50, 2500–2505. doi: 10.1128/AAC.00131-06

Martinez-Martinez, L., Pascual, A., and Jacoby, G. A. (1998). Quinolone resistance from a transferable plasmid. *Lancet* 351, 797–799. doi: 10.1016/S0140-6736(97)07322-4

McArthur, A. G., Waglechner, N., Nizam, F., Yan, A., Azad, M. A., Baylay, A. J., et al. (2013). The comprehensive antibiotic resistance database. *Antimicrob. Agents Chemother.* 57, 3348–3357. doi: 10.1128/AAC.00419-13

McIntosh, D., Cunningham, M., Ji, B., Fekete, F. A., Parry, E. M., Clark, S. E., et al. (2008). Transferable, multiple antibiotic and mercury resistance in Atlantic Canadian isolates of Aeromonas salmonicida subsp. salmonicida is associated with carriage of an IncA/C plasmid similar to the *Salmonella enterica* plasmid pSN254. *J. Antimicrob. Chemother.* 61, 1221–1228. doi: 10.1093/jac/dkn123

Miranda, C. D., Kehrenberg, C., Ulep, C., Schwarz, S., and Roberts, M. C. (2003). Diversity of tetracycline resistance genes in bacteria from Chilean salmon farms. *Antimicrob. Agents Chemother.* 47, 883–888. doi: 10.1128/AAC.47.3.883-888.2003

Miranda, C. D., Tello, A., and Keen, P. L. (2013). Mechanisms of antimicrobial resistance in finfish aquaculture environments. *Front. Microbiol.* 4:233. doi: 10.3389/fmicb.2013.00233

Moleres, J., Santos-López, A., Lázaro, I., Labairu, J., Prat, C., Ardanuy, C., et al. (2015). Novel blaROB-1-bearing plasmid conferring resistance to β-lactams in Haemophilus parasuis isolates from healthy weaning pigs. *Appl. Environ. Microbiol.* 81, 3255–3267. doi: 10.1128/AEM.03865-14

Overbeek, R., Olson, R., Pusch, G. D., Olsen, G. J., Davis, J. J., Disz, T., et al. (2014). The SEED and the rapid annotation of microbial genomes using Subsystems Technology (RAST). *Nucleic Acids Res.* 42, D206–D214. doi: 10.1093/nar/gkt1226

Petersen, A., Andersen, J. S., Kaewmak, T., Somsiri, T., and Dalsgaard, A. (2002). Impact of integrated fish farming on antimicrobial resistance in a pond environment. *Appl. Environ. Microbiol.* 68, 6036–6042. doi: 10.1128/AEM.68.12.6036-6042.2002

Psifidi, A., Dovas, C. I., and Banos, G. (2010). A comparison of six methods for genomic DNA extraction suitable for PCR-based genotyping applications using ovine milk samples. *Mol. Cell. Probes* 24, 93–98. doi: 10.1016/j.mcp.2009.11.001

Qin, J., Rosen, B. P., Zhang, Y., Wang, G., Franke, S., and Rensing, C. (2006). Arsenic detoxification and evolution of trimethylarsine gas by a microbial arsenite S-adenosylmethionine methyltransferase. *Proc. Natl. Acad. Sci. USA* 103, 2075–2080. doi: 10.1073/pnas.0506836103

Rådström, P., Swedberg, G., and Sköld, O. (1991). Genetic analyses of sulfonamide resistance and its dissemination in gram-negative bacteria illustrate new aspects of R plasmid evolution. *Antimicrob. Agents Chemother.* 35, 1840–1848. doi: 10.1128/AAC.35.9.1840

Ramirez, M. S., and Tolmasky, M. E. (2010). Aminoglycoside modifying enzymes. *Drug Resist. Updat.* 13, 151–171. doi: 10.1016/j.drup.2010.08.003

Reichley, S. R., Waldbieser, G. C., Tekedar, H. C., Lawrence, M. L., and Griffin, M. J. (2016). Complete genome sequence of *Edwardsiella piscicida* isolate S11-285 recovered from channel catfish (*Ictalurus punctatus*) in Mississippi, USA. *Genome Announc.* 4:e01259-16. doi: 10.1128/genomeA.01259-16

Reichley, S. R., Ware, C., Steadman, J., Gaunt, P. S., García, J. C., LaFrentz, B. R., et al. (2017). Comparative phenotypic and genotypic analysis of Edwardsiella

isolates from different hosts and geographic origins, with emphasis on isolates formerly classified as *E. tarda*, and evaluation of diagnostic methods. *J. Clin. Microbiol.* 55, 3466–3491. doi: 10.1128/JCM.00970-17

Rhodes, G., Huys, G., Swings, J., McGann, P., Hiney, M., Smith, P., et al. (2000). Distribution of oxytetracycline resistance plasmids between aeromonads in hospital and aquaculture environments: implication of Tn1721 in dissemination of the tetracycline resistance determinant tet A. *Appl. Environ. Microbiology.* 66, 3883–3890. doi: 10.1128/AEM.66.9.3883-3890.2000

Roberts, M. C. (1994). Epidemiology of tetracycline-resistance determinants. *Trends Microbiol.* 2, 353–357. doi: 10.1016/0966-842X(94)90610-6

Robinson, J. T., Thorvaldsdottir, H., Winckler, W., Guttman, M., Lander, E. S., Getz, G., et al. (2011). Integrative genomics viewer. *Nat. Biotechnol.* 29, 24–26. doi: 10.1038/nbt.1754

Sapkota, A., Sapkota, A. R., Kucharski, M., Burke, J., McKenzie, S., Walker, P., et al. (2008). Aquaculture practices and potential human health risks: current knowledge and future priorities. *Environ. Int.* 34, 1215–1226. doi: 10.1016/j.envint.2008.04.009

Schmidt, A. S., Bruun, M. S., Dalsgaard, I., Pedersen, K., and Larsen, J. L. (2000). Occurrence of antimicrobial resistance in fish-pathogenic and environmental bacteria associated with four danish rainbow trout farms. *Appl. Environ. Microbiol.* 66, 4908–4915. doi: 10.1128/AEM.66.11.4908-4915.2000

Schmidt, A. S., Bruun, M. S., Larsen, J. L., and Dalsgaard, I. (2001). Characterization of class 1 integrons associated with R-plasmids in clinical Aeromonas salmonicida isolates from various geographical areas. *J. Antimicrob. Chemother.* 47, 735–743. doi: 10.1093/jac/47.6.735

Schwarz, S., Kehrenberg, C., Doublet, B., and Cloeckaert, A. (2004). Molecular basis of bacterial resistance to chloramphenicol and florfenicol. *FEMS Microbiol. Rev.* 28, 519–542. doi: 10.1016/j.femsre.2004.04.001

Shao, S., Lai, Q., Liu, Q., Wu, H., Xiao, J., Shao, Z., et al. (2015). Phylogenomics characterization of a highly virulent Edwardsiella strain ET080813T encoding two distinct T3SS and three T6SS gene clusters: propose a novel species as *Edwardsiella anguillarum* sp. nov. *Syst. Appl. Microbiol.* 38, 36–47. doi: 10.1016/j.syapm.2014.10.008

Shintani, M., Sanchez, Z. K., and Kimbara, K. (2015). Genomics of microbial plasmids: classification and identification based on replication and transfer systems and host taxonomy. *Front. Microbiol.* 6:242. doi: 10.3389/fmicb.2015.00242

Smillie, C., Garcillan-Barcia, M. P., Francia, M. V., Rocha, E. P., and de la Cruz, F. (2010). Mobility of plasmids. *Microbiol. Mol. Biol. Rev.* 74, 434–452. doi: 10.1128/MMBR.00020-10

Tekedar, H. C., Karsi, A., Williams, M. L., Vamenta, S., Banes, M. M., Duke, M., et al. (2013a). Complete genome sequence of channel catfish gastrointestinal septicemia isolate *Edwardsiella tarda* C07-087. *Genome Announc.* 1, e00959–e00913. doi: 10.1128/genomeA.00959-13

Tekedar, H. C., Waldbieser, G. C., Karsi, A., Liles, M. R., Griffin, M. J., Vamenta, S., et al. (2013b). Complete genome sequence of a channel catfish epidemic isolate, *Aeromonas hydrophila* strain ML09-119. *Genome Announc.* 1:e00755-13. doi: 10.1128/genomeA.00755-13

Tschäpe, H. (1994). The spread of plasmids as a function of bacterial adaptability. *FEMS Microbiol. Ecol.* 15, 23–31. doi: 10.1111/j.1574-6941.1994.tb00226.x

USDA (2019). *Catfish Production, by the National Agricultural Statistics Service (NASS), Agricultural Statistics Board, United States Department of Agriculture (USDA)*. Available online at: https://www.nass.usda.gov/Publications/Todays_Reports/reports/cfpd0419.pdf

van Treeck, U., Schmidt, F., and Wiedemann, B. (1981). Molecular nature of a streptomycin and sulfonamide resistance plasmid (pBP1) prevalent in clinical *Escherichia coli* strains and integration of an ampicillin resistance transposon (TnA). *Antimicrob. Agents Chemother.* 19, 371–380. doi: 10.1128/AAC.19.3.371

Wagner, B. A., Wise, D. J., Khoo, L. H., and Terhune, J. S. (2002). The epidemiology of bacterial diseases in food-size channel catfish. *J. Aquat. Anim. Health* 14, 263–272. doi: 10.1577/1548-8667(2002)014<0263:TEOBDI>2.0.CO;2

Walker, B. J., Abeel, T., Shea, T., Priest, M., Abouelliel, A., Sakthikumar, S., et al. (2014). Pilon: an integrated tool for comprehensive microbial variant detection and genome assembly improvement. *PLoS ONE* 9:e112963. doi: 10.1371/journal.pone.0112963

Welch, T. J., Evenhuis, J., White, D. G., McDermott, P. F., Harbottle, H., Miller, R. A., et al. (2009). IncA/C plasmid-mediated florfenicol resistance in the catfish pathogen *Edwardsiella ictaluri*. *Antimicrob. Agents Chemother.* 53, 845–846. doi: 10.1128/AAC.01312-08

Wu, C., Lin, C., Zhu, X., Liu, H., Zhou, W., Lu, J., et al. (2018). The β-lactamase gene profile and a plasmid-carrying multiple heavy metal resistance genes of *Enterobacter cloacae*. *Int. J. Genomics* 2018:12. doi: 10.1155/2018/4989602

Zeng, X., Ardeshna, D., and Lin, J. (2015). Heat shock-enhanced conjugation efficiency in standard *Campylobacter jejuni* strains. *Appl. Environ. Microbiol.* 81, 4546–4552. doi: 10.1128/AEM.00346-15

Conflict of Interest: The authors declare that the research was conducted in the absence of any commercial or financial relationships that could be construed as a potential conflict of interest.

frontiers in Cellular and Infection Microbiology

ORIGINAL RESEARCH
published: 21 February 2020
doi: 10.3389/fcimb.2020.00054

Antibiotic Resistance Profile, Outer Membrane Proteins, Virulence Factors and Genome Sequence Analysis Reveal Clinical Isolates of *Enterobacter* Are Potential Pathogens Compared to Environmental Isolates

Mitali Mishra[1,2], *Sasmita Panda*[3†], *Susmita Barik*[4], *Arup Sarkar*[4], *Durg Vijai Singh*[3†] and *Harapriya Mohapatra*[1,2*]

[1] School of Biological Sciences, National Institute of Science Education and Research, HBNI, Bhubaneswar, India, [2] Homi Bhabha National Institute (HBNI), Mumbai, India, [3] Infectious Disease Biology, Institute of Life Sciences, Bhubaneswar, India, [4] Trident School of Biotech Sciences, Trident Academy of Creative and Technology, Bhubaneswar, India

Outer membrane proteins (OMPs) of gram-negative bacteria play an important role in mediating antibacterial resistance, bacterial virulence and thus affect pathogenic ability of the bacteria. Over the years, prevalence of environmental antibiotic resistant organisms, their transmission to clinics and ability to transfer resistance genes, have been studied extensively. Nevertheless, how successful environmental bacteria can be in establishing as pathogenic bacteria under clinical setting, is less addressed. In the present study, we utilized an integrated approach of investigating the antibiotic resistance profile, presence of outer membrane proteins and virulence factors to understand extent of threat posed due to multidrug resistant environmental *Enterobacter* isolates. Also, we investigated clinical *Enterobacter* isolates and compared the results thereof. Results of the study showed that multidrug resistant environmental *Enterobacter* isolates lacked OmpC, lacked cell invasion abilities and exhibited low reactive oxygen species (ROS) production in neutrophils. In contrast, clinical isolates possessed OmpF, exhibited high invasive and adhesive property and produced higher amounts of ROS in neutrophils. These attributes indicated limited pathogenic potential of environmental *Enterobacter* isolates. Informations obtained from whole genome sequence of two representative bacterial isolates from environment (DL4.3) and clinical sources (EspIMS6) corroborated well with the observed results. Findings of the present study are significant as it highlights limited fitness of multidrug resistant environmental *Enterobacter* isolates.

Keywords: aquatic environment, outer membrane proteins (OMPs), *Enterobacter* spp., association, antibiotic resistance, virulence, multidrug resistance (MDR)

OPEN ACCESS

Edited by:
Bo Peng,
Sun Yat-sen University, China

Reviewed by:
Prasanth Manohar,
Zhejiang University-University of Edinburgh Institute, China
Renxiang Yan,
Fuzhou University, China

****Correspondence:***
Harapriya Mohapatra
hm@niser.ac.in;
hmsbsniser@gmail.com

†Present address:
Sasmita Panda,
Deptartment of Pathology and Microbiology, University of Nebraska Medical Center, Omaha, NE, United States
D. V. Singh,
Department of Biotechnology, Central University of South Bihar, Gaya, India

Specialty section:
This article was submitted to Molecular Bacterial Pathogenesis, a section of the journal Frontiers in Cellular and Infection Microbiology

Received: *08 December 2019*
Accepted: *31 January 2020*
Published: *21 February 2020*

Citation:
Mishra M, Panda S, Barik S, Sarkar A, Singh DV and Mohapatra H (2020) Antibiotic Resistance Profile, Outer Membrane Proteins, Virulence Factors and Genome Sequence Analysis Reveal Clinical Isolates of Enterobacter Are Potential Pathogens Compared to Environmental Isolates. Front. Cell. Infect. Microbiol. 10:54. doi: 10.3389/fcimb.2020.00054

INTRODUCTION

Development of antibiotic resistance in pathogens has emerged as global health problem. Our knowledge about the resistance mechanisms has been significantly enriched during last decade (O'Neill, 2014). Extensive research has provided credible information that have pointed toward co-evolution of antibiotic resistance in both natural environment and clinics (Davies and Davies, 2010). So far, our understanding on origin and escalation of environmental antibiotic resistance, infers that bacterial isolates possess inherent and adaptive resistance mechanisms that upon exposure to antibiotics/stimuli gets induced. Such antibiotic resistance determinants are transmitted to other strains by various means, ultimately resulting in emergence of resistant strains (Wellington et al., 2013; Bengtsson-Palme et al., 2018). Environmental antibiotic resistant bacteria (eARB) act as a reservoir of antibiotic resistance genes (ARGs), which under selective pressure could transform into pathogenic antibiotic resistant bacteria (pARB), that pose serious health risk resulting in treatment failure (Ashbolt et al., 2013).

The gram-negative, facultative anaerobic, rod-shaped bacteria belonging to Enterobacteriaceae family, *Enterobacter* is a nosocomial pathogen, having ubiquitous distribution in natural environment including sewage and dairy products (Grimont and Grimont, 2006; Davin-Regli and Pagès, 2015). These bacteria are increasingly exhibiting multidrug resistance phenotype, thus becoming resilient to available treatment therapies. The aforementioned fact has resulted in them being included in the "ESKAPE" group of opportunistic pathogens that represents a group for which in a given scenario, no effective therapeutic options would be available (Boucher et al., 2009; Rice, 2010). Also, there is escalation in reports of *Enterobacter* spp. exhibiting resistance toward the last line of antibiotics *viz.* carbapenems and colistin (Thiolas et al., 2005; Le-Ha et al., 2019). *Enterobacter cloacae* and *Enterobacter aerogenes*, are associated with a plethora of diseases such as lower respiratory tract infections, pneumonia, urinary tract infections, skin/soft-tissue infections, septicemia, wound infections, meningitis and nosocomial infections in intensive care units (Davin-Regli and Pagès, 2015).

Outer membrane of gram-negative bacteria is an asymmetric lipid bilayer that permits selective influx of solutes into the cell (Pagès et al., 2008). The outer membrane contains water filled open channels that facilitate passive penetration of hydrophilic drugs restricted to <600 kDa. The proteins that constitute these pores are generally referred to as porins (Fernández and Hancock, 2012). Based on their function and architecture, the porins or outer-membrane proteins (OMPs) are categorized into small β-barrel membrane anchors (e.g., OmpA, OmpX), general non-specific porins (e.g., OmpF, OmpC), substrate specific porins (e.g., PhoE, LamB) and TonB-dependent receptors (e.g., FhuA, FepA; Koebnik et al., 2000). Besides their roles as solute carriers, OMPs have diverse physiological roles in bacteria (Lin et al., 2002); for example, OmpX neutralizes host defense mechanisms, OmpA establishes a physical linkage between outer membrane, and peptidoglycan layer (Buchanan, 1999), OmpC and OmpF are responsible for influx of antibiotics and other solutes. While porins, like OmpA, are expressed constitutively in cells, expression of others such as LamB, PhoE, FhuA, are induced in presence of either specific substrate or by environmental stimuli (Koebnik et al., 2000). Development of multidrug resistance phenotype in such gram-negative pathogens has been associated with porin modification in three ways: by alterations in porin expression, by decreased porin expression, and by mutation in porins. All of the above aspects, individually or in combination affect bacterial susceptibility toward antibiotics, particularly the β-lactams (Pagès et al., 2008). A coordinated interplay between outer membrane protein expression and subsequent folding, increased efflux activity and controlled outer membrane permeability, have been associated with multidrug resistant (MDR) phenotype in *E. coli* (Viveiros et al., 2007). In *Acinetobacter baumannii*, OmpA disruption lead to severe reduction in minimum inhibitory concentration for multiple antibiotics, suggesting its contribution toward MDR phenotype (Smani et al., 2014).

Besides facilitating antibiotic resistance, OMPs serve as receptors for bacteriocins, hemolysin, other toxins and antibodies (Smani et al., 2014). OMPs are also believed to play a pivotal role in bacterial pathogenesis. OmpA, facilitates bacterial adhesion to mucosal surfaces, invasion, serum resistance and antimicrobial peptide resistance (Confer and Ayalew, 2013). In *Cronobacter sakazakii*, compared to the wild type isolates, deletion mutants of OmpA and OmpX isolates exhibited reduced adhesion and invasion to human epithelial cell INT-407 and human enterocyte like epithelial CaCo-2 cells (Kim et al., 2010). Similar observations were also made in avian pathogenic *E. coli*, where inactivation of OmpF and OmpC were shown to significantly hamper its adhesive, invasive and colonization abilities (Hejair et al., 2017). Previous report in clinical *Enterobacter aerogenes* isolates, suggested the significance of OMPs in modulating membrane permeability, which in turn affected its susceptibility to antibiotics and colonization abilities in nematodes (Lavigne et al., 2012).

Overall literature suggests OMPs to play a significant role in conferring antibiotic resistance, boosting virulence properties of many opportunistic bacterial pathogens (Delcour, 2009; Sato et al., 2017) and helping the pathogen to adapt to adverse situations. Despite these observations, population level association studies between OMPs, antibiotic resistance and virulence is still not completely explored (Silva and Mendonça, 2012). This prompted us to question, whether there exists any association between the OMPs, antibiotic resistance and virulence in a given population. Such pilot scale population association studies are important to understand the potential health risks associated with opportunistic multidrug resistant environmental bacteria.

MATERIALS AND METHODS

Bacterial Strains and Growth Conditions

Pure cultures of 20 environmental *Enterobacter* isolates, obtained from aquatic environment from Jamshedpur, India, in a prior study (**Table S1**) (Singh et al., 2017) and, 22 clinical *Enterobacter* isolates, obtained as pure cultures from wound, pus, and

urine samples of patients admitted to tertiary care hospitals in Bhubaneswar, India (**Table S1**) were included in this study. Isolation of pure colonies of clinical isolates was done at the tertiary care hospitals by using MacConkey and/or CLED agar followed by identification using routine biochemical tests and automated bacterial identification system VITEK2 (bioMerieux, USA) or a Microscan Walkaway 40/96S system. Bacterial pure cultures were maintained in nutrient agar stab culture at room temperature (Himedia, India). Unless otherwise mentioned, all experiments were carried out at 37°C and rotation of 220 per minute in shaker incubator (New Brunswick, USA) and performed in triplicates. Following sub-culture, the isolates were cryopreserved in 20% glycerol at −80°C. *Salmonella typhi*i ATCC 13324 and *E. cloacae* ATCC 13047 were used as positive controls in *in-vitro* cell adhesion and invasion studies. *Escherichia coli* ATCC 25922 was used as control strain for antibiotic disk diffusion test.

Antibiotic Resistance Profiling

Antibiotic susceptibility profiles of environmental ($n = 20$) and clinical ($n = 22$) *Enterobacter* isolates was determined by disk diffusion method (Bauer et al., 1966) using commercially available antibiotic disks (Hi-Media, India) representing all the major groups *viz.* β-lactams including cephalosporins, aminoglycosides, quinolones, macrolides, polypeptide, sulfonamides and others (**Table S2**). The diameter of the inhibition zone was recorded after overnight incubation and interpreted following CLSI standards for Enterobacteriaceae (CLSI., 2017).

As described by Krumperman (1983), multiple antibiotic resistance (MAR) index for each isolate was calculated using the following equation:

$$\textbf{MAR}\ \text{index} = a/b$$

where, "*a*" represents number of antibiotics to which isolate is resistant and "*b*" represents the number of antibiotics to which isolate was exposed.

Screening of OMP Genes by Multiplex PCR

Hexaplex PCR was developed to detect the presence of genes encoding prototype porins *viz.* OmpA, OmpF, OmpX, OmpC, LamB, and FhuA, using oligonucleotides designed for this study (**Table S3**). Briefly, bacterial cell lysates were prepared by heat denaturation followed by snap chilling, and were used as the source of template DNA. Final volume of 100 μl reaction mixture, contained 20 μl of (5X) Gotaq Flexi buffer (Promega, USA), 2 μl of (2.5 mM/dNTP) dNTP mix (Promega, USA), 2.5 μl of 25 mM MgCl2, 1.5 μl of (10 μM) forward, and (10 μM) reverse primer each, 2.5 μl of cell lysate as template DNA and 0.2 μl (100U) of Gotaq flexi DNA polymerase (Promega, USA) in a thermal cycler (Eppendorf, Germany). Reaction cycles was programmed with an initial denaturation at 94°C for 2 min, followed by 35 cycles with initial denaturation at 94°C for 45 s, annealing temperature of 53°C for 45 s, and extension at 72°C for 45 s which was followed by a final extension at 72°C for 10 min. PCR products were run in 1.5% agarose gels prepared in 1X Tris-Acetate Buffer (TAE) and gel images were recorded using the gel documentation system (Bio-Rad, USA). Following gel extraction and purification the nucleotide sequence of PCR products was determined in an automated 3130XL Genetic Analyzer (Applied Biosystems, USA).

Slot Blot Hybridization for Confirming Presence of OMP Genes

In addition to the PCR and sequence confirmation, we had validated our results by slot blot hybridization utilizing bacterial genomic DNA extracted from clinical and environmental isolates using Gentra Puregene bacteria/yeast DNA isolation kit (Qiagen, USA), as described previously (Singh et al., 2002). Bacterial genomic DNA was extracted using Gentra Puregene bacteria/yeast DNA isolation kit (Qiagen, USA). Two hundred nanogram of genomic DNA were lysed with equal volume of denaturation buffer (0.5 M NaOH, 1.5 M NaCl). Slot blots were prepared with nylon filters (Hybond; Amersham International, London, UK) using PR648 Slot Blot Manifold (GE healthcare Life Sciences, USA) and neutralized in neutralizing solution (0.5 M Tris-HCl [pH 8.0], 1.5 M NaCl). Finally, the liberated DNA was fixed to nylon membranes by exposure to UV light for 1 min (1800×100 uJ/cm^2) in a UV-crosslinker, in accordance with the manufacturer's instructions.

The membrane was probed using purified PCR products (whose identity was confirmed by sequencing) randomly labeled with [α-32P] dCTP (3,000 Ci/mmol, BARC, Bombay, India). The membrane was hybridized at 65°C in phosphate buffer containing 500 mM Na_2HPO_4 (pH 7.2), 7% (wt/vol) sodium dodecyl sulfate, 1 mM EDTA, and 1% (wt/vol) bovine serum albumin. Hybridized blots were washed once in 2 × SSC buffer (1 × SSC is 0.15 M NaCl with 0.015 M sodium citrate) for 5 min at room temperature, two times in 2 × SSC-0.1% sodium dodecyl sulfate for 10 min at 65°C, and once in 0.1 × SSC-0.1% sodium dodecyl sulfate for 15 min at 65°C. Autoradiographs were developed from the hybridized filters with the Bio-Rad Phosphor Imager screen and visualized in a Phosphor Imager (Bio-Rad, USA).

Phenotypic Detection of Virulence Factors

Clinical and environmental MDR *Enterobacter* isolates with MAR index >= 0.3 (taken as cut off) and presence of OMPs, were checked for presence of different virulence factors (**Table S4**). The presence of type-1 fimbriae in clinical isolates was determined by Hemagglutination assay (Hennequin and Forestier, 2009). The biofilm formation ability of both clinical and environmental *Enterobacter* isolates was also determined (**Figure S1**) by using crystal violet method (Stepanović et al., 2000), with some modifications reported previously (Singh et al., 2017), and were interpreted as weak, moderate and strong biofilm producer. Bacterial resistance to human serum was assessed following the protocol as described earlier (Sahly et al., 2004), with and without heat-inactivated serum. Serum resistance profile was categorized into grade-1 being non-resistant to grade-6 with highest level of resistance (**Table S5**), as described previously (Sahly et al., 2004).

Determination of Host-Dependent Virulence Factors

Essential steps for initiation of pathogenesis include adhesion and invasion to the host cells. Based on our previous observations, six environmental and six clinical MDR *Enterobacter* isolates exhibiting a MAR index >= 0.3, positive for presence of different combinations of OMPs and positive for serum resistance and biofilm production, were further selected for *in-vitro* gentamycin protection assay.

In-vitro Adhesion and Invasion in Murine Macrophage

To confirm the adhesive and invasive properties of selected MDR clinical and environmental *Enterobacter* isolates gentamicin protection assay, with *Enterobacter* isolate ATCC 13047 as control, was performed. Briefly, RAW 264.7 murine macrophage cell line was maintained in RPMI-1640 media (Himedia, India) supplemented with antibiotic cocktail containing 1X penicillin-streptomycin and 250 μg of amphotericin (Himedia, India) and 10% FBS (PAN Biotech, India). Initially, RAW 264.7 cells were trypsinized, counted with and plated into 12 well tissue culture plate with 2×10^5 cells/ml in each well without antibiotics and incubated overnight at 37°C with 5% CO_2 in New Brunswick incubator (Eppendorf, India). Bacterial pure culture was inoculated into 3 ml of tryptic soy broth (Himedia, India) and incubated at 37°C overnight. Culture was then diluted 1:1000 in fresh 5 ml of Tryptic Soy Broth and allowed to grow for 3–4 h till OD_{600nm} reaches to 0.6–0.8. Bacterial cultures were then centrifuged at 4,500 rpm for 10 min at 4°C, bacterial pellet was washed once with in 1X PBS (pH 7.4) and before challenge was mixed with RPMI-1640 without antibiotics. For all further bacterial challenge studies, an optimized multiplicity of infection (MOI) 1:50 and infection time of 60 min at 37°C with 5% CO_2 was used. Using aforementioned conditions, co-cultured plates following incubation, were washed twice with 1X PBS (pH 7.4). Of them, one plate was further incubated with RPMI-1640 containing 200 μg/ml of gentamycin. After incubation, plates were washed twice with PBS and cells were lysed with 0.05% Triton-X100 and plated onto Tryptic Soya Agar. Plates were incubated overnight at 37°C for enumeration of viable counts. The observations were tabulated and statistical analysis of the data obtained from three individual experiments was performed. Moreover, *in-vitro* cell adhesion and invasion frequency were calculated for individual isolates as mentioned earlier (Wilson et al., 2011) to enumerate the percent fraction of populations infecting host cells.

Determination of Reactive Oxygen Species (ROS) Production

On the basis of *in-vitro* cell adhesiveness and invasiveness property, three clinical (EspIMS6, EcTATAH41, ATCC 13047) and three environmental (DL4.3, DL5.1, and SR4.9) MDR *Enterobacter* isolates were selected further. The selection of these isolates was based on the results of gentamycin protection assay, where isolates having higher invasive ability were selected for reactive oxygen species (ROS) production. To assess the production of ROS, we had infected the freshly isolated neutrophils with these six MDR *Enterobacter* isolates. Briefly neutrophils were extracted from peripheral blood from healthy volunteers using histopaque 1119 (Sigma Aldrich, USA) and Percoll (Sigma Aldrich, USA) gradient method, as described previously (Sarkar et al., 2012).

Cells were counted using hemocytometer and 1×10^6 cells were seeded in a 48-well tissue culture plate. Bacterial cells were challenged at MOI 1:50 in triplicate and plates were incubated for 1 h at 37°C with 5% CO_2. After incubation, infected neutrophils were centrifuged at 2,200 rpm for 10 min at room temperature; pellet was suspended with 1X PBS pH 7.4 (Himedia, India). The cell suspension was transferred to FACS tubes and then incubated with ROS indicator fluorescent dye Dihydrorhodamine 123 (Thermofisher Scientific, USA) at a final concentration of 1 μM at 37°C in a water bath for 5 min. Samples were immediately processed for acquisition and flow cytometric assessment of ROS production by BD FACS Calibur™ flow cytometer (BD Biosciences, USA) and analyzed by CellQuest Pro software (BD Biosciences, USA).

Whole Genome Sequencing of Two *Enterobacter* Isolates

In a prior work, we have reported draft genome sequence of environmental *Enterobacter cloacae* isolate DL4.3 (showing multi-drug resistance phenotype) and clinical *Enterobacter cloacae* isolate EspIMS6 (having extreme drug resistance phenotype; Mishra et al., 2017). To further understand and validate experimental results obtained, we analyzed our draft genomic sequences in an internet-based platform (Center for genomic epidemiology http://www.genomicepidemiology.org), which provides a platform for rapid analysis of whole genome DNA-sequences and retrieve information from the sequence data.

Statistical Softwares Used

Bionumeric software (v.7.0, Applied Maths, Biomeriux, USA) was used to analyze antibiotic resistance pattern of the isolates used in the study and dendrogram was generated using UPGMA algorithm inbuilt in the software. Pearson correlation coefficient of OMPs and *in-vitro* adhesion and invasion frequency were generated using XLSTAT software (v. 2017, www.xlstat.com/en/). Analyzed matrix was then plotted in biplot to assess the association between attributes and the pathogenic potential was derived from the biplot generated from principal component analysis. GraphPad prism v. 7.0 was used to generate graphs from *in-vitro* infection assays.

RESULTS

Antibiotic Susceptibility Profile of *Enterobacter* Isolates

Antibiogram profile of the isolates was determined against 40 antibiotics representing major classes of therapeutic agents. Results revealed marked differences in antibiotic susceptibility profiles of environmental and clinical isolates used in the study (**Figure 1**). Alarmingly 50% ($n = 11$) of clinical isolates were resistant to colistin, and 30% ($n = 7$) of them were resistant to imipenem and meropenem, but all environmental isolates

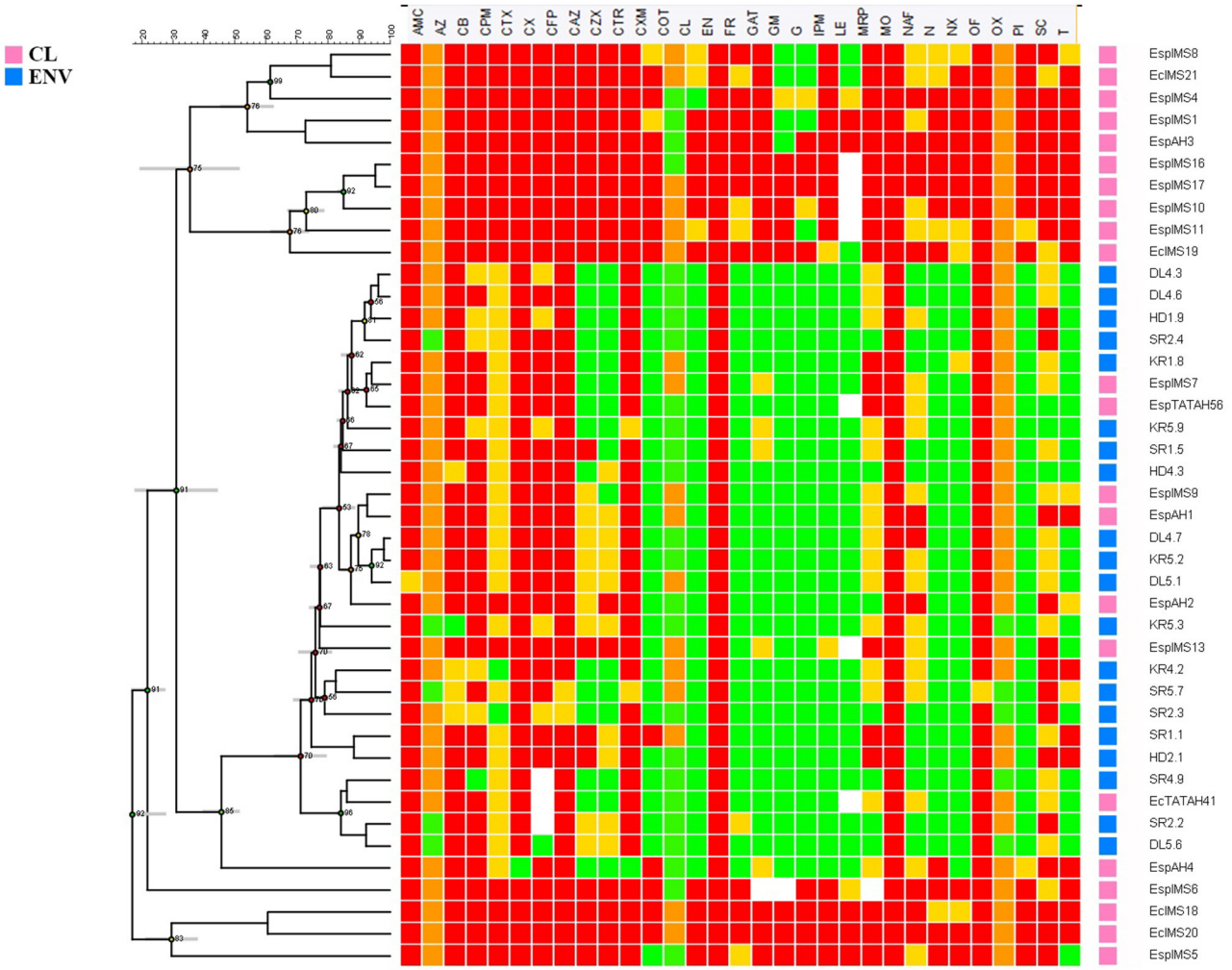

FIGURE 1 | Comparative antibiotic susceptibility profile of environmental and clinical *Enterobacter* isolates. Antibiotic susceptibility of environmental ($n = 20$) and clinical ($n = 22$) *Enterobacter* isolates toward 40 different antibiotics belonging to different classes was performed by disk diffusion method. Zone of inhibition was recorded to represent the Resistant (Red), Intermediate (Yellow) and Susceptible (Green) isolates. The antibiogram profiles of all these isolates are represented here as a heat map with dendrogram, which was generated using Bionumerics v7.0 software.

were sensitive to the above mentioned drugs (**Figure 1**). The clinical isolates were completely resistant to β-lactams, first and second generation of cephalosporins while around 75% of clinical isolates were resistant to third generation cephalosporins *viz.* ceftriaxone, cefotaxime, ceftazidime. All of the clinical isolates ($n = 22$) showed resistance toward fourth generation cephalosporins like cefpirome and cefepime (**Figure 1**). In contrast, environmental isolates were mostly resistant toward first generation of cephalosporins like cefuroxime. While majority of the environmental *Enterobacter* isolates were susceptible to quinolones, resistance toward the drug was exhibited by more than 50% of clinical isolates.

Multiplex PCR for Simultaneous Detection of OMP Genes

We developed a hexaplex PCR for screening of different OMPs present in *Enterobacter* isolates under study. Hexaplex PCR followed by slot blot hybridization and sequencing of the purified PCR products confirmed the presence of *OmpA*, *OmpX*, *LamB,* and *OmpF* in the isolates (**Figures 2A,B** and **Figures S2A,B**, **S3**). Results indicated that majority of environmental isolates ($n = 13$) were positive for *OmpA* and *OmpX* (**Figure 2A**), out of which five were also positive for *LamB* and, two co-harbored *OmpF*. In contrast, eight clinical isolates co-harbored *OmpA, OmpX,* and *LamB*; out of which two isolates were positive for *OmpF* (**Figure 2B**).

It was interesting to note that none of the isolates tested were positive for presence of *OmpC* gene (**Figures S2A,B**). When investigated for the presence of substrate-specific porins such as *LamB* and *FhuA* in the *Enterobacter* isolates, we did not find any isolate positive for *FhuA*. However, *LamB* was present in 25% of environmental and 37% of clinical isolates, making *LamB* as the third most abundant OMPs, among *Enterobacter* isolates (**Figures 2A,B**).

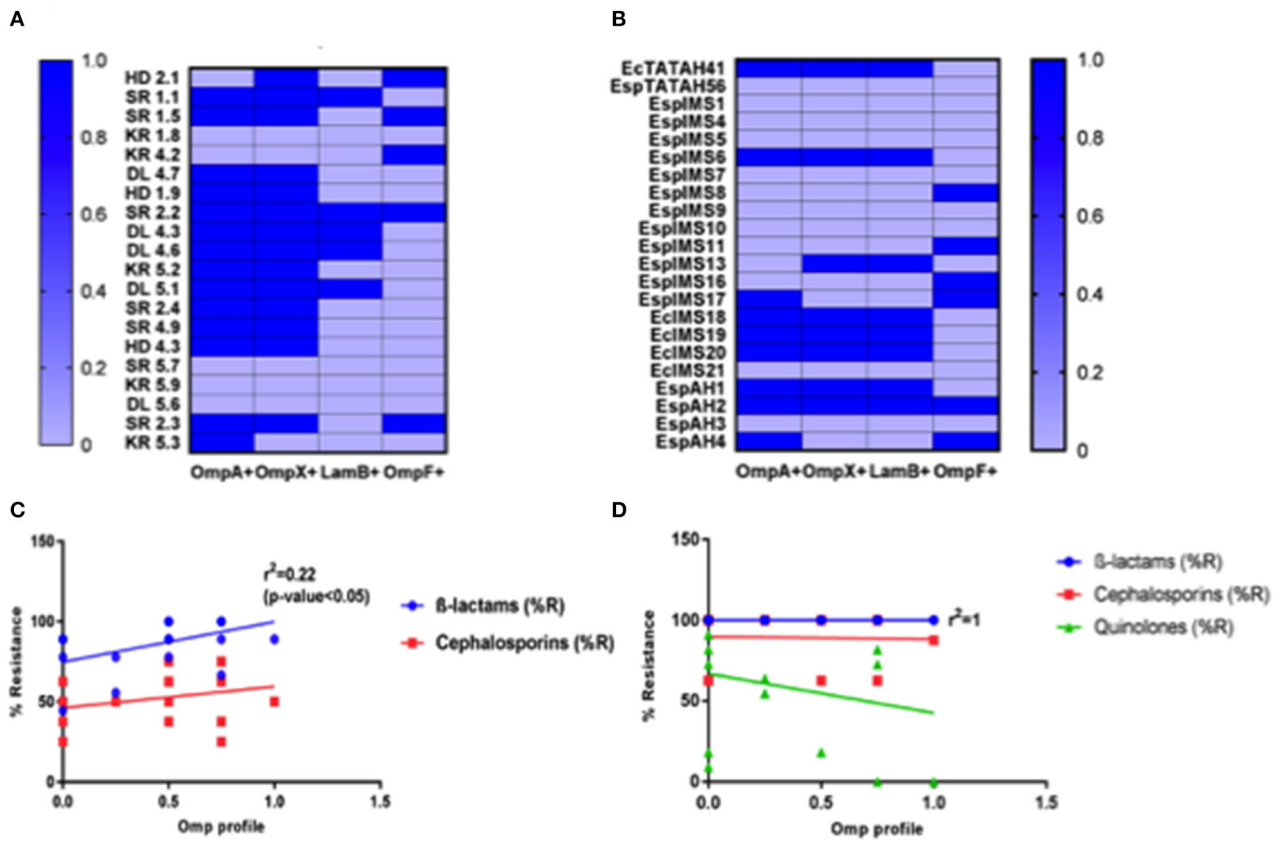

FIGURE 2 | Determination of OMP profile and its association with antibiotic resistance. Distribution of *OmpA*, *OmpX*, *LamB,* and *OmpF* in environmental **(A)** and clinical **(B)** *Enterobacter* isolates is presented, as deduced from multiplex PCR and slot blot hybridization experiments. OMP profile of individual isolates was then compared with their respective % resistance toward β-lactams, cephalosporins antibiotics to assess the association of OMPs with observed drug resistance, presented here as linear regression curve for environmental **(C)** and clinical **(D)** *Enterobacter* isolates, done by GraphPad Prism software.

Association of OMPs With Antibiotic Resistance

We analyzed association between OMPs and antibiotic resistance in the sample population under study using linear regression. Among the environmental isolates, we observed an association between OMP positive isolates and β-lactam, cephalosporins resistance (**Figure 2C**). Moreover, environmental isolates possessing *OmpA* and *OmpX* ($n = 11$) exhibited MDR as against those not harboring *OmpA* and *OmpX genes* (results not shown). It also indicated that isolates devoid of *LamB* and *OmpF* were resistant toward higher number of β-lactam, cephalosporins antibiotics. On the contrary, it was well-understood that OMPs in clinical *Enterobacter* isolates had significantly less or no association with observed antibiotic resistance (**Figure 2D**), attributed to presence of multiple chromosomally encoded resistance determinants.

Phenotypic Detection of Virulence Factors

Clinical isolates ($n = 7$) and environmental *Enterobacter* isolates ($n = 5$) along with prototype strain, *Enterobacter* ATCC 13047, exhibiting MAR index >= 0.3 and positive for presence OMPs, were checked for presence of virulence factors such as type-1 fimbraie, biofilm formation and serum resistance (**Table S4**). Hemagglutination assay for detection of type-1 fimbriae revealed that all environmental and clinical *Enterobacter* isolates tested were positive for fimbriae. Environmental isolates DL4.3, DL4.6, SR5.7, and DL5.1 displayed low and moderate serum resistance, whereas SR4.9 showed high serum resistant phenotype. On the contrary, clinical isolates EcTATAH41, EspIMS6, and EcIMS18 were highly serum resistant indicating strong pathogenic potential. Most of the clinical *Enterobacter* isolates tested, including EcTATAH41, EspIMS6, EcIMS21, EspAH3, and EspAH4 were strong biofilm producer unlike environmental *Enterobacter* isolates like SR4.9, DL4.3, and DL4.6 that were weakly adherent in nature.

In-vitro Cell Adhesion/Invasion of MDR *Enterobacter* Isolates

Bacterial challenge to murine macrophage RAW 264.7 cell line evaluated the pathogenicity of *Enterobacter* isolates. Compared to *in-vitro* cell-attachment and invasion potential of control pathogenic strain of *Salmonella typhii* isolate ATCC 13324, *Enterobacter* isolates used in the present study were categorized into three major groups: (A) Highest pathogenic potential

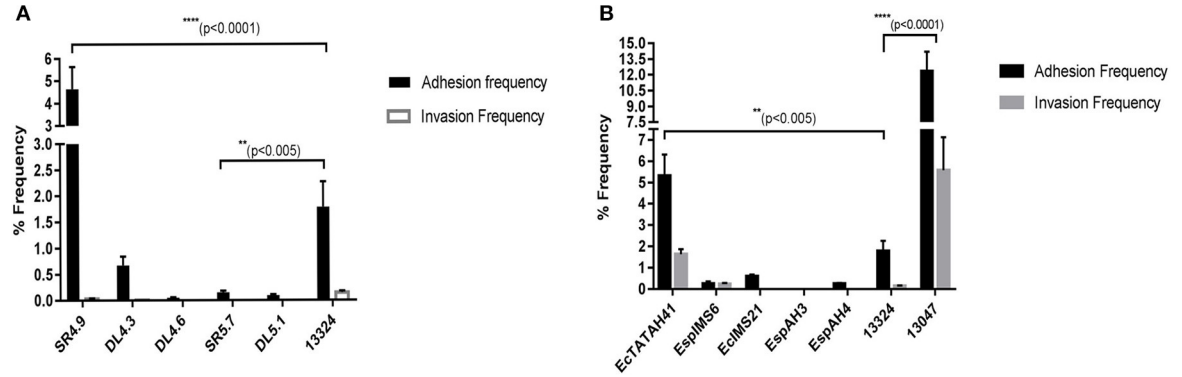

FIGURE 3 | Cell adhesion and invasion frequency of *Enterobacter* isolates. The bar graph represented the % adhesion and invasion frequency of selected MDR environmental **(A)** and clinical **(B)** *Enterobacter* isolates, which was calculated by the % ratio of the number of viable bacterial cells (as in mean $\log_{10}$CFU/ml) after infection to RAW 264.7 cell line and the initial inoculum given. Statistical significance was determined using two-way ANNOVA test using GraphPad Prism software and *S. typhii* ATCC 13324 as control, where $^{****}p < 0.0001$ and $^{**}p < 0.005$.

[P.P.(*Entero.*) $\geq$ P.P.(*S. typhii*)]; (B) Moderate pathogenic potential [P.P.(*Entero.*) $\leq$ P.P.(*S. typhii*)] and (C) Minimal pathogenic potential [P.P.(*Entero.*) $<<$ P.P.(*S. typhii*)]; where P.P. refers to pathogenic potential of the tested organism.

Cell attachment assay revealed that environmental isolate SR4.9, with 4.65% of adhesion frequency showed highest *in-vitro* cell attachment, emulating results as observed with *Salmonellae typhii* ATCC 13324 having adhesion frequency of 1.78% (**Figure 3A**). Further, with ∼0.1% adhesion frequency environmental isolates DL5.1 and SR5.7 exhibited moderate attachment (**Figure 3A**). However, none of the environmental isolates could show cell invasion ability *in-vitro* (**Figure 3A**).

On the contrary, clinical *Enterobacter cloacae* ATCC 13047 isolate with 12.34% adhesion frequency and 5.57% invasion frequency, displayed highest cell attachment and cell invasion *in vitro*, respectively (**Figure 3B**). Moreover, clinical isolate EcTATAH41, EspIMS6, and EcIMS21 showed moderate cell attachment with the former also exhibiting moderate cell invasion *in vitro* (**Figure 3B**). It was worth noting that, the clinical isolate EspIMS6 exhibited almost complete invasion following attachment *in vitro* (**Figure 3B**), as evident from their nearly similar adhesion and invasion frequency. With the % ratio of invasion to adhesion frequency, it was noted that clinical isolates EcTATAH41, EspAH3, and Ec13047 showed 30–45% of invading populations while EspIMS6 displayed >90% of invading populations to macrophage cells.

Flow Cytometric Assessment of ROS Production

Production of reactive oxygen species by neutrophils plays a pivotal role in innate immune response to pathogens. Hence, based on the results of gentamycin protection assay, we determined the activation of neutrophils by estimating the ROS production upon co-culture of neutrophils with six MDR *Enterobacter* isolates. Flow cytometry results of ROS generation by *Enterobacter* isolates as against LPS control were compiled (**Figures 4A–F**). Results of this study suggested that clinical MDR isolates EcTATAH41 (**Figure 4B**) and EspIMS6 (**Figure 4C**) produced significant amount of ROS, which was evident from the shift in fluorescence indicating activation of neutrophils upon infection. It was interesting to note that environmental *Enteorbacter* isolates DL4.3 (**Figure 4E**) and DL5.1 (**Figure 4F**) too were capable of producing ROS similar to clinical counterparts. On the other hand, aquatic isolate SR4.9 (**Figure 4D**) and ATCC strain 13047 (**Figure 4A**) displayed minimal production of ROS upon neutrophil infections.

Association of OMPs With Pathogenic Potential of *Enterobacter* Isolates

After determining the presence of different virulence factors, we analyzed the association of OMPs with *in-vitro* cell adhesion and invasion frequencies. From the Pearson correlation matrix, it was evident that *OmpA* and *OmpX* were strongly correlated ($r = 0.8$). *LamB* displayed a positive correlation with other OMPs; significantly with *OmpX* ($r = 0.8$) followed by *OmpA* ($r = 0.6$) (**Table S6**). Further, a positive correlation between *OmpF* and invasion frequency ($r = 0.6$) was observed.

The results of this Pearson correlation matrix were further evaluated, where the *Enterobacter* isolates were grouped into four quadrants based on their OMP profile and respective *in–vitro* adhesion and invasion frequencies (**Figure 5A**). *E. cloacae* ATCC 13047 that was positive for *OmpA*, *OmpX*, *LamB*, *OmpF* exhibited highest adhesion-invasion frequency, indicating its greater pathogenic ability. Further, clinical (EcTATAH41 and EspIMS6) and environmental (DL4.3, DL4.6, DL5.1) isolates positive for *OmpA*, *OmpX,* and *LamB* showed moderate and weak adhesion-invasion frequency, respectively (**Figure 5A**). In addition, environmental isolate SR4.9 that was positive for *OmpA* and *OmpX* showed strong cell-adhesive property. Interestingly, EspAH4 that was positive only for *OmpA* displayed weaker cell adhesive quality, whereas isolates like SR5.7, EcIMS21, EspAH3 which were devoid of OMPs, did not show *in-vitro* adhesion or invasion ability (**Figure 5A**).

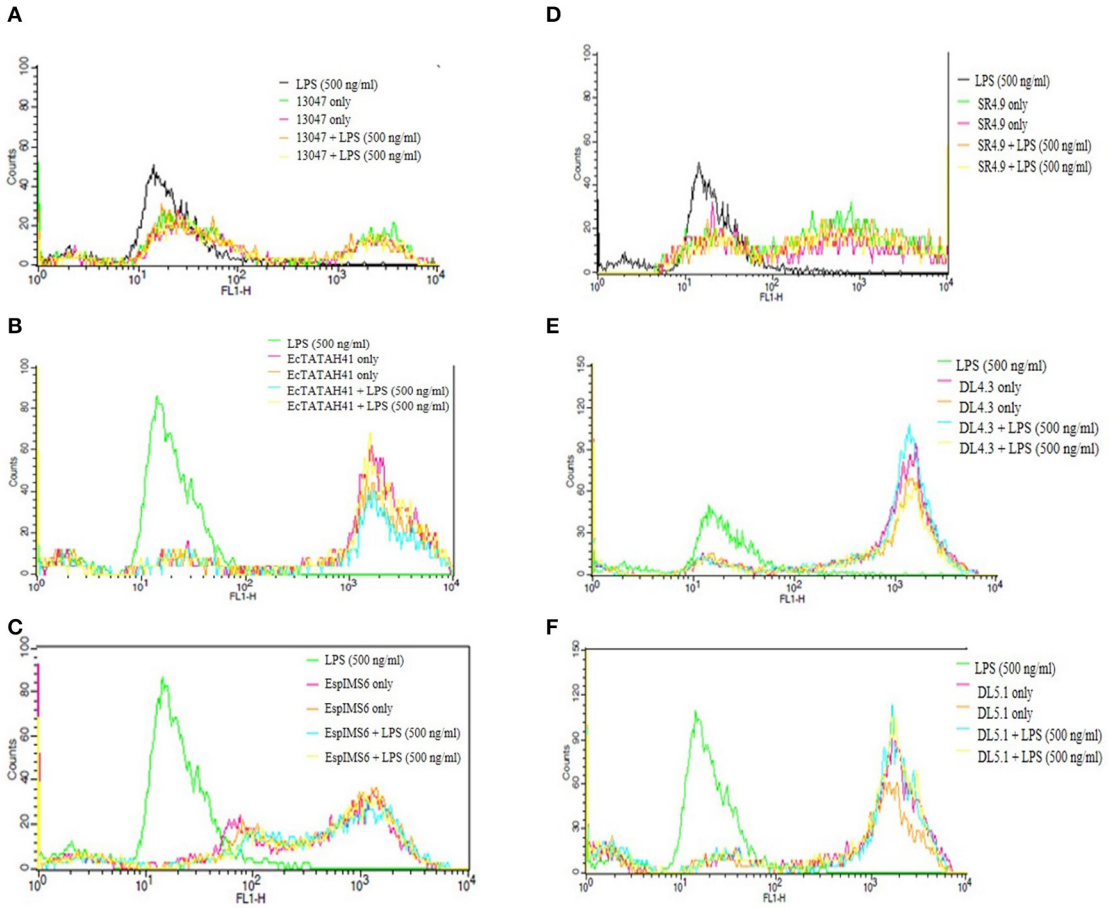

FIGURE 4 | Determination of ROS generation in neutrophils challenged with MDR *Enterobacter* isolates. The histograms of Dihydrorhodamine 123 fluorescence emitted due to activation of neutrophils by the MDR pathogens with and without LPS (in duplicate) and LPS control were recorded and represented here with gated populations for clinical *E. cloacae* ATCC 13047 **(A)**, EcTATAH41 **(B)** and EspIMS6 **(C)** and environmental SR4.9 **(D)**, DL4.3 **(E)**, DL5.1 **(F)** *Enterobacter* isolates.

To give a clear picture of this observed association of OMPs with pathogenic potential, we calculated the virulence index of each of these six MDR isolates taking into considerations: presence of fimbriae, serum resistance, biofilm production, adhesion and invasion frequency (using the formula virulence index = total no. of virulence factors possessed/total no. of virulence factors tested), and analyzed association of virulence index with their respective OMP profile (**Figure 5B**). This data clearly showed that clinical isolates (e.g., EcTATH41, EspIMS6, and ATCC 13047) exhibited greater pathogenic ability as observed from their higher virulence index and OMP profile. Nonetheless, environmental isolates (including SR4.9, DL5.1, and DL4.3), though harbored multiple OMPs, they displayed minimal pathogenic ability, that could be attributed to lower virulence indices.

Virulence Mechanisms of *E. cloacae* Isolates Revealed by Genome Analysis

In a prior work, we had reported draft genome sequence of DL4.3 (environmental-aquatic isolate) and EspIMS6 (Clinical-UTI isolate; Mishra et al., 2017). To further understand and validate experimental results obtained, we analyzed sequence data further. In both *E. cloacae* isolates, number of genes associated with functions were in the order carbohydrates > amino acids and derivatives > protein metabolism > cofactors, vitamins, prosthetic groups, pigments > RNA metabolism > cell wall and capsule > membrane transport (**Figure S4**). We had also segregated individual category and its sub-systems involved to get a blueprint of the similarities and dissimilarities amongst these two *E. cloacae* isolates (**Figures 6A–C**).

In case of membrane transport machinery, both isolates harbored ABC transporters, cation transporters along with protein secretion systems. However, protein secretion system type VII and type VIII were more prevalent in clinical isolate EspIMS6 (**Figure 6A**). Both the organisms were genetically similar in terms of their stress response ability, including oxidative stress, osmotic stress, heat shock, cold shock etc. (**Figure 6C**). Moreover, in case of virulence, defense and disease subcategory (**Figure 6B**), both DL4.3 and EspIMS6 contained machineries for flagellar motility, chemotaxis, capsules, antibacterial peptides, invasion and intracellular

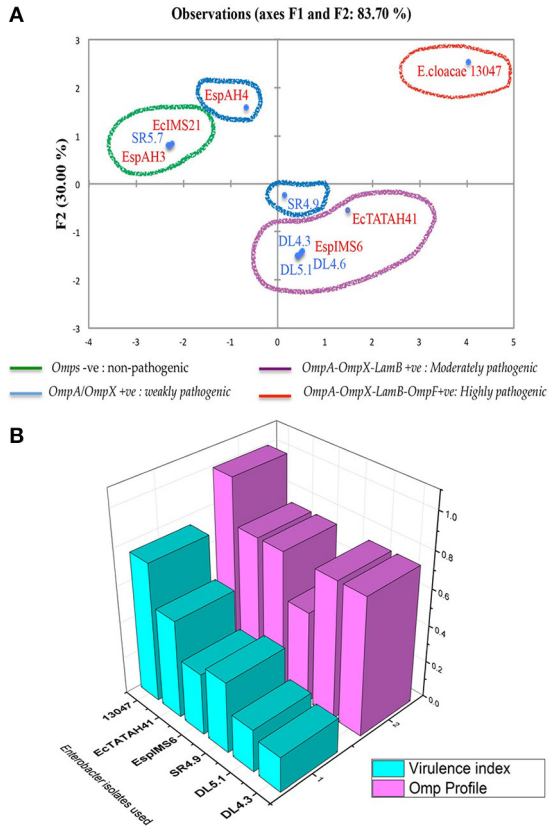

FIGURE 5 | Association of OMPs with pathogenic potential in clinical and environmental *Enterobacter* isolates. Principal component analysis represented as biplot **(A)** associating pathogenic potential and expression of OMPs has categorized into four groups, where organisms in red indicated clinical *Enterobacter* isolates and in blue indicated environmental *Enterobacter* isolates. **(B)** is a 3D plot showing the association between of OMP profile with virulence index of individual *Enterobacter* isolates.

resistance. But, clinical isolate EspIMS6 outnumbered DL4.3, in terms of capsular and extracellular polysaccharides, resistance to antibiotics and toxic compounds, phages and prophages (**Figure 6B**). Interestingly, clinical isolate EspIMS6 also possessed transposable elements and plasmids, which were absent in the environmental isolate DL4.3 (**Figure 6B**).

DISCUSSION

In the present study, we utilized an integrated approach investigating antibiotic resistance profile, presence of outer membrane proteins, virulence factors and utilizing genome sequence data to understand pathogenic potential and extent of threat posed due to multidrug resistant environmental *Enterobacter* isolates. In a previous study conducted by us (Singh et al., 2017), we had quantitatively evaluated threat posed by multidrug-resistant bacteria from environment both at population and genus level. Also, we had reported environmental multidrug *Enterobacter* isolates posed no threat. Detailed investigation in the present study corroborated well with our previous observations.The environmental isolates exhibited low ROS production in neutrophils, lacked OmpC and lacked cell invasion abilities. In contrast clinical isolates produced higher amounts of ROS in neutrophils, possessed all OMPs screened for, and exhibited extremely high invasive and adhesive capabilities. Whole genome sequencing revealed presence of integrons, type VII and type VIII secretion systems in clinical isolate only. Thus, findings of our studies indicate that multidrug resistant environmental *Enterobacter* isolates investigated in this study are limited in their pathogenic ability compared to clinical isolates.

We investigated environmental ($n = 20$) and clinical ($n = 22$) *Enterobacter* isolates, belonging to two major species- *E. cloacae* and *E. aerogenes*, indicating ubiquitous existence of these two species in aquatic and clinical environments. As reported by us previously (Singh et al., 2017), majority of the environmental *Enterobacter* isolates were multi-drug resistant ($n = 15$), whereas, majority of the clinical isolates tested in this study, exhibited resistance to all the antibiotics tested and accordingly could be categorized as MDR ($n = 13$), extreme drug resistant (XDR) ($n = 6$) and pan drug resistant (PDR) ($n = 3$) (Paterson and Doi, 2007). These results indicated the emergence of potential multi-drug resistant strains of *Enterobacter* in both aquatic environment and clinical settings.

Previous reports have cited existence of enzymatic barrier coupled with porin loss/reduction in *Enterobacter* spp. to play a significant role in eliciting resistance toward carbapenems like ertapenem and/or imipenem (Doumith et al., 2009; Lavigne et al., 2012; Yang et al., 2012). Study conducted on the dynamic changes in membrane permeability of *E. aerogenes* clinical isolates subjected to imipenem treatment, revealed no difference in expression of OmpA and OmpX between resistant and intermediate susceptible isolates (Lavigne et al., 2012). Majewski et al. (2016) have studied OMP expression in carbapenem-resistant *Enterobacter* isolates. The authors have reported either downregulation of OmpF and OmpC gene and/or OmpC-directed polarization of the outer membrane to affect carbapenem resistance. This altered outer membrane protein balance in the context of OmpF/OmpC greatly regulates the β-lactam resistance by selecting porins with preferable transmembrane channel diameter (Yigit et al., 2002). This prompted us to investigate the distribution of prototype OMPs (both non-specific and substrate-specific porins) in clinical and environmental *Enterobacter* isolates.

Hexaplex PCR revealed predominance of *OmpA* and *OmpX* in the isolates under study, coinciding with earlier reports, which suggest these two OMPs to be integral part of gram-negative bacterial membrane (Dupont et al., 2004). Overexpression of *OmpX* in *E. coli* and *E. aerogenes* strains was found to reduce expression of non-specific porins i.e., *OmpC* and *OmpF*, leading to restricted permeability of β-lactams (Dupont et al., 2004; Viveiros et al., 2007). A study conducted by Jaskulski et al. (2013) with carbapenem resistant *E. cloacae* isolates ($n = 106$), reported expression of OmpF and OmpC protein in only 6.6% isolates ($n = 7$); out of these seven isolates, only four co-expressed OmpF and OmpC protein. It was interesting to note that none of the isolates we tested, were positive for OmpC. Reduced or no expression of two major non-specific porins, OmpC and OmpF

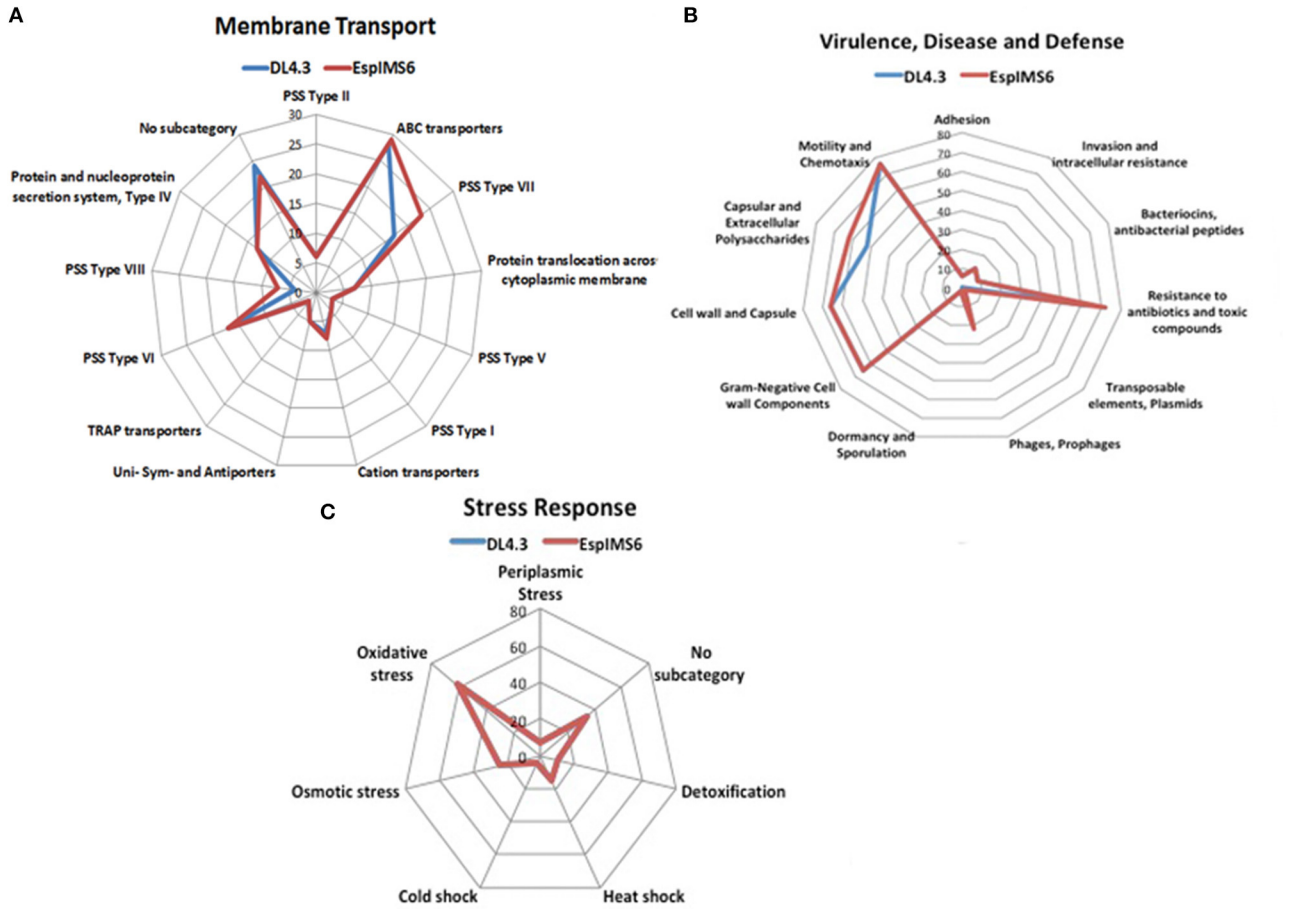

FIGURE 6 | Genetic makeup of environmental (DL4.3) and clinical (EspIMS6) *Enterobacter* isolates. Spider plots generated using the number of genes involved in each function revealed critical genomic differences and similarities between wild type environmental DL4.3 and clinical EspIMS6 isolate in different categories like **(A)** membrane transport, **(B)** virulence, disease and defense, and **(C)** stress response.

in *E. cloacae* isolates, could be due to point mutations affecting their transcription/translation/insertion into outer membrane (Doumith et al., 2009). We also observed that in our present study *LamB* as the third most abundant OMP, after *OmpA* and *OmpX*. Constitutive expression of LamB was previously reported in many clinical isolates of *Enterobacter aerogenes*, and overproduction of LamB and OmpX was associated with major porin loss (Gayet et al., 2003). Utilizing multiplex PCR based screening, results of our study established differences in occurrence of OMPs in *Enterobacter* spp. isolated from clinical and environmental origin.

Antimicrobial susceptibility profile of the *Enterobacter* isolates had exhibited wide spread resistance to β-lactams and cephalosporins. Hence, we investigated the association of OMPs (*OmpA*, *OmpX*, *LamB,* and *OmpF*) in mediating antibiotic resistance. We observed significant association of *OmpA* and *OmpX* with β-lactam and cephalosporin resistance. This indicated probable role of these two porins in mediating resistance to β-lactams in environmental *Enterobacter* isolates. Co-ordinated and similar association of both these OMPs might be, because of the common global regulatory pathways involved in such porin regulation, such as CpxAR and EnvZ/OmpR in response to antibiotics (Dam et al., 2018). OmpA is a multifaceted porin, and is widely conserved in many pathogens like *E. coli*, *Enterobacter* spp., *Klebsiella* spp., *Acinetobacter baumanii* (Confer and Ayalew, 2013). Apart from maintaining cellular integrity, OmpA plays a vital role in biofilm formation and adherence to biotic and abiotic surfaces (Gaddy et al., 2009). We observed that the clinical isolates which possessed *OmpA* namely, *Enterobacter cloacae* 13047, EspAH4, EcTATAH41, and EspIMS6, to be strong biofilm producers. OmpX, a structural homolog of OmpA has been reported, to be important for bacterial pathogenesis (Maisnier-Patin et al., 2003). This finding corroborates with the recent reports, suggesting that bacterial OMPs play a major role in developing antibiotic resistance, since these porins are responsible for intrusion of antibiotics (Ghai and Ghai, 2018).

We observed higher percent of antibiotic resistant isolates to be negative for *LamB* and *OmpF*, suggesting significant low association of *LamB* and *OmpF* in antibiotic resistance amongst

environmental isolates. Though we have discussed loss/reduction of OmpF expression in resistant isolates above, but association of LamB with drug resistance is less explored. We could not find any reports on association of LamB with virulence factors either. But there is one report that explored role of LamB as a vaccine candidate among *Vibrio* species (Lun et al., 2014). LamB porin, known to be responsible for transport of maltose and maltodextrin in gram-negative bacteria, are reported to exhibit poor immunological characteristics. Nonetheless, LamB-one of the first OMPs characterized, are evolutionary significant irrespective of their contribution toward antibiotic resistance and virulence (Koebnik et al., 2000).

Bacterial virulence factors enable the pathogen to replicate and disseminate within host cells in part by evading the host-defense system, hence determination of such virulence factors is important to assess their pathogenic potential (Schroeder et al., 2017). For any opportunistic pathogen like *Enterobacter* spp., cell adherence and invasion are essential steps for successful colonization and subsequent infection. Hence, we investigated the ability of selected MDR aquatic and clinical isolates to adhere and invade murine macrophage cells (RAW 264.7). The prototype *E. cloacae* isolate ATCC 13047 exhibited highest pathogenic potential, as it mimicked adhesive and invasive competence similar to the positive control *S. typhii* ATCC 13324 used in the present study. This was coinciding with an earlier report (Pati et al., 2018), which suggested the *E. cloacae* 13047 to be the most virulent strain of *Enterobacter* spp. known similar to the pathogenic *S. typhii*. Unlike clinical isolates, which displayed moderate cell invasion, none of the environmental isolates showed cell-invasiveness. In addition, greater percentage of invading populations in clinical isolates (EspIMS6, EcTATAH41, and Ec13047) than aquatic isolates (DL4.3, DL5.1, SR4.9), suggested their higher pathogenic potential. Moreover, upon EspIMS6 infection to macrophage cells, ∼90% of adherent cells were actually invading macrophage cells, indicative of its greater pathogenic index. Clinical *Enterobacter* isolates possessed edge over environmental isolates in terms of their biofilm formation, serum resistance and ROS production in neutrophils. Noteworthy was the relatively low ROS production in clinical *Enterobacter* isolates (EspIMS6 and EcTATAH41) as compared to aquatic isolates (DL4.3 and DL5.1), which produced higher ROS in neutrophils. This observation coincided with the reports suggesting that potential opportunistic pathogens reduce ROS level, facilitating their survival and colonization in their target host cells (Spooner and Yilmaz, 2011; Hirschfeld et al., 2017).

Based on the results obtained, we further analyzed the association of OMPs and virulence attributes in MDR *Enterobacter* isolates by principal component analysis. It was evident from the analysis that isolates positive for *OmpA*, *OmpX*, *OmpF,* and *LamB* exhibited greater pathogenic ability *in-vitro*, and presence of *OmpF* was found to be associated with higher pathogenic ability. Overall, the findings suggested that presence of OmpF facilitates *Enterobacter* spp. in establishing infection in host cells. Importance of OmpF in adhesive and invasive abilities of avian pathogenic *E. coli* had been currently elucidated (Hejair et al., 2017), which is coinciding with our observations in *Enterobacter* isolates. Significant association between OmpA and OmpX too was evident from the matrix. Similar synergy amongst OmpA and OmpX was reported earlier in *Cronobacter sakazakii* in the context of their invasiveness (Kim et al., 2010). When the virulence index of an organism was determined taking into consideration of all these virulence factors (as mentioned previously), we noticed that the clinical *Enterobacter* isolates exhibited higher virulence index as compared to aquatic isolates, even though they did not have a distinct difference in their respective OMP profile.

The draft genome sequences obtained from aquatic isolate DL4.3 and clinical isolate EspIMS6 validated our earlier observations, as EspIMS6 harbored multiple antibiotic resistance determinants that were reflected in their XDR phenotype. Also, EspIMS6 contained integrons and type VII and type VIII protein secretion systems, making this clinical strain more robust virulent pathogen, even greater than *E. cloacae* 13047, which do possess secretion system type VII but not type VIII (Liu et al., 2013). Presence of genes for bacterial persistence and intracellular survival in clinical EspIMS6 explained its higher pathogenic potential as compared to the aquatic isolate DL4.3. Therefore, such comparative genome analysis helped us to understand the internal genetic background of isolates that is reflected in their observed phenotype (Mishra et al., 2017).

CONCLUSION

Put together, the present study indicated association of OMPs with both antibiotic resistance and virulence factors in *Enterobacter* spp in the isolates studied. It was also interesting to note that though environmental *Enterobacter* isolates showed multidrug resistance but possessed limited pathogenic potential, whereas clinical MDR *Enterobacter* isolates possess higher pathogenic index indicative of their potential human health risks. Thus, findings of the present study are significant as it highlights limited fitness of multidrug resistant environmental *Enterobacter* isolates. Such investigations provide much needed information on the pathogenic potential of environmental multidrug resistant bacteria thereby assisting identification of potential high-risk pathogenic populations/clones among opportunistic pathogens like *Enterobacter* spp.

DATA AVAILABILITY STATEMENT

All datasets generated for this study are included in the article/**Supplementary Material**.

ETHICS STATEMENT

The present study did not involve human subjects. Approval was obtained from Institutional Biosafety Committee to work on BSL2 organisms. Institutional Ethical Committee approval was obtained for the studies on Human or Animal Cells studies.

AUTHOR CONTRIBUTIONS

HM supervised, conceptualized, and designed the study. MM performed the experiments and analyzed the results. SP and

DS supported in conducting hybridization experiments and gave critical inputs for preparing the manuscript. SB and AS helped with their expertise in neutrophil-based experiments. MM drafted and edited the manuscript. HM reviewed and finalized the draft. All authors approve and gave their inputs in the final manuscript.

FUNDING

MM acknowledges Department of Science and Technology (DST), New Delhi for INSPIRE fellowship for her graduate research. MM and HM greatly acknowledge intramural financial support from DAE through NISER for carrying out this study.

ACKNOWLEDGMENTS

The authors would like to sincerely acknowledge the doctors and hospital personnel for providing clinical *Enterobacter* samples used in this study: Dr. Nagendra Debata (Institute of Medical Sciences Hospital, Bhubaneswar), Dr. Suneeta Sahu (Dept. of Microbiology, Apollo Hospital, Bhubaneswar). The authors would also like to acknowledge Dr. Santosh K. Singh for identification and characterization of environmental *Enterobacter* isolates. Authors greatly acknowledge the timely help of Mr. Chandan Mahish in facilitating with Flow cytometry data acquisitions and generous help of Dr. Subhashis Chattopadhyay (SBS, NISER) for providing RAW 264.7 cell line for *in-vitro* infection studies.

SUPPLEMENTARY MATERIAL

The Supplementary Material for this article can be found online at: https://www.frontiersin.org/articles/10.3389/fcimb.2020.00054/full#supplementary-material

REFERENCES

Ashbolt, N. J., Brandt, K. K., Lawrence, J. R., Finley, R., Amézquita, A., Heberer, T., et al. (2013). Human Health Risk Assessment (HHRA) for environmental development and transfer of antibiotic resistance. *Environ. Health Perspect.* 121, 993–1001. doi: 10.1289/ehp.1206316

Bauer, A. W., Kirby, W. M. M., Sherris, J. C., Turck, A. M., and Von Graevenitz, A. (1966). 40 Microbiology: a centenary perspective 1966 antibiotic susceptibility testing by a standardized single disk method. *Am. J. Clin. Pathol.* 45, 493–496. doi: 10.1093/ajcp/45.4_ts.493

Bengtsson-Palme, J., Kristiansson, E., and Larsson, D. G. J. (2018). Environmental factors influencing the development and spread of antibiotic resistance. *FEMS Microbiol. Rev.* 42, 68–80. doi: 10.1093/femsre/fux053

Boucher, H. W., Talbot, G. H., Bradley, J. S., Edwards, J. E., Gilbert, D., Rice, L. B., et al. (2009). Bad bugs, no drugs: no ESKAPE! an update from the Infectious Diseases Society of America. *Clin. Infect. Dis.* 48, 1–12. doi: 10.1086/595011

Buchanan, S. K. (1999). ß-Barrel proteins from bacterial function and refolding. *Curr. Opin. Struct. Biol.* 9, 455–461. doi: 10.1016/S0959-440X(99)80064-5

CLSI. (2017). *National Committee for Clinical Laboratory Standards. 2000. Performance Standard for Antimicrobial Susceptibility Testing. Document M100–S10*. Wayne, PA: National Committee for Clinical Laboratory Standards.

Confer, A. W., and Ayalew, S. (2013). The OmpA family of proteins: roles in bacterial pathogenesis and immunity. *Vet. Microbiol.* 163, 207–222. doi: 10.1016/j.vetmic.2012.08.019

Dam, S., Pagès, J. M., and Masi, M. (2018). Stress responses, outer membrane permeability control and antimicrobial resistance in enterobacteriaceae. *Microbiology* 164, 260–267 doi: 10.1099/mic.0.000613

Davies, J., and Davies, D. (2010). Origins and evolution of antibiotic resistance. *Microbiol. Mol. Biol. Rev.* 74, 417–433. doi: 10.1128/MMBR.00016-10

Davin-Regli, A., and Pagès, J. M. (2015). *Enterobacter aerogenes* and *Enterobacter cloacae*; Versatile bacterial pathogens confronting antibiotic treatment. *Front. Microbiol.* 6:392. doi: 10.3389/fmicb.2015.00392

Delcour, A. H. (2009). Outer membrane permeability and antibiotic resistance. *Biochim. Biophys. Acta*. 1794, 808–816. doi: 10.1016/j.bbapap.2008.11.005

Doumith, M., Ellington, M. J., Livermore, D. M., and Woodford, N. (2009). Molecular mechanisms disrupting porin expression in ertapenem-resistant *Klebsiella* and *Enterobacter* spp. clinical isolates from the UK. *J. Antimicrob. Chemother.* 63, 659–667. doi: 10.1093/jac/dkp029

Dupont, M., Emmanuelle, D., Chollet, R., Chevalier, J., and Pag, J. (2004). *Enterobacter aerogenes* OmpX, a cation-selective channel mar- and osmo-regulated. *FEBS Lett.* 569, 27–30. doi: 10.1016/j.febslet.2004.05.047

Fernández, L., and Hancock, R. E. W. (2012). Adaptive and mutational resistance: role of porins and efflux pumps in drug resistance. *Clin. Microbiol. Rev.* 25, 661–681. doi: 10.1128/CMR.00043-12

Gaddy, J. A., Tomaras, A. P., and Actis, L. A. (2009). The *Acinetobacter baumannii* 19606 OmpA protein plays a role in biofilm formation on abiotic surfaces and in the interaction of this pathogen with eukaryotic cells. *Infect. Immun.* 77, 3150–3160. doi: 10.1128/IAI.00096-09

Gayet, S., Chollet, R., Molle, G., Pagès, J. M., and Chevalier, J. (2003). Modification of outer membrane protein profile and evidence suggesting an active drug pump in *Enterobacter aerogenes* clinical strains. *Antimicrob. Agents Chemother.* 47, 1555–1559. doi: 10.1128/AAC.47.5.1555-1559.2003

Ghai, I., and Ghai, S. (2018). Understanding antibiotic resistance via outer membrane permeability. *Infect. Drug Resist.* 11, 523–530. doi: 10.2147/IDR.S156995

Grimont, F., and Grimont, P. A. D. (2006). The genus *Enterobacter*. *Prokaryotes.* 6, 197–214. doi: 10.1007/0-387-30746-X_9

Hejair, H. M. A., Zhu, Y., Ma, J., Zhang, Y., Pan, Z., Zhang, W., et al. (2017). Microbial pathogenesis functional role of ompF and ompC porins in pathogenesis of avian pathogenic *Escherichia coli*. *Microb. Pathog.* 107, 29–37. doi: 10.1016/j.micpath.2017.02.033

Hennequin, C., and Forestier, C. (2009). oxyR, a LysR-type regulator involved in *Klebsiella pneumoniae* mucosal and abiotic colonization. *Infect. Immun.* 77, 5449–5457. doi: 10.1128/IAI.00837-09

Hirschfeld, J., White, P. C., Milward, M. R., Cooper, P. R., and Chapple, I. L. C. (2017). Modulation of neutrophil extracellular trap and reactive oxygen species release by periodontal bacteria. *Infect. Immun.* 85, 1–14. doi: 10.1128/IAI.00297-17

Jaskulski, M. R., Medeiros, B. C., Borges, J. V., Zalewsky, R., Fonseca, M. E. C., Marinowic, D. R., et al. (2013). Assessment of extended-spectrum β-lactamase, KPC carbapenemase and porin resistance mechanisms in clinical samples of *Klebsiella pneumoniae* and *Enterobacter* spp. *Int. J. Antimicrob. Agents* 42, 76–79. doi: 10.1016/j.ijantimicag.2013.03.009

Kim, K. K., Kim, K. K., Choi, J., Lim, J., Lee, J., Hwang, S., et al. (2010). Outer membrane proteins A (OmpA) and X (OmpX) are essential for basolateral invasion of *Cronobacter sakazakii*. *Appl. Environ. Microbiol.* 76, 5188–5198. doi: 10.1128/AEM.02498-09

Koebnik, R., Locher, K. P., and Van, P. (2000). MicroReview Structure and function of bacterial outer membrane proteins : barrels in a nutshell. *Mol. Microbiol.* 37, 239–253. doi: 10.1046/j.1365-2958.2000.01983.x

Krumperman, P. H. (1983). Multiple antibiotic resistance indexing of *Escherichia coli* to identify high-risk sources of faecal contamination of water. *Appl. Environ. Microbiol.* 46, 165–170. doi: 10.1128/AEM.46.1.165-170.1983

Lavigne, J. P., Sotto, A., Nicolas-Chanoine, M. H., Bouziges, N., Bourg, G., Davin-Regli, A., et al. (2012). Membrane permeability, a pivotal function involved in

antibiotic resistance and virulence in *Enterobacter aerogenes* clinical isolates. *Clin. Microbiol. Infect.* 18, 539–545 doi: 10.1111/j.1469-0691.2011.03607.x

Le-Ha, T.-D., Le, L., Le-Vo, H.-N., Anda, M., Motooka, D., Nakamura, S., et al. (2019). Characterization of a carbapenem- and colistin-resistant *Enterobacter cloacae* carrying Tn 6901 in bla NDM-1 genomic context. *Infect. Drug Resist.* 12, 733–739. doi: 10.2147/IDR.S194495

Lin, J., Huang, S., and Zhang, Q. (2002). Outer membrane proteins: key players for bacterial adaptation in host niches. *Microb. Infect.* 4, 325–331. doi: 10.1016/S1286-4579(02)01545-9

Liu, W. Y., Wong, C. F., Chung, K. M. K., Jiang, J. W., and Leung, F. C. C. (2013). Comparative genome analysis of *Enterobacter cloacae*. *PLoS ONE* 8:e74487. doi: 10.1371/journal.pone.0074487

Lun, J., Xia, C., Yuan, C., Zhang, Y., Zhong, M., Huang, T., et al. (2014). The outer membrane protein, LamB (maltoporin), is a versatile vaccine candidate among the *Vibrio* species. *Vaccine* 32, 809–815. doi: 10.1016/j.vaccine.2013.12.035

Maisnier-Patin, K., Malissard, M., Jeannin, P., Haeuw, J. F., Corbière, J. C., Hoeffel, G., et al. (2003). The outer membrane protein X from *Escherichia coli* exhibits immune properties. *Vaccine* 21, 3765–3774. doi: 10.1016/S0264-410X(03)00316-5

Majewski, P., Wieczorek, P., Ojdana, D., Sienko, A., Kowalczuk, O., Sacha, P., et al. (2016). Altered outer membrane transcriptome balance with AmpC overexpression in carbapenem-resistant *Enterobacter cloacae*. *Front. Microbiol.* 7:2054. doi: 10.3389/fmicb.2016.02054

Mishra, M., Patole, S., and Mohapatra, H. (2017). Draft genome sequences of non-clinical and clinical *Enterobacter cloacae* isolates. *Genome Announc.* 5, 5–6. doi: 10.1128/genomeA.01218-17

O'Neill, J. (2014). *Review on Antimicrobial Resistance: Tackling a Crisis for the Health and Wealth of Nations*. London, UK: Welcome Trust.

Pagès, J. M., James, C. E., and Winterhalter, M. (2008). The porin and the permeating antibiotic: a selective diffusion barrier in Gram-negative bacteria. *Nat. Rev. Microbiol.* 6, 893–903. doi: 10.1038/nrmicro1994

Paterson, D. L., and Doi, Y. (2007). A step closer to Extreme Drug Resistance (XDR) in Gram-Negative Bacilli. *Clin. Infect. Dis.* 45, 1179–1181. doi: 10.1086/522287

Pati, N. B., Doijad, S. P., Schultze, T., Mannala, G. K., Yao, Y., Jaiswal, S., et al. (2018). *Enterobacter bugandensis*: a novel Enterobacterial species associated with severe clinical infection. *Sci. Rep*. 8:5392. doi: 10.1038/s41598-018-23069-z

Rice, L. B. (2010). Progress and challenges in implementing the research on ESKAPE pathogens. *Infect. Control Hosp. Epidemiol.* 31, S7–S10. doi: 10.1086/655995

Sahly, H., Aucken, H., Benedí, V. J., Forestier, C., Fussing, V., Hansen, D. S., et al. (2004). Increased serum resistance in *Klebsiella pneumoniae* strains producing extended-spectrum β-lactamases. *Antimicrob. Agents Chemother.* 48, 3477–3482. doi: 10.1128/AAC.48.9.3477-3482.2004

Sarkar, A., Hellberg, L., Bhattacharyya, A., Behnen, M., Wang, K., Lord, J. M., et al. (2012). Infection with *Anaplasma phagocytophilum* activates the phosphatidylinositol 3-Kinase/Akt and NF-κB survival pathways in neutrophil granulocytes. *Infect. Immun.* 80, 1615–1623. doi: 10.1128/IAI.05219-11

Sato, Y., Unno, Y., Kawakami, S., Ubagai, T., and Ono, Y. (2017). Virulence characteristics of *Acinetobacter baumannii* clinical isolates vary with the expression levels of omps. *J. Med. Microbiol.* 66, 203–212. doi: 10.1099/jmm.0.000394

Schroeder, M., Brooks, B. D., and Brooks, A. E. (2017). The complex relationship between virulence and antibiotic resistance. *Genes* 8:39. doi: 10.3390/genes8010039

Silva, G. J., and Mendonça, N. (2012). Association between antimicrobial resistance and virulence in *Escherichia coli*. *Virulence* 3, 18–28. doi: 10.4161/viru.3.1.18382

Singh, D. V., Matte, M. H., Matte, G. R., Jiang, S., Sabeena, F., Shukla, B. N., et al. (2002). Non-O139 strains : clonal relationships between clinical and environmental isolates. *J. Clin. Microbiol.* 67, 910–921. doi: 10.1128/AEM.67.2.910-921.2001

Singh, S. K., Ekka, R., Mishra, M., and Mohapatra, H. (2017). Association study of multiple antibiotic resistance and virulence: a strategy to assess the extent of risk posed by bacterial population in aquatic environment. *Environ. Monit. Assess.* 189:320. doi: 10.1007/s10661-017-6005-4

Smani, Y., Roca, I., and Vila, J. (2014). Role of OmpA in the multidrug resistance phenotype of *Acinetobacter baumannii*. *Antimicrob. Agents Chemother.* 58, 1806–1808. doi: 10.1128/AAC.02101-13

Spooner, R., and Yilmaz, Ö. (2011). The role of reactive-oxygen-species in microbial persistence and inflammation. *Int. J. Mol. Sci.* 12, 334–352. doi: 10.3390/ijms12010334

Stepanović, S., Vuković, D., Dakić, I., Savić, B., and Švabić-Vlahović, M. (2000). A modified microtiter-plate test for quantification of staphylococcal biofilm formation. *J. Microbiol. Methods* 40, 175–179. doi: 10.1016/S0167-7012(00)00122-6

Thiolas, A., Bollet, C., Scola, B. L., Raoult, D., and Pages, J.-M. (2005). Successive emergence of *Enterobacter aerogenes* strains resistant to imipenem and colistin in a patient. *Antimicrob. Agents Chemother.* 49, 1354–1358. doi: 10.1128/AAC.49.4.1354-1358.2005

Viveiros, M., Dupont, M., Rodrigues, L., Couto, I., Davin-Regli, A., Martins, M., et al. (2007). Antibiotic stress, genetic response and altered permeability of *E. coli*. *PLoS ONE* 2:e365. doi: 10.1371/journal.pone.0000365

Wellington, E. M. H., Boxall, A. B. A., Cross, P., Feil, E. J., Gaze, W. H., Hawkey, P. M., et al. (2013). The role of the natural environment in the emergence of antibiotic resistance in Gram-negative bacteria. *Lancet Infect. Dis.* 13, 155–165. doi: 10.1016/S1473-3099(12)70317-1

Wilson, B. A., Salyers, A. A., Whitt, D. D., and Winkler, M. E. (2011). *Bacterial Pathogenesis-A Molecular Approach. 3rd ed*. Washington, DC: ASM Press, American Society for Microbiology, 130–146. doi: 10.1128/9781555816162

Yang, F. C., Yan, J. J., Hung, K. H., and Wu, J. J. (2012). Characterization of ertapenem-resistant *Enterobacter cloacae* in a Taiwanese University Hospital. *J. Clin. Microbiol.* 50, 223–226. doi: 10.1128/JCM.01263-11

Yigit, H., Anderson, G. J., Biddle, J. W., Steward, C. D., Rasheed, J. K., Valera, L. L., et al. (2002). Carbapenem resistance in a clinical isolate of *Enterobacter aerogenes* is associated with decreased expression of OmpF and OmpC porin analogs. *Antimicrob. Agents Chemother.* 46, 3817–3822. doi: 10.1128/AAC.46.12.3817-3822.2002

Conflict of Interest: The authors declare that the research was conducted in the absence of any commercial or financial relationships that could be construed as a potential conflict of interest.

frontiers in Cellular and Infection Microbiology

ORIGINAL RESEARCH
published: 28 February 2020
doi: 10.3389/fcimb.2020.00084

5-Methylindole Potentiates Aminoglycoside Against Gram-Positive Bacteria Including *Staphylococcus aureus* Persisters Under Hypoionic Conditions

Fengqi Sun[1†], *Mengmeng Bian*[1†], *Zhongyan Li*[1†], *Boyan Lv*[1], *Yuanyuan Gao*[1,2], *Yan Wang*[1*] *and Xinmiao Fu*[1,2*‡]

[1] *Provincial University Key Laboratory of Cellular Stress Response and Metabolic Regulation, College of Life Sciences, Fujian Normal University, Fuzhou, China,* [2] *Engineering Research Center of Industrial Microbiology of Ministry of Education, College of Life Sciences, Fujian Normal University, Fuzhou, China*

Antibiotic resistance/tolerance has become a severe threat to human and animal health. To combat antibiotic-resistant/tolerant bacteria, it is of significance to improve the efficacy of traditional antibiotics. Here we show that indole potentiates tobramycin to kill stationary-phase *Staphylococcus aureus* cells after a short, combined treatment, with its derivative 5-methylindole being the most potent compound tested and with the absence of ions as a prerequisite. Consistently, this combined treatment also kills various types of *S. aureus* persister cells as induced by the protonophore CCCP, nutrient shift, or starvation, as well as methicillin-resistant *S. aureus* (MRSA) cells. Importantly, 5-methylindole potentiates tobramycin killing of *S. aureus* persisters in a mouse acute skin wound model. Furthermore, 5-methylindole facilitates killing of many strains of gram-positive pathogens such as *Staphylococcus epidermidis*, *Enterococcus faecalis*, and *Streptococcus pyogenes* by aminoglycoside antibiotics, whereas it suppresses the action of aminoglycoside against the gram-negative pathogens *Escherichia coli* and *Shigella flexneri*. In conclusion, our work may pave the way for the development of indole derivatives as adjuvants to potentiate aminoglycosides against gram-positive pathogens.

Keywords: 5-Methylindole, indole, aminoglycoside, antibiotic resistance, antibiotic tolerance, persister, gram-positive bacteria, *Staphylococcus aureus*

OPEN ACCESS

Edited by:
Patrícia Poeta, University of Trás-os-Montes and Alto Douro, Portugal

Reviewed by:
Jose Yuste, Carlos III Health Institute, Spain
William Schwan, University of Wisconsin–La Crosse, United States

***Correspondence:**
Yan Wang
wangyan@fjnu.edu.cn
Xinmiao Fu
xmfu@fjnu.edu.cn

[†] *These authors have contributed equally to this work*

[‡] ***ORCID:***
Xinmiao Fu
orcid.org/0000-0003-3361-6904

Specialty section:
This article was submitted to Molecular Bacterial Pathogenesis, a section of the journal Frontiers in Cellular and Infection Microbiology

Received: *19 November 2019*
Accepted: *18 February 2020*
Published: *28 February 2020*

Citation:
Sun F, Bian M, Li Z, Lv B, Gao Y, Wang Y and Fu X (2020) 5-Methylindole Potentiates Aminoglycoside Against Gram-Positive Bacteria Including Staphylococcus aureus Persisters Under Hypoionic Conditions. Front. Cell. Infect. Microbiol. 10:84. doi: 10.3389/fcimb.2020.00084

INTRODUCTION

Antibiotic resistance/tolerance has become a severe threat to public health and global economic development (Lewis, 2010; WHO, 2014; O'Neill, 2016; Balaban et al., 2019). Currently, no single or simple strategy suffices to fully contain the emergence and spread of antibiotic-resistant/tolerant pathogens. The discovery and development of new antibiotics have played a dominant role in these attempts. Nevertheless, the new types of antibiotics brought into clinical application since the 1990s are very limited (WHO, 2014; Hoagland et al., 2016), presumably due to both scientific and financial barriers. Besides developing new antibiotics, improving the efficacy of traditional antibiotics is an important strategy for combating antibiotic-resistant/tolerant pathogens (WHO, 2014; Trusts, 2016). Accordingly, advantages of this strategy include the good documentation of the toxicity, pharmacokinetics, administration, and mechanisms of action of traditional antibiotics.

In the last decade, many adjuvants have been reported to enhance the action of existing antibiotics. For instance, iron chelators (Moreau-Marquis et al., 2009), plant steroid tomatidine (Mitchell et al., 2012), glycerol monolaurate and lauric acid (Hess et al., 2014), resveratrol (Nohr-Meldgaard et al., 2018), and β-lactam aztreonam (Yu et al., 2012) were found to enhance the aminoglycoside tobramycin against different pathogens. Further, various metabolites, such as glucose and alanine, were found to facilitate aminoglycoside antibiotics to eradicate different pathogenic persister cells by enhancing proton motive force (PMF)-dependent aminoglycoside uptake (Allison et al., 2011; Barraud et al., 2013; Peng et al., 2015; Meylan et al., 2017; Su et al., 2018). Notably, rhamnolipids, synthesized by *Pseudomonas aeruginosa*, potentiate aminoglycoside against *Staphylococcus aureus* persisters by enhancing aminoglycoside uptake in a PMF-independent manner (Radlinski et al., 2019).

Indole, an interkingdom signaling molecule, has important biological functions in bacteria and animals (Lee and Lee, 2010). For instance, it has been shown to increase the antibiotic tolerance of *Escherichia coli* cells (Lee et al., 2010; Han et al., 2011; Vega et al., 2013), likely by activating stress response-related pathways (Vega et al., 2012) and/or upregulating the expression of antibiotic-efflux pump genes (Hirakawa et al., 2005). Conversely, several studies have revealed that indole is able to reduce the antibiotic tolerance of *E. coli* (Hu et al., 2015; Kwan et al., 2015) and *Lysobacter enzymogenes* (Han et al., 2017; Wang et al., 2019), highlighting its potential as an adjuvant for antibiotic potentiation. In particular, halogenated indoles are even able to directly eradicate bacterial persister cells and biofilms (Lee et al., 2016). These studies suggest that indole may exert diverse effects under antibiotic challenge conditions in the context of growth conditions and cell status.

We recently reported that hypoionic shock (i.e., shock with an ion-free solution) could markedly facilitate aminoglycosides to kill stationary-phase *E. coli* cells, but exhibited limited effects against stationary-phase *S. aureus* cells (Jiafeng et al., 2015) and triggered *S. aureus* persister cells (Chen et al., 2019). We sought to enhance the efficacy of this unique approach against *S. aureus* persister cells. Here we found that not only *S. aureus* but also several gram-positive pathogens could be killed by a short, combined treatment using aminoglycoside and indole derivatives, with 5-methylindole (5M-indole) being the most potent. Our study may open an avenue to develop new strategies against gram-positive pathogens.

MATERIALS AND METHODS

Bacterial Strains, Medium, and Reagents

Various gram-positive and gram-negative bacterial strains were used in this study (refer to **Table S1**). Over-night culture of each strain was diluted at 1:500 in Luria-Bertani (LB) medium (Note: MRS medium was used for *L. lactis* and *E. faecalis*) and agitated in a shaker (37°C, 220 rpm) for 3–6 and 20–24 h to prepare exponential-phase and stationary-phase cells, respectively. Aminoglycoside antibiotics are described in **Table S2**. Carbonyl cyanide m-chlorophenylhydrazone (CCCP) was purchased from Sigma-Aldrich. All other chemical reagents are of analytical purity. Indole, 2M-indole, 5M-indole and paraben, as dissolved in DMSO solution, were stocked in brown, opaque Eppendorf tubes to avoid photo-induced damage.

Aminoglycoside Potentiation by Indole Under Hypoionic Condition

Briefly, 100 μL cell cultures were centrifuged (12, 000, *g*, 1 min) in Eppendorf tube and the supernatant was completely removed. Cell pellets were re-suspended and thoroughly mixed with the working solution, which was prepared by dissolving aminoglycoside antibiotic plus indole, 2M-indole, 5M-indole or paraben in pure water at concentrations as described in **Table S2**. Cell suspension was kept at room temperature for 5 min before washing twice with phosphate-buffered saline (PBS: 0.27 g/L KH_2PO_4, 1.42 g/L Na_2HPO_4, 8 g/L NaCl, 0.2 g/L KCl, pH 7.4), and then 4 μL of 10-fold serially diluted cell suspension were spot plated onto LB agar dishes for cell survival assay. Cycled combined treatments were performed by washing the treated cells with PBS once and then subjected to another round of treatment. The effect of salts and EDTA was examined by re-suspending the cell pellets with the working solution containing NaCl, KCl, $MgCl_2$, $BaCl_2$, $CaCl_2$, or EDTA at various concentrations.

Preparation and Eradication of Antibiotic-Tolerant *S. aureus* Persister Cells

ATP depletion-associated persisters were prepared by agitating *S. aureus* stationary-phase cell culture in the presence of 100 μM protonophore CCCP or 15 μM NaN_3 for 1 h, and cells were then treated with the working solution containing CCCP or NaN_3 at corresponding concentrations. Nutrient shift-induced persisters were prepared as previously reported (Radzikowski et al., 2016; Chen et al., 2019). Starvation-induced persisters were prepared as previously reported (Eng et al., 1991; Chen et al., 2019). Tobramycin-tolerant persister cells were prepared by adding tobramycin at a final concentration of 500 μg/mL into *S. aureus* stationary-phase cell culture and further agitating for 1 h prior to the combined treatment.

Intracellular ATP Level Assay

A luciferase-based kit (BacTiter-Glo™ Microbial Cell Viability Assay, Promega Corporation, USA; Cat.# G8093) was used to measure ATP level according to the manufacturer's instruction. Briefly, *S. aureus* persister cells, with or without pretreatment of 100 μM CCCP or 15 μM NaN_3 for 1 h, was lysed using the lysis buffer and centrifuged (12, 000, *g*, 4°C, 5 min). The supernatant was quickly mixed with the working solution at equal volumes and then transferred into a 96-well plate before light recording on a FLUOstar Omega Microplate Reader using the Luminometer method.

Animal Experiments

A skin acute wound model was applied to test the *in vivo* efficacy of the combined treatment by referring to an earlier report (Davidson, 1998). Briefly, 8-week-old ICR male mice (around 28 g) were purchased from the Animal Center of

Fujian Medical University and maintained in the Animal Center of Fujian Normal University. Mice were housed for 1 or 2 days and then randomly divided into four groups for surgery experiments (Group A: treatment with 0.9% NaCl solution; Group B: treatment with tobramycin in 0.9% NaCl solution; Group C: treatment with tobramycin in pure water; Group D: treatment with tobramycin and 5M-indole in pure water; $n = 3$). Mice were anesthetized by intraperitoneal injection of 4% chloral hydrate, barbered on the right back and sterilized, and then a 1 cm × 1 cm whole skin section was removed to make an acute skin wound. Five microliter of 10-fold-concentrated stationary-phase *S. aureus* cells were seeded on the wound and fully absorbed before adding 120 μL working solution (4 mM 5M-indole plus 100 μg/mL tobramycin) and further incubating for 5 min. Residue solution was removed by absorbing with medical cotton and then subjected to another round of the combined treatment. The whole muscle on the wound site was removed and homogenized, with the lysates being spot-plated on LB agar dishes for bacterial survival assay.

Ethics

The animal use protocol was approved by the Animal Ethical and Welfare Committee of Fujian Normal University (approval No.: IACUC 20190006) and performed in accordance with the U.K. Animals (Scientific Procedures) Act, 1986 and associated guidelines, EU Directive 2010/63/EU for animal experiments, as well as with the National Standards of the People's Republic of China (GB/T 35892-2018: Laboratory animals-Guideline for ethical review of animal welfare; GB/T 35823-2018: Laboratory animals-General requirements for animal experiment).

Statistics

CFU (colony-forming units) on LB agar dishes were counted and cell density was calculated according to the dilution fold and volume of cell suspension droplet. Quantitative data, as calculated by Microsoft Excel, represent means ± SD of three replicates from one independent experiment; independent experiments were repeated at least three times. A statistical analysis was performed in the MicroOrigin software using the ANOVA algorithm at a significance level of 0.05.

RESULTS

Respective Potentiating and Suppressive Effects of 5M-Indole on Tobramycin Against Stationary- and Exponential-Phase *S. aureus* Cells Under Hypoionic Conditions

We first confirmed that the aminoglycoside antibiotics tobramycin, gentamicin, and kanamycin, when dissolved in pure water, but not in NaCl containing solution, were all able to effectively and rapidly (within a few minutes) kill stationary-phase *E. coli* cells (**Figure S1A**) but only had a limited lethal effect on stationary-phase *S. aureus* cells (**Figure S1B**). We sought to improve the efficacy of hypoionic shock-induced aminoglycoside potentiation by adding paraben, indole, 2-methylindole (2M-indole), or 5-methylindole (5M-indole).

We found that a 5-min combined treatment with tobramycin plus each adjuvant could eradicate stationary-phase *S. aureus* cells (left part in **Figure 1A**). In particular, no colony forming units (CFUs) were detected on LB dishes after the cells underwent the combined treatment three times (left part in **Figure 1B**), indicating that the number of viable cells was reduced by more than six orders of magnitude. In comparison, treatments with each adjuvant alone for three times did not kill the cells (**Figure S1C**). As expected, the presence of NaCl in the working solution significantly suppressed such tobramycin potentiation by paraben and indole (right parts in **Figures 1A,B**).

We also examined the effects of indole on other aminoglycoside antibiotics (streptomycin, gentamicin, and kanamycin). We found that they were hardly enhanced by indole, 2M-indole, 5M-indole, or paraben against *S. aureus* cells (**Figure S2A**). Similar observations were made with stationary-phase cells of other *S. aureus* strains, with gentamicin and kanamycin being slightly potentiated (**Figures S2B**, **S2C**). These results suggest that 5M-induced potentiation against *S. aureus* cells is largely specific to tobramycin. In addition, we examined β-lactams (mecillinam and meropenem) and fluoroquinolones (ofloxacin and ciprofloxacin), two types of commonly used bactericidal antibiotics. We found (i) that indole and 2M-indole potentiated ciprofloxacin, but not mecillinam, meropenem, and ofloxacin, by about one order of magnitude against stationary-phase *S. aureus* cells and (ii) that 5M-indole exhibited stronger potentiating effects, of around two orders of magnitude (**Figure S2D**). These observations suggest that 5M-indole-induced potentiation is largely specific to aminoglycosides.

Strikingly, we observed suppressive effects of each adjuvant on the action of tobramycin against exponential-phase *S. aureus* cells, i.e., they all suppressed the hypoionic shock-induced tobramycin potentiation to a certain degree (**Figure 1C**). Prompted by these observations, we examined the effects of these adjuvants on the action of tobramycin against stationary-phase *S. aureus* cells at different culturing time points. When the cells were cultured for 12, 16, 20, and 24 h and subsequently subjected to the combined treatment, the hypoionic shock-induced tobramycin potentiation was additively reduced, but each adjuvant was able to enhance the potentiation in each sample, with 5M-indole being the most potent (**Figure 1D**).

5M-Indole Potentiates Tobramycin Against Stationary-Phase *S. aureus* Cells in a Time- and Dose-Dependent Manner

We next examined the time and dose dependency of the combined treatment. The stationary-phase *S. aureus* cells grown in LB medium for 16 h were subjected to the combined treatment for varying lengths of time. The cell survival assay revealed that 1- or 3-min combined treatment already reached a maximum killing efficiency (except for the 1-min combined treatment with paraben) (**Figure 2A**), and extension

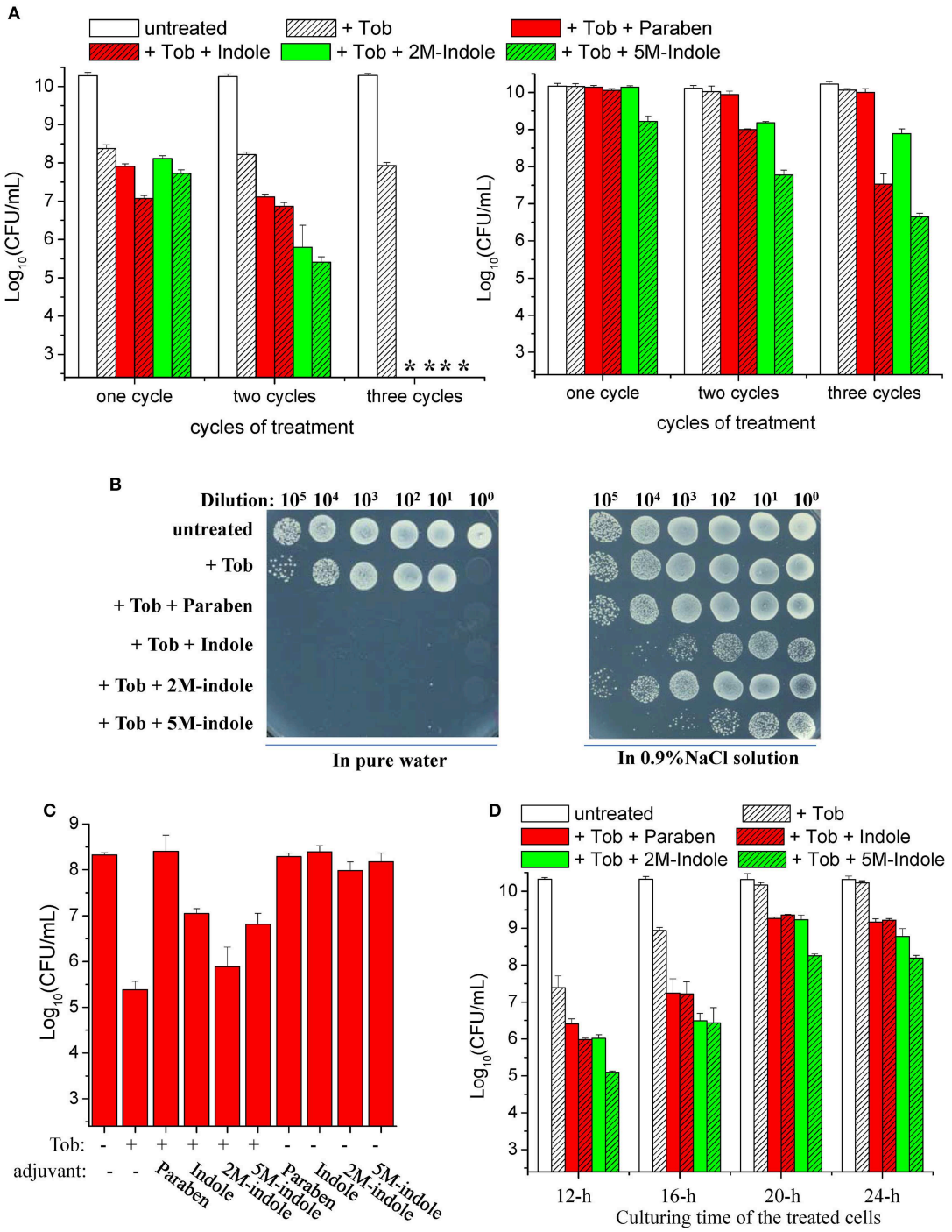

FIGURE 1 | Indole derivatives potentiate tobramycin against stationary-phase *S. aureus*. **(A,B)** Survival of stationary-phase *S. aureus* following three cycles of 5-min treatment with 500 μg/ml tobramycin (Tob) plus 4 mM indicated adjuvant dissolved (left) in pure water or (right) in 0.9% NaCl solution. After centrifugation and complete removal of the supernatant, cell pellets were resuspended with the working solution and incubated for 5 min before spots were plated on LB agar dishes to count CFUs. **(A)** Quantitative results. The asterisk (*) means CFUs were undetectable. **(B)** Original cell survival results on dishes. Cycled treatment was performed by washing the treated cells with PBS once before the following round of treatment. $P<0.001$ for the majority of the values indicated and $P < 0.01$ for 2M-indol. **(C,D)** Survival of **(C)** exponential-phase ($OD_{600} \approx 0.6$) and **(D)** stationary-phase *S. aureus* cells following 5 min treatment with **(C)** 100 μg/ml or **(D)** 500 μg/ml Tob plus 4 mM indicated adjuvant dissolved in pure water. **(D)** Stationary-phase cells at different culturing time points were examined. Data represent the mean ± SD of three replicates, with independent experiments being performed at least three times.

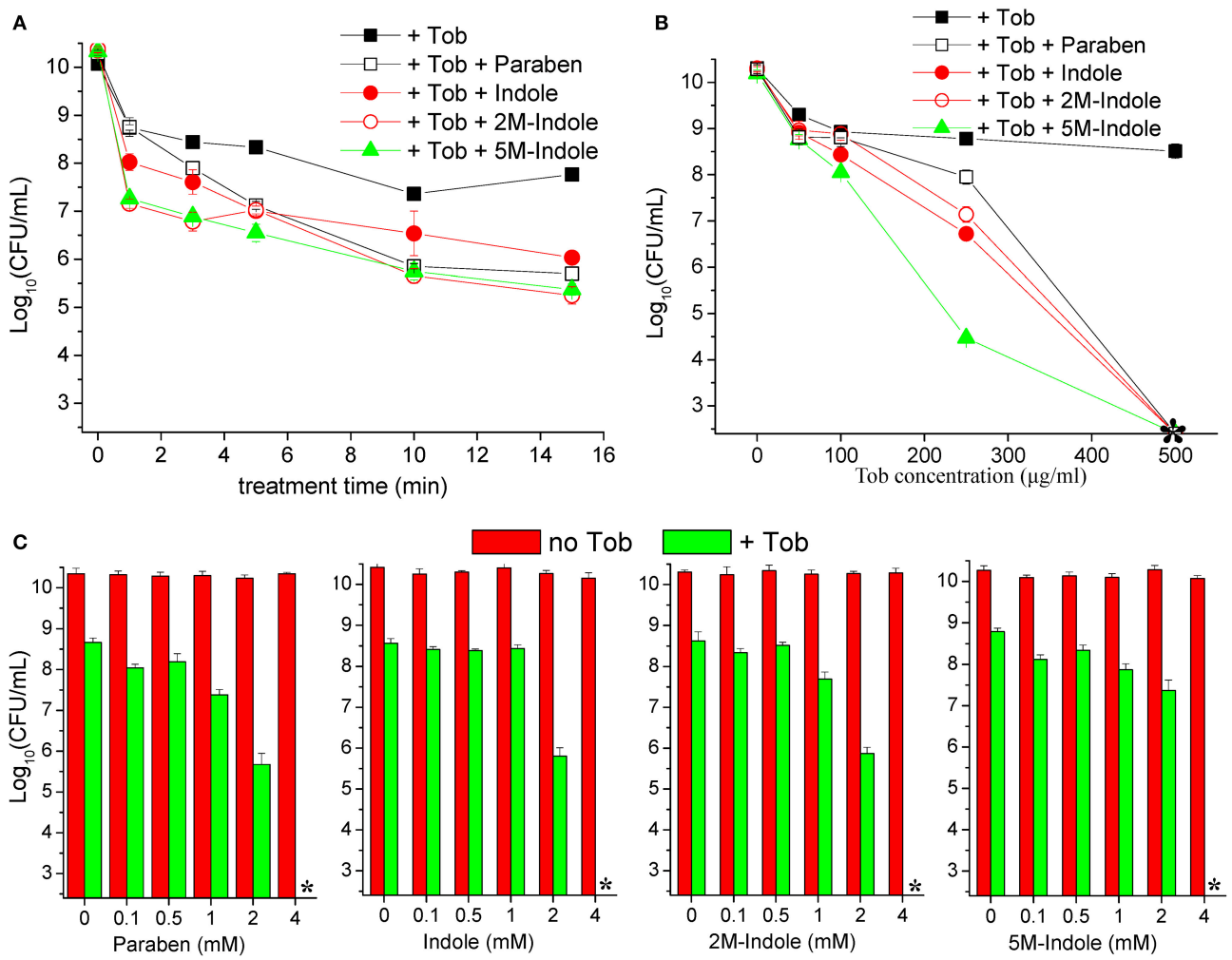

FIGURE 2 | Indole derivatives potentiate tobramycin against stationary-phase *S. aureus* in a time- and dose-dependent manner. **(A)** Survival of stationary-phase *S. aureus* (from 16 h cultures) following treatment with 500 μg/ml tobramycin (Tob) plus 4 mM indicated adjuvant for varying lengths of time. **(B,C)** Survival of stationary-phase *S. aureus* following three cycles of 5-min treatment with **(B)** varying concentrations of Tob plus 4 mM indicated adjuvant or **(C)** 500 μg/ml Tob plus varying concentrations of adjuvant. Data represent the mean ± SD of three replicates, with independent experiments being performed at least three times. The asterisk (*) means CFUs were undetectable.

of the treatment from 3 to 15 min only resulted in a limited increase in the killing efficiency. This observation indicates that tobramycin potentiation by these adjuvants can be achieved within a couple of minutes. As expected, such potentiation depends on the concentration of tobramycin. Specifically, weak potentiation was observed when the tobramycin concentration was below 100 μg/ml, and significant potentiation was detected at tobramycin concentrations above 250 μg/ml (**Figure 2B**). When 250 μg/ml tobramycin was used, 5M-indole and paraben were again the most and the least potent, respectively. In particular, no CFUs were detected on LB dishes when the cells were treated with 500 μg/ml tobramycin plus 4 mM adjuvant (indicated by an asterisk in **Figure 2B**). Furthermore, each adjuvant was found to reinforce tobramycin in a concentration-dependent manner (**Figure 2C**).

5M-Indole Potentiates Tobramycin and Streptomycin Killing of Antibiotic-Tolerant *S. aureus* Persisters and MRSA Cells

Stationary-phase *S. aureus* cells, which are highly tolerant to bactericidal antibiotics (Keren et al., 2004), are usually considered as one type of *S. aureus* persisters (Allison et al., 2011; Wang et al., 2018). Therefore, our aforementioned observations suggested that 5M-indole enables aminoglycosides to kill *S. aureus* persisters. To confirm this, we tested other types of *S. aureus* persisters. We omitted paraben, because it is less potent than indole, 2M-indole, and 5M-indole (**Figures 2A,B**).

The ATP level is critical for bacterial persistence (Conlon et al., 2016; Shan et al., 2017; Pu et al., 2019). Therefore, we first examined ATP depletion-associated *S. aureus* persisters (Conlon et al., 2016) which were prepared by pretreating *S.*

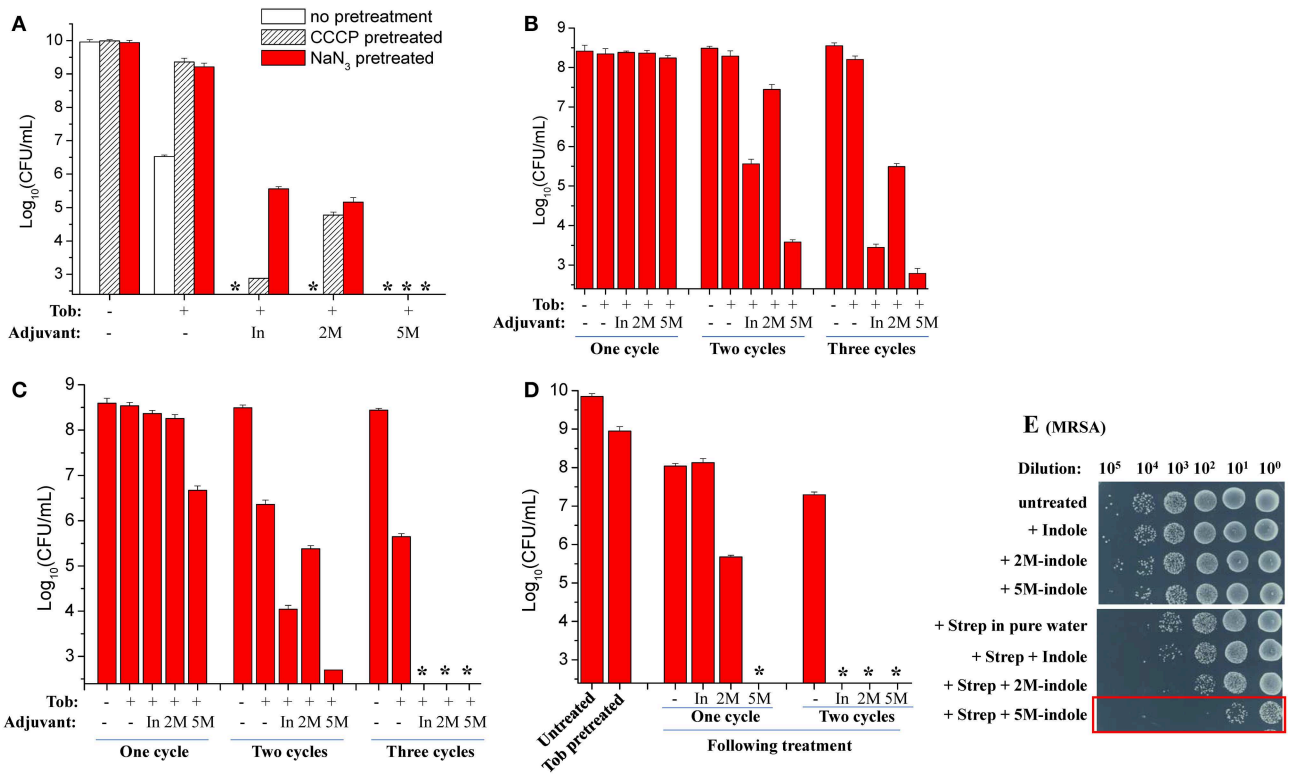

FIGURE 3 | 5M-indole potentiates tobramycin against *S. aureus* persisters and streptomycin against MRSA. **(A–D)** Survival of **(A)** ATP depletion-associated, **(B)** nutrient shift-induced, **(C)** starvation-induced, and **(D)** tobramycin (Tob)-tolerant *S. aureus* persister cells following cycled 5-min treatments with Tob plus 4 mM adjuvant (indole, 2M-indole, or 5M-indole) dissolved in pure water. In, indole; 2M, 2M-indole; 5M, 5M-indole. **(A)** Stationary-phase cells (from 12 h cultures) were pretreated with 100 μM CCCP or 15 μM NaN_3 for 1 h prior to two cycles of treatments with 500 μg/ml Tob plus 4 mM adjuvant. **(B)** Exponential-phase cells (OD_{600} = 0.5–0.6) were transferred to fumarate containing M9 medium to prepare nutrient shift-induced persister cells, which were then subjected to cycled treatments with 100 μg/ml Tob plus 4 mM adjuvant. **(C)** Stationary-phase cells were transferred to yeast nitrogen broth medium without amino acids to prepare starvation-induced persister cells, which were then subjected to cycled treatments with 250 μg/ml Tob plus 4 mM adjuvant. **(D)** Stationary-phase cells were treated with 500 μg/ml Tob for 1 h under agitation at 37°C before being subjected to cycled treatments with 250 μg/ml Tob plus 4 mM adjuvant. For experimental details, refer to the Methods section. Data represent the mean ± SD of three replicates, with independent experiments being performed at least three times. The asterisk (*) means CFUs were undetectable. **(E)** Survival of stationary-phase MRSA cells following 5-min treatment with 7 mM adjuvant (indole, 2M-indole, or 5M-indole) plus 2,000 μg/ml streptomycin (Strep). MRSA cells (10 μl) were centrifuged and the cell pellets were resuspended in 100 μl working solution for treatment; MRSA cells without dilution were treated similarly (for the results see **Figure S4A**). It should be pointed out that 4 mM adjuvants exhibited little potentiating effect on Strep against MRSA cells (**Figure S4B**).

aureus cells with the protonophore CCCP for 1 h (Grassi et al., 2017). The cell survival assay revealed that CCCP pretreatment only exhibited marginal suppressive effects on indole- or 2M-indole-induced tobramycin potentiation and had little effect on 5M-indole-induced potentiation (**Figure 3A**). In line with these observations, NaN_3 (an inhibitor of the electron transport chain), although it marginally suppressed indole- or 2M-indole-induced tobramycin potentiation, had no effects on 5M-indole-induced potentiation (**Figure 3A**). We confirmed that pretreatment with CCCP or NaN_3 did significantly decrease the intracellular ATP level of *S. aureus* cells (**Figure S3A**). These results thus suggest 5M-indole-induced tobramycin potentiation could kill ATP depletion-associated *S. aureus* persisters, largely in a PMF-independent manner.

Second, we examined nutrient shift-induced *S. aureus* persisters by switching the carbon source of exponential-phase *S. aureus* cells to fumarate (Radzikowski et al., 2016). Such *S. aureus* persister cells exhibited high tolerance to tobramycin under conventional treatment conditions (**Figure S3B**). However, they could be effectively killed by two or three cycles of combined treatment with tobramycin plus indole or 5M-indole, with 2M-indole being less effective (**Figure 3B**).

Third, we examined starvation-induced *S. aureus* persisters by transferring stationary-phase *S. aureus* cells to medium without any nutrients (Chen et al., 2019). Such starvation-induced *S. aureus* persister cells were hardly killed by tobramycin under conventional treatment condition (**Figure S3C**). However, approximately 99% of the cells were killed by one cycle of combined treatment with tobramycin plus 5M-indole, and two or three cycles of treatments could further kill the persisters, with indole being the least potent (**Figure 3C** and **Figure S3D**).

Lastly, we directly examined antibiotic-tolerant cells, which were selected by agitating a stationary-phase *S. aureus* cell culture with supralethal (500 μg/ml) tobramycin concentrations for 1 h. The cell survival assay revealed that around 90% of cells present in the stationary-phase culture were tolerant to the

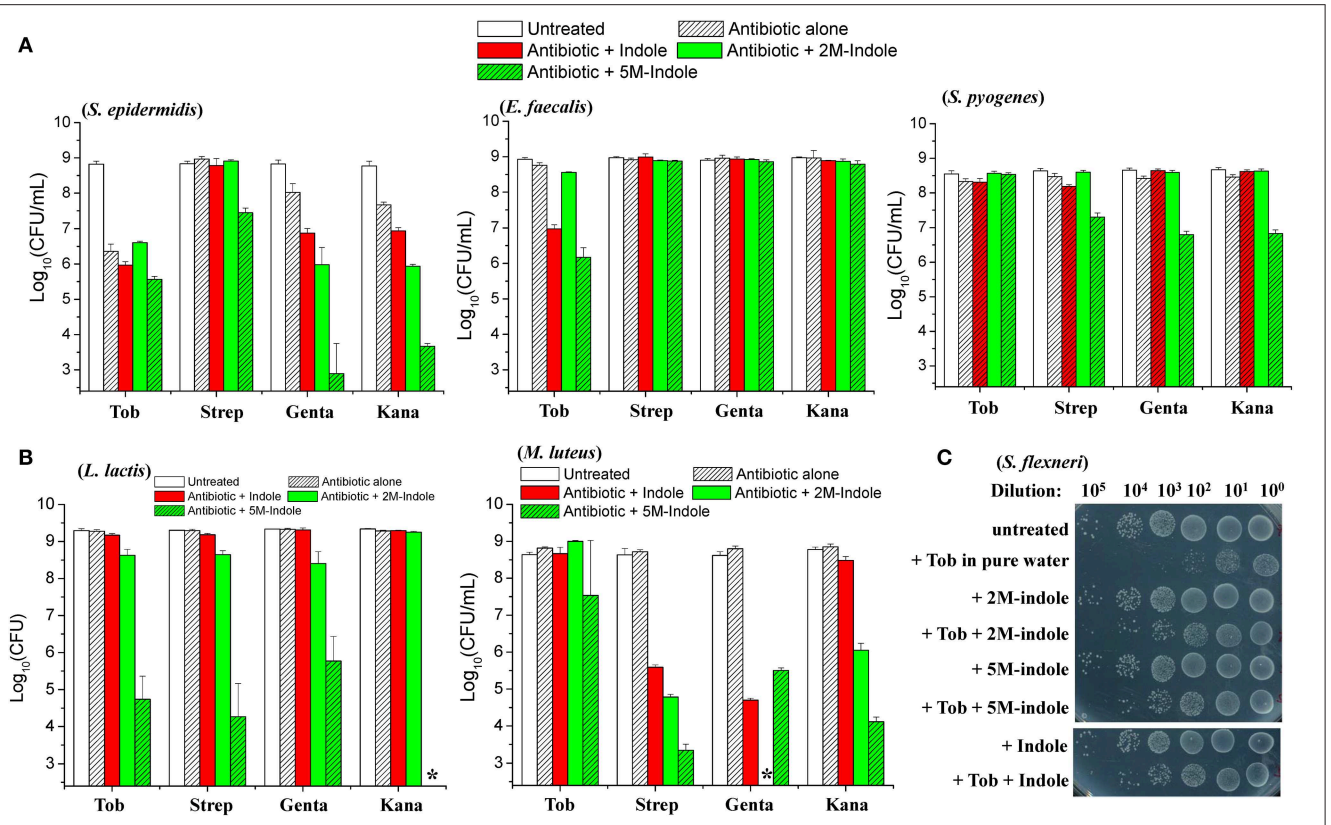

FIGURE 4 | 5M-indole potentiates aminoglycosides against many strains of gram-positive bacteria, including MRSA, but not gram-negative bacteria. **(A,B)** Survival of stationary-phase cells of indicated bacterial strains following 5-min treatment with 10 mM adjuvant (indole, 2M-indole, or 5M-indole) plus 500 μg/ml tobramycin (Tob), 2,000 μg/ml streptomycin (Strep), 500 μg/ml gentamycin (Genta), or 1,000 μg/ml kanamycin (Kana) dissolved in pure water. Data represent the mean ± SD of three replicates, with independent experiments being performed at least three times. **(C)** Survival of stationary-phase *S. flexneri* following 5-min treatment with 1 mM adjuvant plus 200 μg/ml Tob dissolved in pure water. Similar results for *E. coli* are shown in **Figure S6E**. The asterisk (*) means CFUs were undetectable.

1 h tobramycin treatment, and that such tobramycin-tolerant persisters cells could be completely killed by the combined treatment with tobramycin plus 5M-indole (indicated by the asterisk in **Figure 3D** and **Figure S3E**), with indole and 2M-indole being less effective. One more cycle of the combined treatment with indole and 2M-indole completely eradicated the persisters (**Figure 3D** and **Figure S3E**). Collectively, these observations demonstrate that 5M-indole is highly potent in potentiating tobramycin to kill various types of antibiotic-tolerant *S. aureus* persister cells, with indole and 2M-indole being less effective.

In addition, we demonstrate that the combined treatment is able to kill methicillin-resistant *S. aureus* (MRSA), which is listed as one of most dangerous bacterial pathogens by the WHO (WHO, 2014, 2017). The cell survival assay showed that only three cycles of combined treatments with streptomycin plus 5M-indole exerted certain lethal effects on stationary-phase MRSA cells (red frame, **Figure S4A**). We then diluted the MRSA cells 10-fold before treating them once, and found that around 99.9% of the MRSA cells were killed by the combined treatment with streptomycin plus 5M-indole (red frame, **Figure 3E**), while only 90% of the cells were killed by streptomycin alone. It should be pointed out that the concentration of adjuvants used in this assay was 7 mM, and that 4 mM adjuvants exhibited no or limited potentiating effects (**Figure S4B**).

5M-Indole Potentiates Aminoglycosides Against Many Strains of Gram-Positive Bacteria but Not Gram-Negative Bacteria

We next examined whether indole could potentiate aminoglycoside antibiotics against other bacterial strains than *S. aureus*. When in the exponential-phase stage, these bacteria exhibit varying sensitivity to the aminoglycoside antibiotics tobramycin, streptomycin, gentamicin, and kanamycin (**Figure S5**). Regarding the gram-positive pathogens *Staphylococcus epidermidis*, *Enterococcus faecalis*, and *Streptococcus pyogenes*, we found that (i) indole, 2M-indole, and 5M-indole reinforced gentamicin and kanamycin against *S. epidermidis* (left part in **Figure 4A**); (ii) indole and 5M-indole potentiated tobramycin against *E. faecalis* (middle part in **Figure 4A**); and (iii) 5M-indole potentiated streptomycin, gentamicin, and kanamycin against *S. pyogenes* (right part in **Figure 4A**). We also examined two industrial,

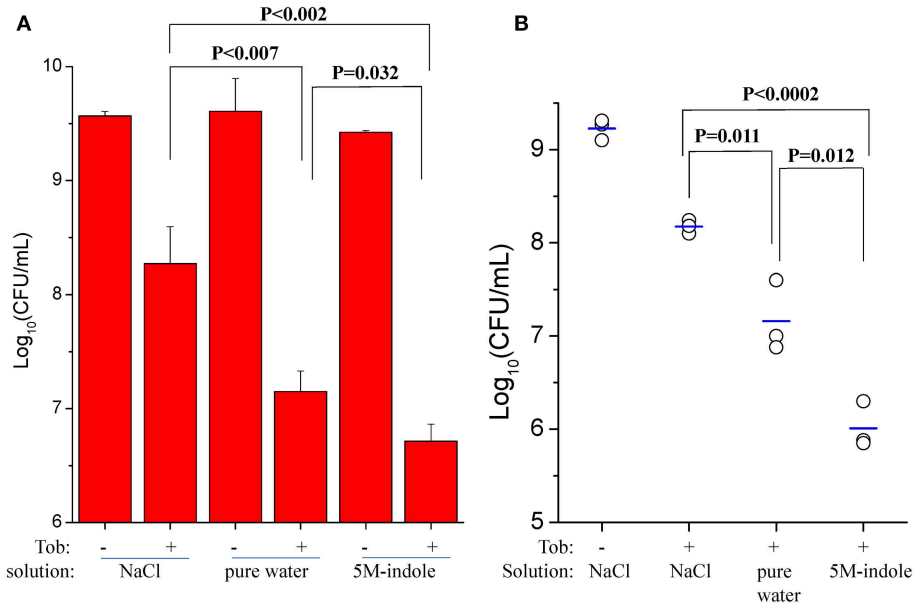

FIGURE 5 | 5M-indole potentiates tobramycin against *S. aureus* in mice. **(A,B)** Survival of stationary-phase *S. aureus* in **(A)** isolated mouse skin or **(B)** wounds in mice following 5-min treatment with 100 μg/ml tobramycin (Tob) and 5M-indole dissolved in NaCl solution or pure water. Data represent the mean ± SD of three replicates, with independent experiments being performed at least three times. For experimental details, please refer to the Methods section.

non-pathogenic gram-positive bacterial strains, *Micrococcus luteus* and *Lactococcus lactis*, and found that (i) all these aminoglycosides were potentiated by 5M-indole to kill *L. lactis* (left part of **Figure 4B**); and (ii) streptomycin, gentamicin, and kanamycin were potentiated by 2M-indole and 5M-indole to kill *M. luteus* (right part of **Figure 4B**). It should be pointed out that the concentration of adjuvants used in these assay is 10 mM, and that 4 mM adjuvants exhibited no (**Figures S6A–S6C**) or limited (**Figure S6D**) potentiating effects.

Lastly, we examined two gram-negative bacteria. Unexpectedly, indole, 2M-indole, and 5M-indole all effectively suppressed the bactericidal action of tobramycin against stationary-phase *Shigella flexneri* (**Figure 4C**) and *E. coli* (**Figure S6E**) under hypoionic condition. Prompted by these observations, we further examined exponential-phase *E. coli* cells and observed similar suppressive effects (**Figure S6F**). These observations on different bacterial strains, though not exhaustive, indicate that 5M-indole is able to enhance the hypoionic shock-induced tobramycin potentiation against gram-positive bacteria in the stationary phase, but suppresses the potentiating effect against gram-positive bacteria in the exponential phase and against gram-negative bacteria in both phases.

5M-Indole Potentiates Tobramycin Against *S. aureus* Persisters in Mice

We also investigated whether 5M-indole is able to facilitate aminoglycoside antibiotics to eradicate *S. aureus* cells in animals. First, we removed skin from sacrificed mice and then placed stationary-phase *S. aureus* cells on the skin before subjecting them to the combined treatment. The cell survival assay showed that tobramycin dissolved in pure water killed the *S. aureus* cells more effectively than it did in 0.9% NaCl solution ($P < 0.007$, **Figure 5A** and **Figure S7A**), demonstrating the hypoionic shock-induced tobramycin potentiation under *ex vivo* conditions. More importantly, the presence of 5M-indole could further enhance tobramycin against *S. aureus* in comparison with tobramycin treatment alone ($P = 0.035$, **Figure 5A**).

Second, we utilized an acute skin wound model (Davidson, 1998) to measure the *in vivo* efficacy of the combined treatment. To this end, a piece of skin of 1 cm × 1 cm was removed from the right back of anesthetized mice (**Figure S7B**), and *S. aureus* cells were placed on the wound before subjecting the mice to the combined treatment. Initially, we analyzed stationary-phase *S. aureus* cells and observed a marginal potentiating effect of 5M-indole on tobramycin (**Figure S7C**). Then we analyzed ATP depletion-associated *S. aureus* persister cells as induced by CCCP pretreatment (**Figure 3A**), and found that 5M-indole significantly enhanced the bactericidal action of tobramycin ($P = 0.012$, **Figure 5B** and **Figure S7D**). Again, tobramycin dissolved in pure water killed the cells more much efficiently than it did in NaCl solution ($P = 0.011$, **Figure 5B**).

Effective Abolishment of 5M-Indole-Induced Tobramycin Potentiation Against *S. aureus* by Cations and EDTA

We attempted to dissect the biochemical mechanisms underlying this unique 5M-indole-induced tobramycin potentiation against stationary-phase *S. aureus* cells. Considering that the absence of electrolyte is a prerequisite for the

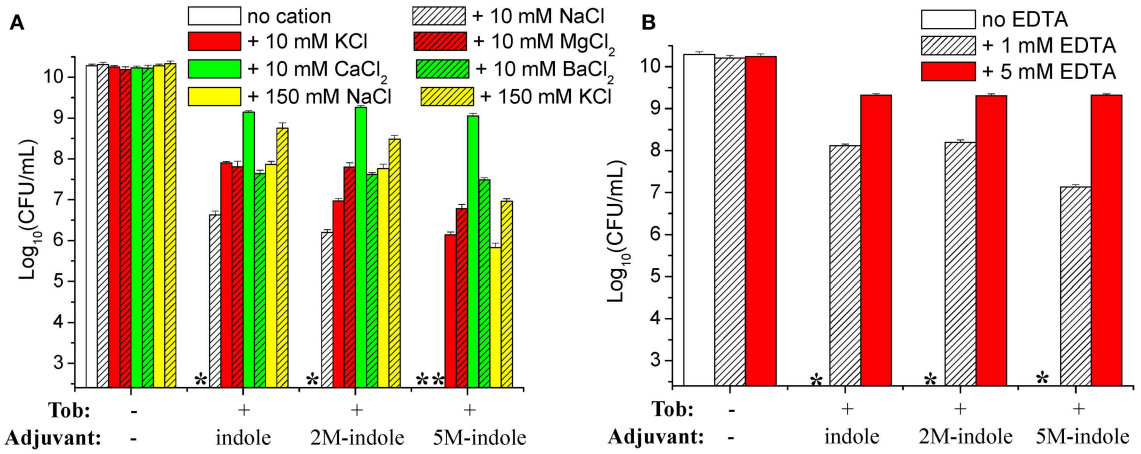

FIGURE 6 | Salts and EDTA effectively abolish 5M-indole-induced tobramycin potentiation against *S. aureus*. **(A,B)** Survival of stationary-phase *S. aureus* following three cycles of 5-min treatment with 500 μg/ml tobramycin (Tob) plus 4 mM adjuvant (indole, 2M-indole, or 5M-indole) dissolved in pure water, in the absence or presence of **(A)** indicated salts or **(B)** EDTA. Data represent the mean ± SD of three independent experiments. The asterisk (*) means CFUs were undetectable.

hypoionic shock-induced aminoglycoside potentiation, as we reported previously (Jiafeng et al., 2015), and the presence of 0.9% NaCl significantly suppressed 5M-indoled-induced tobramycin potentiation (right parts in **Figures 1A,B**), we systematically examined the effects of salts.

The cell survival assay revealed that the presence of 10 mM KCl, $MgCl_2$, $CaCl_2$, or $BaCl_2$ in the treatment solution effectively suppressed indole-, 2M-indole-, or 5M-indole-induced tobramycin potentiation against *S. aureus* cells, with $CaCl_2$ being the most potent (**Figure 6A**). Notably, the presence of 10 mM NaCl significantly suppressed tobramycin potentiation by indole or 2M-indole, but not that by 5M-indole (indicated by the fourth asterisk in **Figure 6A**), and the presence of 150 mM NaCl or KCl significantly suppressed 5M-indole-induced tobramycin potentiation.

If the presence of $MgCl_2$, $CaCl_2$, or $BaCl_2$ can suppress indole-induced tobramycin potentiation, can the absolute absence of them enhance such potentiation? We examined this question by treating the cells with solutions containing EDTA, a divalent cation chelator. Unexpectedly, the cell survival assay revealed that the presence of 1 mM or 5 mM EDTA almost abolished the tobramycin potentiation by indole, 2M-indole, and 5M-indole (**Figure 6B**). The mechanisms underlying this EDTA-mediated suppressive effect were not investigated in this study; we hypothesize it results from the disturbing effect of EDTA on the cell envelope of *S. aureus* cells (Felix, 1982; Hancock, 1984).

DISCUSSION

Several notable findings have been made in this study. First, indole derivatives are able to effectively and rapidly potentiate aminoglycoside killing of antibiotic-tolerant *S. aureus* persister cells, MRSA cells, and other gram-positive pathogens, with 5M-indole being the most potent. Second, 5M-indole-induced potentiation is largely independent of the PMF. Third, 5M-indole facilitates aminoglycoside to kill *S. aureus* in a mouse model. These findings may guide the development of indole derivatives as adjuvants for aminoglycoside potentiation against gram-positive pathogens.

Our approach differs from earlier reports in several aspects (Lee et al., 2010; Han et al., 2011; Vega et al., 2012, 2013; Hu et al., 2015; Kwan et al., 2015; Wang et al., 2019). First, 5M-induced aminoglycoside potentiation is achieved within a couple of minutes. In contrast, bacterial eradication by a combined treatment with indole and antibiotics under conventional conditions takes a couple of hours (Hu et al., 2015; Han et al., 2017; Wang et al., 2019). Second, salts are able to abolish the potentiating effect. In other words, the absence of ions is a prerequisite for such aminoglycoside potentiation. Third, the potentiating effect is largely independent of the PMF; the PMF is well-known to be indispensable for aminoglycoside actions under conventional treatment conditions (as reviewed in Taber et al., 1987) and also for metabolite-stimulated aminoglycoside potentiation (Allison et al., 2011; Barraud et al., 2013; Peng et al., 2015; Meylan et al., 2017; Su et al., 2018). In this regard, indole-induced aminoglycoside potentiation represents a unique mechanism. Notably, Conlon and colleagues recently reported that rhamnolipid-induced aminoglycoside potentiation was also independent of the PMF and only effective against gram-positive, but not gram-negative, pathogens (Radlinski et al., 2019), in agreement with our present findings. Nevertheless, this approach, as the metabolite-based approach, takes several hours to achieve a significant potentiating effect.

Indole, an endogenous metabolite in many bacteria, has multiple and diverse roles in signaling (Lee et al., 2010), and it even mediates the signaling between enteric bacteria and

their mammalian host (Bansal et al., 2010). Opposite effects of indole on the antibiotic resistance of bacteria have been reported previously. For instance, indole was shown to increase (Lee et al., 2010; Han et al., 2011; Vega et al., 2012, 2013) or decrease (Hu et al., 2015; Kwan et al., 2015) the antibiotic tolerance of *E. coli*, depending on experimental conditions. In addition, indole was recently reported to dramatically reduce the antibiotic resistance of *L. enzymogenes* at the early exponential phase, but it exhibited little effect on the same bacterium in late exponential and stationary phases (Wang et al., 2019). In our study, indole derivatives appeared to potentiate aminoglycoside only against stationary-phase gram-positive bacteria under hypoionic conditions but they suppressed the effects of aminoglycosides against gram-positive bacteria in exponential-phase stage and gram-negative bacteria in both stages. These distinct or opposite effects are likely linked to different signaling pathways or biomolecules, which are activated or inhibited by indole under different experimental conditions and/or bacterial statuses. Considering that 5M-indole only effectively potentiates tobramycin, but not other aminoglycosides, against *S. aureus* cells, it seems that such biomolecules have a certain preference toward different aminoglycoside antibiotics (**Figures S2A–S2C**).

The precise mechanisms underlying indole-induced aminoglycoside potentiation remain unclear. We speculate that such potentiation is linked to the bacterial cell membrane based on the following considerations. First, the potentiating effect was only observed in gram-positive bacteria, but not in gram-negative bacteria, which are different mainly in their cell membranes. Second, indole has been shown to be able to act as an ionophore to dissipate the PMF across the cell membrane (Chimerel et al., 2012). In addition, we found that EDTA, which is well-known to disintegrate the bacterial cell membrane (Felix, 1982; Hancock, 1984), abolished the potentiating effect (**Figure 6B**). Lastly, aminoglycosides have been shown to kill bacteria by inducing membrane protein aggregation and cell membrane damage (Davis et al., 1986). If the molecular mechanisms underlying indole-induced aminoglycoside potentiation can be dissected, certain indole derivatives may be developed that are able to potentiate aminoglycoside as effectively as 5M-indole but are inhibited by salts to a lower extent. Studies of the precise underlying mechanisms are currently underway in our laboratory.

DATA AVAILABILITY STATEMENT

All datasets generated for this study are included in the article/**Supplementary Material**.

ETHICS STATEMENT

The animal study was reviewed and approved by the Animal Ethical and Welfare Committee of Fujian Normal University.

AUTHOR CONTRIBUTIONS

XF designed the research. FS, MB, ZL, and BL performed the research. YG managed the project. XF and YW analyzed the data. XF wrote the paper.

FUNDING

This work was supported by research grants from the National Natural Science Foundation of China (Nos. 31972918, 31770830 and 31570778 to XF), the Natural Science Foundation of Fujian Province (No. 2018J01725 to XF), and the Scientific Research Innovation Team Construction Program of Fujian Normal University (Z1707219021).

ACKNOWLEDGMENTS

We thank Professor Luhua Lai and Dr. Xiaoyun Liu (both from Peking University) and Dr. Qingeng Huang (from Fujian Normal University) for their kindness in providing bacterial strains as described in **Table S1**.

SUPPLEMENTARY MATERIAL

The Supplementary Material for this article can be found online at: https://www.frontiersin.org/articles/10.3389/fcimb.2020.00084/full#supplementary-material

REFERENCES

Allison, K. R., Brynildsen, M. P., and Collins, J. J. (2011). Metabolite-enabled eradication of bacterial persisters by aminoglycosides. *Nature* 473, 216–220. doi: 10.1038/nature10069

Balaban, N. Q., Helaine, S., Lewis, K., Ackermann, M., Aldridge, B., Andersson, D. I., et al. (2019). Definitions and guidelines for research on antibiotic persistence. *Nat. Rev. Microbiol.* 17, 441–448. doi: 10.1038/s41579-019-0196-3

Bansal, T., Alaniz, R. C., Wood, T. K., and Jayaraman, A. (2010). The bacterial signal indole increases epithelial-cell tight-junction resistance and attenuates indicators of inflammation. *Proc. Natl. Acad. Sci. U.S.A.* 107, 228–233. doi: 10.1073/pnas.0906112107

Barraud, N., Buson, A., Jarolimek, W., and Rice, S. A. (2013). Mannitol enhances antibiotic sensitivity of persister bacteria in Pseudomonas aeruginosa biofilms. *PLoS ONE* 8:e84220. doi: 10.1371/journal.pone.0084220

Chen, Z., Gao, Y., Lv, B., Sun, F., Yao, W., Wang, Y., et al. (2019). Hypoionic shock facilitates aminoglycoside killing of both nutrient shift- and starvation-induced bacterial persister cells by rapidly enhancing aminoglycoside uptake. *Front. Microbiol.* 10:2028. doi: 10.3389/fmicb.2019.02028

Chimerel, C., Field, C. M., Pinero-Fernandez, S., Keyser, U. F., and Summers, D. K. (2012). Indole prevents Escherichia coli cell division by modulating membrane potential. *Biochim. Biophys. Acta* 18, 1590–1594. doi: 10.1016/j.bbamem.2012.02.022

Conlon, B. P., Rowe, S. E., Gandt, A. B., Nuxoll, A. S., Donegan, N. P., Zalis, E. A., et al. (2016). Persister formation in *Staphylococcus aureus* is associated with ATP depletion. *Nat. Microbiol.* 1:16051. doi: 10.1038/nmicrobiol.2016.51

Davidson, J. M. (1998). Animal models for wound repair. *Arch. Dermatol. Res.* 290, S1–S11. doi: 10.1007/PL00007448

Davis, B. D., Chen, L. L., and Tai, P. C. (1986). Misread protein creates membrane channels: an essential step in the bactericidal action of aminoglycosides. *Proc. Natl. Acad. Sci. U.S.A.* 83, 6164–6168. doi: 10.1073/pnas.83.16.6164

Eng, R. H., Padberg, F. T., Smith, S. M., Tan, E. N., and Cherubin, C. E. (1991). Bactericidal effects of antibiotics on slowly growing and nongrowing bacteria. *Antimicrob. Agents Chemother.* 35, 1824–1828. doi: 10.1128/AAC.35.9.1824

Felix, H. (1982). Permeabilized cells. *Anal. Biochem.* 120, 211–234. doi: 10.1016/0003-269790340-2

Grassi, L., Di Luca, M., Maisetta, G., Rinaldi, A. C., Esin, S., Trampuz, A., et al. (2017). Generation of persister cells of pseudomonas aeruginosa and staphylococcus aureus by chemical treatment and evaluation of their susceptibility to membrane-targeting agents. *Front. Microbiol.* 8:1917. doi: 10.3389/fmicb.2017.01917

Han, T. H., Lee, J. H., Cho, M. H., Wood, T. K., and Lee, J. (2011). Environmental factors affecting indole production in *Escherichia coli*. *Res. Microbiol.* 162, 108–116. doi: 10.1016/j.resmic.2010.11.005

Han, Y., Wang, Y., Yu, Y., Chen, H., Shen, Y., and Du, L. (2017). Indole-induced reversion of intrinsic multiantibiotic resistance in lysobacter enzymogenes. *Appl. Environ. Microbiol.* 83:e00995-17. doi: 10.1128/AEM.00995-17

Hancock, R. E. (1984). Alterations in outer membrane permeability. *Annu. Rev. Microbiol.* 38, 237–264. doi: 10.1146/annurev.mi.38.100184.001321

Hess, D. J., Henry-Stanley, M. J., and Wells, C. L. (2014). Antibacterial synergy of glycerol monolaurate and aminoglycosides in *Staphylococcus aureus* biofilms. *Antimicrob. Agents. Chemother.* 58, 6970–6973. doi: 10.1128/AAC.03672-14

Hirakawa, H., Inazumi, Y., Masaki, T., Hirata, T., and Yamaguchi, A. (2005). Indole induces the expression of multidrug exporter genes in Escherichia coli. *Mol. Microbiol.* 55, 1113–1126. doi: 10.1111/j.1365-2958.2004.04449.x

Hoagland, D. T., Liu, J., Lee, R. B., and Lee, R. E. (2016). New agents for the treatment of drug-resistant Mycobacterium tuberculosis. *Adv. Drug Deliv. Rev.* 102, 55–72. doi: 10.1016/j.addr.2016.04.026

Hu, Y., Kwan, B. W., Osbourne, D. O., Benedik, M. J., and Wood, T. K. (2015). Toxin YafQ increases persister cell formation by reducing indole signaling. *Environ. Microbiol.* 17, 1275–1285. doi: 10.1111/1462-2920.12567

Jiafeng, L., Fu, X., and Chang, Z. (2015). Hypoionic shock treatment enables aminoglycosides antibiotics to eradicate bacterial persisters. *Sci. Rep.* 5:14247. doi: 10.1038/srep14247

Keren, I., Kaldalu, N., Spoering, A., Wang, Y., and Lewis, K. (2004). Persister cells and tolerance to antimicrobials. *FEMS Microbiol. Lett.* 230, 13–18. doi: 10.1016/S0378-109700856-5

Kwan, B. W., Osbourne, D. O., Hu, Y., Benedik, M. J., and Wood, T. K. (2015). Phosphodiesterase DosP increases persistence by reducing cAMP which reduces the signal indole. *Biotechnol. Bioeng.* 112, 588–600. doi: 10.1002/bit.25456

Lee, H. H., Molla, M. N., Cantor, C. R., and Collins, J. J. (2010). Bacterial charity work leads to population-wide resistance. *Nature* 467, 82–85. doi: 10.1038/nature09354

Lee, J. H., Kim, Y. G., Gwon, G., Wood, T. K., and Lee, J. (2016). Halogenated indoles eradicate bacterial persister cells and biofilms. *AMB Exp.* 6:123. doi: 10.1186/s13568-016-0297-6

Lee, J. H., and Lee, J. (2010). Indole as an intercellular signal in microbial communities. *FEMS Microbiol. Rev.* 34, 426–444. doi: 10.1111/j.1574-6976.2009.00204.x

Lewis, K. (2010). Persister cells. *Annu. Rev. Microbiol.* 64, 357–372. doi: 10.1146/annurev.micro.112408.134306

Meylan, S., Porter, C. B. M., Yang, J. H., Belenky, P., Gutierrez, A., Lobritz, M. A., et al. (2017). Carbon sources tune antibiotic susceptibility in *Pseudomonas aeruginosa* via tricarboxylic acid cycle control. *Cell. Chem. Biol.* 24, 195–206. doi: 10.1016/j.chembiol.2016.12.015

Mitchell, G., Lafrance, M., Boulanger, S., Seguin, D. L., Guay, I., Gattuso, M., et al. (2012). Tomatidine acts in synergy with aminoglycoside antibiotics against multiresistant *Staphylococcus aureus* and prevents virulence gene expression. *J. Antimicrob. Chemother.* 67, 559–568. doi: 10.1093/jac/dkr510

Moreau-Marquis, S., O'Toole, G. A., and Stanton, B. A. (2009). Tobramycin and FDA-approved iron chelators eliminate *Pseudomonas aeruginosa* biofilms on cystic fibrosis cells. *Am. J. Respir. Cell. Mol. Biol.* 41, 305–313. doi: 10.1165/rcmb.2008-0299OC

Nohr-Meldgaard, K., Ovsepian, A., Ingmer, H., and Vestergaard, M. (2018). Resveratrol enhances the efficacy of aminoglycosides against *Staphylococcus aureus*. *Int. J. Antimicrob. Agents* 52, 390–396. doi: 10.1016/j.ijantimicag.2018.06.005

O'Neill, J. (2016). *Tackling Drug-Resistant Infections Globally. Final Report and Recommendations. The Review on Antimicrobial Resistance*. Available online at: https://amr-review.org/sites/default/files/160525_Final%20paper_with%20cover.pdf

Peng, B., Su, Y. B., Li, H., Han, Y., Guo, C., Tian, Y. M., et al. (2015). Exogenous alanine and/or glucose plus kanamycin kills antibiotic-resistant bacteria. *Cell. Metab.* 21, 249–261. doi: 10.1016/j.cmet.2015.01.008

Pu, Y., Li, Y., Jin, X., Tian, T., Ma, Q., Zhao, Z., et al. (2019). ATP-dependent dynamic protein aggregation regulates bacterial dormancy depth critical for antibiotic tolerance. *Mol. Cell.* 73, 143–156.e144. doi: 10.1016/j.molcel.2018.10.022

Radlinski, L. C., Rowe, S. E., Brzozowski, R., Wilkinson, A. D., Huang, R., Eswara, P., et al. (2019). Chemical induction of aminoglycoside uptake overcomes antibiotic tolerance and resistance in staphylococcus aureus. *Cell. Chem. Biol.* 26, 1355–1364. doi: 10.1016/j.chembiol.2019.07.009

Radzikowski, J. L., Vedelaar, S., Siegel, D., Ortega, A. D., Schmidt, A., and Heinemann, M. (2016). Bacterial persistence is an active sigmaS stress response to metabolic flux limitation. *Mol. Syst. Biol.* 12:882. doi: 10.15252/msb.20166998

Shan, Y., Brown Gandt, A., Rowe, S. E., Deisinger, J. P., Conlon, B. P., and Lewis, K. (2017). ATP-Dependent persister formation in escherichia coli. *MBio* 8:e02267-16. doi: 10.1128/mBio.02267-16

Su, Y. B., Peng, B., Li, H., Cheng, Z. X., Zhang, T. T., Zhu, J. X., et al. (2018). Pyruvate cycle increases aminoglycoside efficacy and provides respiratory energy in bacteria. *Proc. Natl. Acad. Sci. U.S.A.* 115, E1578–E1587. doi: 10.1073/pnas.1714645115

Taber, H. W., Mueller, J. P., Miller, P. F., and Arrow, A. S. (1987). Bacterial uptake of aminoglycoside antibiotics. *Microbiol. Rev.* 51, 439–457. doi: 10.1128/MMBR.51.4.439-457.1987

Trusts, T. P. C. (2016). *A Scientific Roadmap for Antibiotic Discovery*. The Pew Charitable Trusts.

Vega, N. M., Allison, K. R., Khalil, A. S., and Collins, J. J. (2012). Signaling-mediated bacterial persister formation. *Nat. Chem. Biol.* 8, 431–433. doi: 10.1038/nchembio.915

Vega, N. M., Allison, K. R., Samuels, A. N., Klempner, M. S., and Collins, J. J. (2013). Salmonella typhimurium intercepts Escherichia coli signaling to enhance antibiotic tolerance. *Proc. Natl. Acad. Sci. U.S.A.* 110, 14420–14425. doi: 10.1073/pnas.1308085110

Wang, Y., Bojer, M. S., George, S. E., Wang, Z., Jensen, P. R., Wolz, C., et al. (2018). Inactivation of TCA cycle enhances *Staphylococcus aureus* persister cell formation in stationary phase. *Sci. Rep.* 8:10849. doi: 10.1038/s41598-018-29123-0

Wang, Y., Tian, T., Zhang, J., Jin, X., Yue, H., Zhang, X. H., et al. (2019). Indole reverses intrinsic antibiotic resistance by activating a novel dual-function importer. *MBio* 10:e00676-19. doi: 10.1128/mBio.00676-19

WHO (2014). *Antimicrobial Resistance GLOBAL Report on Surveillance*.

WHO (2017). *Global Priority List of Antibiotic-Resistant Bacteria to Guide Research, Discovery, and Development of New Antibiotics*.

Yu, Q., Griffin, E. F., Moreau-Marquis, S., Schwartzman, J. D., Stanton, B. A., and O'Toole, G. A. (2012). *In vitro* evaluation of tobramycin and aztreonam versus *Pseudomonas aeruginosa* biofilms on cystic fibrosis-derived human airway epithelial cells. *J. Antimicrob. Chemother.* 67, 2673–2681. doi: 10.1093/jac/dks296

Conflict of Interest: The authors declare that the research was conducted in the absence of any commercial or financial relationships that could be construed as a potential conflict of interest.

frontiers in Cellular and Infection Microbiology

ORIGINAL RESEARCH
published: 28 February 2020
doi: 10.3389/fcimb.2020.00044

Absence of tmRNA Increases the Persistence to Cefotaxime and the Intercellular Accumulation of Metabolite GlcNAc in *Aeromonas veronii*

Wenjing Yu[1,2†], *Daiyu Li*[1†], *Hong Li*[1], *Yanqiong Tang*[1], *Hongqian Tang*[1], *Xiang Ma*[1*] and *Zhu Liu*[1*]

[1] Key Laboratory of Tropical Biological Resources of Ministry of Education, School of Life and Pharmaceutical Sciences, Hainan University, Haikou, China, [2] School of Tropical Crops, Hainan University, Haikou, China

OPEN ACCESS

Edited by:
Xiangmin Lin,
Fujian Agriculture and Forestry University, China

Reviewed by:
George Liechti,
Uniformed Services University of the Health Sciences, United States
Jarek Dziadek,
Institute for Medical Biology (PAN), Poland

***Correspondence:**
Xiang Ma
993034@hainanu.edu.cn
Zhu Liu
zhuliu@hainanu.edu.cn

[†] These authors have contributed equally to this work

Specialty section:
This article was submitted to Molecular Bacterial Pathogenesis, a section of the journal Frontiers in Cellular and Infection Microbiology

Received: 04 September 2019
Accepted: 23 January 2020
Published: 28 February 2020

Citation:
Yu W, Li D, Li H, Tang Y, Tang H, Ma X and Liu Z (2020) Absence of tmRNA Increases the Persistence to Cefotaxime and the Intercellular Accumulation of Metabolite GlcNAc in Aeromonas veronii. Front. Cell. Infect. Microbiol. 10:44. doi: 10.3389/fcimb.2020.00044

Bacterial persisters are a small proportion of phenotypically heterogeneous variants with the transient capability to survive in high concentrations of antibiotics, causing recurrent infections in both human and aquatic animals. Transfer-messenger RNA (tmRNA), which was encoded by the *ssrA* gene, was identified as a determinant regulator mediating the persistence to β-lactams in the pathogenic *Aeromonas veronii* C4. The deletion of tmRNA exhibited the increased ability of persister formation most probably due to the reduction of protein synthesis. Transcriptomic and metabolomic analyses revealed that the absence of tmRNA not only significantly elevated the intercellular levels of metabolite GlcNAc and promoted NaCl osmotic tolerance, but also upregulated the expression of metabolic genes in both the upstream biosynthesis pathway and the downstream metabolic flux of peptidoglycan (PG) biosynthesis. Finally, exogenous GlcNAc stimulated significant bacterial growth, enhanced content of GlcNAc in the cell wall, higher resistance to osmotic response, and higher persistence to cefotaxime in a concentration-dependent manner, implying its potential role in promoting the multiple phenotypes observed in tmRNA deletion strains. Taken together, these results hint at a potential mechanism of persister formation mediated by tmRNA against the β-lactam challenges in *A. veronii*.

Keywords: *Aeromonas veronii*, β-lactams, persisters, GlcNAc, peptidoglycan biosynthesis

INTRODUCTION

When treated with a lethal concentration of antibiotic, the great majority of bacteria are killed, whereas a small proportion of persisters survive in a dormant state (Fisher et al., 2017). Persister cells never exhibit genetic mutations and thus recover to normal growth and sensitivity after the removal of antibiotics (Helaine and Kugelberg, 2014). Bacterial persistence exists in nearly all bacterial pathogens and acts as the major contributor to the emergence of antibiotic resistance and the relapse of many chronic infectious diseases affecting humans and aquaculture (Michiels et al., 2016).

Despite intensive attempts, the underlying mechanism of persister cell formation is still elusive. It has been reported that bacterial persister formation is associated with trans-translation

(Li et al., 2013; Liu et al., 2017), toxin–antitoxin modules (TA modules) (Li and Zhang, 2007), SOS response (Dorr et al., 2009), stringent response (Liu et al., 2017), transporter or efflux mechanism (Pu et al., 2016), and metabolic pathways (Amato et al., 2013). Trans-translation is mediated by transfer-messenger RNA (tmRNA) and small protein B (SmpB) (de la Cruz and Vioque, 2001). It is a vital quality control system for rescuing stalled ribosomes on defective mRNAs (Keiler, 2008). Besides, persister formation can be induced by glucose metabolism and stringent stress via inhibiting peptidoglycan biosynthesis (PGB) in the challenge of β-lactams (Amato and Brynildsen, 2015). Peptide polysaccharide is the final product of PGB and the major component of the bacterial envelope. It is composed of *N*-acetylglucosamine (GlcNAc) and *N*-acetylmuramic acid (MurNAc) bridged by β-1,4 glycosidic bonds (Johnson et al., 2013). Establishing a solid relationship between PGB or trans-translation with persisters production is urgent for both the clinical treatment of chronic infections and aquaculture development (Girgis et al., 2012).

The gram-negative bacterium *Aeromonas veronii* (*A. veronii*) is one of the most threatening pathogens in aquaculture, which initiates massive mortalities in fish species and causes catastrophic economic losses in the fish-farming industry (Li et al., 2011; Reyes-Becerril et al., 2015). *A. veronii* exhibits natural resistance to multiple antibiotics, including sulfonamides and ampicillin (Liu et al., 2018). Deficiency of trans-translation in *Escherichia coli* significantly enhances the sensitivity to aminoglycosides (Luidalepp et al., 2005), while the deletion of tmRNA leads to strong resistance to the β-lactam antibiotics cefotaxime in *A. veronii*. Herein, we explored the role of tmRNA in bacterial persister formation of *A. veronii* against a representative of β-lactam cefotaxime. The results suggested that the absence of tmRNA increased persister formation of *A. veronii* C4 against cefotaxime through a potential mechanism involved in primarily the reduction of protein synthesis, and partly the accumulation of intercellular abundance of elementary metabolite GlcNAc. The results illustrated that trans-translation acted as the critical mediator to connect the carbon resource metabolism with persister formation by changing the levels of an intracellular metabolite, and thereby uncovered a novel model of persistence formation against cefotaxime.

MATERIALS AND METHODS

Bacterial Strains and Growth Conditions

The tmRNA deletion strain of *A. veronii* C4 was constructed previously (Liu et al., 2015). Bacterial culture was shaken (150 rpm) at 30°C for 16 h in LB medium, or grown on LB agar plate at 30°C for 24 h. M9 or LB medium was supplemented with 50 μg/ml ampicillin. Different concentrations of GlcNAc (5, 10, 15, and 20 mM) were added to the media for research purposes.

The Growth Curve Measurement

Bacteria were cultured for 36 h at the initial turbidity of 0.02 optical densities (OD) per milliliter, and the OD values were measured at 600 nm wavelength with 2-h intervals.

Minimum Inhibitory Concentration and Minimum Bactericidal Concentration (MBC) Assays

The culture was inoculated into a 96-well-plate with the initial 0.005 OD per milliliter and grown at 30°C for 22 h. The serial two-fold dilutions were performed with the additions of cefotaxime. Three replicates were performed for each strain of bacteria. The MIC values were determined as the lowest antibiotic concentration that inhibited visible growth, and the MBC values were defined as the lowest concentration that killed 99.9% of the bacteria (Liu et al., 2018).

Persister Assay

Persistence was determined by evaluating the viable bacteria per 1 ml. After shaking at 30°C in M9 or LB medium overnight, bacterial cultures were collected and washed, and then transferred to M9 or LB medium containing 5 μg/ml cefotaxime with initial 1.8×10^7 cells per ml. To test the contribution of GlcNAc to persister formation, the cells were cultured in the presence of 20 mM GlcNAc, washed, and then challenged with 5 μg/ml cefotaxime at 30°C for 11 h. To eliminate the effect of trans-translation malfunction, 50 μg/ml chloramphenicol was added as a protein synthesis inhibitor. The volume of 1 ml culture was collected and serially diluted in phosphate-buffered saline (PBS), and 50 μl of which was plated onto LB agar. The colony-forming units (CFUs) were counted after 22 h incubation at 30°C (Zhang et al., 2019).

RNA Sequencing and Bioinformatics Analysis

Bacterial strains were cultured in 10 ml of M9 medium containing 50 μg/ml ampicillin at 30°C, shaking at 150 rpm for 20 h. The cells were collected and total RNA was extracted using the traditional phenol/chloroform method. After determining the concentration and quality of the extracted RNA using Agilent 2100 Bio analyzer, the RNA sample was treated with DNase I to remove DNA, followed by the depletion of rRNA with the RiboZero Magnetic Kit. Then, the resulting RNA was used as the template for generating the double-stranded cDNA in a reverse transcription reaction. The synthesized cDNA was subjected to repair and adenylated in the 3′-end and ligated to the adapters. The cDNA fragments were enriched by PCR amplification with a PCR Primer Cocktail, and the purified products were sequenced using a Hiseq Xten (Illumina, San Diego, CA, USA), and 50 bp single-end RNA-seq reads were obtained. Sequence files were generated in the FASTQ format. The RNA-seq raw data were assembled and analyzed in comparison to the translational region of the annotated DNA sequence in reference genomes (GCA_001593245.1 and GCA_000204115.1) using HISAT (Kim et al., 2015). To identify the differential expression between wild type and tmRNA deletion, Bowtie 2(v2.2.5) was used to analyze the mRNA expression (Langmead and Salzberg, 2012). The unit of measurement is fragmented per kilobase of per million fragments mapped (FPKM). It was measured to normalize the gene expression levels, and the *p* value was evaluated for each gene, and Benjamini–Hochberg false discovery rate (FDR) was

applied for the correction. Only the comparisons with "FDR" <0.05 and expression fold change greater than two-fold in the Cuffdiff output were represented as significant differential expression. GEO accession number is GSE120603, the URL of the accession website is https://submit.ncbi.nlm.nih.gov/subs/sra/SUB6133286. The DESeq 2 packages in R was applied to estimate the fold changes and to perform other analysis (Love et al., 2014).

Metabolomic Analysis

The bacteria were cultured for 20 h and were collected and lysed using 1 ml extraction solvent (volume ratios of methanol and acetonitrile and water were 2:2:1, stored at −20°C before use). The extracts were homogenized in ball mill for 4 min, and subjected to ultrasonic treatments in ice water three times, followed by incubating at −20°C for 1 h to precipitate the proteins. After centrifugation at 12,000 rpm for 15 min at 4°C, the supernatant was transferred into EP tubes and dried in a vacuum concentrator. Then, the extraction solvent (volume ratios of acetonitrile and water were 1:1) was added for reconstitution. After vortex and ultrasonication for 10 min at 4°C in the water bath, the reconstituted extracts were spun down, and the supernatant was transferred into an LC/MS glass vial. A total of 10 μl supernatant was taken from each sample and pooled as QC samples, from which 60 μl was used for the UHPLC-QTOF-MS analysis. LC-MS/MS analyses were performed using a UHPLC system (1290, Agilent Technologies) with a UPLC BEH Amide column (1.7 μm 2.1*100 mm, Waters) coupled to TripleTOF 6600 (Q-TOF, AB Sciex). AB 6600 Triple TOF mass spectrometer can collect primary and secondary mass spectrometer data based on the IDA function under the control of Analyst TF 1.7 and AB Sciex. In each data acquisition cycle, the molecular ions with the strongest strength >100 were selected as the corresponding secondary mass spectrometry data. MS raw data (.wiff) files were converted to the mzXML format using ProteoWizard and processed by R package XCMS (version 3.2). The preprocessing results generated a data matrix that consisted of the retention time (RT), mass-to-charge ratio (m/z) values, and peak intensity. R package CAMERA was used for peak annotation after XCMS data processing. In-house MS2 database was applied in metabolite identification. The website of metabolomics raw data was accessed at https://www.ebi.ac.uk/metabolights/MTBLS1191.

Determination of the Relative Content of GlcNAc

The isolation of cell walls was performed according to a previous protocol (Glauner et al., 1988). To compare the content of GlcNAc, the bacteria were harvested and counted, and a total of 1.2×10^{11} cells were resuspended in PBS (pH = 7.4) supplemented with 5% SDS for boiling. The pellet was dissolved in PBS appending with 300 μg/ml of α-trypsin shaking overnight at 37°C, followed by lysing with additional 300 μg/ml α-trypsin for 4 h, and incubated in a final concentration of 1% SDS for 1 h at 95°C. After repeated washes to remove SDS, the peptidoglycan was suspended and hydrolyzed with 6 mol/L HCl in boiling water. The relative content of GlcNAc in peptidoglycan was calculated as follows: Relative content of GlcNAc = mass of GlcNAc/mass of peptidoglycan (Zhang and Wu, 1990).

Measurement of the Response to NaCl Osmotic Stress

To compare the tolerance under NaCl osmotic stress, the bacteria were cultured with initial 1.8×10^6 cells/ml overnight, and a total of 1.8×10^8 cells were collected by centrifugation and resuspended in 1 ml of 2 mol/L NaCl solutions. After culturing at 30°C for 1 h, the suspension was diluted with sterile water to form a series of NaCl gradients, 4 μl of which was plated onto LB solid medium and cultured at 30°C for about 16 h. The colony-forming units (CFUs) were counted after 22 h incubation at 30°C.

Statistical Analysis

The data were presented as the mean plus standard deviation, and the differences were analyzed with a one-way analysis of variance (ANOVA).

RESULTS

The Absence of tmRNA May Increase Persister Formation Under Cefotaxime by Reduction of Protein Synthesis

Both the growth curve and the tolerance against cefotaxime were determined in the deletion of *ssrA* strain and the wild type. The results showed that the deletion of *ssrA* did not change the growth rate of *A. veronii* C4 in LB or M9 media, while both the deletion of *ssrA* and the wild type grew slower in M9 media because of the lack of nutrients (**Figure 1A** and **Figures S1A,B**). The MIC values of cefotaxime for both wild type and *ssrA* mutants were 0.05 μg/ml, and the MBC values for both were 2 μg/ml, indicating that *A. veronii* C4 was sensitive to cefotaxime and the deletion of *ssrA* did not affect the susceptibility against cefotaxime. Although *A. veronii* C4 encoded beta-lactamases including AMS64_18215, AMS64_00580, and AMS64_13110, cefotaxime was inherently resistant to most beta-lactamase enzymes, similarly with the previous report in *E. coli* (Barour et al., 2019). However, the biphasic kill curve revealed that significant differences in persister cell formation were observed in both LB and M9 media between wild type and *ssrA* mutants under the treatment of 5 μg/ml cefotaxime (**Figure 1B**). Consistently, the enumeration of persister cells showed that the deletion of *ssrA* significantly increased the persister production by five- and four-fold in LB and M9 media (**Figure 1C**) after incubation with 5 μg/ml cefotaxime for 11 h, respectively. The concentration of 5 μg/ml cefotaxime was selected as the suggested concentration, which should be 10 times the MIC value in persister assay, to distinguish the persistence from transient modes of resistance (Balaban et al., 2019).

To verify whether the promoted persistence was caused by the reduction of the protein synthesis, both wild type and *ssrA* deletion mutants were pretreated with a protein synthesis inhibitor chloramphenicol, and subsequently, the persister formation was determined to challenge with cefotaxime. The

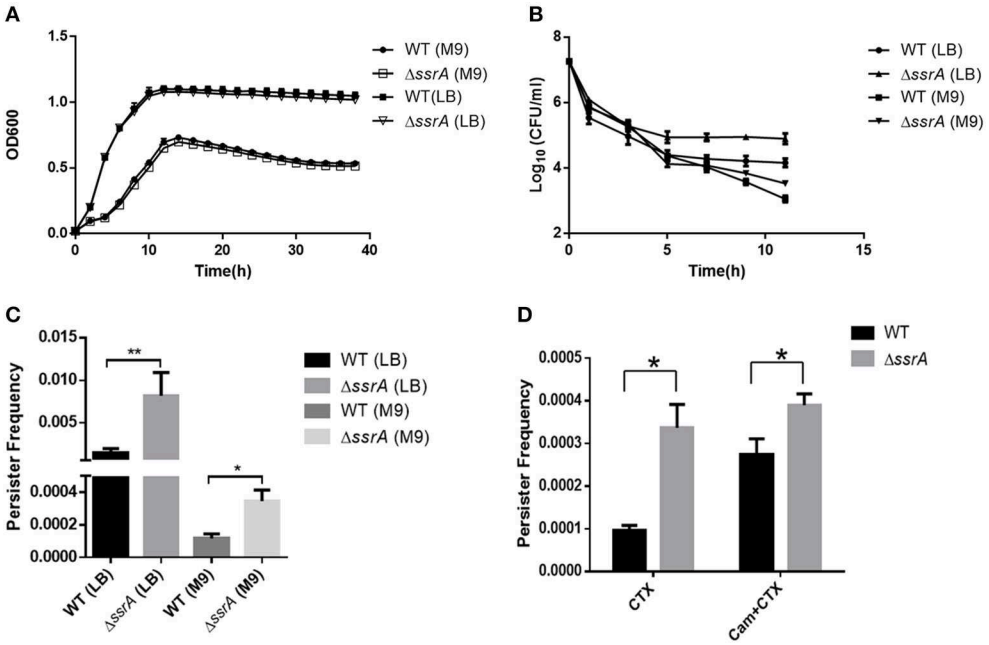

FIGURE 1 | The deletion of tmRNA increases persister formation under cefotaxime treatment. **(A)** Growth curves of wild type (WT) and tmRNA deletion strain (Δ*ssrA*) in LB and M9 medium. **(B)** Bacterial survival of WT and Δ*ssrA* in LB and M9 medium after treatment with cefotaxime for 11 h. *a significant difference with $p < 0.05$, and **an extremely significant result with $p < 0.01$, followed by one-way ANOVA, Tukey post-test. **(C)** Persister frequency of WT and Δ*ssrA* in LB and M9 medium after treatment with cefotaxime for 11 h, wherein persister frequency = CFU post-cefotaxime treatment/CFU pre-cefotaxime treatment. **(D)** Persister frequency of WT and Δ*ssrA* in M9 medium under the treatment of 5 μg/ml cefotaxime (CTX) for 11 h, in the absence or presence of the pretreatment with 50 μg/ml chloramphenicol (Balaban et al., 2019) to inhibit the protein synthesis. *A significant difference with $p < 0.05$, followed by one-way ANOVA, Tukey post-test.

results showed that persister frequency was only elevated in wild type rather than tmRNA deletion strains, suggesting that both the absence of *ssrA* and chloramphenicol treatment produced a slow-growing or dormant state through the inhibition of translation (**Figure 1D**). Moreover, the formations of persister cells were significantly reduced compared to *ssrA* deletion mutants when cells were propagated in LB (**Figures 1B,C**), likely due to the higher frequency of protein synthesis and more susceptibility to cefotaxime as the results of richer nutrients in LB media (VanHook, 2019). Taken together, these results suggested that the deletion of tmRNA strain might mediate higher persister cell formation under the pressure of cefotaxime by reduction of protein synthesis.

The Absence of tmRNA Led to the Accumulation of Metabolite GlcNAc

To explore the genes and pathways responsible for the effects of tmRNA on persister production, the transcriptional differences were compared between wild type and *ssrA* deletion strains. The results showed that 47% of the total detected genes exhibited altered expression levels in the *ssrA* deletion strain, wherein 36% increased and 11% decreased (**Figure 2A**). KEGG pathway enrichment indicated that the genes with varied expression levels were mostly involved in metabolic pathways and biosynthesis of secondary metabolites, with significant changes of 89 and 43 genes, respectively (**Figure 2B**). The metabolic-related genes constituted the most dominant portion, occupying 54% of the total genes with significant changes, followed by the biosynthesis-related genes that shared 35% proportion (**Figure 2C**). These results implied that the deletion of *ssrA* in *A. veronii* C4 primarily influenced the metabolism- and biosynthesis-related genes.

Accordingly, the variations of the essential metabolites were compared between wild type and *ssrA* deletion strains through untargeted metabolomic analysis using UHPLC-QTOF-MS, which identified the primary metabolites essential for bacteria growth, development, and reproduction of bacteria (Sanchez and Demain, 2008). The results showed that 13% of the total detected metabolites exhibited higher abundances in the *ssrA* deletion strain, while 8 and 79% of which were found to have lower or unchanged abundances, separately (**Figure 3A**). The primarily differential metabolites included organic nitrogen compounds, carboxylic acids and derivatives, benzene and substituted derivatives, phenols, etc. (**Table S1**). Primary functional classification in the Venn diagram illustrated that the metabolic group occupied the highest numbers of unique metabolites, followed by the biosynthesis group (**Figure 3B**). This result is consistent with that found by transcriptomic analysis (**Figure 2C**). Further KEGG pathway analysis demonstrated that the alterations of metabolic pathways contributed dominantly, with 26 compounds changed, followed by purine metabolism, pyrimidine metabolism, and fructose and mannose metabolism, etc. (**Figure 3C**). Considering that the antibiotic cefotaxime takes actions by inhibiting the activity of peptidoglycan transpeptidase and thus the bacterial cell wall synthesis, which results in

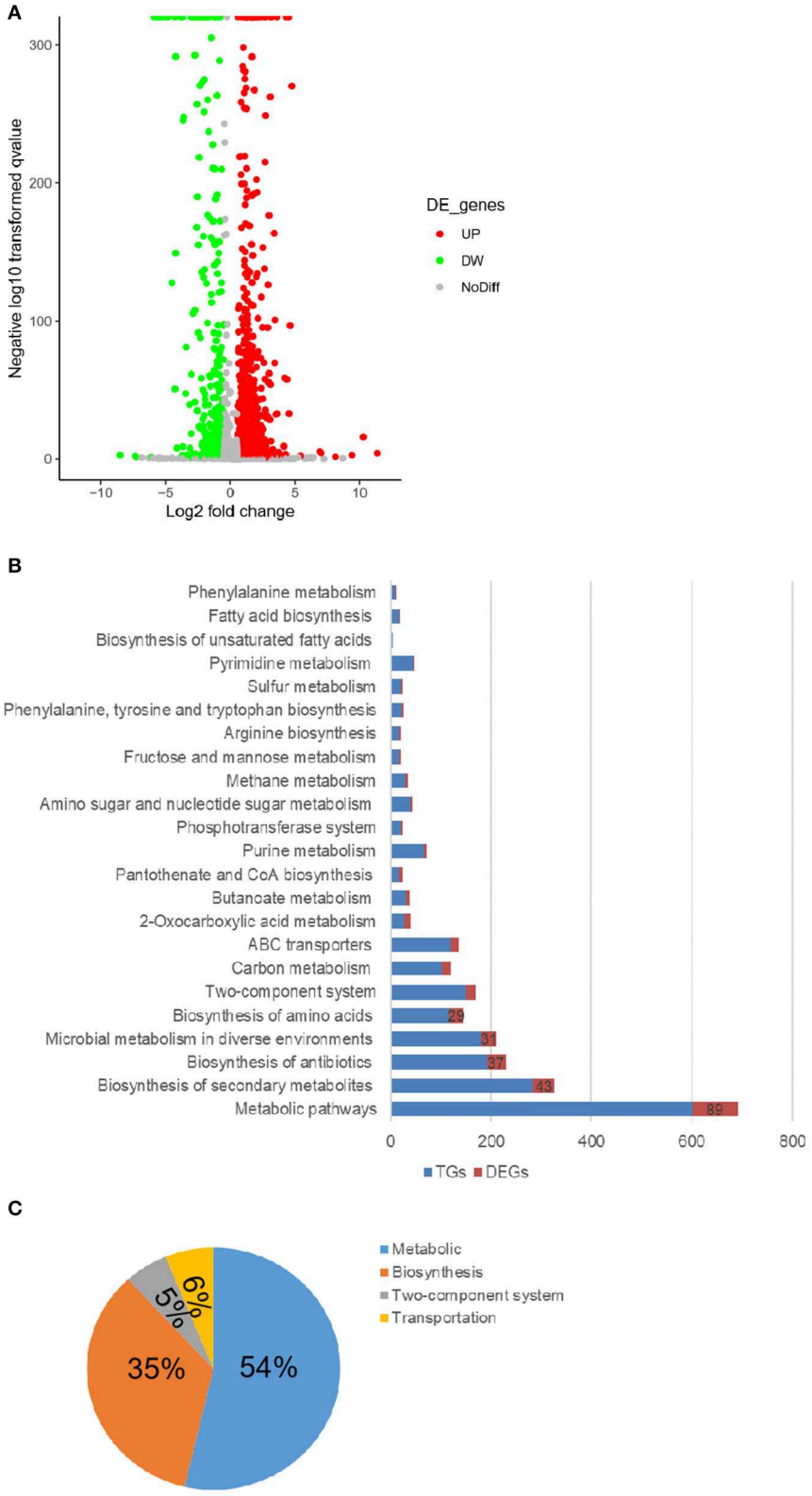

FIGURE 2 | The deletion of tmRNA dominantly changes the metabolic-related genes. **(A)** Volcanic map showing the changes of individual genes in WT and Δ*ssrA* strains, wherein the red circles represent the upregulated genes (UP), and green circles represent the downregulated genes (DW) in Δ*ssrA* strain, which exhibit at least two-fold changes with $p < 0.05$. Gray circles represent the genes without expression differences (NoDiff). **(B)** Enrichment of genes with differential changes in the

(Continued)

FIGURE 2 | KEGG pathway, wherein the blue bars represent the number of all the detected genes in the pathway (TGs), and red bars represent the number of the genes with significant changes (DEGs). **(C)** The primary classification of the altered genes in the KEGG pathway in terms of their basic functions, wherein the blue portion represents the metabolic-related pathway, the orange portion represents the synthetic-related pathway, the gray portion represents the two-component system, and the yellow portion represents the transport-related pathway.

cell lysis and death (Lefrock et al., 2012), we emphasized the amino sugar and nucleoside sugar metabolism pathways and discovered that two metabolites, i.e., GlcNAc (C00140 in **Table S2**) and L-arabinose (C00259 in **Table S2**), exhibited higher abundance in the *ssrA* deletion strain. Besides the amino sugar and nucleoside sugar metabolism, GlcNAc functions in phosphotransferase system (PTS) and ABC transporters, while L-arabinose participates in ABC transporters, ascorbate, and aldarate metabolism (**Table S2**). GlcNAc exhibited a higher abundance level than L-arabinose in the *ssrA* deletion strain (**Figure S2** and **Table S3**).

We investigated the GlcNAc-involved pathways and found further that GlcNAc is a preliminary substrate to form the precursor UDP-GlcNAc for peptidoglycan biosynthesis (**Figure 4A**). The transcriptional data revealed that the upregulation of *HEXA_B* might contribute to the increase of GlcNAc. Besides, enhanced expression of the *nag* operon may stimulate the formation of UDP-GlcNAc (the regulators in red in **Figure 4A** and **Figure S3A**). The *nag* operon in *A. veronii* C4 was composed of the genes *nagE*, *nagB*, *nagA*, and *nagC*, which were located adjacently on the chromosome and arranged similarly in other bacterial species such as *E. coli* and *Vibrio cholerae non-O1* (**Figure 4B**). The phylogenetic analysis revealed that each gene in the *nag* operon was clustered into the genus *Aeromonas*, implying that they may exhibit the same functionality (**Figure S3B**). The heightened expression of *nagE* and *nagK* probably promoted the phosphorylation of GlcNAc for the formation of GlcNAc-6p, subsequently transforming GlcNAc-6p to glucosamine-6-phosphate (GlcN-6p) by elevated expression of *nagA*, and eventually producing fructose-6-phosphate (Fru-6p) by upregulated *nagB* (**Figure 4A**). In addition, the enhanced expression of the *amgK* gene facilitated the formation of UDP-MurNAc (**Figure 4A**). As for the downstream pathways, the transcription levels of the genes involved peptidoglycan synthesis were investigated (**Figure S3C**). The related genes were categorized into two subgroups encoding Mur ligases and penicillin-binding proteins (PBPs), both of which function in peptidoglycan biosynthesis and the assembly of the bacterial cell wall. The Mur ligases (*murC*, *murD*, *murE*, and *murF*) were significantly upregulated in the *ssrA* deletion mutant. Similarly, so did PBPs (*mrcB*, *mrcA*, *ftsI*, *mrdA*, and *pbpC*) (**Figure 4C** and **Figures S3C,D**). They are attractive targets for designing novel antibacterial agents to inhibit cell wall synthesis (Barreteau et al., 2010; Welsh et al., 2017). In particular, the high-molecular-weight PBPs (*mrcB*, *mrcA*, and *ftsI*) have been identified as the targets of cefotaxime, which catalyze the synthesis of the major component of the cell wall (Denome et al., 1999).

In order to validate the effects of the accumulation of cellular GlcNAc, we extracted the peptidoglycans and determined the content of GlcNAc in wild type and *ssrA* deletion strains. Consistent with the transcriptional data, the results showed that the GlcNAc content in the peptidoglycan of the deletion strain was significantly higher than that of the wild type (**Figure 5A**). Moreover, considering that the enhanced peptidoglycan usually leads to improved tolerance to osmotic stress (Vollmer et al., 2008), we determined the responses of wild type and *ssrA* deletion strains to NaCl osmotic stress. The results showed that the *ssrA* deletion strain exhibited remarkably enhanced tolerance in comparison to the wild type (**Figure 5B**). Taken together, these results confirmed that the tmRNA deletion strain increases the intercellular stores of metabolite GlcNAc.

Exogenous GlcNAc Promotes the Multiple Phenotypes as Observed in tmRNA Deletion Strains

In order to validate the contributions of the accumulated GlcNAc for the multiple phenotypes observed in the *ssrA* deletion strain, different concentrations of exogenous GlcNAc were added to wild type of *A. veronii* C4, followed by evaluations of the bacterial growth, persister formations, GlcNAc contents in peptidoglycan, and response to osmotic stress. The growth curve demonstrated that addition of GlcNAc caused faster growth rates and higher cell mass at stationary phase in a concentration-dependent manner, while there were no significant growth differences at the exponential phase in both wild type and *ssrA* deletion mutants (**Figures 6A,B** and **Figures S4A,B**). Moreover, accompanied by an increased content of GlcNAc in the cell wall (**Figure 6C**), the resistance to NaCl osmotic stress was enhanced (**Figure 6D**). These results illustrated that GlcNAc acted as the major contributor for the enhanced peptidoglycan and resistance to osmotic stress in the *ssrA* deletion strain. In addition, when the wild type was treated with 5 μg/ml cefotaxime in M9 medium, persister production was doubled in the presence of 20 mM of GlcNAc in both the biphasic kill curve and persister cell enumeration assay (**Figures 6E,F**). Similar results were displayed in the LB medium **Figures S4C,D**). We proposed that the additive of GlcNAc may contribute in part to persister cell formation. These results illustrated that enhanced GlcNAc levels may account for the phenotypes associated with the deletion of *ssrA* strain.

DISCUSSION

The trans-translation system is required for antibiotic tolerance, growth, and persistence under antibiotic and environmental stresses (Keiler, 2008). In this study, the role of tmRNA, encoded by the *ssrA* gene as one of the core factors in the trans-translation system, in persister formation was investigated in the aquatic

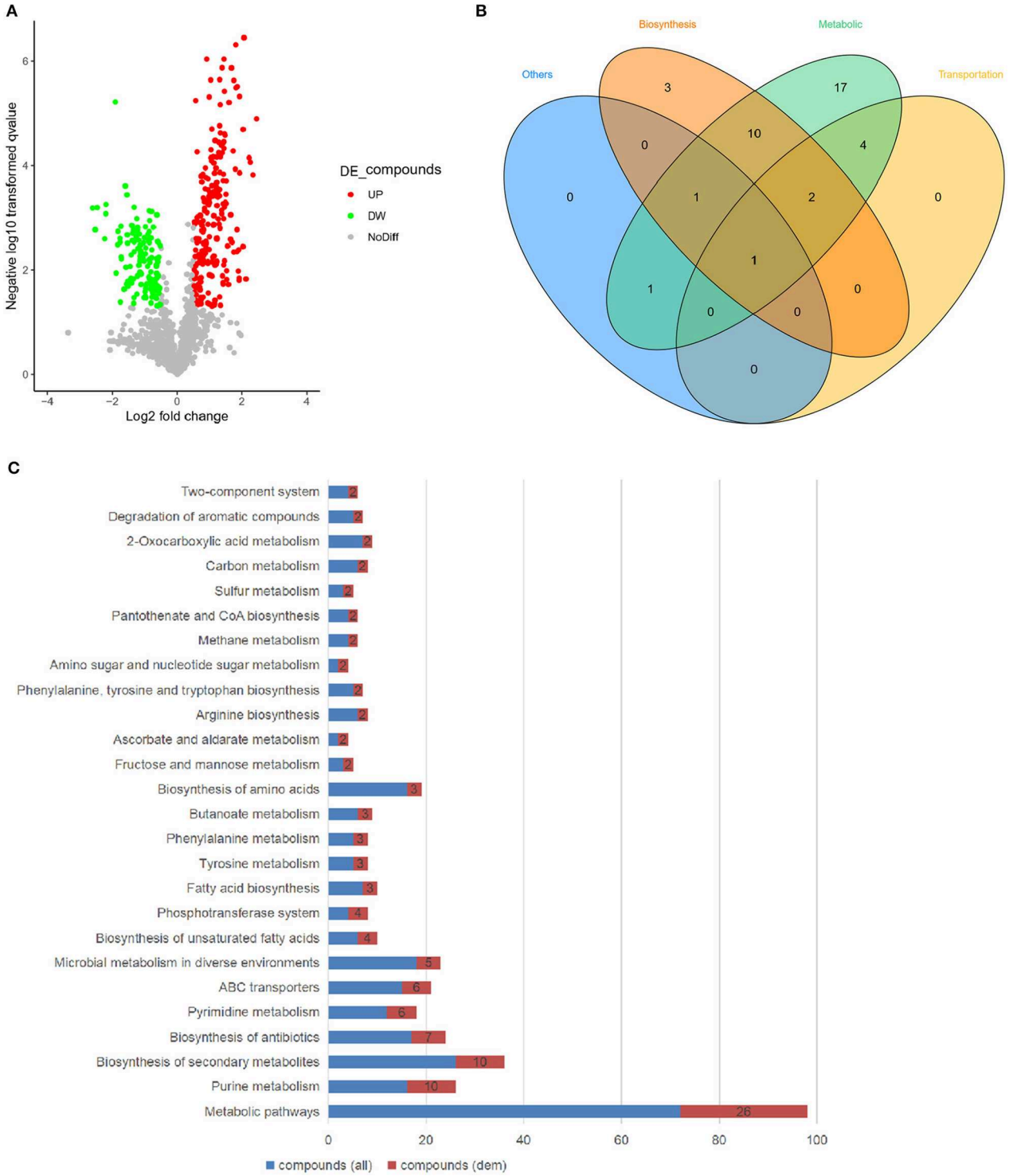

FIGURE 3 | The deletion of tmRNA significantly upregulates the level of the metabolite GlcNAc. **(A)** Volcanic map showing changes of essential metabolites in WT and Δ*ssrA* strains, wherein the red circles represent the metabolites with increased abundance (UP), and green circles represent the metabolites with reduced abundance (DW) in Δ*ssrA* strain, which exhibit at least two-fold changes with $p < 0.05$. The gray circles represent the metabolites without differences in abundance (NoDiff). **(B)** Venn graph showing the unique and overlapping relationships between the altered metabolites in terms of their basic classifications of functions, with the blue portion representing other pathways, the orange portion representing synthetically related pathways, the green portion representing metabolically related pathways, and the yellow portion representing transport-related pathways. **(C)** Enrichment of the differential metabolites in the KEGG pathway, wherein the blue bars represent the number of all the detected compounds in the pathway [compound (all)] and the red bars represent the number of the detected compounds with changes [compound (dem)].

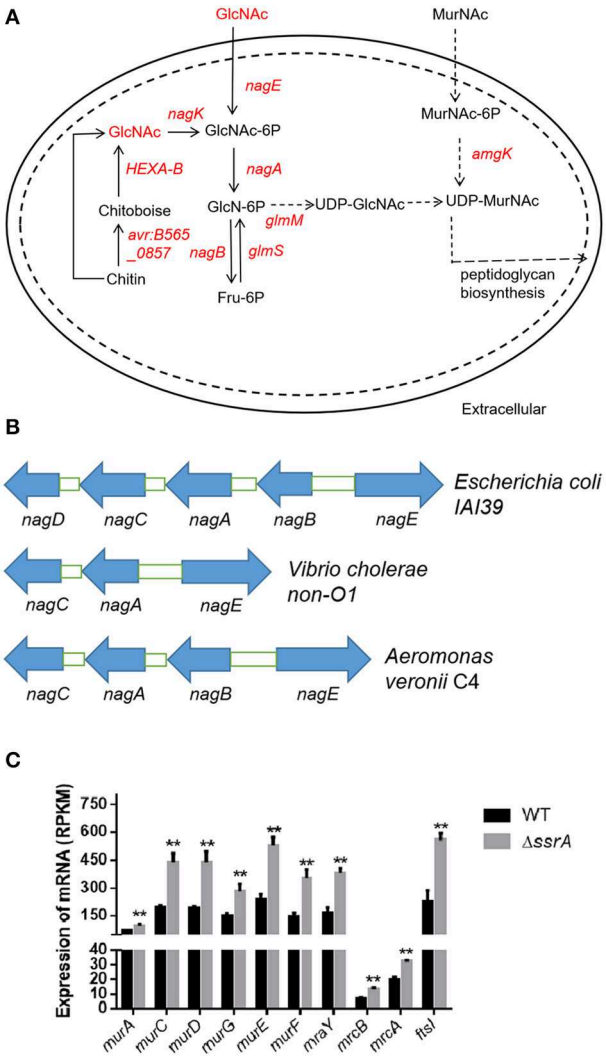

FIGURE 4 | The deletion of tmRNA enhances the expression of genes associated with the metabolism of GlcNAc. **(A)** Intercellular amino sugar metabolic pathways involved by GlcNAc. The significantly upregulated genes and metabolites are shown in red, and those with no significant differences are shown in black. The arrows indicate the direction of the metabolic flux. **(B)** The genetic locations of *nagE*, *nagA*, *nagB*, *nagC*, and *nagD* on the chromosome in *Escherichia coli IAI39*, *Vibrio cholerae non-O1*, and *Aeromonas veronii* C4. Blue arrows indicate the transcriptional directions of the genes. **(C)** The gene expression levels of peptidoglycan synthesis. **An extremely significant result with $p < 0.01$, followed by one-way ANOVA, Tukey post-test.

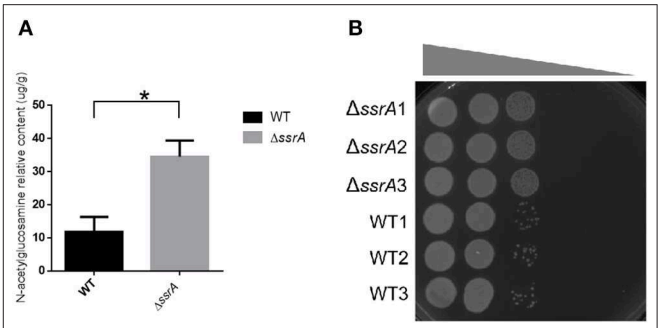

FIGURE 5 | The deletion of tmRNA promotes the peptidoglycan biosynthesis. **(A)** The relative contents of GlcNAc in the peptidoglycan of the cell wall in WT and Δ*ssrA* strains. *A significant difference with $p < 0.05$, followed by one-way ANOVA, Tukey post-test. **(B)** The response of WT and Δ*ssrA* strains to NaCl osmotic stress. An identical number of initial bacteria (2.88×10^4 cells) were cultured in the growth medium containing a series of NaCl gradients. The gray wedge indicates that the osmotic stress decreases from left to right.

pathogen *A. veronii* C4. Our results showed that the *ssrA* deletion mutant had a growth rate identical to that of wild type (**Figure 1A** and **Figures S1A,B**), indicating that the tmRNA was dispensable to bacterial growth in *A. veronii* C4. The same result was reported for some other bacterial species (de la Cruz and Vioque, 2001). However, the results surprisingly showed that the deletion of *ssrA* promoted significantly higher persister production under the treatment of cefotaxime (**Figures 1B,C**), although it did not cause different MIC/MBC values as compared with wild type. Although the deletion of *ssrA* strain promotes higher susceptibility to fosfomycin and ampicillin (Luidalepp et al., 2005), it does not significantly affect responses to ampicillin (de la Cruz and Vioque, 2001). In *Streptococcus pneumoniae*, tmRNA deficiency may reduce ROS production and chromosome breakage through the trans-translation process, thus increasing the tolerance to fluoroquinolones (Liliana et al., 2016).

Herein, for the first time, the effect of the *ssrA* mutant was delineated on the persistence to cefotaxime. Our results suggested that the inhibition of translation probably constituted the primary reason for the boost of persister cell formation in the presence of cefotaxime (**Figure 1D**). Although chloramphenicol treatment led to the lower translation frequency and prompted a slow-growing or dormant state, there was still a slight difference in the persistence compare to in *ssrA* deletion strains (**Figure 1D**). Further, the transcriptomic and metabolomic analyses were conducted to identify the related genes and pathways. By analyzing the transcriptomic profile, the absence of tmRNA elevated the expressions of the key enzymes in the metabolic and the biosynthesis pathways (**Figures 2A–C**). Besides, metabolomic analyses indicated that the *ssrA* deletion significantly increased the abundance of metabolite GlcNAc, which was involved in the amino sugar and nucleotide sugar metabolism (**Figure 3C** and **Table S3**). GlcNAc is an excellent energy source for gram-negative pathogenic bacteria, which can be utilized more efficiently than glucose in multiple metabolic pathways (Hsing-Chen et al., 2002). The supplementation with GlcNAc significantly promoted the growth rate of wild type (**Figures 6A,B**), including increased relative content of GlcNA in the cell wall (**Figure 6C**) and higher resistance to osmotic stress (**Figure 6D**), and promoted persister formation under cefotaxime (**Figures 6E,F**).

Taken together, the persister formation may be modulated by multiple pathways under cefotaxime in *A. veronii*. First, the reduction of protein synthesis likely acted as the primary contributor (**Figure 1D**). Secondly, the accumulation of metabolite GlcNAc also promoted the persister formation, probably through accelerating the bacteria growth

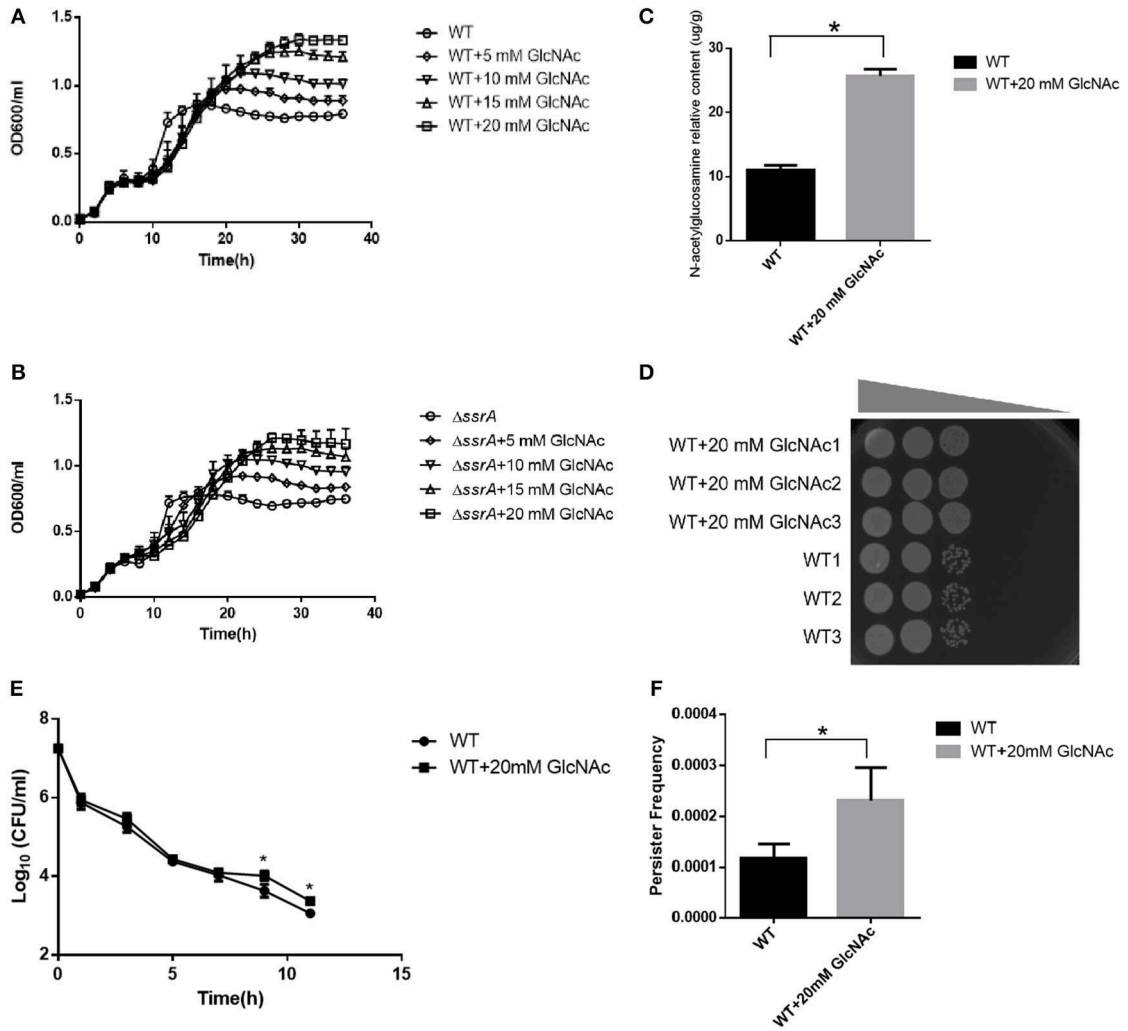

FIGURE 6 | Metabolites GlcNAc promotes the peptidoglycan biosynthesis and the persister formation. **(A,B)** Growth curves of WT and Δ*ssrA* strain supplemented without and (WT/Δ*ssrA*) with 5 mM GlcNAc (5 mM GlcNAc + WT/Δ*ssrA*), 10 mM GlcNAc (10 mM GlcNAc + WT/Δ*ssrA*), 15 mM GlcNAc (15 mM GlcNAc + WT/Δ*ssrA*), and 20 mM GlcNAc (20 mM GlcNAc + WT/Δ*ssrA*) in M9 medium. **(C)** The relative contents of GlcNAc in the peptidoglycan of the cell wall in WT supplemented without or with 20 mM GlcNAc, *a significant difference with $p < 0.05$, followed by one-way ANOVA, Tukey post-test. **(D)** The bacterial response to NaCl osmotic stress. An identical number of initial bacteria (2.88×10^4 cells) were adopted in the osmotic response experiment, with the gray wedge indicating that the osmotic stress decreases from left to right. **(E,F)** Bacterial survival curve and persister frequency showing the persister formations in WT in the absence and presence of 20 mM GlcNAc in M9 medium under the treatment with cefotaxime for 11 h. *A significant result with $p < 0.05$, followed by one-way ANOVA, Tukey post-test.

(**Figures 6A,B,E,F**). Finally, the upregulation of PBPs in the *ssrA* mutant (**Figure S3C**) offered a potential explanation for the enhanced tolerance to cefotaxime, probably by providing more target enzymes of cefotaxime (Fani et al., 2013). Although the inhibition of trans-translation by the deletion of *ssrA* caused the depletion of some ribosomes, the reasonable explanation was that the upregulated transcription of PBPs promoted the production. Collectively, these three alternative ways were responsible for persistence. However, which way was dominant depended on the triggering of circumstance effects, and the underlying mechanism needed to be further investigated.

Both trans-translation and metabolism play critical roles in the process of persistence (Li et al., 2013; Amato et al., 2014). The malfunction of SmpB or tmRNA modulates the effector (p)ppGpp to obstruct the persister formation in the presence of aminoglycosides, quinolones, and β-lactams (Liu et al., 2017), and SmpB knockout reduces the number of persisters under gentamicin stress (Liu et al., 2018). Moreover, metabolic inactivity increases persistence (Girgis et al., 2012). Although tmRNA regulates the metabolism of some sugars through the mechanism of trans-translation (Roche and Sauer, 2001), the interactive relationship between trans-translation and metabolism in persister formation remains unclear. The alternations of metabolic flux stimulate the persister formation against fluoroquinolone in a manner of TA behavior by a metabolite–enzyme interaction model, in which the metabolite ppGpp acts as a toxin, and the ppGpp hydrolase SpoT acts as an

antitoxin (Amato et al., 2013; Maisonneuve and Gerdes, 2014). Besides, the glucose exhaustion stimulates persister formation to β-lactams through the action of the metabolite ppGpp, mediated by the actions of trans-translation (Amato and Brynildsen, 2015). Dissimilar types of antibiotics may stimulate diverse metabolite–enzyme interaction models under the regulation and control of various mechanisms, thereby inducing different persister levels. Our present study was preliminarily presumed that carbon metabolism was associated with persister formation to β-lactams through the action of the metabolite GlcNAc, which exhibits similar function to ppGpp. Although Mur ligases and penicillin-binding proteins (PBPs) were upregulated and utilized for peptidoglycan biosynthesis and the assembly of the bacterial cell wall, GlcNAc was accumulated curiously. Our explanations assume that GlcNAc participates in various metabolic pathways, and some other metabolic pathways will be downregulated. The contributors that reduce the utilization of GlcNAc remain to be investigated in the *ssrA* mutant. The targeted enzymes that interact with GlcNAc for mediating the persister formation will facilitate the discovery of novel therapeutic strategies against the threatening bacterial pathogens.

DATA AVAILABILITY STATEMENT

The datasets generated for this study can be found in the NCBI: GSE120603, https://submit.ncbi.nlm.nih.gov/subs/sra/SUB6133286, Metabolights: https://www.ebi.ac.uk/metabolights/MTBLS1191.

AUTHOR CONTRIBUTIONS

ZL, XM, and WY contributed to the conception and design of the study. WY and DL performed the experiments. WY, DL, HL, YT, and HT performed the statistical analysis. WY, XM, and ZL drafted the manuscript. All authors contributed to manuscript revision and approved the submitted version.

FUNDING

This work was supported by grants from the Hainan Natural Science Foundation Nos. 317015 (to YT) and 319QN161 (to HL). This work was also partially supported by grants from the National Natural Science Foundation of China Nos. 31560021, 31772887 (to ZL), 31860676 (to YT), and 31960027 (to XM).

ACKNOWLEDGMENTS

We are very grateful to Dr. Chiju Wei, who is a professor at Shantou University to help us revise the manuscript carefully.

SUPPLEMENTARY MATERIAL

The Supplementary Material for this article can be found online at: https://www.frontiersin.org/articles/10.3389/fcimb.2020.00044/full#supplementary-material

REFERENCES

Amato, S., and Brynildsen, M. (2015). Persister heterogeneity arising from a single metabolic stress. *Curr. Biol.* 25, 2090–2098. doi: 10.1016/j.cub.2015.06.034

Amato, S. M., Fazen, C. H., Henry, T. C., Mok, W. W., Orman, M. A., Sandvik, E. L., et al. (2014). The role of metabolism in bacterial persistence. *Front. Microbiol.* 5:70. doi: 10.3389/fmicb.2014.00070

Amato, S. M., Orman, M. A., and Brynildsen, M. P. (2013). Metabolic control of persister formation in *Escherichia coli*. *Mol. Cell* 50, 475–487. doi: 10.1016/j.molcel.2013.04.002

Balaban, N. Q., Helaine, S., Lewis, K., Ackermann, M., Aldridge, B., Andersson, D. I., et al. (2019). Definitions and guidelines for research on antibiotic persistence. *Nat. Rev. Microbiol.* 17, 441–448. doi: 10.1038/s41579-019-0196-3.

Barour, D., Berghiche, A., and Boulebda, N. (2019). Antimicrobial resistance of *Escherichia coli* isolates from cattle in Eastern Algeria. *Vet World* 12, 1195–1203. doi: 10.14202/vetworld.2019.1195-1203

Barreteau, H., Kovač, A., Boniface, A., Sova, M., Gobec, S., Blanot, D., (2010). Cytoplasmic steps of peptidoglycan biosynthesis. *FEMS Microbiol. Rev.* 32, 168–207. doi: 10.1111/j.1574-6976.2008.00104.x

de la Cruz, J., and Vioque, A. (2001). Increased sensitivity to protein synthesis inhibitors in cells lacking tmRNA. *RNA* 7, 1708–1716.

Denome, S. A., Elf, P. K., Henderson, T. A., Nelson, D. E., and Young, K. D. (1999). *Escherichia coli* mutants lacking all possible combinations of eight penicillin binding proteins: viability, characteristics, and implications for peptidoglycan synthesis. *J. Bacteriol.* 181, 3981–3993. doi: 10.1128/JB.181.13.3981-3993.1999

Dorr, T., Lewis, K., and Vulic, M. (2009). SOS response induces persistence to fluoroquinolones in *Escherichia coli*. *PLoS Genet.* 5:e1000760. doi: 10.1371/journal.pgen.1000760

Fani, F., Brotherton, M. C., Leprohon, P., and Ouellette, M. (2013). Genomic analysis and reconstruction of cefotaxime resistance in *Streptococcus pneumoniae*. *J. Antimicrob. Chemother.* 68, 1718–1727. doi: 10.1093/jac/dkt113

Fisher, R. A., Gollan, B., and Helaine, S. (2017). Persistent bacterial infections and persister cells. *Nat. Rev. Microbiol.* 15, 453–464. doi: 10.1038/nrmicro.2017.42

Girgis, H. S., Harris, K., and Tavazoie, S. (2012). Large mutational target size for rapid emergence of bacterial persistence. *Proc. Natl. Acad. Sci. U.S.A.* 109, 12740–12745. doi: 10.1073/pnas.1205124109

Glauner, B., Höltje, J. V., and Schwarz, U. (1988). The composition of the murein of *Escherichia coli*. *J. Biol. Chem.* 263, 10088–10095.

Helaine, S., and Kugelberg, E. (2014). Bacterial persisters: formation, eradication, and experimental systems. *Trends Microbiol.* 22, 417–424. doi: 10.1016/j.tim.2014.03.008

Hsing-Chen, C., Chiao-Ching, C., Wei-Juin, M., and Lin-Shiun, Y. (2002). Evaluation of N-acetylchitooligosaccharides as the main carbon sources for the growth of intestinal bacteria. *FEMS Microbiol. Lett.* 209, 51–54. doi: 10.1016/S0378-1097(02)00483-4

Johnson, J. W., Fisher, J. F., and Mobashery, S. (2013). Bacterial cell-wall recycling. *Ann. N. Y. Acad. Sci.* 1277, 54–75. doi: 10.1111/j.1749-6632.2012.06813.x

Keiler, K. C. (2008). Biology of trans-translation. *Annu. Rev. Microbiol.* 62, 133–151. doi: 10.1146/annurev.micro.62.081307.162948

Kim, D., Langmead, B., and Salzberg, S. L. (2015). HISAT: a fast spliced aligner with low memory requirements. *Nat. Methods.* 12, 357–360. doi: 10.1038/nmeth.3317

Langmead, B., and Salzberg, S. L. (2012). Fast gapped-read alignment with Bowtie 2. *Nat. Methods.* 9, 357–359. doi: 10.1038/nmeth.1923

Lefrock, J. L., Prince, R. A., and Leff, R. D. (2012). Mechanism of action, antimicrobial activity, pharmacology, adverse effects, and clinical efficacy of cefotaxime. *Pharmacotherapy* 2, 174–184. doi: 10.1002/j.1875-9114.1982.tb03185.x

Li, J., Ji, L., Shi, W., Xie, J., and Zhang, Y. (2013). Trans-translation mediates tolerance to multiple antibiotics and stresses in *Escherichia coli*. *J. Antimicrob. Chemother.* 68, 2477–2481. doi: 10.1093/jac/dkt231

Li, Y., Liu, Y., Zhou, Z., Huang, H., Ren, Y., Zhang, Y., et al. (2011). Complete genome sequence of *Aeromonas veronii* strain B565. *J. Bacteriol.* 193, 3389–3390. doi: 10.1128/JB.00347-11

Li, Y., and Zhang, Y. (2007). PhoU is a persistence switch involved in persister formation and tolerance to multiple antibiotics and stresses in *Escherichia coli*. *Antimicrob. Agents Chemother.* 51, 2092–2099. doi: 10.1128/AAC.00052-07

Liliana, B., Joana, W. J., Ferrándiz M. J., Alicia, G.-S., de la Campa A. G., et al. (2016). Absence of tmRNA has a protective effect against fluoroquinolones in streptococcus pneumoniae. *Front. Microbiol.* 7:2164. doi: 10.3389/fmicb.2016.02164

Liu, S., Wu, N., Zhang, S., Yuan, Y., Zhang, W., and Zhang, Y. (2017). Variable persister gene interactions with (p)ppGpp for persister formation in *Escherichia coli*. *Front. Microbiol.* 8:1795. doi: 10.3389/fmicb.2017.01795

Liu, Z., Hu, K., Tang, Y., Li, H., Tang, H., Hu, X., et al. (2018). SmpB down-regulates proton-motive force for the persister tolerance to aminoglycosides in *Aeromonas veronii*. *Biochem. Biophys. Res. Commun.* 507, 407–413. doi: 10.1016/j.bbrc.2018.11.052

Liu, Z., Peng, L., Shuanshuan, L., Haichao, S., Hongqian, T., and Xinwen, H. (2015). Small protein B upregulates sensor kinase bvgS expression in *Aeromonas veronii*. *Front. Microbiol.* 6:579. 00579 doi: 10.3389/fmicb.2015.00579

Love, M. I., Huber, W., and Anders, S. (2014). Moderated estimation of fold change and dispersion for RNA-seq data with DESeq2. *Genome Biol.* 15:550. doi: 10.1186/s13059-014-0550-8

Luidalepp, H., Hallier, M., Felden, B., and Tenson, T. (2005). tmRNA decreases the bactericidal activity of aminoglycosides and the susceptibility to inhibitors of cell wall synthesis. *RNA Biol.* 2, 70–74. doi: 10.4161/rna.2.2.2020.

Maisonneuve, E., and Gerdes, K. (2014). Molecular mechanisms underlying bacterial persisters. *Cell* 157, 539–548. doi: 10.1016/j.cell.2014.02.050

Michiels, J. E., van den Bergh, B., Verstraeten, N., and Michiels, J. (2016). Molecular mechanisms and clinical implications of bacterial persistence. *Drug Resist. Updat.* 29, 76–89. doi: 10.1016/j.drup.2016.10.002

Pu, Y., Zhao, Z., Li, Y., Zou, J., Ma, Q., Zhao, Y., et al. (2016). Enhanced efflux activity facilitates drug tolerance in dormant bacterial cells. *Mol. Cell.* 62, 284–294. doi: 10.1016/j.molcel.2016.03.035

Reyes-Becerril, M., Angulo, C., and Ascencio, F. (2015). Humoral immune response and TLR9 gene expression in Pacific red snapper (Lutjanus peru) experimentally exposed to *Aeromonas veronii*. *Fish Shellfish Immunol.* 42, 289–296. doi: 10.1016/j.fsi.2014.11.002

Roche, E. D., and Sauer, R. T. (2001). Identification of endogenous SsrA-tagged proteins reveals tagging at positions corresponding to stop codons. *J. Biol. Chem.* 276, 28509–28515. doi: 10.1074/jbc.M103864200

Sanchez, S., and Demain, A. L. (2008). Metabolic regulation and overproduction of primary metabolites. *Microb. Biotechnol.* 1, 283–319. doi: 10.1111/j.1751-7915.2007.00015.x

VanHook, A. (2019). Slow growth for bacterial persistence. *Science* 365, 459–459. doi: 10.1126/science.365.6452.458-i

Vollmer, W., Blanot, D., and de Pedro, M. A. (2008). Peptidoglycan structure and architecture. *FEMS Microbiol. Rev.* 32, 149–167. doi: 10.1111/j.1574-6976.2007.00094.x

Welsh, M. A., Taguchi, A., Schaefer, K., Van Tyne, D., Lebreton, F., et al. (2017). Identification of a functionally unique family of penicillin-binding proteins. *J. Am. Chem. Soc.* 139:jacs.7b10170. doi: 10.1021/jacs.7b10170

Zhang, L., Yu, W., Tang, Y., Li, H., Ma, X., and Liu, Z. (2019). RNA chaperone hfq mediates persistence to multiple antibiotics in *Aeromonas veronii*. *Microb. Pathog.* 132, 124–128. doi: 10.1016/j.micpath.2019.04.045

Zhang, S., and Wu, M. (1990). Determination of various neutral sugars, amino hexoses and acetamido hexoses. *J. Second Mil. Med. Univers.* 11, 450–453.

Conflict of Interest: The authors declare that the research was conducted in the absence of any commercial or financial relationships that could be construed as a potential conflict of interest.

frontiers in Cellular and Infection Microbiology

ORIGINAL RESEARCH
published: 28 April 2020
doi: 10.3389/fcimb.2020.00183

A T3SS Regulator Mutant of *Vibrio alginolyticus* Affects Antibiotic Susceptibilities and Provides Significant Protection to *Danio rerio* as a Live Attenuated Vaccine

Shihui Zhou[1,2,3,4,5,6], *Xueting Tu*[1,2,3,4,5,6], *Huanying Pang*[1,2,3,4,5,6]*, *Rowena Hoare*[7], *Sean J. Monaghan*[7], *Jiajun Luo*[2,3,4] and *Jichan Jian*[2,3,4,5,6]

[1] Shenzhen Institute of Guangdong Ocean University, Shenzhen, China, [2] Fisheries College, Guangdong Ocean University, Zhanjiang, China, [3] Guangdong Provincial Key Laboratory of Pathogenic Biology and Epidemiology for Aquatic Economic Animals, Zhanjiang, China, [4] Guangdong Key Laboratory of Control for Diseases of Aquatic Economic Animals, Zhanjiang, China, [5] Key Laboratory of Experimental Marine Biology, Institute of Oceanology, Chinese Academy of Sciences, Qingdao, China, [6] Laboratory for Marine Biology and Biotechnology, Qingdao National Laboratory for Marine Science and Technology, Qingdao, China, [7] Institute of Aquaculture, University of Stirling, Stirling, United Kingdom

OPEN ACCESS

Edited by:
Xiao-Peng Xiong,
Sanford-Burnham Institute for Medical Research, United States

Reviewed by:
Zhijie Xia,
Sanford Burnham Prebys Medical Discovery Institute, United States
Jing Xing,
Ocean University of China, China
Jingting Yu,
Salk Institute for Biological Studies, United States

***Correspondence:**
Huanying Pang
phying1218@163.com

Specialty section:
This article was submitted to Molecular Bacterial Pathogenesis, a section of the journal Frontiers in Cellular and Infection Microbiology

Received: 28 January 2020
Accepted: 06 April 2020
Published: 28 April 2020

Citation:
Zhou S, Tu X, Pang H, Hoare R, Monaghan SJ, Luo J and Jian J (2020) A T3SS Regulator Mutant of Vibrio alginolyticus Affects Antibiotic Susceptibilities and Provides Significant Protection to Danio rerio as a Live Attenuated Vaccine. Front. Cell. Infect. Microbiol. 10:183. doi: 10.3389/fcimb.2020.00183

Vibrio alginolyticus is a major cause of Vibriosis in farmed marine aquatic animals and has caused large economic losses to the Asian aquaculture industry in recent years. Therefore, it is necessary to control *V. alginolyticus* effectively. The virulence mechanism of *V. alginolyticus*, the Type III secretion system (T3SS), is closely related to its pathogenicity. In this study, the T3SS gene *tyeA* was cloned from *V. alginolyticus* wild-type strain HY9901 and the results showed that the deduced amino acid sequence of *V. alginolyticus tyeA* shared 75–83% homology with other *Vibrio* spp. The mutant strain HY9901Δ*tyeA* was constructed by Overlap-PCR and homologous recombination techniques. The HY9901Δ*tyeA* mutant exhibited an attenuated swarming phenotype and an ∼40-fold reduction in virulence to zebrafish. However, the HY9901Δ*tyeA* mutant showed no difference in growth, biofilm formation and ECPase activity. Antibiotic susceptibility test was observed that wild and mutant strains were extremely susceptible to Amikacin, Minocycline, Gentamicin, Cefperazone; and resistant to oxacillin, clindamycin, ceftazidime. In contrast wild strains are sensitive to tetracycline, chloramphenicol, kanamycin, doxycycline, while mutant strains are resistant to them. qRT-PCR was employed to analyze the transcription levels of T3SS-related genes, the results showed that compared with HY9901 wild type, Δ*tyeA* had increased expression of vscL, vscK, vscO, vopS, vopN, vscN, and hop. Following vaccination with the mutant strain, zebrafish had significantly higher survival than controls following infection with the wild-type HY9901 (71.2% relative percent survival; RPS). Analysis of immune gene expression by qPCR showed that vaccination with HY9901Δ*tyeA* increased the expression of IgM, IL-1β, IL-6, and TNF-α in zebrafish. This study provides evidence of protective efficacy of a live attenuated vaccine targeting the T3SS of *V. alginolyticus* which may be facilitated by up-regulated pro-inflammatory and immunoglobulin-related genes.

Keywords: *Vibrio alginolyticus*, live attenuated vaccine, type III secretory system, tyeA, regulator

INTRODUCTION

Vibrio alginolyticus, a Gram-negative motile rod bacterium, is widely found in seawater and estuaries in various regions of the world (Thompson et al., 2004; Jones et al., 2013) *V. alginolyticus* is highly pathogenic in marine animals (Ben Kahla-Nakbi et al., 2009; Jun et al., 2015) and is associated with diseases of fish, shellfish, shrimp, and coral (Chang et al., 2008; Sadok et al., 2013). It is also a potential zoonotic pathogenic bacteria and incurs great economic losses to the aquaculture industry with raised pressures for the industry to develop controls in recent years. Zoonotic infections can result from human food poisoning causing diarrhea and other symptoms (Li et al., 2009; Sganga et al., 2009). Therefore, it is of great importance to understand the pathogenic mechanisms of *V. alginolyticus* in order to develop an effective vaccine.

Type III secretory system (T3SS) is a highly conserved secretory system in several Gram-negative bacteria such as *Yersinia* spp., *Salmonella* spp., *Vibrio cholerae*, *Pseudomonas* spp. (Anand et al., 2003; Masato et al., 2014; Khavong and Lorena, 2016; Dorothea et al., 2017). When *V. alginolyticus* infects the host, the T3SS can secrete virulence proteins outside the cell or on the surface of the host cell, or even directly inject virulent proteins into the host cell, resulting in cell death (Pallen et al., 2005). Although the T3SS mechanism is usually conserved in Gram-negative pathogens, the functions of its regulator vary widely. Comparative genome analysis showed that the T3SS of *V. alginolyticus* was similar to that of *Vibrio parahaemolyticus* (Martinez-Argudo and Blocker, 2010), but little is known about the regulator TyeA of *V. alginolyticus* T3SS.

Until now, there was no related research on *tyeA* gene in *Vibrio alginolyticus*, and its function was still being explored. It has been found that TyeA is a regulator of T3SS and involved in regulation of effector proteins expression (Sundberg and Forsberg, 2003). Numerous studies have shown that the YopN-TyeA heterodimer plays a particularly important role in regulating the secretion of effector proteins in *Yersinia* (Iriarte et al., 1998; Cheng and Schneewind, 2000; Schubot et al., 2004; Ferracci et al., 2005). In order to understand the function of TyeA in T3SS, we first constructed a mutant of *tyeA* gene, studied the biology and pathogenicity of the HY9901Δ*tyeA* strain and the transcription levels of T3SS-related genes were then analyzed by qRT-PCR. In addition, we found that HY9901Δ*tyeA* mutant can be used as an effective live vaccine against *Vibrio alginolyticus* in zebrafish and induces the expression of zebrafish pro-inflammatory and immunoglobulin-related genes.

MATERIALS AND METHODS

Bacterial Strains, Plasmid, and Experimental Fish

The bacterial strains, plasmids, and zebrafish used in this study are listed in **Table 1**. *V. alginolyticus* HY9901 was isolated from diseased red snapper (*Lutjanus sanguineus*) (Cai et al., 2007) in Zhanjiang Port, Guangdong Province. *E. coli* DH5 α, *E. coli* MC1061 (λ pir) (Rubirés et al., 1997), S17-1 (λ Pir) (Simon et al., 2019), and suicide plasmid pRE112 (Edwards et al., 1998) were preserved in our laboratory. Healthy zebrafish (*Danio rerio*) were purchased from Zhanjiang Aquatic Market, 3–4 cm long and ∼0.2 g in weight. The zebrafish were tested by bacteriological recovery tests and kept in seawater in a circulation system at 28°C for 2 weeks before the experiment.

Reagents and Primers

TIANamp Bacteria DNA Kit (Beijing, Tiangen Biotech Co., Ltd.); Easy PureTMQuick GelExtraction Kit and Easy PureTM Plasmid MiniPrepKit (Beijing, TransGen Biotech Co., Ltd.); pMD18-T vector, ExTaqDNA polymerase, Prime START MHS DNA polymerase, KpnI, SacI, and T4DNA ligase were all purchased from TaKaRa (Japan). The primers were synthesized by Sangon Biotech Co., Ltd.

Cloning and Sequencing of the *tyeA* Gene From *V. alginolyticus* HY9901

A pair of primers tyeAP1-F/tyeAP1-R were designed as shown in **Table 2** according to the *V. alginolyticus* gene sequence (GenBank Number: GU074526.1). PCR was performed in a Thermocycler (Bio-Rad, CA, USA) under the following optimized amplification conditions: an initial denaturation at 95°C for 5 min, followed by 35 cycles of 94°C for 30 s, 55°C for 30 s and 72°C for 30 s. Five microlitre of each amplicon was examined on a 1% agarose gel stained with ethidium bromide. The PCR product was recovered from the agarose gel to ligate into the pMD18-T vector and transformed into *E. coli* DH5α (**Table 1**). The inserted fragment was sequenced by Sangon Biological Engineering Technology & Services Co., Ltd. (Shanghai, China). Similarity analyses of the determined nucleotide sequences and deduced amino acid sequences were performed by BLAST programs (http://blast.ncbi.nlm.nih.gov /Blast.cgi) and aligned using the program Clustal-X (version 1.81). Protein analysis was conducted with ExPASy tools (http://expasy.org/tools/). Location of the domain

TABLE 1 | Bacterial strains, plasmids, and experimental fish used in this study.

Strains, plasmids	Relevant characteristics	Source
V.alginolyticus HY9901	Wild type, isolated from diseased *Lutjanus sanguineus* off the Southern China coast	(Cai et al., 2007)
E. coli DH5α	supE44 ΔlacU169 (ϕ80 lacZDM15) hsdR17 recA1 gyrA96 thi-1 relA1	TakaRa
MC1061 (λpir)	lacY1 galK2 ara-14 xyl-5 supE44 λpir	(Rubirés et al., 1997)
pRE112	pGP704 suicide plasmid, pir dependent, oriT, oriV, sacB, C mr	(Edwards et al., 1998)
S17-1 (λpir)	T prSmrrecA thi pro hsdR-M+RP4:2-Tc: Mu: K m T n7 λpir	(Simon et al., 2019)
S17-1-pRE-ΔtyeA	S17-1 containing plasmid of pRE-Δ*tyeA*, C mr	This study
pMD18-T	Cloning vector, Ampr	TakaRa
Zebrafish	experimental fish, purchased from Zhanjiang Aquatic Market	Zhanjiang Aquatic Market

TABLE 2 | Sequences of primers used in this study.

Primer name	Primer sequence(5′-3′)	Accession number
tyeA-for	GGAATCTAGACCTTGAGTCG ATATCTCGACCATCGCGCAA	MN328351
tyeA-int-rev	ATCTTCCCACGCTTCCTCTT CAACTTGATAAGCCATAATTCGTCC	
tyeA-int-for	GGACGAATTATGGCTTATCA AGTTGAAGAGGAAGCGTGGGAAGAT	
tyeA-rev	ACAGCTAGCGACGATATGTCA GGCCGGAGGTCATAGAGCT	
tyeA-up	CACATGAACTCGTTTCGGACTATT	
tyeA-down	TTTCTGGACGCAACAACTCTGA	
tyeAP1-F	ATGGCTTATCAAGTTTCTA	
tyeAP1-R	TCAATCCAACTCATCTTCC	
IL-6-F	GGTCAGACTGAATCGGAGCG	NM_001079833.1
IL-6-R	CAGCCATGTGGCGAACG	
IL-6R-F	GCATGTGCTTAAAGTATCCTGGTC	NM_001114318.1
IL-6R-R	TGCAAATTGTGGTCGGTATCTC	
IL-1β-F	TGGACTTCGCAGCACAAAATG	AY340959.1
IL-1β-R	GTTCACTTCACGCTCTTGGATG	
IL-8-F	GTCGCTGCATTGAAACAGAA	XM_001342570.2
IL-8-R	CTTAACCCATGGAGCAGAGG	
IgM-F	GTTCCTGACCAGTGCAGAGA	AF246193
IgM-R	CCTGATCACCTCCAGCATAA	
TNF-α-F	TAGAACAACCCAGCAAAC	NC_007130.7
TNF-α-R	ACCAGCGGTAAAGGCAAC	
rag-1-F	GAAGTATACCAGAAGCCTAAT	NC_007136.7
rag-1-R	TTCCATTCATCCTCATCACA	
TLR5-F	GAAACATTCACCTGGCACA	NC_007131.7
TLR5-R	CTACAACCAGCACCACCAGAATG	
c/ebpβ-F	GCCGTACCAGACTGCTCCGA	NC_007119.7
c/ebpβ-R	AGCCGCTTCTTGCCTTTCCC	
β-actin-F	ATGGATGAGGAAATCGCTGCC	NM_131031.1
β-actin-R	CTCCCTGATGTCTGGGTCGTC	
vscL-F	TACCACGGTGAGTGTAGTTC	ACY41051.1
vscL-R	CGTAACCGACTTCAGGGA	
hop-F	CTTCGCTTTCGGTTTGCT	KX245315
hop-R	AATACCATCCCACCCTGT	
vscO-F	GAGCTGGAAACATTAAGACA	ACY41065.1
vscO-R	TTGCTGCAACTGAACGAA	
vscK-F	GGCGTTATCTCCCGTTCC	ACY41050.1
vscK-R	CTCCGCCCACCATCAATA	
vopN-F	TGAACTCGTTTCGGACTA	ACY41067.1
vopN-R	ACTTTCTGGACTCGCACT	
vscN-F	TAGGCGAAGAAGGAATGG	ACY41066.1
vscN-R	GCGATAGAAGTGGCAACAA	
vopS-F	AGTTTTGGAAGTGTTAGCG	ACY41053.1
vopS-R	ACATTGCCTCTGTCATCG	
16S-F	TTGCGAGAGTGAGCGAATCC	NR_044825.2
16S-R	ATGGTGTGACGGGCGGTGTG	

was predicted using the InterProScan program (http://www.ebi.ac.uk/Tools/pfa/iprscan/).

Construction of In-frame Deletion Mutant of *tyeA* Gene

According to the method previously described Zujie et al. (2019), Overlap extension PCR was applied to generate an in-frame deletion of the *tyeA* gene on the *V. alginolyticus* wild-type HY9901 chromosome. The in-frame deletion of *tyeA* in the *V. alginolyticus* was generated according to the method of Rubirés et al. (1997). For the construction of Δ*tyeA*, two PCR fragments were generated from HY9901 genomic DNA. The first fragment was amplified using primers tyeA-for (contains a KpnI site at the 5′-end) and tyeA-int-rev, whereas primers tyeA-int-for and tyeA-rev (contains a SmaI site at the 5′-end) were used to amplify the second fragment. Both fragments contained a 20 bp overlapping sequence and were used as templates for the subsequent PCR procedure, which used primers tyeA-for and tyeA-rev. The PCR product was ligated into suicide vector pRE112 (Cmr) to generate pRE-Δ*tyeA*. This recombinant suicide plasmid was transformed into *E. coli* MC1061λpir and subsequently S17-1λpir. The single crossover mutants were obtained by conjugal transfer of the resulting plasmid into *V. alginolyticus* HY9901. Deletion mutants were screened on 10% sucrose TSA plates. Its presence was subsequently confirmed by PCR and sequencing using primers tyeA-up and tyeA-down.

Characterization of the Δ*tyeA*

Genetic Stability of Mutants HY9901ΔtyeA

HY9901Δ*tyeA* was inoculated onto a TSA plate and passaged blindly for 30 generations. In brief, a single colony was picked from Tryptic Soya agar (TSA) plates and cultured in Tryptic soya broth (TSB, HKM, Guangzhou, China) medium, shaking for 12 h, bacterial broth culture was streaked out on a TSA plate, and this process repeated 30 times. Its genetic stability was determined by the PCR method.

Growth Curve of Bacteria

The wild-type HY9901 strain and the Δ*tyeA* were cultured in TSB for 24 h. The HY9901 and HY9901 Δ*tyeA* were inoculated into TSB at the ratio of 1: 100 (OD_{600} = 0.5) at 28°C, with determination of OD_{600} every 2 h. This procedure was repeated three times per group.

Detection of Extracellular Protease Activity

According to the previously published method (Windle and Kelleher, 1997) wild-type strain HY9901 and HY9901Δ*tyeA* were coated on TSA plates coated with sterile cellophane, and cultured at 28°C for 24 h, washed with sterile PBS, centrifuged at 4°C for 30 min, and the supernatant filtered to obtain extracellular products. Inactivated sample (supernatant was boiled for 10 min) was used as a blank control.

Swarming Motility

Single colonies of wild-type strain HY9901 and HY9901Δ*tyeA* were selected by sterile toothpick and plated on TSA plates with agar content of 0.5%. Each group was incubated for 24 h at 28°C. The diameter of swarming circle was measured by Vernier calipers.

Detection of Biofilm Formation Ability Using Crystal Violet Ammonium Oxalate

With reference to the method described previously (Katharine and Watnick, 2003), wild strains HY9901 and HY9901 Δ*tyeA* (OD_{600} = 0.5) were transferred to a 96-well plate. Each well was inoculated with 200 μL of bacterium with 6 replicates per sample, the negative control was an inoculum of TSB only, and the culture temperature was 28°C. Samples were taken from the 96 well plate at 12, 24, 48, and 72 h, methanol fixed for 20 min, stained with Crystal violet ammonium oxalate dye for 15 min, rinsed with water and dried. Finally, 95% alcohol was added and incubated at room temperature for 30 min. OD_{570} was determined by Multimode Plate Reader(PerkinElmer EnSpire, EnSpire, Singapore) (OD_{600} = 1, bacterial concentration = 1×10^9 cfu/mL).

Detection of Biofilm Formation Ability Using *Laser Scanning Confocal Microscope (LSCM)*

The wild strain HY9901 and the mutant strain HY9901Δ*tyeA* (OD_{600} = 0.5) were diluted 50-fold, added to a glass bottom culture dishes (spec: type 28.2 mm, class diameter 20 mm) (Wuxi NEST, Wuxi, China) and statically cultured in a 28°C biochemical incubator for 24 h, gently washed three times with physiological saline, and then combined with 10% SYTO9 green. Bacteria were incubated with fluorescent dyes in the dark for 20 min, washed three times with saline, mounted in 40% saline-glycerol and observed by confocal microscopy (Zeiss, LSM710, Germany). The excitation wavelength was 488 nm, scanned from the bottom to the top of the biofilm, Z-section was 1 μm apart, and biofilm parameters—biomass and maximum thickness were determined. Three samples were made for each strain and the average amount calculated.

Dose Response Challenge Test (LD_{50})

The injection concentrations used for the dose response of wild-type strain HY9901 and Δ*tyeA* were 10^4, 10^5, 10^6, 10^7, and 10^8 CFU/mL. A total of 330 fish were randomly divided into three groups (**Table 3**). The water temperature was adjusted to 28°C. The experiment was repeated three times. Five microlitre of bacterial solution was injected into fish by intramuscular injection. The control group was injected with equivalent volumes of PBS. Fish were monitored for 14 days or until no morbidities occurred. Specific mortality was determined by streaking head-kidney onto TSA. The LD_{50} of the mutant and wild strains was calculated by the Koch method (Reed and Muench, 1938).

Antibiotic Susceptibility

The susceptibility patterns of the HY9901 and HY9901Δ*tyeA* strains to 30 different antibiotics were determined according to the disc diffusion method using TSA (Bauer et al., 1966), and the diameters of the inhibition zones were measured using Vernier calipers. Resistant, intermediate and susceptible phenotype determinations were based on previously published susceptibility paper guidelines (HANGWEI, S1100, China). The strains were inoculated onto TSA plates and allowed to absorb onto agar for 10 min, and antibiotic discs were added after 24 h of incubation at 28°C (Cai et al., 2016).

TABLE 3 | Experiment of LD_{50}.

Concentration HY9901 (CFU/mL)		Death rate (%)	Δ*tyeA*	Death rate (%)	Control (PBS)	Death rate (%)
10^8	10 × 3	90	10 × 3	66.7	–	–
10^7	10 × 3	80	10 × 3	40	–	–
10^6	10 × 3	60	10 × 3	10	–	–
10^5	10 × 3	20	10 × 3	0	–	–
10^4	10 × 3	20	10 × 3	0	–	–
0(PBS)	–	–	–	–	10 × 3	0

Each experiment involved 110 zebrafish with 10 fish per group in three replicate tanks and the experiment was repeated three times (total fish = 330).

Expression Analysis of T3SS-Related Genes

T3SS secretion was induced by Dulbecco's Modified Eagle Medium (DMEM) media, and strains HY9901 and HY9901 Δ*tyeA* were cultured for 12 h. The primers for T3SS related genes are shown in **Table 2** (All primers were designed within the current study). The genes in this study were hop (Pang et al., 2018), vopN, vscN (Yonghong et al., 2016), vscO (Zhou et al., 2013), vopS, vscL, and vscK (Nguyen et al., 2000). 16S rRNA is used as an internal reference. According to the experimental method of Li et al. (2016), RNA was extracted, synthetic cDNA and real-time PCR were used to analyze the expression of T3SS related genes.

Preparation of Vaccine and Vaccination

The Δ*tyeA* immune concentration of 10^5 CFU/mL was selected by LD_{50} experiments, which has no mortality to zebrafish (**Table 3**). The mutant Δ*tyeA* was cultured in a shaking flask at 28°C for 18 h, washed and suspended in sterile artificial seawater, and the concentration of the bacterial solution was adjusted to 10^5CFU mL^{-1} by spectrophotometer. The experimental fish were randomly divided into two groups with 80 fish in each group. The water temperature was adjusted to 28°C. Each fish was injected with 5 μL Δ*tyeA* bacterial solution (10^5 CFU mL^{-1}) by intramuscular injection and control fish were injected with 5 μL PBS per fish.

Determination of Vaccine Efficacy

Fish were challenged 28 days post vaccination. Thirty fish were randomly selected from each group (in triplicate) and given intramuscular injection of 5 μL *V. alginolyticus* the wild-type HY9901 (1×10^8 CFU mL^{-1}). The water temperature was adjusted to 28°C and the number of moribund/mortalities was recorded for 14 days. Calculation of the relative percentage survival was performed at the end of the experiment (RPS (%) = (1-immunized group mortality / control group mortality) × 100%).

Immune Gene Expression of Zebrafish Induced by HY9901Δ*tyeA* Vaccine

Liver and spleen samples were taken from three fish from each group, respectively, 1 day before challenge. Immune-related genes expression levels were detected with real-time qPCR. Primers for IL6, IL6R, IL-1β, IL-8, IgM, TNF-α, rag-1, TLR5, and c/ebpβ are shown in **Table 2**, and β-actin was used as internal reference. The procedures of RNA extraction, cDNA synthesis, real-time qPCR for analysis of immune gene expression were described by Li et al. (2016).

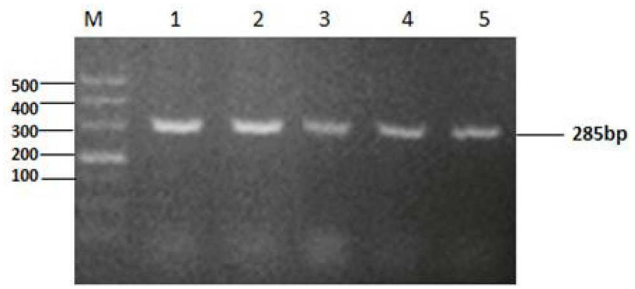

FIGURE 1 | Cloning of *tyeA* gene. M: DL2000 marker. Lane 1-5:The 285bp fragment was amplified from genomic DNA of the wild-type strain HY9901 using primer pairs of tyeAP1-for/tyeAP1-rev (Lane 1, 2, 3, 4, 5:Tm = 56°C, 57°C, 58°C, 59°C, 60°C).

Ethics Statement

All animal experiments were conducted strictly based on the recommendations in the "Guide for the Care and Use of Laboratory Animals" set by the National Institutes of Health. The animal protocols were approved by the Animal Ethics Committee of Guangdong Ocean University (Zhanjiang, China).

Biosecurity

The bacteria protocols were approved by the Biosecurity Committee of Guang dong Ocean University (Zhanjiang, China).

Statistical Analysis

The experimental data were analyzed by single factor analysis of variance (ANOVA) with SPSS17.0 software. **indicates extremely significant difference compared with the control group ($p < 0.01$). *indicates significant difference compared with the control group ($p < 0.05$).

RESULTS

Cloning of *tyeA* Gene and Construction of Mutant

The *tyeA* gene consists of an open reading frame of 285 bp (**Figure 1**), encoding 95 amino acids (aa) with a predicted molecular weight of 10.98 kDa (tyeA accession no. MN328351). The deduced amino acid sequence analysis of TyeA show it has high homology of 75–83% with other *Vibrio* spp. (**Figure 2**),

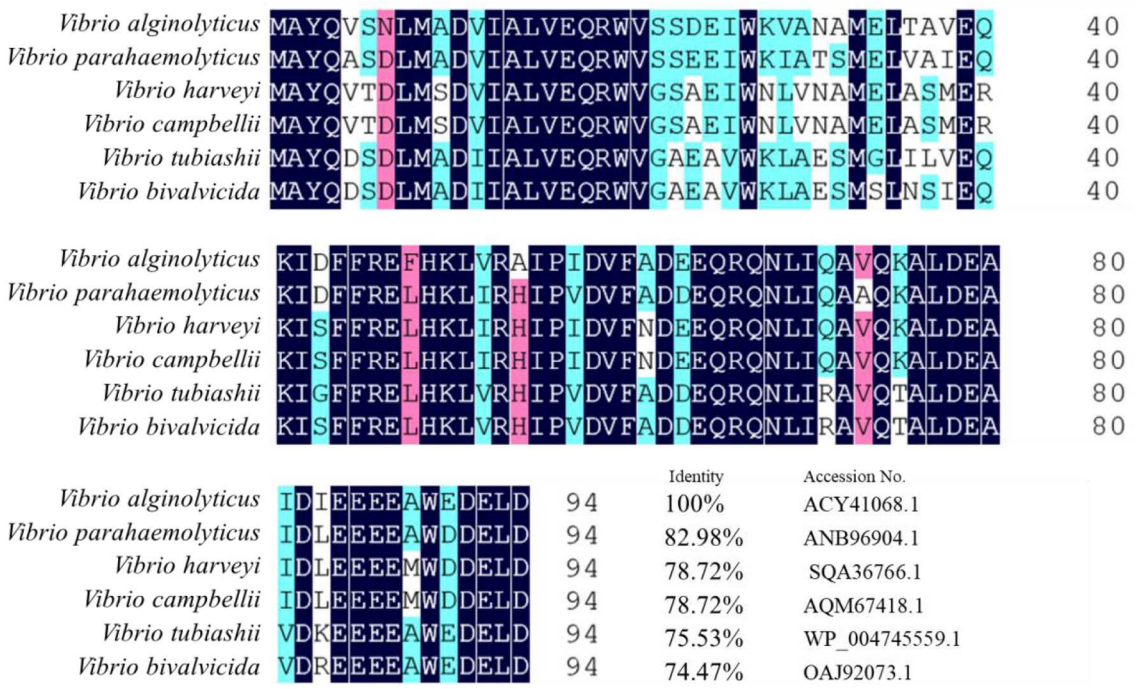

FIGURE 2 | Homology comparison of *Vibrio parahaemolyticus* HY9901 T3SS Regulator Protein TyeA. *Vibrio alginolyticus* T3SS regulatory protein TyeA Accession No.ACY41068.1; *Vibrio parahaemolyticus* T3SS regulatory protein TyeA Accession No.ANB96904.1; *Vibrio harveyi* T3SS regulatory protein TyeA Accession No.SQA36766.1; *Vibrio campbellii* T3SS regulatory protein TyeA Accession NO.AQM67418.1; *Vibrio tubiashii* T3SS regulatory protein TyeA Accession No.WP_004745559.1; *Vibrio bivalvicida* T3SS regulatory protein TyeA Accession No.OAJ92073.1.

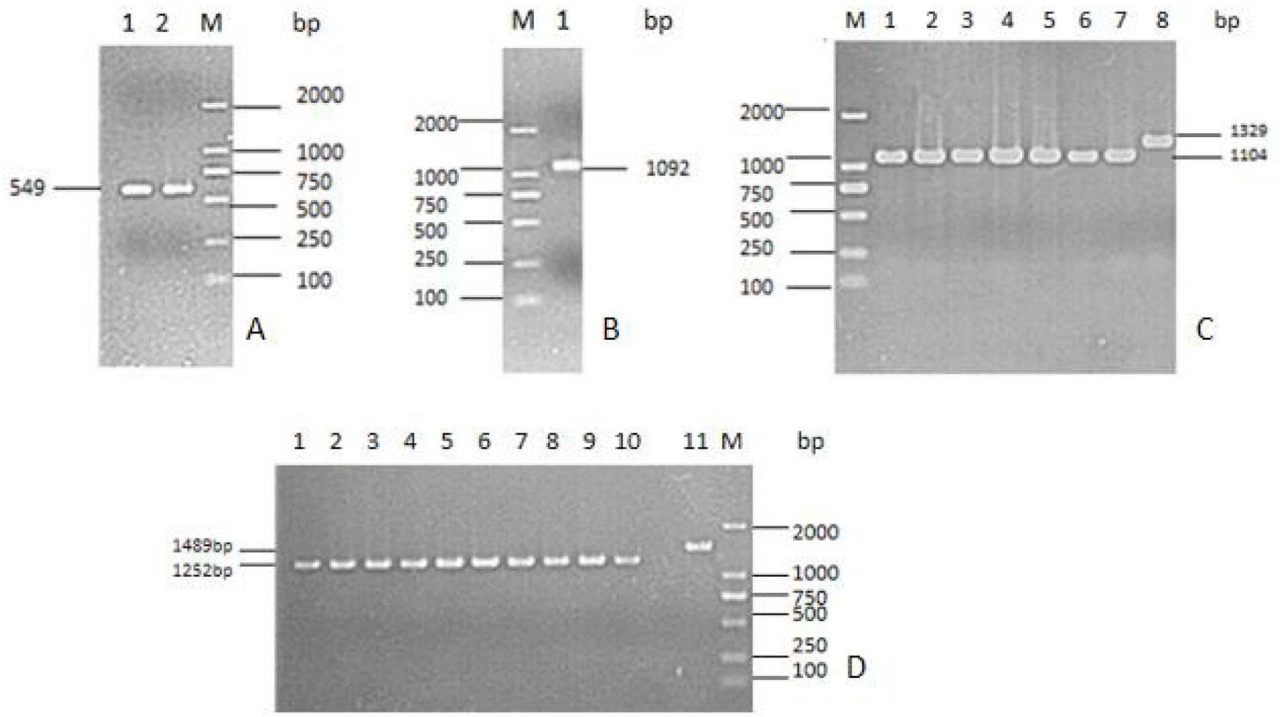

FIGURE 3 | Construction and confirmation of the knockout mutant strain HY9901Δ*tyeA*. **(A)** M: DL2000 marker; Lane 1. The 549 bp upstream fragment amplified from genomic DNAs of the strain HY9901 using primer pairs of tyeA-for/tyeA-int-rev; Lane 2. The 543 bp downstream fragment amplified from genomic DNAs of the strain HY9901 using primer pairs of tyeA-int-for / tyeA-rev. **(B)** M: DL2000 marker; Lane 1. The 1,092 bp fragment amplified from genomic DNAs of HY9901Δ*tyeA* using primer pairs of tyeA-for/tyeA-rev. **(C)** M: DL2000 marker; Lane 1–7. The 1,104 bp fragment amplified from genomic DNAs of the HY9901Δ*tyeA* using primer pairs of tyeA-for/tyeA-rev; Lane 8. The 1,329 bp fragment amplified from genomic DNAs of the wild-type strain HY9901 using primer pairs of tyeA-for/tyeA-rev. **(D)** M: DL2000 marker; Lane 1–10. The 1,252 bp fragment amplified from genomic DNAs of HY9901Δ*tyeA*; Lane11. The 1,489 bp fragment amplified from genomic DNAs of the strain HY9901 using primer pairs of tyeA-up / tyeA-down.

with the highest homology shared with *V. parahaemolyticus* (83%). An untagged in-frame deletion mutant HY9901Δ*tyeA* was constructed by over-lap PCR and forward and reverse screening methods. The mutant was confirmed by inabilityto grow on TSA supplemented with chloramphenicol, and verified by PCR by generating a fragment of ∼1,092 bp. Using PCR the genome of HY9901Δ*tyeA* and wild-type strain HY9901 by primer *tyeA*-up/*tyeA*-down, a 1,252 bp fragment was obtained for HY9901Δ*tyeA* and fragment of 1,489 bp was obtained for HY9901 (**Figure 3**).

Characterization of the *tyeA*

Genetic Stability of Mutants

After 30 generations of continuous passages of mutant Δ*tyeA*, the PCR genome of HY9901Δ*tyeA* and wild-type strain HY9901 using primers *tyeA*-up/*tyeA*-down, a fragment of 1,489 bp was obtained for HY9901, and fragment of 1,252 bp was obtained for HY9901Δ*tyeA*. This shows that the wild-type strain HY9901 has 237 bp more than the mutant Δ*tyeA*, and the mutant Δ*tyeA* has deleted the gene tyeA, which can stabilize the inheritance (**Figure 4**).

Comparison of Growth Rates of Wild Type and Mutant Bacteria

The growth rate of wild-type strain HY9901 and HY9901Δ*tyeA* was similar and not statistically significant ($p > 0.05$) (**Figure 5**), the deletion of *tyeA* gene has no effect on the growth of *V. alginolyticus*. The exponential growth phase of the two bacterial strains was from 0 to 4 h, with growth stationary at 18 h, OD600 ≈ 1.7.

Extracellular Protease Activity

Extracellular proteases, as metabolites of bacteria, play an important role as virulence factors in the process of infecting the host. Extracellular proteins have a variety of protease activities, including lecithin, amylase, lipase, and casein. The extracellular protease activity was not significantly different between HY9901Δ*tyeA* and the wild-type strain HY9901 ($p > 0.05$) (**Table 4**).

Detection of Biofilm Formation Ability

No significant differences were observed in biofilm formation at 24 h ($p > 0.05$) between wild strains and mutants of *V. alginolyticus* using the crystal violet ammonium oxalate assay (**Figure 6**) or by confocal microscopy (**Figure 7** and **Table 4**).

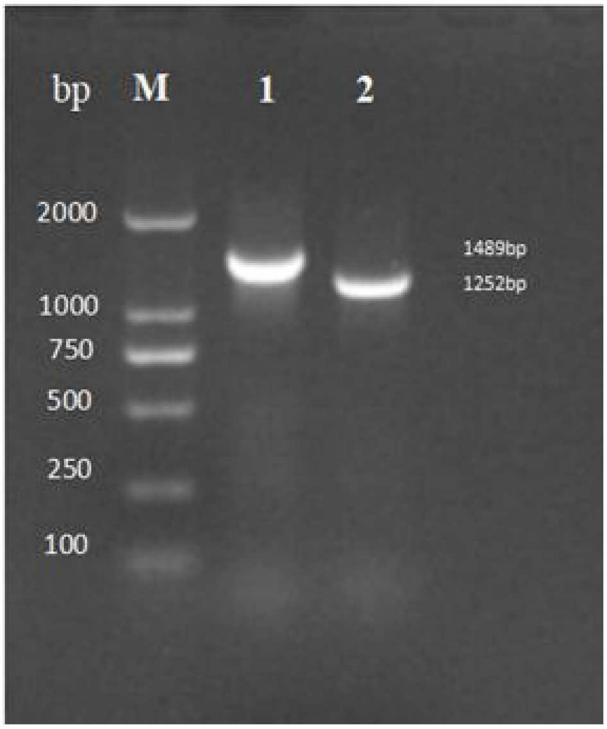

FIGURE 4 | Genetic stability detection of HY9901Δ*tyeA* deletion mutant. M: DL2000 marker, Lane 1. A fragment of 1,489 bp is obtained for HY9901 using primer pairs of tyeA-up/tyeA-down. Lane 2. A fragment of 1,252 bp is obtained for HY9901Δ*tyeA* using primer pairs of tyeA-up/tyeA-down.

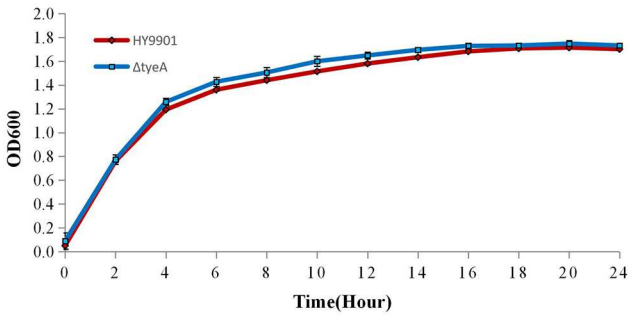

FIGURE 5 | Growth rates of HY9901Δ*tyeA* and HY9901. Aliquots of cell culture were taken at various time points and measured for cell density at OD_{600}.

TABLE 4 | Comparison of biological characteristics between HY9901 and HY9901Δ*tyeA*.

Characteristics	HY9901	HY9901Δ*tyeA*
Activity of ECPase(A_{422})[a]	1.03 ± 0.2	0.97 ± 0.2
Biofilm thickness(μm)[b]	60 ± 10	90 ± 20
Swarming (mm)[c]	34.9 ± 0.2	20.6 ± 0.4**
LD_{50}(CFU mL^{-1})[d]	5.8×10^5	2.6×10^{7}**

Values are mean ± standard deviation for three trials. Significant differences between HY9901 and HY9901ΔtyeA indicated by asterisk.
***p < 0.01.*
[a]Bacteria were incubated in TSB for 18 h at 28°C.
[b]Bacteria were incubated in a glass bottom culture dish (NEST) for 24 h at 28°C.
[c]Swarming diameters were measured after 24 h incubation on TSA containing 0.3% agar plates.
[d]LD_{50} were evaluated in healthy zebrafish with an average weight of 0.2 g.

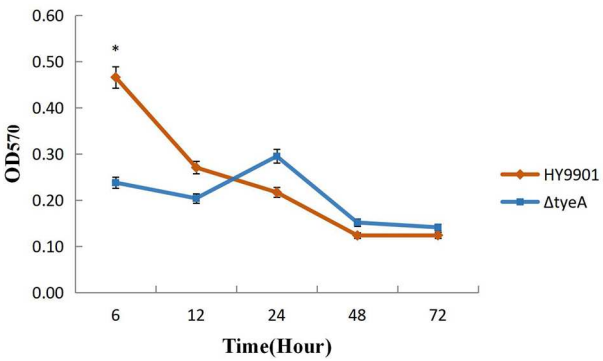

FIGURE 6 | Measurement of biofilm by crystal violet ammonium oxalate. *indicates significant difference compared with the control group ($p < 0.05$). **indicates extremely significant difference compared with the control group ($p < 0.01$).

The biofilm fluctuates up and down within 72 h in crystal violet ammonium oxalate. The biofilm was thicker in HY9901 than in the mutant at 6 h ($p < 0.05$). After 12 h, the biofilm thickness was basically equal, and there was no significant change according to biological statistical analysis.

Swarming Motility

The wild-type strain HY9901 and HY9901Δ*tyeA* were inoculated on the swarming plate, and the results were as follows: the swarming circle of wild strain was 34.9 ± 0.2 mm, mutant was 20.6 ± 0.4 mm (**Table 4**). The swarming circle diameter of HY9901Δ*tyeA* was significantly smaller than that of wild strain ($p < 0.01$), indicating that the swarming ability of HY9901Δ*tyeA* was significantly weakened.

LD_{50} Determination

Zebrafish from quarantined stocks recognized as disease free (Xu et al., 2010) were used as models (Sullivan and Kim, 2008) to assess the virulence of the strain HY9901 and HY9901Δ*tyeA*. The results showed that the 50% lethal dose of HY9901Δ*tyeA* was 40 times higher than that of wild strain (**Tables 3**, **4**). The symptoms of body surface hyperemia, abdominal redness and swelling and slow swimming were observed in the diseased fish. The results showed that the virulence of HY9901 Δ*tyeA* was significantly decreased when compared with the wild strain ($p < 0.01$).

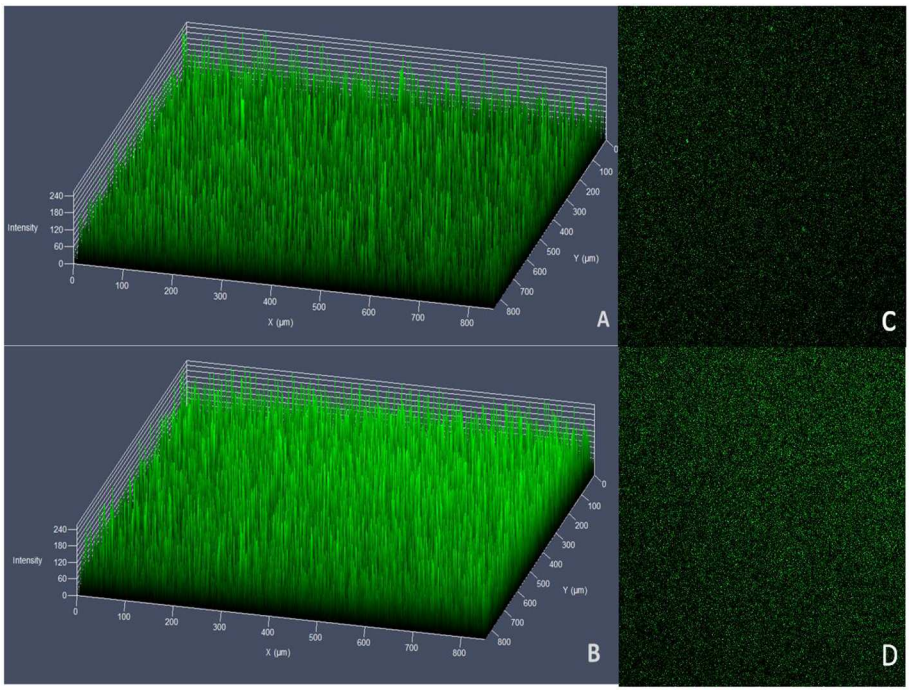

FIGURE 7 | Measurement of biofilm by LSCM. **(A)** HY9901 2.5d diagram. **(B)** HY9901Δ*tyeA* 2.5d diagram. **(C)** HY9901 2d diagram. **(D)** HY9901Δ*tyeA* 2d diagram; HY9901 Biofilm thickness:60 ± 10 μm, HY9901Δ*tyeA* Biofilm thickness:90 ± 20 μm.

Antibiotic Susceptibility

Both wild and mutant strains were extremely susceptible to amikacin, minocycline, gentamicin, Cefperazone; resistant to oxacillin, clindamycin, ceftazidime, penicillin, ampicillin, caebenicillin, cefazolin, ceftriaxone, cephradine, piperacillin. Wild strains were sensitive to tetracycline, chloramphenicol, kanamycin, doxycycline, while mutant strains were resistant to them (**Table 5**).

T3SS-related Gene Expression Analysis

QRT-PCR was employed to analyze the transcription levels of T3SS-related genes including *vscL*, *vscK*, *vopN*, *vscO*, *vscN*, *vopS,* and *hop*. The results showed that compared with HY9901 wild type, Δ*tyeA* had significantly increased expression of *vscL*, *vscK*, *vscO*, *vopS* ($p < 0.05$), *vopN*, *vscN* and *hop* ($p < 0.01$) (**Figure 8**).

Vaccine Efficacy

Fish vaccinated with the mutant strain HY9901Δ*tyeA* were challenged 28 days post-vaccination with the wild strain. Within 14 days, the mortality rate in the control group injected with sterile PBS was 87%, the mortality rate in the injection immunization group was 25%, and the relative percentage survival was 71.2% (**Figure 9**).

Immune Gene Expression of Zebrafish Induced by HY9901Δ*tyeA* Vaccine

Detection of immune gene expression in zebrafish immunized with HY9901Δ*tyeA* live attenuated vaccine was assessed by qPCR to analyze the transcriptional levels of pro-inflammatory and immunoglobulin-related immune genes. The results showed that, the group vaccinated with the mutant strain HY9901Δ*tyeA* had significantly increased expression of IL6, IL6R, IL-1β, TNF-α, rag-1, TLR5, c/ebpβ genes in liver and IL6, IL8, IgM, TNF-α, rag-1 genes in spleen compared to control fish injected with PBS ($p < 0.01$) (**Figure 10**).

DISCUSSION

At present, the interaction mechanisms between some fish pathogens and hosts have been studied in depth. Based on these studies, the development of efficient new vaccines has become highly desirable in aquaculture (Pang et al., 2016). Attenuated live vaccines are one of the more efficient vaccines, especially compared to inactivated vaccines due to their greater activation of cellular immunity. Currently, the construction of attenuated strains by gene knockout is an important method to obtain candidate attenuated live vaccines.

In the current study, we knocked out the T3SS gene *tyeA* of *V. alginolyticus*, explored its biology and pathogenicity, and evaluated its effect as a live attenuated vaccine. Zhou et al. (2013) found that the mutant of T3SS chaperone escort *vscO* of *V. alginolyticus* showed an attenuated swarming ability and a 10-fold decrease in the virulence to fish. However, the Δ*vscO* mutant showed no difference in the biofilm formation and ECPase activity. The authors concluded that *vscO* is associated with the flagella of *V. alginolyticus*. The knockout of *vscO* gene results in the decline of group movement ability and thus reduced virulence

TABLE 5 | Drug sensitivity test results of the HY9901 and HY9901Δ*tyeA*.

Antibiotic	Dose (μg)	Bacteriostatic circle diameter (mm)			
		HY9901	Sensitivity	Δ*tyeA*	Sensitivity
Cefperazone	75	0	R	0	R
Oxacillin	1	0	R	0	R
Clindamycin	2	0	R	0	R
Ceftazidime	30	0	R	0	R
Penicillin	10U	0	R	0	R
Ampicillin	100	0	R	0	R
Caebenicillin	100	0	R	0	R
Cefazolin	30	8.0 ± 0.2	R	0	R
Ceftriaxone	30	9.3 ± 0.3	R	0	R
Cephradine	30	0	R	0	R
Piperacillin	100	0	R	0	R
Cefuroxime	30	0	R	0	R
SMZ/TMP	23.75/1.25	0	R	0	R
Aboren	30	0	R	0	R
Vancomycin	30	0	R	0	R
Cephalexin	30	0	R	0	R
polymxinB	200IU	0	R	0	R
Norfloxacin	10	0	R	0	R
Ofloxacin	5	0	R	0	R
Ciprofloxacin	5	0	R	0	R
Amikacin	30	13.3 ± 0.3	I	10.0 ± 0.1	I
Minocyline	30	18.5 ± 0.2	S	14.3 ± 0.3	I
Tetracyline	30	13.5 ± 0.2	I	12.5 ± 0.2	R
Gentamicin	10	14.5 ± 0.1	I	12.5 ± 0.2	I
Furazolidone	300	10.5 ± 0.4	R	8.0 ± 0.1	R
Chloramphenicol	30	17.2 ± 0.3	S	0	R
kanamycin	30	14.1 ± 0.2	I	12.1 ± 0.2	R
Erythromycin	15	10.1 ± 0.2	R	0	R
Doxycycline	30	16.5 ± 0.3	S	10.6 ± 0.1	R
Cefperazone	30	14.2 ± 0.3	I	13.3 ± 0.3	I

S(susceptible) I(intermediate) R(resistance).

(Zhou et al., 2013). Another mutant of *V. alginolyticus*, Δ*sodB* did not show any difference in growth when compared with wild type strains HY9901. However, the Δ*sodB* mutant resulted in the formation of biofilm, increased SOD activity and toxicity, increased ECPase activity and sensitivity to hydrogen peroxide, a decreased group movement ability and decreased adhesion to cytokine-induced killer (CIK) cells (Yanyan et al., 2019). Even though the mutant of T3SS effector Hop revealed an attenuated swarming phenotype and a 2,600-fold decrease in the virulence to grouper, the HY9901Δ*hop* mutant showed no difference in morphology, growth, biofilm formation and ECPase activity (Pang et al., 2018). Similarly in the present study, there was no significant difference between HY9901Δ*tyeA* and wild type strains HY9901 in growth, biofilm formation and ECPase activity but the HY9901Δ*tyeA* mutant showed an attenuated swarming phenotype and a nearly 40-fold decrease in virulence to zebrafish. A polar flagellum and numerous lateral flagella contribute to the swimming and swarming motilities respectively, by which some bacteria access an appropriate niche inside the host after infection, as observed in *V. parahaemolyticus* (Enos-Berlage et al., 2005). Therefore, swarming ability is closely related to the virulence of some bacteria. Biofilm formation is a multicellular behavior through which bacteria colonize the surface of host tissues and tank surfaces and are thereby highly resistant to antibiotics and host immune defense mechanisms (Parsek and Singh, 2003; Verstraeten et al., 2008). Extracellular products (ECP) produced by bacteria include proteases, hemolysins and siderophores. As a metabolite of bacteria, extracellular proteases used as virulence factors by *V. alginolyticus* play an important role in the process of infection. Flagella assist in swimming and can help bacteria enter the appropriate niche in the host after *Vibrio spp*. infection. Motility is an important index used to judge the virulence of bacteria (Watnick et al., 2001). Numerous studies have shown that flagellin is essential for flagellum formation, trivial movement and symbiosis, and it also greatly affects the colonizing ability of *Vibrio spp*. (Millikan and Ruby, 2004). The results of this study showed that there was no significant difference in bacterial growth rate, biofilm, and extracellular enzyme activity between the *tyeA* knockout and the wild strain of *V. alginolyticus*, suggesting that TyeA may not affect these characteristics in *V. alginolyticus*. Nevertheless, this study found that HY9901Δ*tyeA* had significantly decreased swarming motility, which may be associated with bacterial flagellar movement. Therefore, the *tyeA* gene may have a positive regulation in the swarming motility of *Vibrio alginolyticus*, and its regulatory mechanism needs further investigation.

It is generally agreed that T3SS can be secreted by bacteria *in vitro* or by contacting host cells (Buttner and Bonas, 2002; Blondel Carlos et al., 2016). The secretory pathway of T3SS *in vitro* and *in vivo* is complex, sometimes the regulation is completed by a single regulatory protein, and sometimes the regulation is completed by multiple interacting regulatory proteins. For example, the transcriptional expression of the T3SS1 gene cluster of *V. parahaemolyticus* in DMEM can be regulated by the regulatory proteins ExsA and ExsD. Among them, ExsA is a positive transcriptional regulation protein and ExsD is a negative transcriptional regulation protein. It was hypothesize that ExsA might play a direct role in the T3SS1 promoter sequence (Zhou et al., 2008) based on the discovery that ExsA protein directly binds the upstream region of effector protein VP1668 and VP1687 in gel retardation assay (EMSA). Furthermore, the co-expression of recombinant proteins labeled with different antigens showed that: the combination of ExsD and ExsA blocks the expression of T3SS1; the combination of ExsC and ExsD releases ExsA, thus allowing the expression of T3SS1 (Zhou et al., 2010).

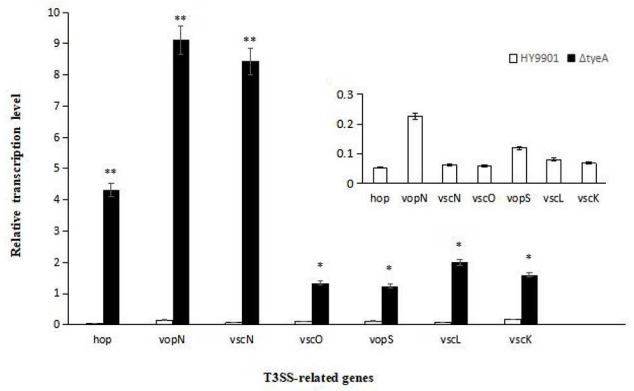

FIGURE 8 | Expression of HY9901 and HY9901Δ*tyeA* T3SS-related genes induced by DMEM. Δ*tyeA* had significantly increased expression of *vscL*, *vscK*, *vscO*, *vopS* ($p < 0.05$), *vopN*, *vscN*, and *hop* ($p < 0.01$). * indicates significant difference compared with the control group ($p < 0.05$). ** indicates extremely significant difference compared with the control group ($p < 0.01$).

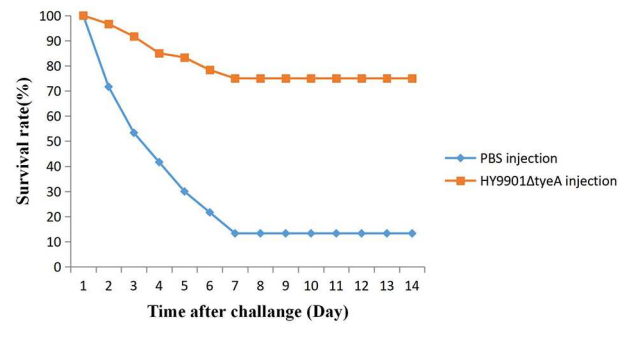

FIGURE 9 | Survival in groups vaccinated with HY9901Δ*tyeA* and PBS following challenge with *Vibrio alginolyticus* HY9901.

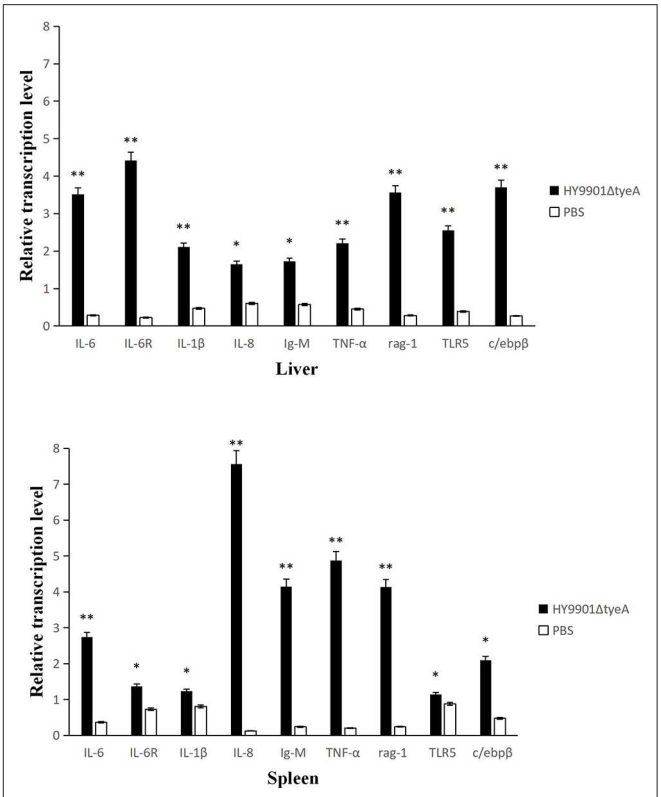

FIGURE 10 | Comparative analysis of the expression of immune-related genes in liver and spleen of zebrafish given the live attenuated vaccine and unvaccinated zebrafish. The head kidney and spleen of grouper were sampled at 1 day before challenge, and the mRNA level of each immune-related gene was normalized to that of β-actin. Bars represent the mean relative expression of three biological replicates and error bars represent standard deviation.

According to Miller et al. (2016), in a bile salt environment, VttRA and VttRB of *V.o cholerae* can regulate the secretion of T3SS structural genes and some effector proteins. In terms of *V. alginolyticus*, ExsA and ExsC play a positive regulatory role on the effector proteins Va1686 and Va1687, ExsD, and ExsE play a negative regulatory role, ExsA and ExsC act as stimulus to the swarming of the side flagella of *V. alginolyticus* and on the contrary, ExsD and ExsE act as hindrance to the swarming of the side flagella (Liu et al., 2016). Interestingly, the results of fluorescence quantification and drug susceptibility tests in this study indicated that TyeA negatively regulated T3SS protein (vscL, vscK and vscO are apparatus proteins, while vopN, vscN, and hop are effector or regulatory proteins) and drug resistance genes. However, the systematic research of the network regulatory mechanism of various *V. alginolyticus* regulatory proteins on effector proteins *in vitro* and *in vivo* is still needed. TyeA, a regulator in T3SS, is widely studied in other strains (Sundberg and Forsberg, 2003; Schubot et al., 2004; Amer et al., 2016), and some progress has been made (Joseph and Plano, 2007; Plano and Schesser, 2013). However, its regulation mechanism in *V. alginolyticus* remains unknown. In order to further reveal the pathogenic mechanism of *V. alginolyticus*, so as to achieve the purpose of controlling vibriosis, the research on the regulatory mechanism of the regulatory gene *tyeA* in *V. alginolyticus* will be followed-up in future investigations.

Moreover, although zebrafish will not specifically be the target of the vaccine in the future, studies have shown that zebrafish are a good model for teleost immune responses (Streisinger et al., 1981). For example, Zhang et al. (2012) used zebrafish to investigate the immune response following administration of a live attenuated *V. anguillarum* vaccine. Hua and co-author's results showed that Th17 cells were activated following vaccination of zebrafish (Hua et al., 2013). At the same time, a large number of studies have shown that zebrafish can be infected by marine vibrios (O'toole et al., 2004; Rojo et al., 2007; Rodríguez et al., 2008). Therefore, it is feasible to use zebrafish to study the effectiveness of a marine *Vibrio* vaccine. In this study, genes associated with innate immunity or inflammatory factors: IL-1 β, IL6, IL8, and TNF- α were studied. Additionally the expression profiles of bacterial flagellum recognition factor TLR5, adaptive immune factors including

rag-1, and immunoglobulin IgM were assessed, as well as blood corpuscle specific marker genes c/elbp. In summary, the results show that HY9901Δ*tyeA* can effectively induce the protective immune response of zebrafish associated with pro-inflammatory and immunoglobulin activity. *V. alginolyticus* has been resistant to most antibiotics according to the results of drug sensitivity testing in this study. Antibiotic resistance is closely linked to antibiotic abuse (Chee-Sanford et al., 2001; Burridge et al., 2010). In the future, the direction for the prevention and control of aquatic diseases such as Vibriosis is to develop *Vibrio* vaccine and thereby reduce the use of antibiotics, which has great significance for protecting the environment and developing aquaculture sustainably. In the current study, the relative percentage survival rate of zebrafish immunized with the vaccine candidate strain Δ*tyeA* was 71.2%, which indicated that the construction of the deletion strain could be used as one of the effective ways to develop a vaccine against this pathogen. It provides an experimental basis for the prevention and control of *Vibrio spp*. in aquaculture. Studies have shown that compared with inactivated vaccines, live attenuated vaccines have the advantages of long-lasting efficacy and inducing strong cellular immunity, which is in line with the current needs of aquaculture, however their use is not permitted under current regulations in Europe.

CONCLUSION

To sum up, we have successfully constructed the deletion strain of HY9901Δ*tyeA*. We found that the HY9901Δ*tyeA* strain exhibited decreased virulence to zebrafish, but the wild strain and the mutant strains were resistant to most antibiotics. The attenuated live vaccine was highly protective against *V. alginolyticus* and can induce protective immune responses in zebrafish. These results provide further evidence for the importance of T3SS in *V. alginolyticus* and provide reference for further study of this virulence factor. The immune effect and safety of the attenuated live vaccine will be tested and evaluated in aquaculture species in order to provide further theoretical basis and technical support for its application for the prevention and control of fish diseases caused by *V. alginolyticus*.

DATA AVAILABILITY STATEMENT

The datasets generated for this study can be found in the NCBI Accession No. MN328351.

ETHICS STATEMENT

The animal study was reviewed and approved by Guangli Li and Guangdong Ocean University of ethics committee.

AUTHOR CONTRIBUTIONS

SZ and HP designed the experiments. SZ, XT, and JL generated experimental data and wrote the manuscript. HP, RH, SM, and JJ conceived the work and critically reviewed the manuscript. All authors contributed extensively to the work presented in this manuscript.

FUNDING

This work was funded by Shenzhen Science and Technology Project (JCYJ20170818111629778), the National Key Research and Development Program of China (2018YFD0900501), National Natural Science Foundation of China (No. 31402344, 31670129), Natural Science Foundation of Guangdong Province (No. 2017A030313174), Independent Project of Southern Marine Science and Engineering Guangdong Laboratory (Zhanjiang) (No. ZJW-2019-05), projects subsidized by special funds for science technology innovation and industrial development of Shenzhen Dapeng New District (No. PT202001-13).

REFERENCES

Amer, A. A., Gurung Jyoti, M., Costa Tiago, R. D., Kristina, R., Zavialov, A. V., Forsberg, A., et al. (2016). TyeA hydrophobic contacts required for regulating ysc-yop type, III secretion activity by yersinia pseudotuberculosis. *Front. Cell. Infect. Microbiol.* 6:66. doi: 10.3389/fcimb.2016.00066

Anand, S., Tomoko, K., and Galán J. E. (2003). Synthesis and localization of the *Salmonella* SPI-1 type III secretion needle complex proteins PrgI and PrgJ. *J. Bacteriol.* 185, 3480–3883. doi: 10.1128/JB.185.11.3480-3483.2003

Bauer, A. W., Kirby, W. M., Sherris, J. C., and Turck, M. (1966). Antibiotic susceptibility testing by a standardized single disk method. *Am. J. Clin. Pathol.* 45, 493–496. doi: 10.1093/ajcp/45.4_ts.493

Ben Kahla-Nakbi, A., Chaieb, K., and Bakhrouf, A. (2009). Investigation of several virulence properties among *Vibrio* alginolyticus strains isolated from diseased cultured fish in Tunisia. *Dis. Aquat. Organ.* 86, 21–28. doi: 10.3354/dao02091

Blondel Carlos, J., Park Joseph, S., Hubbard Troy, P., Pacheco Alline, R., Kuehl Carole, J., Walsh Michael, J., et al. (2016). CRISPR/Cas9 screens reveal requirements for host cell sulfation and fucosylation in bacterial type III secretion system-mediated cytotoxicity. *Cell Host Microbe* 20, 226–237. doi: 10.1016/j.chom.2016.06.010

Burridge, L., Weis, J. S., Cabello, F., Pizarro, J., and Bostick, K. (2010). Chemical use in salmon aquaculture: a review of current practices and possible environmental effects. *Aquaculture* 306, 7–23. doi: 10.1016/j.aquaculture.2010.05.020

Buttner, D., and Bonas, U. (2002). Getting across–bacterial type III effector proteins on their way to the plant cell. *EMBO J.* 21, 5313–5322. doi: 10.1093/emboj/cdf536

Cai, S. H., Wu, Z. H., Jian, J. C., and Lu, Y. S. (2007). Cloning and expression of gene encoding the thermostable direct hemolysin from *Vibrio* alginolyticus strain HY9901, the causative agent of vibriosis of crimson snapper (*Lutjanus erythopterus*). *J. Appl. Microbiol.* 103, 289–296. doi: 10.1111/j.1365-2672.2006.03250.x

Cai, X. H., Peng, Y. H., Wang, Z. C., Huang, T., Xiong, X. Y., Huang, Y. C., et al. (2016). Characterization and identification of streptococci from golden pompano in China. *Dis. Aquat. Organ.* 119, 207–217. doi: 10.3354/dao02998

Chang, C. C., Yeh, M. S., Lin, H. K., and Cheng, W. (2008). The effect of *Vibrio* alginolyticus infection on caspase-3 expression and activity in white shrimp *Litopenaeus* vannamei. *Fish Shellfish Immunol.* 25, 672–678. doi: 10.1016/j.fsi.2008.09.004

Chee-Sanford, J. C., Aminov, R. I., Krapac, I. J., Garrigues-Jeanjean, N., and Mackie, R. I. (2001). Occurrence and diversity of tetracycline resistance genes in lagoons and groundwater underlying two swine production facilities. *Appl. Environ. Microbiol.* 67, 1494–1502. doi: 10.1128/AEM.67.4.1494-1502.2001

Cheng, L. W., and Schneewind, O. (2000). Yersinia enterocolitica TyeA, an intracellular regulator of the type III machinery, is required for specific

targeting of YopE, YopH, YopM, and YopN into the cytosol of eukaryotic cells. *J. Bacteriol.* 182, 3183–3190. doi: 10.1128/JB.182.11.3183-3190.2000

Dorothea, R. A., Enrica, B., Selma, M., Da-Kang, S., Xia, L., Maria, P., et al. (2017). Steps for shigella gatekeeper protein mxic function in hierarchical type III secretion regulation. *J. Biol. Chem.* 292, 1705–1723. doi: 10.1074/jbc.M116.746826

Edwards, R. A., Keller, L. H., and Schifferli, D. M. (1998). Improved allelic exchange vectors and their use to analyze 987P fimbria gene expression. *Gene* 207, 149–57. doi: 10.1016/S0378-1119(97)00619-7

Enos-Berlage, J. L., Guvener, Z. T., Keenan, C. E., and Mccarter, L. L. (2005). Genetic determinants of biofilm development of opaque and translucent *Vibrio* parahaemolyticus. *Mol. Microbiol.* 55, 1160–1182. doi: 10.1111/j.1365-2958.2004.04453.x

Ferracci, F., Schubot, F. D., Waugh, D. S., and Plano, G. V. (2005). Selection and characterization of Yersinia pestis YopN mutants that constitutively block Yop secretion. *Mol. Microbiol.* 57, 970–987. doi: 10.1111/j.1365-2958.2005.04738.x

Hua, Z., Chao, F., Haizhen, W., Minjun, Y., Qin, L., Qiyao, W., et al. (2013). Transcriptome profiling reveals Th17-like immune responses induced in zebrafish bath-vaccinated with a live attenuated *Vibrio anguillarum*. *PLoS ONE* 8:e73871. doi: 10.1371/journal.pone.0073871

Iriarte, M., Sory, M. P., Boland, A., Boyd, A. P., Mills, S. D., Lambermont, I., et al. (1998). TyeA, a protein involved in control of Yop release and in translocation of Yersinia Yop effectors. *EMBO J.* 17, 1907–18. doi: 10.1093/emboj/17.7.1907

Jones, E. H., Feldman, K. A., Palmer, A., Butler, E., Blythe, D., and Mitchell, C. S. (2013). Vibrio infections and surveillance in Maryland, 2002-2008. *Public Health Rep*. 128, 537–45. doi: 10.1177/003335491312800613

Joseph S. S., and Plano G. V. (2007). Identification of TyeA residues required to interact with YopN and to regulate Yop secretion. *Adv. Exp. Med. Biol.* 603, 235–345. doi: 10.1007/978-0-387-72124-8_21

Jun, W., Yu-Hong, S., Xue-Heng, Z., Chang-Hong, L., Ming-Yun, L., and Jiong, C. (2015). Molecular characterization of an IL-1β gene from the large yellow croaker (*Larimichthys crocea*) and its effect on fish defense against *Vibrio alginolyticus* infection. *Dongwuxue Yanjiu*. 36, 133–141. doi: 10.13918/j.issn.2095-8137.2015.03.003

Katharine, K., and Watnick, I. P. (2003). Environmental determinants of *Vibrio* cholerae biofilm development. *Appl. Environ. Microbiol.* 69, 5079–88. doi: 10.1128/AEM.69.9.5079-5088.2003

Khavong, P., and Lorena, N. (2016). Yersinia type III effectors perturb host innate immune responses. *World J. Biol. Chem.* 7, 1–13. doi: 10.4331/wjbc.v7.i1.1

Li, W. X., Yao, Z. J., Sun, L. N., Hu, W. J., Cao, J. J., Lin, W. X., et al. (2016). Proteomics analysis reveals a potential antibiotic cocktail therapy strategy for aeromonas hydrophila infection in biofilm. *J. Proteome Res.* 15, 1810–1820. doi: 10.1021/acs.jproteome.5b01127

Li, X. C., Xiang, Z. Y., Xu, X. M., Yan, W. H., and Ma, J. M. (2009). Endophthalmitis caused by vibrio alginolyticus. *J. Clin. Microbiol.* 47, 3379–3381. doi: 10.1128/JCM.00722-09

Liu, J., Lu, S. Y., Orfe, L. H., Ren, C. H., Hu, C. Q., Call, D. R., et al. (2016). ExsE is a negative regulator for T3SS gene expression in vibrio alginolyticus. *Front. Cell Infect. Microbiol.* 6:177. doi: 10.3389/fcimb.2016.00177

Martinez-Argudo, I., and Blocker, A. J. (2010). The *Shigella* T3SS needle transmits a signal for MxiC release, which controls secretion of effectors. *Mol. Microbiol.* 78, 1365–1378. doi: 10.1111/j.1365-2958.2010.07413.x

Masato, S., Olga, D., and Mekalanos, J. J. (2014). Vibrio cholerae T3SS effector VopE modulates mitochondrial dynamics and innate immune signaling by targeting Miro GTPases. *Cell Host Microbe* 16, 581–591. doi: 10.1016/j.chom.2014.09.015

Miller, K. A., Sofia, M. K., Weaver, J. W. A., Seward, C. H., and Dziejman, M. (2016). Regulation by ToxR-like proteins converges on vttRB expression to control type 3 secretion system-dependent Caco2-BBE cytotoxicity in vibrio cholerae. *J. Bacteriol.* 198, 1675–1682. doi: 10.1128/JB.00130-16

Millikan, D. S., and Ruby, E. G. (2004). *Vibrio fischeri* flagellin a is essential for normal motility and for symbiotic competence during initial squid light organ colonization. *J. Bacteriol.* 186, 4315–4325. doi: 10.1128/JB.186.13.4315-4325.2004

Nguyen, L., Paulsen, I. T., Tchieu, J., Hueck, C. J., and Saier, M. H. (2000). Phylogenetic analyses of the constituents of Type III protein secretion systems. *J. Mol. Microbiol. Biotechnol.* 2, 125–44.

O'toole, R., Hofsten, J. V., Rosqvist, R., Olsson, P.-E., and Wolf-Watz, H. (2004). Visualisation of zebrafish infection by GFP-labelled *Vibrio* anguillarum. *Microbial. Pathog.* 37, 41–6. doi: 10.1016/j.micpath.2004.03.001

Pallen, M. J., Beatson, S. A., and Bailey, C. M. (2005). Bioinformatics analysis of the locus for enterocyte effacement provides novel insights into type-III secretion. *BMC Microbiol.* 5:9. doi: 10.1186/1471-2180-5-9

Pang, H., Chen, L., Hoare, R., Huang, Y., Zaohe, W., and Jian, J. (2016). Identification of DLD, by immunoproteomic analysis and evaluation as a potential vaccine antigen against three *Vibrio* species in *Epinephelus* coioides. *Vaccine* 34, 1225–31. doi: 10.1016/j.vaccine.2015.11.001

Pang, H. Y., Qiu, M. S., Zhao, J. M., Hoare, R., Monaghan, S. J., Song, D. W., et al. (2018). Construction of a *Vibrio* alginolyticus hopPmaJ (hop) mutant and evaluation of its potential as a live attenuated vaccine in orange-spotted grouper (*Epinephelus coioides*). *Fish Shellfish Immunol.* 76, 93–100. doi: 10.1016/j.fsi.2018.02.0

Parsek, M. R., and Singh, P. K. (2003). Bacterial biofilms: an emerging link to disease pathogenesis. *Annu. Rev. Microbiol.* 57, 677–701. doi: 10.1146/annurev.micro.57.030502.090720

Plano, G. V. and Schesser, K. (2013). The *Yersinia pestis* type III secretion system: expression, assembly and role in the evasion of host defenses. *Immunol. Res.* 57, 237–245. doi: 10.1007/s12026-013-8454-3

Reed, L. J., and Muench, H. (1938). A simple method of estimating fifty per cent endpoints12. *Am. J. Epidemiol.* 27, 493–497. doi: 10.1093/oxfordjournals.aje.a118408

Rodríguez, I., Novoa, B., and Figueras, A. (2008). Immune response of zebrafish (*Danio rerio*) against a newly isolated bacterial pathogen *Aeromonas* hydrophila. *Fish Shellfish Immunol.* 25, 239–49. doi: 10.1016/j.fsi.2008.05.002

Rojo, I., De Ilarduya, O. M., Estonba, A., and Pardo, M. A. (2007). Innate immune gene expression in individual zebrafish after listonella anguillarum inoculation. *Fish Shellfish Immunol.* 23, 1285–1293. doi: 10.1016/j.fsi.2007.07.002

Rubirés, X., Saigi, F., Piqué N., Climent, N., Merino, S., Albertí S., et al. (1997). A gene (wbbL) from *Serratia marcescens* N28b (O4) complements the rfb-50 mutation of *Escherichia coli* K-12 derivatives. *J. Bacteriol.* 179, 7581–7586. doi: 10.1128/JB.179.23.7581-7586.1997

Sadok, K., Mejdi, S., Nourhen, S., and Amina, B. (2013). Phenotypic characterization and RAPD fingerprinting of *Vibrio* parahaemolyticus and *Vibrio* alginolyticus isolated during Tunisian fish farm outbreaks. *Folia Microbiol.* 58, 17–26. doi: 10.1007/s12223-012-0174-x

Schubot, F. D., Jackson, M. W., Penrose, K. J., Cherry, S., Tropea, J. E., Plano, G. V., et al. (2004). Three-dimensional structure of a macromolecular assembly that regulates type III secretion in yersinia pestis. *J. Mol. Biol.* 346, 1147–1161. doi: 10.1016/j.jmb.2004.12.036

Sganga, G., Cozza, V., Spanu, T., Spada, P. L., and Fadda, G. (2009). Global climate change and wound care: case study of an off-season *Vibrio alginolyticus* infection in a healthy man. *Ostomy Wound Manage.* 55, 60–62.

Simon, R., Priefer, U., and Pühler, A. (2019). A broad host range mobilization system for *in vivo* genetic engineering: transposon mutagenesis in gram negative bacteria. *Nat. Biotech.* 1, 784–791. doi: 10.1038/nbt1183-784

Streisinger, G., Walker, C., Dower, N., Knauber, D., and Singer, F. (1981). Production of clones of homozygous diploid zebra fish (*Brachydanio rerio*). *Nature* 291, 293–296. doi: 10.1038/291293a0

Sullivan, C., and Kim, C. H. (2008). Zebrafish as a model for infectious disease and immune function. *Fish Shellfish Immunol.* 25, 341–350. doi: 10.1016/j.fsi.2008.05.005

Sundberg, L., and Forsberg, A. (2003). TyeA of *Yersinia pseudotuberculosis* is involved in regulation of Yop expression and is required for polarized translocation of Yop effectors. *Cell. Microbiol.* 5, 187–202. doi: 10.1046/j.1462-5822.2003.00267.x

Thompson, F. L., Iida, T., and Swings, J. (2004). Biodiversity of vibrios. *Microbiol. Mol. Biol. Rev.* 68, 403–431. doi: 10.1128/MMBR.68.3.403-431.2004

Verstraeten, N., Braeken, K., Debkumari, B., Fauvart, M., Fransaer, J., Vermant, J., et al. (2008). Living on a surface: swarming and biofilm formation. *Trends Microbiol.* 16, 496–506. doi: 10.1016/j.tim.2008.07.004

Watnick, P. I., Lauriano, C. M., Klose, K. E., Croal, L., and Kolter, R. (2001). The absence of a flagellum leads to altered colony morphology, biofilm development and virulence in *Vibrio* cholerae O_{139}. *Mol. Microbiol.* 39, 223–35. doi: 10.1046/j.1365-2958.2001.02195.x

Windle, H. J., and Kelleher, D. (1997). Identification and characterization of a metalloprotease activity from *Helicobacter pylori*. *Infect. Immun.* 65, 3132–3137. doi: 10.1128/IAI.65.8.3132-3137.1997

Xu, Z., Wang, Y., Han, Y., Chen, J., and Zhang, X.-H. (2010). Mutation of a novel virulence-related gene mltD in *Vibrio anguillarum* enhances lethality in zebra fish. *Res. Microbiol.* 162, 144–150. doi: 10.1016/j.resmic.2010.08.003

Yanyan, C., Fenglei, W., Huanying, P., Jufen, T., Shuanghu, C., and Jichang, J. (2019). Superoxide dismutase B (sodB), an important virulence factor of *Vibrio* alginolyticus, contributes to antioxidative stress and its potential application for live attenuated vaccine. *Fish Shellfish Immunol.* 89, 354–360. doi: 10.1016/j.fsi.2019.03.061

Yonghong, Y., Huanying, P., Zejun, Z., Dawei, S., Yu, D., Jichang, J., et al. (2016). Construction of live attenuated vaccine against *Vibrio alginolyticus* and the evaluation on its immunoprotection effect. *Anim. Husbandry Feed Sci.* 8, 85–93. doi: 10.19578/j.cnki.ahfs.2016.02.007

Zhang, Z., Wu, H., Xiao, J., Wang, Q., Liu, Q., and Zhang, Y. (2012). Immune responses of zebrafish (*Danio rerio*) induced by bath-vaccination with a live attenuated *Vibrio anguillarum* vaccine candidate. *Fish Shellfish Immunol.* 33, 36–41. doi: 10.1016/j.fsi.2012.03.031

Zhou, X., Konkel, M. E., and Call, D. R. (2010). Regulation of type III secretion system 1 gene expression in *Vibrio parahaemolyticus* is dependent on interactions between ExsA, ExsC, and ExsD. *Virulence* 1, 260–272. doi: 10.4161/viru.1.4.12318

Zhou, X., Shah, D. H., Konkel, M. E., and Call, D. R. (2008). Type III secretion system 1 genes in *Vibrio parahaemolyticus* are positively regulated by ExsA and negatively regulated by ExsD. *Mol. Microbiol.* 69, 747–764. doi: 10.1111/j.1365-2958.2008.06326.x

Zhou, Z., Pang, H., Ding, Y., Cai, J., Huang, Y., Jian, J., et al. (2013). VscO, a putative T3SS chaperone escort of *Vibrio alginolyticus*, contributes to virulence in fish and is a target for vaccine development. *Fish Shellfish Immunol.* 35, 1523–31. doi: 10.1016/j.fsi.2013.08.017

Zujie, Y., Zhuang, G., Yuqian, W., Wanxin, L., Yuying, F., Yuexu, L., et al. (2019). Integrated succinylome and metabolomics profiling reveals crucial role of S-ribosylhomocysteine lyase in quorum sensing and metabolism of *Aeromonas hydrophila*. *Mol. Cell. Proteomics* 18, 200–215. doi: 10.1074/mcp.RA118.001035

Conflict of Interest: The authors declare that the research was conducted in the absence of any commercial or financial relationships that could be construed as a potential conflict of interest.

frontiers in Cellular and Infection Microbiology

ORIGINAL RESEARCH
published: 25 May 2020
doi: 10.3389/fcimb.2020.00239

SmpB and tmRNA Orchestrate Purine Pathway for the Trimethoprim Resistance in *Aeromonas veronii*

Dan Wang[1,2], *Hong Li*[1], *Wasi Ullah Khan*[2], *Xiang Ma*[1], *Hongqian Tang*[1], *Yanqiong Tang*[1]*, *Dongyi Huang*[2] *and Zhu Liu*[1]*

[1] *Key Laboratory of Tropical Biological Resources of Ministry of Education, School of Life and Pharmaceutical Science, Hainan University, Haikou, China,* [2] *Key Laboratory for Sustainable Utilization of Tropical Bioresource, College of Tropical Crops Hainan University, Haikou, China*

Small protein B(SmpB) cooperates with transfer-messenger RNA (tmRNA) for *trans*-translation to ensure the quality control of protein synthesis in prokaryotes. Furthermore, they regulate cell metabolism separately. According to research, SmpB functions as a transcription factor, and tmRNA acts as a small RNA. Purine pathway has been reported to be related to trimethoprim resistance, including hypoxanthine synthesis, adenosine metabolism and guanosine metabolism. Another reason of drug tolerance is the efflux pump of the bacterium. In transcriptomic data, it was shown that the expression of some related enzymes in adenosine metabolism were raised significantly in *smpB* deletion strain than that of wild type, which led to the differential trimethoprim resistance of *Aeromonas veronii* (*A. veronii)*. Furthermore, the metabolic products of adenosine AMP, cAMP, and deoxyadenosine were accumulated significantly. However, the expressions of the enzymes related to hypoxanthine synthesis and guanosine metabolism were elevated significantly in *ssrA (small stable RNA, tmRNA) deletion strain*, which eventually caused an augmented metabolic product xanthine. In addition, the deletion of *ssrA* also affected the significant downregulations of efflux pump *acrA/acrB*. The minimal inhibitory concentrations (MIC) were overall decreased after the trimethoprim treatment to the wild type, Δ*smpB* and Δ*ssrA*. And the difference in sensitivity between Δ*smpB* and Δ*ssrA* was evident. The MIC of Δ*smpB* was descended significantly than those of wild type and Δ*ssrA* in M9 medium supplemented with 1 mM adenosine, illustrating that the adenosine metabolism pathway was principally influenced by SmpB. Likewise, the strain Δ*ssrA* conferred more sensitivity than wild type and Δ*smpB* in M9 medium supplemented with 1mM guanosine. By overexpressing *acrA/acrB*, the tolerance to trimethoprim was partially recovered in Δ*ssrA*. These results revealed that SmpB and tmRNA acted on different branches in purine metabolism, conferring the diverse trimethoprim resistance to *A. veronii*. This study suggests that the *trans*-translation system might be an effective target in clinical treatment of *A. veronii* and other multi-antibiotic resistance bacteria with trimethoprim.

Keywords: *Aeromonas veronii*, trimethoprim, SmpB, tmRNA, purine metabolism

OPEN ACCESS

Edited by:
Bo Peng,
Sun Yat-sen University, China

Reviewed by:
Vijayakumar Sekar,
Shandong University, Weihai, China
Hyouta Himeno,
Hirosaki University, Japan

***Correspondence:**
Yanqiong Tang
tyq@126.com
Zhu Liu
liuzhuabel@163.com

Specialty section:
This article was submitted to Molecular Bacterial Pathogenesis, a section of the journal Frontiers in Cellular and Infection Microbiology

Received: *27 December 2019*
Accepted: *27 April 2020*
Published: *25 May 2020*

Citation:
Wang D, Li H, Khan WU, Ma X, Tang H, Tang Y, Huang D and Liu Z (2020) SmpB and tmRNA Orchestrate Purine Pathway for the Trimethoprim Resistance in Aeromonas veronii. Front. Cell. Infect. Microbiol. 10:239. doi: 10.3389/fcimb.2020.00239

INTRODUCTION

Aeromonas veronii (*A. veronii*) is a pathogen of aquatic animals and humans. It is widely found in freshwater and seawater with a strong pathogenic ability, causing fish skin ulceration, visceral hemorrhage, ascites, and other symptoms (Liu et al., 2016). Clinical studies have reported that *A. veronii* can also cause human gastroenteritis, endocarditis, bacteremia and other diseases (Aguilera-Arreola et al., 2007; Chuang et al., 2011). *A. veronii* is resistant to spectinomycin, gentamicin, streptomycin, and kanamycin (Zhang et al., 2019). Bacterial drug resistance makes it more difficult to control pathogens (Leal et al., 2019; El Mekes et al., 2020). Studies have shown that *trans*-translation system composed of SmpB (Small protein B) and tmRNA (transfer-messenger RNA) can release ribosomal block caused by translation errors, thus ensuring ribosome efficiency and protein synthesis (Keiler, 2015), which has an important impact on bacterial drug resistance (Venkataraman et al., 2014; Sharkey et al., 2016).

In addition to the *trans*-translation function of SmpB and tmRNA, they also play other roles in bacteria. As a transcription factor, SmpB participates in transcriptional regulation of *bvgS* and sRNA of *A. veronii* (Liu et al., 2015; Wang et al., 2019). SmpB also affects the transcription of sRNA and the tolerance to environmental stress (Wang et al., 2019). Analogously, tmRNA can act as sRNA and interact with *crtMN* mRNA to affect the synthesis of *Staphylococcus aureus* pigment (Liu et al., 2010). Results of the present study show that a double knockout of *smpB* and *ssrA (tmRNA, small stable RNA)* makes *A. veronii* more sensitive to trimethoprim.

It is reported that bacteria could develop acquired drug tolerance when treated with Trimethoprim (Ma et al., 2018). Trimethoprim affects the synthesis of nucleotides and purine metabolism of *A. veronii* by inhibiting dihydrofolate reductase (Sangurdekar et al., 2011). Purine metabolism also affects the bacterial tolerance to trimethoprim (Sah et al., 2015; Stepanek et al., 2016). This study explored the molecular mechanism of SmpB and tmRNA in the tolerance of *A. veronii* to trimethoprim, mainly through purine metabolism. In Δ*smpB*, seven adenine related enzyme expression upregulated, and the content of adenosine increased. In Δ*ssrA*, a large number of guanine related enzymes upregulated, the content guanine and hypoxanthine contents increased. SmpB and tmRNA affect two branches of purine metabolism, adenine synthesis and guanine synthesis, respectively. The sensitivity of *A. veronii* to trimethoprim increased with the addition of exogenous purine products. More different, Δ*ssrA* efflux pump related gene expression was decreased, and the overexpression of *acrAB* made Δ*ssrA* increased the resistance of trimethoprim. This study explained the reason for decreased MIC of trimethoprim, and the different influence between Δ*smpB* and Δ*ssrA* on purine pathway was also found.

TABLE 1 | Strains and plasmids used in this paper.

Strains or plasmids	Traits	Sources
E. coli WM3064	Gene cloning strain	This lab
Aeromonas veronii	Wild type strain	This lab
smpB_ssrA mutant (Δ*smpB_ ssrA)*	*smpB* and *ssrA* deletion mutant	This paper
Δ*smpB_ ssrA*:: c	*A complementary strain of smpB* and *ssrA* deletion mutant	This paper
smpB mutant	*smpB* deletion mutant	This lab
Δ*smpB:: smpB*	*A complementary strain of smpB* deletion mutant	This lab
ssrA mutant	*ssrA* deletion mutant	This lab
Δ*ssrA:: ssrA*	*The complementary strain of ssrA* deletion mutant	This lab
ssrA mutant *with acrAB*	Over-expressing *acrAB* in *ssrA* mutant strain	This paper
pre112	Gene cloning vector	This lab
pBBR1MCS-2	Gene cloning vector	This lab
pBBR *acrAB*	*acrAB* overexpression vector	This paper

METHODS

Strains

The strain information was listed in **Table 1**. *A. veronii* was isolated from the diseased tissues of grass carp (Liu et al., 2015) and cultured with M9 Minimal Medium (M9) at 30°C, 150 r/min, and 50 ug/mL ampicillin. *SmpB* knockout strain and *ssrA* knockout strain was derived from the preserved strain in this laboratory (Liu et al., 2015). The *smpB* and *ssrA* double knockout strain (Δ*smpB_ssrA*) and *ssrA* mutant complemented with *acrAB* sequence (Δ*ssrA::acrAB*) were constructed in this study. *E coli* WM 3064 assisted the vector introduction into *A. veronii* for the construction of overexpressed strains and knockout strains. *E coli* WM3064 was Diaminopimelic acid (DAP) dependent and cultured in LB medium at 37°C with DAP concentration of 0.3mM. All of the medium composition belongs to inorganic salts. For the 5× stock: 64 g Na_2HPO_4, 15 g KH_2PO_4, 5 g NH_4Cl, 2.5 g NaCl, and 1 liter of high-quality distilled water. Mix 1 ml of 1 M $MgSO_4.7H_2O$, 10 ml of 20% glucose, 100ul of 1M $CaCl_2$ and 200mL of 5× stock solution and adjust to 1000ml with distilled H_2O.

Plasmids

The construction vectors and primers used in this study are listed in **Tables 1**, **2**. Suicide plasmid pRE112 was used to construct knockout vectors. And the assembly knockout vectors of *smpB_ssrA* sequence were constructed by double enzyme digestion and specific connection and were integrated with the genome under 6% sucrose to complete homologous recombination (Liu et al., 2015). Plasmid pBBR1MCS-2 was used to construct a vector that overexpressed efflux pump-related gene *acrAB* in *A. veronii*. DNA sequence *acrA* and *acrB* were introduced into the pBBR1MCs-2 plasmid, as well as the upstream and downstream primers needed for vector construction respectively. The plasmid was transferred into Δ*ssrA* strain through affinity experiment to construct the overexpressed strain. The overexpressed strains were screened using plates containing both Kanamycin and Ampicillin resistance and verified by sequencing.

TABLE 2 | Primers and plasmids used in this paper.

Names	Sequences (5′-3′)	Usage
WP_041202667.1-F	ATGGTCGCAGAGCTTGTC	Strain validation
WP_041202667.1-R	CAGCACAATAGAACACCAGAC	Strain validation
acrA Sal I F	ACGCGTCGACTTGGTATCG GCTGGGGATTG	*acrAB* vector construction
acrB EcoR I R	CCGGAATTCATGAGCGTC GGGAGAG	*acrAB* vector construction
pBBR1MCS-2 F	GGCACCCCAGGCTTTACACT	Complement plasmid validation
pBBR1MCS-2 R	GATGTGCTGCAAGGCGATTAAG	Complement plasmid validation
pre112 F	GTGCGTACCGGGTTGAGAAG	pre112 validation
pre112 R	CGCCCTTAAACGCCTGGTTG	pre112 validation
Iden-F	GGTCAGACACCGTATACCTC	Deleted sequence validation
Iden-R	TCAAGAGATCGCCATGAGTC	Deleted sequence validation
Up-*smpB* F	CGGGGTACCGAGATCAAACT CCACCTTGCAG	Upstream arm of *smpB* amplification
Up-*smpB* R	CCGGAATTCGACGGGCGATT TCCGGCAAT	Upstream arm of *smpB* amplification
Down- *ssrA* F	CCGGAATTCGCTCCACCAA ACAATGTTCC	Downstream arm of *ssrA* amplification
Down- *ssrA* R	CCCGAGCTCGCGTTAG CTTCTTGTTCTG	Downstream arm of *ssrA* amplification

Minimum Inhibitory Concentration Test

Micro broth dilution method: Antibiotics were added to the sterile 96-well plates at final concentrations of 64, 32, 16, 8, 4, 2, 1, 0.5, 0.25, and 0.125 ug/mL. Then, 10-E6 CFU broth was added to each well to a final volume of 200 μL. The 96-well plate was sealed with parafilm and cultured at 30°C with shaking at 150 r/min for 24 h. The minimum drug concentration that completely inhibited the growth in the well was considered as the minimum inhibitory concentration. The experiment was repeated 3 times.

Transcriptomic Analysis

The cells were collected, lysed, and the sample RNA was extracted with phenol-chloroform. The concentration and quality of the RNA samples were tested with the Agilent 2100. DNase I was used to remove double-stranded DNA, and a Ribo-Zero Magnetic Kit was used to remove human RNA. Reverse transcription was performed with random primers and first strand cDNA which was used as a template to synthesize the second strand. The linker sequence was attached to the 3′ end of the cDNA fragment. The cDNA sequence was amplified with a primer cocktail, and the purified product was sequenced on a HiSeq Xten (Illumina, San Diego, CA, USA) platform. The sequencing depth was chain-specific sequencing for 2 Gb of clean data. HISAT was attempted for genome assembly, analysis of potential coding sequence analysis and to identify new transcripts that may be present. Differences in gene transcription levels between wild-type and knockout strains were analyzed by Bowtie 2, and RPKM was used to normalize gene expression levels. The results of gene expression were calculated using the Benjamini-Hochberg false discovery rate (FDR). The differentially expressed transcripts were tested for log-fold change and the p value was corrected with FDR < 0.001. The results of the differentially expressed genes were analyzed using GO classification, and differential gene expression in the pathway was com*pared* with the entire genomic background using hyper geometric analysis. Value of $p < 0.05$ is considered to be a differential metabolic pathway. The accession number of reference genome is NO. CP012504.1. GEO accession number is GSE120603, and the URL of accession website is https://submit.ncbi.nlm.nih.gov/subs/sra/SUB6133286. The DESeq.2 package in R was applied to estimate the fold changes and to perform other analysis.

Metabolomics Analysis

The non-target metabolomics and lipidomics detection platform (UHPLC-QTOF-MS) was applied to metabolomics for the detection of *A. veronii* samples. UHPLC-QTOF-MS includes Ultra-Performance Liquid Chromatography 1290UHPLC (Agilent), ACQUITY UPLC BEH Amide column 1.7 um, 2.1*100 mm (Waters) and High-Resolution Mass Spectrometry Triple TOF 6600 (AB Sciex). The original mass spectrum was converted to the mzXML format using Proteo Wizard software, and the peaks were identified using the R Programming Language package (Version 3.2) and self-built secondary mass spectrometry data. URL of accession website is: www.ebi.ac.uk/metabolights/MTBLS1411.

Statistical Analysis

Statistical data were analyzed using the Statistical Package for the Social Science (SPSS) version 20.0 (SPSS, Chicago, IL, USA) and GraphPad Prism version 8.0 (GraphPad, San Diego, CA, USA). The results are presented as the mean values of three independent experiments with standard deviation (SD) using one-way analysis of variance (ANOVA). Values of $p < 0.05$ or 0.01 were represented as significant or extremely significant, respectively.

RESULTS

1. The trimethoprim tolerance of Δ*smpB_ssrA* to was decreased than wild type *A. veronii*.

The minimum inhibitory concentration (MIC) was tested by trimethoprim gradient concentration. The trimethoprim MIC of Δ*smpB_ssrA* was 2 ug/mL. Compared with wild type *A. veronii*, the strain of Δ*smpB_ssrA* was more sensitive to trimethoprim (**Figure 1A**). In order to distinguish the function of SmpB and tmRNA on trimethoprim, Δ*smpB* and Δ*ssrA* strains were used in this study. The MIC data showed that Δ*smpB* and Δ*ssrA* were more sensitive than the wild type,

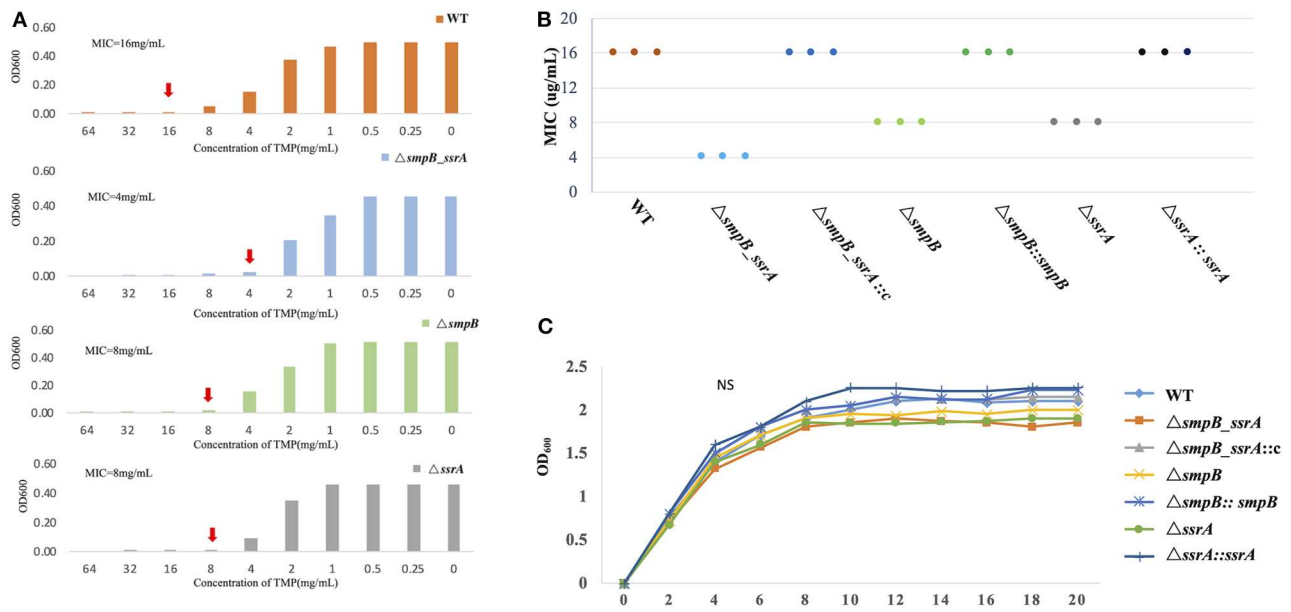

FIGURE 1 | Minimum inhibitory concentration (MIC) value of trimethoprim. **(A)** The red arrow indicates the concentration of trimethoprim in M9 medium that prevented the growth of *Aeromonas veronii*. **(B)** The MIC of the complementary strain of the three mutants. **(C)** The growth curve of wild type *A. veronii,* Δ*smpB*, Δ*ssrA, and* Δ*smpB_ ssrA*, *and the complementary strains*.

which was still higher than Δ*smpB_ssrA*. The MIC data of complementary strain was tested (**Figure 1B**). The changes between wild type and knockout strains were rescued by transferring their pBBR plasmids into the deficient strain. The growth curve was tested to prove that the MIC value was not influenced by the non-obvious difference on growth (**Figure 1C**) This phenomenon suggested that the functions of SmpB and tmRNA were different from *trans*-translation in the presence of trimethoprim.

2. The difference between Δ*smpB* and Δ*ssrA* occurred at the transcriptional level.

In order to explore the differences on function of SmpB and tmRNA, the transcriptomic sequencing was taken to test the expression of stationary phage Δ*smpB* and Δ*ssrA* stains. The transcriptomic results showed that there was a big difference between Δ*smpB* and Δ*ssrA* (**Figure 2A**). As the expression of guanosine related enzymes in Δ*ssrA* purine metabolism was significantly higher than that in wild type *A. veronii*. Simultaneously, the Expression of adenosine related enzymes in Δ*smpB* purine metabolism was significantly higher than wild type *A. veronii* (**Figure 2B**).

3. The content of purine metabolites in Δ*smpB* and Δ*ssrA* were different.

Metabonomic analysis of Δ*smpB* and Δ*ssrA* strains was done because of significant differences in the transcriptomic data. Metabolomics results showed that guanosine metabolites and adenosine metabolites showed up-regulation in the purine metabolic pathway separately in Δ*smpB* and Δ*ssrA* (**Figure 3**). The content of adenosine, AMP, cAMP, and deoxyadenosine in Δ*smpB* were increased significantly. Whereas the contents of xanthine and guanosine in Δ*ssrA* were significantly increased.

4. Trimethoprim tolerance of Δ*ssrA* was enhanced by *acrAB* overexpression.

The expression of efflux pump gene *acrA* and *acrB* in Δ*ssrA* was downregulated, but no significant change in Δ*smpB* (**Figure 4A**). The *acrAB* over-expression vector pBBR_*acrAB*, which was constructed with *acrAB* promoter, were introduced into Δ*ssrA*. Trimethoprim MIC test results showed that the MIC of Δ*ssrA::acrAB* similar to wild type strain (**Figure 4B**). The tolerance to trimethoprim is enhanced by over-expression of *acrAB* in Δ*ssrA*. Under the condition of 1 mM adenosine in M9, the MIC of Δ*ssrA::acrAB* strain increased to 8 mg/mL, which is lower than the wild type.

5. The trimethoprim tolerance of Δ*smpB* and Δ*ssrA* was weakened by exogenous purine metabolites.

Excessive purine metabolites in M9 medium resulted in a decrease in MIC value, making the wildtype of *A. veronii* more sensitive to trimethoprim (**Figure 5A**, **Supplementary Table 1**). The MIC value of Δ*smpB* was decreased by adding exogenous 1mM adenosine and 10mM ATP but was not changed by excessive guanosine (**Figure 5B**) and complementary strains (**Supplementary Table 1**). These results implied that the increase of adenosine in adenosine metabolic pathways could make

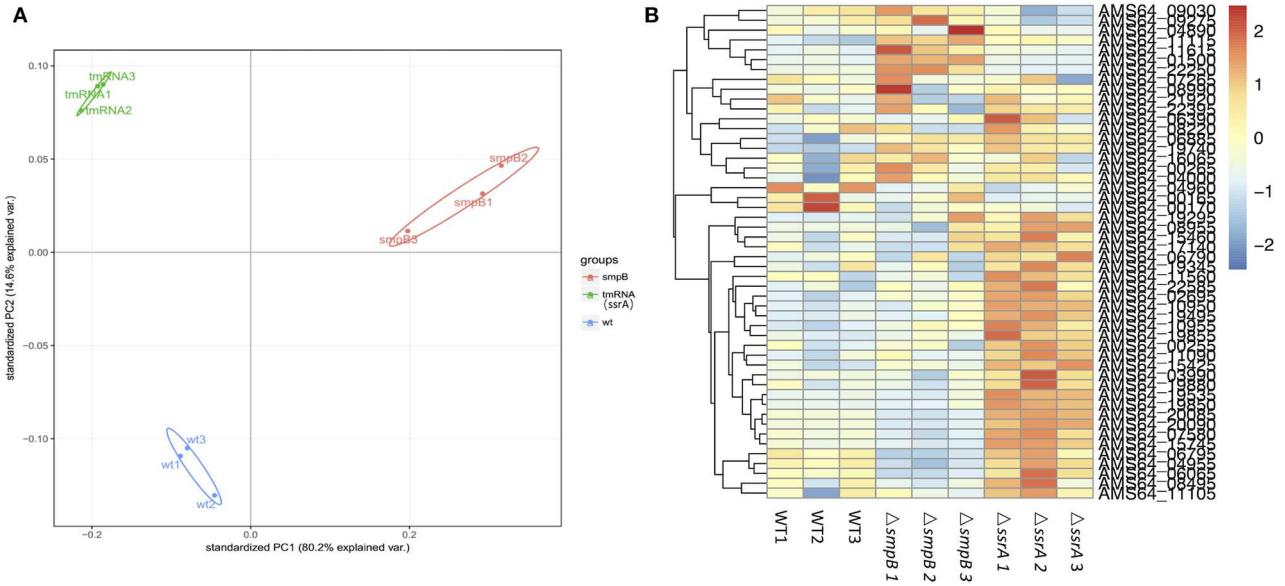

FIGURE 2 | Transcriptomic data of *Aeromonas veronii*. **(A)** Principal component analysis (PCA) diagram of wild type, Δ*smpB* and Δ*ssrA* data. **(B)** Heat map of expression levels of genes involved in purine metabolism and efflux pump synthesis of wild type, Δ*smpB* and Δ*ssrA* strains. There were three samples of wild type, Δ*smpB* and Δ*ssrA* for transcriptome sequencing and analysing. The reads were mapped to reference genome with the accession NO. CP012504.1.

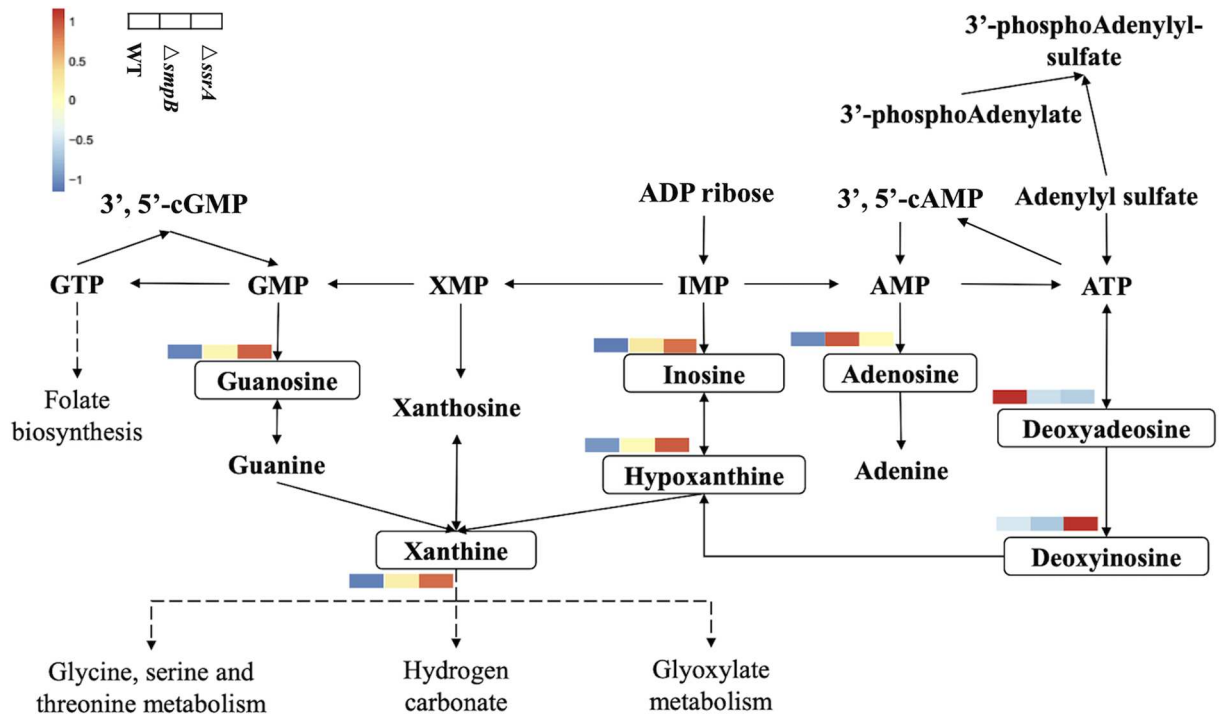

FIGURE 3 | Simplified diagram of *Aeromonas veronii* purine metabolic pathway. The metabolites with a change between wild-type, Δ*smpB* and Δ*ssrA* strains were framed by solid line and presented by heat-map. Compounds with no significant difference in content of the three strains were not labeled.

Δ*smpB* more sensitive to trimethoprim. Adding exogenous adenosine and guanosine, the MIC value of Δ*ssrA* was decreased. Conversely, there was no change between the MIC of Δ*ssrA* and the wild type cultivated by 10 mM ATP in M9 medium (**Figure 5C**). And 1mM guanosine in M9 medium had an effect on MIC value of Δ*ssrA*. These results demonstrated that

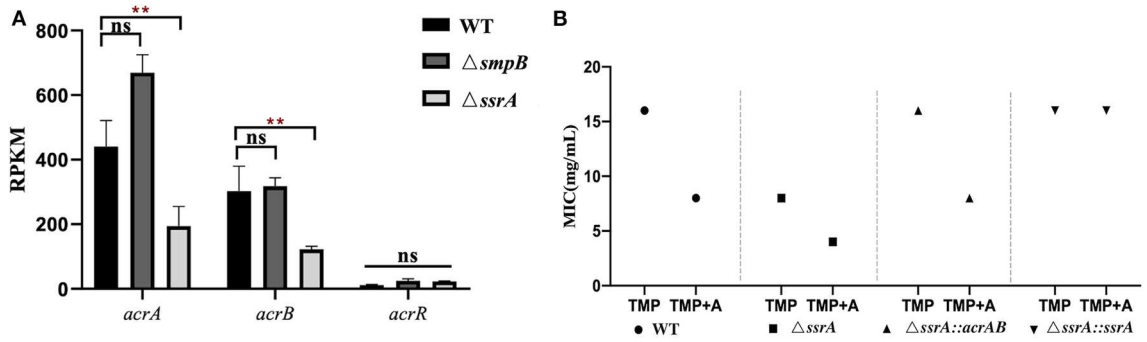

FIGURE 4 | Trimethoprim tolerance of Δ*ssrA* was enhanced by *acrAB* overexpression. **(A)** Expression of efflux pump related gene *acrA* and *acrB* in wild type, Δ*smpB* and Δ*ssrA* strains. **(B)** MIC value of wild type, Δ*ssrA* strains affected by overexpression of *acrAB*. A represents the metabolite substrate 1 mM adenosine. **represents $p < 0.01$, and ns represents no significant difference.

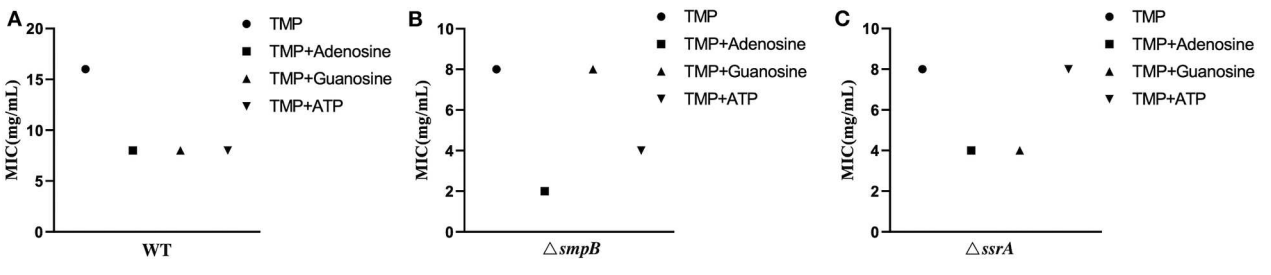

FIGURE 5 | MIC value of trimethoprim under conditions of adenosine, guanosine and adenosine triphosphate. **(A)** MIC value of wild type with 1 mM adenosine, 1 mM guanosine, and 10 mM ATP in M9 medium. **(B)** MIC of Δ*smpB* with 1 mM adenosine, 1 mM guanosine, and 10 mM ATP in M9 medium. **(C)** MIC of Δ*ssrA* with 1 mM adenosine, 1 mM guanosine, and 10 mM ATP in M9 medium.

the differences in the regulation of purine metabolites led to differences in their tolerance to trimethoprim between Δ*smpB* and Δ*ssrA*.

DISCUSSION

Trimethoprim inhibits the synthesis of tetrahydrofolic acid, a carbon unit carrier, by affecting the activity of dihydrofolate reductase, thereby affecting the growth and metabolism of bacteria (Bertacine Dias et al., 2018). The products of purine metabolism will be reduced under the inadequate condition of one carbon unit (Sah et al., 2015). However, in the *A. veronii* metabonomic data, the decrease in folate metabolism and the increase in purine pathway-related enzymes were found to occur at the same time as the significant up-regulation of the purine metabolic pathway. The upregulation trend of Δ*ssrA* was more sensitive to trimethoprim than that of Δ*smpB*. The decrease of MIC value of trimethoprim to Δ*smpB* and Δ*ssrA* were not consistent with the double knockout strain. This indicated different functions of SmpB and tmRNA acting on the tolerance of trimethoprim. These results suggested that the reduced tolerance of trimethoprim in the double-knockout strain may be less relevant to the function of the *trans*-translation system.

ATP is known to be the most effective energy to physiological reactions. As an important products of purine metabolism, ATP was predicted to be beneficial to the growth of *A. veronii*. In this study, 10mM ATP led to a decrease in trimethoprim MIC value, suggesting that excessive ATP weakened the tolerance of *A. veronii* to trimethoprim. It was speculated that the heightened need of ATP increased the challenge to the one carbon unit synthesis of the organism. The role of efflux pump had been explored in drug resistance to fluoroquinolones in gram negative bacteria. AcrAB-TolC efflux system, which has a physiologic role of pumping out bile acids and fatty acids to lower their toxicity. The decreased expression of AcrAB also contributed to the accumulation of ATP. Therefore, it is speculated that ATP in a dynamic balance that It showed little influence upon the value of MIC.

Recent studies had been focused on the assistance of SmpB in binding to the stalled ribosome to release it (Keiler, 2015; Buskirk and Green, 2017). In Δ*ssrA*, the expression of genes related to guanine synthesis was significantly upregulated and the mRNA of genes related to effusion pump was significantly decreased, which did not occur in Δ*smpB*. On the contrary, the expression adenine-related enzymes of Δ*smpB* were significantly increased, which were not repeated in Δ*ssrA*. This indicates that SmpB and tmRNA have independent and non-interference functions.

The difference in tolerance between double knock out strain Δ*smpB_ssrA* and single deletion strain Δ*smpB* and Δ*ssrA* indicated the distinctive functions. The transcriptional and

metabolites data showed separate regulation of SmpB and tmRNA. The changes of Δ*ssrA* were more significant. The trimethoprim MIC value results proved that the efflux pump AcrAB-TolC was affected by *ssrA* deletion. Therefore, this study demonstrated that SmpB and tmRNA act on different branches of purine metabolism, showing an effect on the tolerance to trimethoprim. A second collaboration between SmpB and tmRNA was completed by regulating purine metabolic pathway.

DATA AVAILABILITY STATEMENT

The raw data supporting the conclusions of this article will be made available by the authors, without undue reservation, to any qualified researcher.

AUTHOR CONTRIBUTIONS

ZL, YT, DH, and DW contributed the conception and design of the study. DW, HL, XM, and HT performed the statistical analysis. DW, WK, and ZL drafted the manuscript. All authors contributed to manuscript revision, read and approved the submitted version.

FUNDING

This work was supported by the Hainan Natural Science Foundation No. 319QN161 (to HL), the National Science and Technology Major Project No. 2019ZX08010004 (to ZL), and the grants from the National Natural Science Foundation of China Nos. 31560021 and 31772887 (to ZL) and 31860676 (to YT) and 31960027 (to XM), and the Priming Scientific Research Foundation of Hainan University No. KYQD (ZR) 1929 (to HL).

SUPPLEMENTARY MATERIAL

The Supplementary Material for this article can be found online at: https://www.frontiersin.org/articles/10.3389/fcimb.2020.00239/full#supplementary-material

REFERENCES

Aguilera-Arreola, M. G., Hernandez-Rodriguez, C., Zuniga, G., Figueras, M. J., Garduno, R. A., and Castro-Escarpulli, G. (2007). Virulence potential and genetic diversity of *Aeromonas caviae*, *Aeromonas veronii*, and *Aeromonas hydrophila* clinical isolates from Mexico and Spain: a comparative study. *Can. J. Microbiol.* 53, 877–887. doi: 10.1139/W07-051

Bertacine Dias, M. V., Santos, J. C., Libreros-Zuniga, G. A., Ribeiro, J. A., and Chavez-Pacheco, S. M. (2018). Folate biosynthesis pathway: mechanisms and insights into drug design for infectious diseases. *Future Med. Chem.* 10, 935–959. doi: 10.4155/fmc-2017-0168

Buskirk, A. R., and Green, R. (2017). Ribosome pausing, arrest and rescue in bacteria and eukaryotes. *Philos. Trans. R Soc. Lond. B Biol. Sci.* 372:1716. doi: 10.1098/rstb.2016.0183

Chuang, H. C., Ho, Y. H., Lay, C. J., Wang, L. S., Tsai, Y. S., and Tsai, C. C. (2011). Different clinical characteristics among *Aeromonas hydrophila*, *Aeromonas veronii* biovar sobria and *Aeromonas caviae* monomicrobial bacteremia. *J. Korean Med. Sci.* 26, 1415–1420. doi: 10.3346/jkms.2011.26.11.1415

El Mekes, A., Zahlane, K., Ait Said, L., Tadlaoui Ouafi, A., and Barakate, M. (2020). The clinical and epidemiological risk factors of infections due to multi-drug resistant bacteria in an adult intensive care unit of University Hospital Center in Marrakesh-Morocco. *J. Infect. Public Health*. 13, 637–643. doi: 10.1016/j.jiph.2019.08.012

Keiler, K. C. (2015). Mechanisms of ribosome rescue in bacteria. *Nat. Rev. Microbiol.* 13, 285–297. doi: 10.1038/nrmicro3438

Leal, H. F., Azevedo, J., Silva, G. E. O., Amorim, A. M. L., de Roma, L. R. C., Arraes, A. C. P., et al. (2019). Bloodstream infections caused by multidrug-resistant gram-negative bacteria: epidemiological, clinical and microbiological features. *BMC Infect Dis.* 19:609. doi: 10.1186/s12879-019-4265-z

Liu, P., Chen, Y., Wang, D., Tang, Y., Tang, H., Song, H., et al. (2016). Genetic selection of peptide aptamers that interact and inhibit both small protein B and alternative ribosome-rescue factor A of *Aeromonas veronii* C4. *Front. Microbiol.* 7:1228. doi: 10.3389/fmicb.2016.01228

Liu, Y., Wu, N., Dong, J., Gao, Y., Zhang, X., Shao, N., et al. (2010). SsrA (tmRNA) acts as an antisense RNA to regulate Staphylococcus aureus pigment synthesis by base pairing with crtMN mRNA. *FEBS Lett.* 584, 4325–4329. doi: 10.1016/j.febslet.2010.09.024

Liu, Z., Liu, P., Liu, S., Song, H., Tang, H., and Hu, X. (2015). Small protein B upregulates sensor kinase bvgS expression in *Aeromonas veronii*. *Front. Microbiol.* 6:579. doi: 10.3389/fmicb.2015.00579

Ma, Q. P., Su, L., Liu, J. W., Yao, M. X., and Yuan, G. Y. (2018). Study on the association between drugresistance and gene mutations of the active efflux pump acrABtolC gene and its regulatory genes. *Mol. Med. Rep.* 17, 8228–8236. doi: 10.3892/mmr.2018.8916

Sah, S., Aluri, S., Rex, K., and Varshney, U. (2015). One-carbon metabolic pathway rewiring in Escherichia coli reveals an evolutionary advantage of 10-formyltetrahydrofolate synthetase (Fhs) in survival under hypoxia. *J. Bacteriol.* 197, 717–726. doi: 10.1128/JB.02365-14

Sangurdekar, D. P., Zhang, Z., and Khodursky, A. B. (2011). The association of DNA damage response and nucleotide level modulation with the antibacterial mechanism of the anti-folate drug trimethoprim. *BMC Genomics* 12:583. doi: 10.1186/1471-2164-12-583

Sharkey, L. K., Edwards, T. A., and O'Neill, A. J. (2016). ABC-F proteins mediate antibiotic resistance through ribosomal protection. *MBio* 7:e01975. doi: 10.1128/mBio.01975-15

Stepanek, J. J., Schäkermann, S., Wenzel, M., Prochnow, P., and Bandow, J. E. (2016). Purine biosynthesis is the bottleneck in trimethoprim-treatedBacillus subtilis. *Proteomics Clin. Appl.* 10, 1036–1048. doi: 10.1002/prca.201600039

Venkataraman, K., Guja, K. E., Garcia-Diaz, M., and Karzai, A. W. (2014). Non-stop mRNA decay: a special attribute of trans-translation mediated ribosome rescue. *Front. Microbiol.* 5:93. doi: 10.3389/fmicb.2014.00093

Wang, D., Li, H., Ma, X., Tang, Y., Tang, H., Hu, X., et al. (2019). Small RNA AvrA regulates IscR to increase the stress tolerances in SmpB deficiency of *Aeromonas veronii*. *Front. Cell Infect. Microbiol.* 9:142. doi: 10.3389/fcimb.2019.00142

Zhang, L., Yu, W., Tang, Y., Li, H., Ma, X., and Liu, Z. (2019). RNA chaperone hfq mediates persistence to multiple antibiotics in *Aeromonas veronii*. *Microb Pathog* 132, 124–128. doi: 10.1016/j.micpath.2019.04.045

Conflict of Interest: The authors declare that the research was conducted in the absence of any commercial or financial relationships that could be construed as a potential conflict of interest.

frontiers in Cellular and Infection Microbiology

ORIGINAL RESEARCH
published: 17 July 2020
doi: 10.3389/fcimb.2020.00348

Identification of Antimicrobial Resistance Determinants in *Aeromonas veronii* Strain MS-17-88 Recovered From Channel Catfish (*Ictalurus punctatus*)

*Hasan C. Tekedar[1], Mark A. Arick II[2], Chuan-Yu Hsu[2], Adam Thrash[2], Jochen Blom[3], Mark L. Lawrence[1] and Hossam Abdelhamed[1]**

[1] College of Veterinary Medicine, Mississippi State University, Mississippi State, MS, United States, [2] Institute for Genomics, Biocomputing and Biotechnology, Mississippi State University, Mississippi State, MS, United States, [3] Bioinformatics & Systems Biology, Justus-Liebig-University Giessen, Giessen, Germany

Aeromonas veronii is a Gram-negative species ubiquitous in different aquatic environments and capable of causing a variety of diseases to a broad host range. *Aeromonas* species have the capability to carry and acquire antimicrobial resistance (AMR) elements, and currently multi-drug resistant (MDR) *Aeromonas* isolates are commonly found across the world. *A. veronii* strain MS-17-88 is a MDR strain isolated from catfish in the southeastern United States. The present study was undertaken to uncover the mechanism of resistance in MDR *A. veronii* strain MS-17-88 through the detection of genomic features. To achieve this, genomic DNA was extracted, sequenced, and assembled. The *A. veronii* strain MS-17-88 genome comprised 5,178,226-bp with 58.6% G+C, and it encoded several AMR elements, including *imiS, ampS, mcr-7.1, mcr-3, catB2, catB7, catB1, floR, vat(F), tet(34), tet(35), tet(E), dfrA3,* and *tetR*. The phylogeny and resistance profile of a large collection of *A. veronii* strains, including MS-17-88, were evaluated. Phylogenetic analysis showed a close relationship between MS-17-88 and strain Ae5 isolated from fish in China and ARB3 strain isolated from pond water in Japan, indicating a common ancestor of these strains. Analysis of phage elements revealed 58 intact, 63 incomplete, and 15 questionable phage elements among the 53 *A. veronii* genomes. The average phage element number is 2.56 per genome, and strain MS-17-88 is one of two strains having the maximum number of identified prophage elements (6 elements each). The profile of resistance against various antibiotics across the 53 *A. veronii* genomes revealed the presence of *tet(34), mcr-7.1, mcr-3,* and *dfrA3* in all genomes (100%). By comparison, *sul1* and *sul2* were detected in 7.5% and 1.8% of *A. veronii* genomes. Nearly 77% of strains carried *tet(E)*, and 7.5% of strains carried *floR*. This result suggested a low abundance and prevalence of sulfonamide and florfenicol resistance genes compared with tetracycline resistance among *A. veronii* strains. Overall, the present study provides insights into the resistance patterns among 53 *A. veronii* genomes, which can inform therapeutic options for fish affected by *A. veronii*.

Keywords: *Aeromonas veronii*, antibiotic resistant, phage elements, comparative genomics, phylogenetic tree

OPEN ACCESS

Edited by:
Xiangmin Lin,
Fujian Agriculture and Forestry University, China

Reviewed by:
Shengkang Li,
Shantou University, China
Xiaofeng Shan,
Jilin Agricultural University, China

***Correspondence:**
Hossam Abdelhamed
abdelhamed@cvm.msstate.edu

Specialty section:
This article was submitted to Molecular Bacterial Pathogenesis, a section of the journal Frontiers in Cellular and Infection Microbiology

Received: *31 March 2020*
Accepted: *08 June 2020*
Published: *17 July 2020*

Citation:
Tekedar HC, Arick MA II, Hsu C-Y, Thrash A, Blom J, Lawrence ML and Abdelhamed H (2020) Identification of Antimicrobial Resistance Determinants in Aeromonas veronii Strain MS-17-88 Recovered From Channel Catfish (Ictalurus punctatus). Front. Cell. Infect. Microbiol. 10:348. doi: 10.3389/fcimb.2020.00348

INTRODUCTION

Aeromonas species are Gram-negative rods in the family *Aeromonadaceae*. They are among the most common bacteria in aquatic environments and have been isolated from virtually all water source types including freshwater, estuarine environments, drinking waters, wastewaters, and sewage (Janda and Abbott, 2010). The disease caused by *Aeromonas* species affects a broad host range, including freshwater fish, amphibians, reptiles, and birds (Barony et al., 2015). Mesophilic *Aeromonas* species such as *A. hydrophila*, *A. caviae*, and *A. veronii*, are associated with several kinds of human infections, including gastroenteritis, wound infections, septicemia, and respiratory infections (Figueras, 2005; Igbinosa et al., 2012). *A. veronii* is one member of the genus *Aeromonas*, which is known for causing hemorrhagic septicemia in both wild and farmed fish such as channel catfish (*Ictalurus punctatus*) (Liu et al., 2016; Yang et al., 2017), snakehead (*Ophiocephalus argus*), whitefish (*Coregonus clupeaformis*) (Loch and Faisal, 2010), obscure puffer (*Takifugu obscurus*), Nile tilapia (*Oreochromis niloticus*) (Hassan et al., 2017), and common carp (*Cyprinus carpio*) (Sun et al., 2016). In recent years, an increasing number of *Aeromonas* species have become associated with disease of predominantly freshwater fish in most countries (Goni-Urriza et al., 2000), which results in causing severe outbreaks in different important aquaculture industries.

Sulfonamides potentiated with trimethoprim or ormethoprim, oxytetracycline, florfenicol, and erythromycin are the most commonly used antimicrobial (AM) agents for treatment of *Aeromonas*-related diseases in global aquaculture (Serrano, 2005). Although the judicious use of AM-medicated feeds is important for treatment purposes when faced with outbreaks of bacterial infections (Okocha et al., 2018), a substantial number of reports suggest that indiscriminate use of AMs can foster selection pressure and enable development of multi-drug resistant (MDR) bacteria in aquatic environments (Arslan and Küçüksari, 2015). MDR in bacterial pathogens can result in therapeutic challenges for control of bacterial diseases (Marshall and Levy, 2011).

Over the past two decades, *A. veronii* has gained epidemiological and ecological importance by several research groups due to its potential as an opportunistic and primary pathogen for fish and the prevalence of MDR strains (Sanchez-Cespedes et al., 2008). Previous studies have reported the isolation of MDR *A. veronii* strains from different regions of the world such as Sri Lanka (Jagoda et al., 2017), China (Yang et al., 2017), and United States (Abdelhamed et al., 2019; Tekedar et al., 2019). The resistance elements in *Aeromonas* species are often harbored in mobile genetic elements such as class 1 integrons, plasmids, IS elements, transposons, and genomic islands (Piotrowska and Popowska, 2015). These mobile elements can facilitate the spread of resistance among bacteria via transduction and conjugation (Sanchez-Cespedes et al., 2008; Hossain et al., 2013; Piotrowska and Popowska, 2015). Therefore, it is important to investigate the pattern of resistance, genetic relatedness, and mobile elements in *Aeromonas* species. High-throughput sequencing provides an opportunity to detect MDR bacteria, discover potential resistance mechanisms, and explore the mechanisms underlying resistance gene transfer (Liu et al., 2012).

The purpose of the current work was to uncover mechanisms of resistance in *A. veronii* strain MS-17-88, which was isolated from catfish in the southeastern U.S., and to assess the diversity, resistance profiles, and mobile elements in a large collection of *A. veronii* strains. Here we present the draft genome of *A. veronii* and results from a comparative analysis with 52 publicly available *A. veronii* genomes with a special emphasis on patterns of AMR genes and prophage elements distribution. To the best of our knowledge, no study has been published reporting a core-genome based phylogenetic relationship of sequenced *A. veronii* genomes, AMR profiles, and their mobilomes. Overall, our work provides a basis to understand the AMR profile for *A. veronii* in aquatic environments, which is an important step toward curtailing AMR spread and informing a treatment of disease caused by *A. veronii*.

MATERIALS AND METHODS

Bacterial Strains and Data Source for Comparative Genome Analysis

A. veronii strain MS-17-88 was recovered from a diseased channel catfish in 2017 from the Aquatic Diagnostic Laboratory at the College of Veterinary Medicine, Mississippi State University. The isolate was confirmed phenotypically as *A. veronii*. A 20% glycerol stock culture was stored at −80°C. *A. veronii* strain MS-17-88 was cultured in brain heart infusion (BHI) agar or broth (Difco) and incubated at 30°C. Fifty-two *A. veronii* genomes were retrieved from the National Center for Biotechnology Information (NCBI) genomes database on October 9, 2018, including five complete genome sequences and forty-seven draft genome sequences (**Table 1**).

Antibiotic Resistance Phenotypes of *A. veronii* Strain MS-17-88

The AM susceptibility of *A. veronii* strain MS-17-88 was determined by the Kirby-Bauer disk diffusion method (Bauer et al., 1966). Strain MS-17-88 was streaked on Mueller-Hinton agar plates, and the AM disks were applied on the streaked cultures with a Dispens-O-Disc dispenser. The AM agents tested were florfenicol (30 μg), chloramphenicol (30 μg), tetracycline (30 μg), doxycycline (30 μg), oxytetracycline (30 μg), sulfamethoxazole-trimethoprim (23:75; 1.25 μg), sulfamethoxazole (25 μg), erythromycin (15 μg), gentamicin (10 μg), streptomycin (10 μg), spectinomycin (100 μg), amoxicillin/clavulanic acid (30 μg), ampicillin (30 μg), penicillin (10 μg), ceftriaxone (30 μg), cefpodoxime (10 μg), ceftiofur (30 μg), ciprofloxacin (5 μg), enrofloxacin (15 μg), azithromycin (15 μg), nalidixic acid (30 μg), bacitracin (10 μg), and novobiocin (30 μg). These AM agents were selected based on the World Health Organization's list of the most common classes of antimicrobials (aminoglycosides, tetracyclines, macrolides, beta-lactam, phenicols, quinolones, and sulfonamides) that are regularly used in agriculture and aquaculture and linked to human medicine (Done et al., 2015). After 24 h of incubation

TABLE 1 | The 53 *A. veronii* genomes used in comparative genomic analysis.

Strain names	Country	Source	Level	Size (Mb)	GC%	Scaffolds	Genes	Proteins	Accession	References
Ae52	Sri-Lanka	Goldfish	Contig	4.56	58.7	80	–	–	BDGY00000000.1	Jagoda et al., 2017
MS-17-88	USA	Catfish	Contig	5.18	58.2	12	4,948	4,651	NZ_RAWX01000001.1	This study
ARB3	Japan	Pond water	Contig	4.54	58.8	63	4,074	3,952	NZ_JRBE00000000.1	Kenzaka et al., 2014
CIP 107763	USA	N/A	Contig	4.43	58.8	64	4,040	3,897	NZ_CDDU00000000.1	N/A
VBF557	India	Human	Contig	4.70	58.4	526	4,460	3,325	LXJN00000000.1	N/A
TTU2014-108ASC	USA	Cattle	Contig	4.53	58.7	58	4,103	3,941	NZ_LKJP00000000.1	Webb et al., 2016
TTU2014-108AME	USA	Cattle	Contig	4.53	58.7	62	4,112	3,938	NZ_LKJN00000000.1	Webb et al., 2016
TTU2014-115AME	USA	Cattle	Scaffold	4.53	58.7	53	4,108	3,943	NZ_LKJR00000000.1	Webb et al., 2016
TTU2014-115ASC	USA	Cattle	Contig	4.53	58.7	52	4,102	3,940	NZ_LKJS00000000.1	Webb et al., 2016
TTU2014-142ASC	USA	Cattle	Contig	4.68	58.6	45	4,242	4,065	NZ_LKKF00000000.1	Webb et al., 2016
TTU2014-130ASC	USA	Cattle	Scaffold	4.68	58.6	49	4,243	4,063	NZ_LKJX00000000.1	Webb et al., 2016
TTU2014-134AME	USA	Cattle	Contig	4.68	58.6	50	4,248	4,063	NZ_LKKA00000000.1	Webb et al., 2016
TTU2014-141AME	USA	Cattle	Scaffold	4.68	58.6	48	4,241	4,066	NZ_LKKD00000000.1	Webb et al., 2016
TTU2014-134ASC	USA	Cattle	Contig	4.68	58.6	59	4,242	4,060	NZ_LKKB00000000.1	Webb et al., 2016
TTU2014-143ASC	USA	Cattle	Contig	4.68	58.6	54	4,246	4,061	NZ_LKKH00000000.1	Webb et al., 2016
TTU2014-125ASC	USA	Cattle	Contig	4.68	58.6	58	4250	4,066	NZ_LKJV00000000.1	Webb et al., 2016
TTU2014-141ASC	USA	Cattle	Contig	4.68	58.6	45	4,240	4,062	NZ_LKKE00000000.1	Webb et al., 2016
TTU2014-113AME	USA	Cattle	Scaffold	4.66	58.6	122	4,239	4,037	NZ_LKJQ00000000.1	Webb et al., 2016
TTU2014-130AME	USA	Cattle	Contig	4.68	58.6	64	4,242	4,064	NZ_LKJW00000000.1	Webb et al., 2016
TTU2014-143AME	USA	Cattle	Contig	4.68	58.6	59	4,248	4,066	NZ_LKKG00000000.1	Webb et al., 2016
TTU2014-131ASC	USA	Cattle	Contig	4.68	58.6	70	4,245	4,055	NZ_LKJY00000000.1	Webb et al., 2016
TTU2014-140ASC	USA	Cattle	Contig	4.68	58.6	81	4,249	4,057	NZ_LKKC00000000.1	Webb et al., 2016
pamvotica	Greece	Sediment	Contig	4.92	58.1	21	4,581	4,317	NZ_MRUI00000000.1	N/A
AER397	USA	Human	Scaffold	4.50	58.8	5	4,014	3,888	NZ_AGWV00000000.1	*
B565	China	Pond sediment	Complete	4.55	58.7	1	4,100	3,950	NC_015424	Li et al., 2011
CCM 4359	USA	Human	Contig	4.51	58.9	56	4,170	3,908	NZ_MRZR00000000.1	N/A
CECT 4257	USA	Human	Scaffold	4.52	58.9	52	4,101	3,955	NZ_CDDK00000000.1	Colston et al., 2014
AMC35	USA	Human	Scaffold	4.57	58.5	2	4,064	3,918	NZ_AGWW00000000.1	*
AVNIH1	USA	Human	Complete	4.96	58.47	2	4,551	4,321	NZ_CP014774.1	N/A
AVNIH2	USA	Human	Contig	4.52	58.9	50	4,071	3,918	NZ_LRBO00000000.1	N/A
LMG 13067	USA	N/A	Scaffold	4.74	58.4	72	4,265	4,055	NZ_CDBQ00000000.1	N/A
126-14	China	Human	Scaffold	4.37	58.6	146	4,114	3,884	NZ_PPTE00000000.1	N/A
FC951	India	Human	Contig	4.67	58.5	231	4,479	4,066	NZ_PKSR00000000.1	N/A
5.28.6	Greece	Fish	Contig	4.61	58.6	98	4,337	4,107	NZ_NNSE00000000.1	N/A

(Continued)

TABLE 1 | Continued

Strain names	Country	Source	Level	Size (Mb)	GC%	Scaffolds	Genes	Proteins	Accession	References
VCK	Greece	Fish	Contig	4.63	58.6	120	4,366	4,133	NZ_NNSF00000000.1	N/A
NS	Greece	European bass	Contig	4.71	58.5	140	4,503	4,244	NZ_NMUR00000000.1	N/A
PDB	Greece	Fish	Contig	4.72	58.5	141	4,542	4,285	NZ_NMUS00000000.1	N/A
AER39	USA	Human	Scaffold	4.42	58.8	4	3,987	3,832	NZ_AGWT00000000.1	N/A
X12	China	Wuchang bream	Complete	4.77	58.3	1	4,440	4,183	NZ_CP024933	N/A
A29	South Africa	Surface water	Scaffold	4.48	58.8	54	4,142	3,979	NJGB00000000.1	N/A
X11	China	Wuchang bream	Complete	4.28	58.8	1	3,901	3,716	NZ_CP024930	N/A
CCM 7244	Germany	Surface water	Contig	4.42	58.9	74	4,069	3,807	NZ_MRZQ00000000.1	N/A
CECT 4486	USA	Surface water	Scaffold	4.41	58.9	66	4,022	3,831	NZ_CDBU00000000.1	Colston et al., 2014
Hm21	Turkey	Digestive tract	Contig	4.68	58.7	50	4,252	4,116	NZ_ATFB00000000.1	Bomar et al., 2013
CB51	China	Fish	Complete	4.58	58.6	1	4,152	3,623	CP015448	N/A
ZWY-AV1	China	Liver	Contig	4.62	58.6	31	4,317	4,153	NZ_PXYZ00000000.1	N/A
Z2-7	China	N/A	Scaffold	4.41	58.7	48	4,092	3,915	NZ_UETI00000000.1	N/A
ZJ12-3	China	Human	Scaffold	4.70	58.4	124	4,380	4,122	NZ_UETM00000000.1	N/A
ML09-123	USA	Fish	Contig	4.75	58.4	32	4,422	4,204	PPUW01000001	N/A
TH0426	China	Catfish	Complete	4.92	58.3	1	4,528	4,282	NZ_CP012504.1	Kang et al., 2016
XH.VA.1	China	Catfish	Contig	5.36	58.5	62	5,207	4,912	NZ_PZKL00000000.1	N/A
XH.VA.2	China	Catfish	Scaffold	4.91	58.1	48	4,637	4,389	NZ_QQOQ00000000.1	N/A
RU31B	N/A	N/A	Scaffold	4.53	58.7	93	4,203	3,976	NZ_FTMU00000000.1	N/A

**Human Microbiome U54 initiative, Broad Institute (broadinstitute.org).*
N/A, Not available.

at 30°C, the zones of inhibition diameter were measured and compared to the criteria of the National Committee for Clinical Laboratory Standards. The assay was performed in triplicate and repeated as two independent experiments.

DNA Extraction, Whole-Genome Sequencing, Assembly, and Annotation

Genomic DNA of *A. veronii* strain MS-17-88 was extracted using the DNeasy Blood & Tissue Kit (Qiagen., USA) according to the manufacturer's instructions. Genome sequencing was conducted using HiSeq X Ten (Illumina, San Diego, CA, USA) and MinION (Oxford Nanopore Technologies, Oxford, UK), producing approximately 848.86X and 229.35X genome coverages, respectively. Together, the genome coverage is 1077X. Trimmomatic (Bolger et al., 2014) was used to trim Illumina reads, Nanopore reads were corrected with Canu (version 1.6) (Koren et al., 2017), and contig errors were corrected using Pilon (version 1.21) (Walker et al., 2014). Assembly of the Illumina and Nanopore reads into contigs was done using MaSuRCA (version 3.2.4 (Zimin et al., 2013). Average nucleotide identity (ANI) was calculated based on whole genome sequencing using BLAST alignments (Richter and Rossello-Mora, 2009).

Phylogenetic Tree

A phylogenetic tree was constructed based on the complete core genome of *A. veronii* strain MS-17-88 and 52 *A. veronii* genomes to evaluate taxonomic positions. All publicly available *A. veronii* genome sequences (52 genomes) were downloaded from NCBI. Gene sets of the core genome were aligned using MUSCLE (Edgar, 2004) and concatenated. Concatenated alignment files were used as an input to compute a Kimura distance matrix, which was followed by using the concatenated files for the Neighbor-Joining algorithm as implemented in PHYLP (Felsenstein, 1989).

Subsystem Coverages and Genomes Structure Variation

A. veronii strain MS-17-88 and 52 *A. veronii* genomes were submitted to Rapid Annotations using Subsystems Technology (RAST) for annotation, subsystem categorization, and comparison purposes (Aziz et al., 2008). The following criteria were used for annotation pipeline: classic RAST for annotation, RAST gene caller for open reading frame (ORF) identification, and Figfam (version release70 with automatic fix errors and fix frameshifts options). *A. veronii* strain MS-17-88 genome was compared against 52 *A. veronii* using BRIG (BLAST Ring Image Generator) (Alikhan et al., 2011).

Prophages

The presence of prophages in the 53 *A. veronii* genomes was determined using PHASTER (PHAge Search Tool Enhanced Release) (Arndt et al., 2016, 2019). Nucleotide sequences from 53 genomes were concatenated using Sequencher 5.4.5 to serve as an input file prior to submission to the PHASTER server. Results from PHASTER were arranged into three categories: score > 90 was considered intact phage element; a score between 70 and 90 was deemed questionable; and score < 70 was considered incomplete phage region (Arndt et al., 2019).

Comparative Analysis of Putative AMR Elements

The potential AMR genes and related elements for each genome were identified using ResFinder 3.1 (Zankari et al., 2012). ResFinder database was downloaded and used in CLC Workbench version 11.0.1 (CLC Bio) for the BLAST search. The contig files for each genome were concatenated, and concatenated nucleotide files were uploaded to CLC Workbench. A BLAST search was run with the following settings: 40% minimum identity and 40% minimum matching length.

RESULTS AND DISCUSSION

General Genome Features of *A. veronii* Strain MS-17-88

The present study reported the draft genome of *A. veronii* strain MS-17-88 isolated from diseased catfish in the southeastern U.S. The draft genome of *A. veronii* strain MS-17-88 consisted of 5,178,226 bp with 58.6% G+C content and encoded 4,944 predicted coding sequences (CDSs). A total of 181 RNA genes were predicted in the genome including 139 tRNAs, 4 ncRNAs, and 38 rRNAs (12, 13, 13 for 5, 16, and 23 s, respectively). The final assembly contained 13 contigs. The largest contig assembled was 1,457,362-bp length, and the smallest contig was 7,082-bp. The genome has been deposited in GenBank (accession number NZ_RAWX01000000). *A. veronii* contains two biovars (*A. veronii* biovar veronii and *A. veronii* biovar sobria) (Janda and Abbott, 2010). ANI and phylogenetic tree calculation confirmed that strain MS-17-88 belongs to *A. veronii* biovar veronii (ANI score higher than 95%).

Genotypic and Phenotypic Characterization of *A. veronii* Strain MS-17-88

The Rasfinder and CARD analysis revealed 14 resistance elements in the *A. veronii* strain MS-17-88 genome (**Table 2**), including beta-lactamase resistance genes (*imiS* and *ampS*), chloramphenicol and florfenicol resistance gene (*floR*), macrolide resistance genes (*mcr-3* and *mcr-7.1*), streptogramin B resistance *vat(F),* tetracycline resistance genes [*tet(34)*, *tet(35),* and *tet(E)*], and acetyltransferase genes conferring resistance to phenicol compounds. The disk diffusion results (**Table 3**) demonstrated that *A. veronii* strain MS-17-88 strain is resistant to phenicol class (florfenicol and chloramphenicol), tetracyclines (tetracycline, doxycycline, and oxytetracycline), macrolides (erythromycin, azithromycin,), aminoglycoside (gentamicin), sulfamethoxazole, beta-lactam class (amoxicillin/clavulanic acid, ampicillin, and penicillin), spectinomycin, bacitracin, and novobiocin.

Resistance to β-lactam antibiotics in *Aeromonas* species is primarily mediated by β-lactamases, whose mode of action involves hydrolyzing the β-lactam ring. Many different β-lactamases have been detected in *Aeromonas* species, such as TEM-, SHV-, OXA-, CMY-, and CTX-M-type β-lactamases. In

TABLE 2 | Predicted antibiotic resistance genes in *A. veronii* strain MS-17-88.

Protein name	Protein ID	Gene	% Identity	Query/HSP Length	Predicted phenotype
CphA family subclass B2 metallo-beta-lactamase	RKJ87494.1	*imiS*	89.7	767/768	Beta-lactam resistance
Class D beta-lactamase	RKJ86357.1	*ampS*	93.84	795/795	Beta-lactam resistance
Phosphoethanolamine-lipid A transferase	RKJ90059.1	*mcr-3*	67.19	756/1,626	Colistin resistance
Phosphoethanolamine–lipid A transferase	RKJ90059.1	*mcr-7.1*	73.2	1,601/1,620	Colistin resistance
Antibiotic acetyltransferase	D6R50_13775	*catB2*	65.85	201/633	Phenicol resistance
Antibiotic acetyltransferase	D6R50_13775	*catB7*	68.78	235/639	Phenicol resistance
Antibiotic acetyltransferase	RKJ86442.1	*catB7*	66.61	565/639	Phenicol resistance
Vat family streptogramin A O-acetyltransferase	RKJ85500.1	*catB1*	70.79	265/630	Phenicol resistance
Chloramphenicol/florfenicol efflux MFS	RKJ86396.1	*floR*	98.19	1,214/1,215	Phenicol resistance
Vat family streptogramin A O-acetyltransferase	RKJ85500.1	*vat(F)*	69.52	581/666	Streptogramin B resistance
Xanthine phosphoribosyltransferase	RKJ89311.1	*tet(34)*	66.95	340/465	Tetracycline resistance
Na+/H+ antiporter NhaC family protein	RKJ91399.1	*tet(35)*	70.13	231/1,110	Tetracycline resistance
Tetracycline efflux MFS transporter Tet(E)	RKJ91234.1	*tet(E)*	99.92	1218/1,218	Tetracycline resistance
Type 3 dihydrofolate reductase	RKJ87621.1	*dfrA3*	68.93	348/489	Trimethoprim resistance

the present study, *ampS* and *imiS* were detected in *A. veronii* stain 17-88. AmpS is a class 2d penicillinase and ImiS is a class 3 metallo-β-lactamase. The *imiS* gene has been detected in clinical isolates of *A. veronii* biovar sobria (Wu et al., 2012). MS-17-88 also harbors *floR*, which encodes a major facilitator superfamily efflux pump that exports florfenicol (Schwarz et al., 2004). Florfenicol is one among the three approved AMs for use in catfish aquaculture in the U.S (Bowker et al., 2010). Most fish pathogenic bacteria mediate florfenicol resistance through FloR (Dang et al., 2007; Gordon et al., 2008). Dissemination of florfenicol resistance among bacterial pathogens isolated from aquaculture can limit the efficacy of this agent as an important treatment option.

Phylogenetic Tree

The phylogenetic relationship between the *A. veronii* MS-17-88 genome and 52 other *A. veronii* genomes was assessed. The strains used in this analysis are from different countries and hosts, and they had distinct resistance profiles (**Table 1**). The phylogenetic tree for the 53 *A. veronii* genomes was built from a core genome of 2,563 genes per genome (135,839 genes in total). The core has 2,538,377 bp per genome (134,533,981 bp in total).

The phylogenetic tree showed that there are multiple highly conserved branches that are separated from the other *A. veronii* genomes. MDR *A. veronii* strain MS-17-88 from U.S. channel catfish, goldfish (*Carassius auratus*) MDR strain Ae5 from China, and *A. veronii* ARB3 from pond water in Japan were clustered together, which may indicate a common origin. Similarly, U.S. channel catfish isolate ML09-123 and China catfish isolate TH0426 were closely related, which also may suggest derivation from the same monophyletic origin despite their geographic disparity. Moreover, dairy cattle isolates and Greece surface sediment isolates (strain pamvotica) formed another closely related group. U.S. human isolates (strains AER 397, CECT 4257, and CCM 4359) and China pond sediment isolate B565 formed another clade. Lastly, U.S. surface water and Germany surface water isolates were closely related, and Greece fish isolates (strains 5.28.6, VCK, NS, and PDB) were clustered together. These data clearly suggest that the ecological niche is a more important factor contributing to relatedness among *A. veronii* isolates than geographical location. However, two isolates (CIP 107763 and VBF557) showed a distinct genetic relationship to the other isolates.

It has been postulated that a fish pathogenic *Aeromonas hydrophila* clonal group was transferred to the U.S. channel catfish aquaculture industry from China (Hossain et al., 2014). In the current study, we observed two different clonal groups of *A. veronii* that contain isolates from both U.S. and China. One clade has MDR *A. veronii* strain MS-17-88 from U.S. catfish aquaculture and MDR isolate Ae5 from goldfish in China, and another clade has U.S. channel catfish isolate ML09-123 and China catfish strain TH0426 (**Figure 1**).

Subsystems Coverage

The subsystems categorization based on RAST annotation is shown in **Figure 2**. SEED subsystem categorization analysis predicted 26 different categories for the evaluated *A. veronii* genomes. The most abundant systems are "amino acid and derivatives," followed by "carbohydrates" and "protein metabolism." These subsystems are essential for bacteria to perform basic cellular processes and may indicate the potential ability of *A. veronii* to utilize different kinds of sugars and amino acids available in the environment (Liang et al., 2019). On the other hand, *A. veronii* genomes show remarkably low numbers of mobile genetic elements including phages, prophages, transposable elements, and plasmids. These mobile elements can mediate alteration of genotypes, and these findings may suggest that horizontal gene exchange may not contribute to *A. veronii* genomic variation as much as other species. Interestingly, U.S. catfish isolate strain MS-17-88 carries the most abundant subsystems (63 elements) associated with phages, prophages, transposable elements, and plasmids. Chinese catfish isolate strain TH0426 has the second largest number (52 elements) of phage and transposable elements. Therefore,

TABLE 3 | Antimicrobial resistance phenotype of *A. veronii* strain MS-17-88.

Antimicrobial agents	Disk content (μg)	Diameter of inhibition zone (mm)	Sensitivity
Florfenicol FFC30	30	0	R
Chloramphenicol C30	30	0	R
Tetracycline TE30	30	6.16 ± 0.44	R
Doxycycline D30	30	10.8 ± 0.41	R
Oxytetracycline T30	30	0	R
Sulfamethoxazole	25	0	R
Sulphamethoxazole trimethoprim SXT	25	17.9 ± 0.20	S
Erythromycin E15	15	11.20 ± 0.11	R
Gentamicin GM10	10	16.24 ± 0.40	R
Streptomycin S10	10	11.4 ± 0.23	S
Spectinomycin SPT100	100	12.7 ± 0.14	R
Amoxicillin/clavulanic acid AMC30	30	9.2 ± 0.11	R
Ampicillin AM10	10	0	R
Penicillin P10	10	0	R
Ceftriaxone CRO30	30	29.43 ± 0.31	S
Cefpodoxime CPD10	10	19.63 ± 0.18	S
Ceftiofur XNL30	30	19.76 ± 0.12	S
Ciprofloxacin CIP5	25	24.76 ± 0.14	S
Enrofloxacin E15	15	24.76 ± 0.14	S
Azithromycin AZM15	15	16.3 ± 0.17	R
Nalidixic acid NA30	30	24.8 ± 0.10	S
Bacitracin B10	10	0	R
Novobiocin NB30	30	9.3 ± 0.15	R

R, resistant; S, sensitive.
Data represented as means diameter of inhibition zones (mm) ± SD of two independent experiments in triplicates.

these two strains (MS-17-88 and TH0426) may have acquired significant genome structure changes by gene acquisitions from mobile elements. It is notable that both strains were isolated from aquatic environments, and we speculate that the aquatic environment may be favorable for genetic exchange and horizontal gene acquisition.

Genome Structure Variation

Visualization of the alignment between *A. veronii* MS-17-88 and 52 other *A. veronii* genomes revealed that phage elements, transposons, and genomic islands comprise many of the MS-17-88-specific regions (**Figure 3**). This suggests that mobile elements, especially phages and transposons, play an important role in *A. veronii* genome variation. These mobile elements can result in genomic rearrangements and evolution through acquisition of novel virulence or antibiotic resistance genes which may result in emergence of new phenotypes (Brown-Jaque et al., 2015).

Prophages

Bacteriophages are responsible for loci rearrangements and deletions and are recognized as an important element in bacterial evolution (Tinsley et al., 2006). The vast majority of aquatic bacteria (about 70%) are infected with prophages (Chen et al., 2006). Of particular interest, bacteriophages can mediate horizontal gene transfer, including genes encoding virulence factors and antibiotic resistance (Colomer-Lluch et al., 2011). A higher number of phages may represent a concern because they can expand the pathogenicity of a bacterial strain or convert an avirulent strain into a virulent one (Canchaya et al., 2004). Even though phage elements may not be the main spreading factors of resistance elements, recent studies indicate that they can infrequently contribute to the dissemination of these elements (Allen et al., 2011; Enault et al., 2017). In *Aeromonas*, the transfer of resistance gene by phage elements has never been observed previously (Piotrowska and Popowska, 2015).

In the present study, we identified 58 intact, 63 incomplete, and 15 questionable phage elements among the 53 *A. veronii* genomes (**Figure 4**). The average phage element number is 2.56 per genome (136 identified phage elements/53 *A. veronii* strains). In a previous study, *A. hydrophila* genomes were found to harbor an average of 2.91 phage elements per genome (143 identified phage elements/49 *A. hydrophila* strains) (Awan et al., 2018). Almost all the strains carry one or more prophage elements, with the exceptions being strains FC951, CECT4486, and CCM7244, which do not carry any type of prophage. Strains MS-17-88 and TH0426 had the maximum number of identified prophage elements (6 elements per strain). The maximum number of complete prophage elements (5 complete phages) was present in strain MS-17-88 along with one incomplete phage element (**Figure 4**). The maximum number of incomplete prophage elements (4 incomplete phages) was present in strains TTU2014-108ASC and TTU2014-115AME. Strain MS-17-88 carries three different types of phage elements: vB_AbaM_ME3, phi018P, and RSA1. Interestingly, two of these phage elements (vB_AbaM_ME3 and RSA1) are not carried by any other evaluated *A. veronii* genomes, suggesting that this strain has been exposed to different environments and acquired unique phage elements. Phage vB_AbaM_ME3 was previously isolated from wastewater effluent using the propagating host *Acinetobacter baumannii* DSM 30007 (Kropinski et al., 2009). *A. baumannii* is a known nosocomial pathogen that causes pneumonia, urinary tract infection, and septicemia (Buttimer et al., 2016). Phage vB_AbaM_ME3 of *A. baumannii* has a size of 234,900 bp and 326 ORFs (Buttimer et al., 2016). The Myovirus-type phage RSA1 is relatively small (39 to 40 kb) and has lytic activity. It has restricted host range, mainly *Ralstonia solanacearum*, a soil-borne species pathogenic to many important crops (Yamada et al., 2007; Addy et al., 2019).

Interestingly, the MS-17-88 genome has four prophages sharing structural similarities with temperate Aeromo_phiO18P elements found in *Aeromonas media* isolated from a pond in Germany (Beilstein and Dreiseikelmann, 2008). The phiO18P phage type belongs to the *Myoviridae* phage family and consists of 33 kb. The phiO18P phage elements typically have 46 ORFs encoding proteins responsible for integration and regulation, replication, packaging, head and tail, and lysis (Beilstein and Dreiseikelmann, 2008). Unlike other prophage elements, Aeromo_phiO18P does not have a lytic phase; it replicates lysogenically by integrating its genome into the bacterial

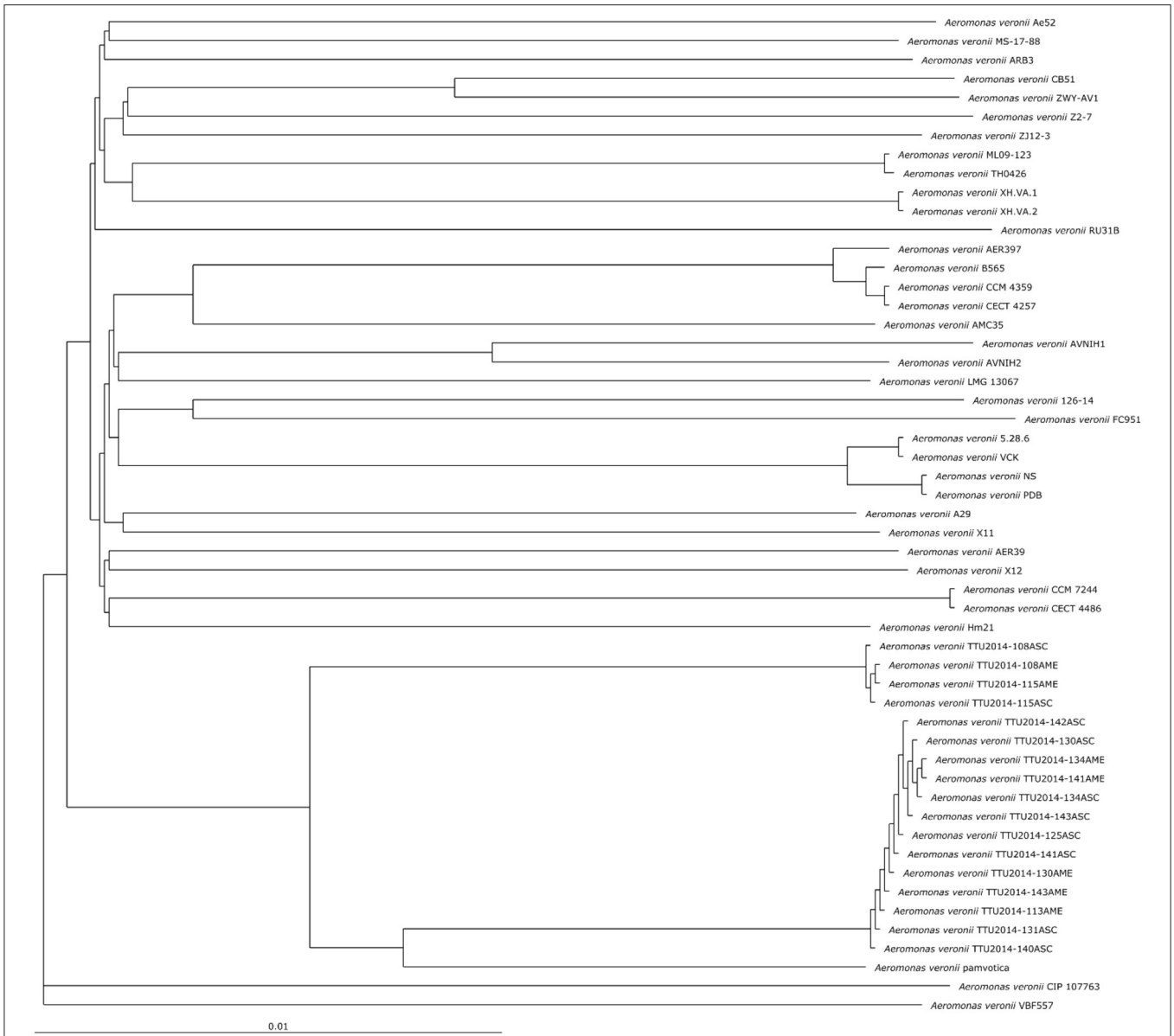

FIGURE 1 | Phylogenetic tree analysis based on the core genomes of *A. veronii*.

chromosome (Vincent et al., 2017). In some instances, the phage-encoded genes are advantageous to the host bacteria (Dziewit and Radlinska, 2016). Aeromo_phiO18P shows significant similarity to the P2 phage family in *Aeromonas salmonicida* and *Vibrio cholerae* K139 genomes (Beilstein and Dreiseikelmann, 2008).

The present study documented 40 different types of phage elements across the 53 *A. veronii* genomes (**Figure 5**). Among these 40 phage elements, phage type "Aeromo_phiO18P" is the most abundant type in all the evaluated *A. veronii* genomes as well as the most abundant in strain MS-17-88. Strains CCM 4359 and XH.VA.1 carry five different phage elements. Incomplete Staphy_SPbeta_like phage element was detected in two strains (MS-17-88 and AVNIH1). In our initial analysis of the MS-17-88 genome using PHASTER, we identified that the strain carries the *floR* gene inside incomplete phage element PHAGE_Staphy_SPbeta_like_NC_029119 (genome position 2631302-2644102), but later analysis with PHASTER showed that this may not be a true phage element. Further investigation of this region is warranted to determine whether a phage element mediated dissemination of the *floR* resistance gene (Garriss et al., 2009).

Comparative Analysis of Antibiotic Resistance Determinants

A comparative analysis of 87 AMR determinants and components was conducted to determine their distribution

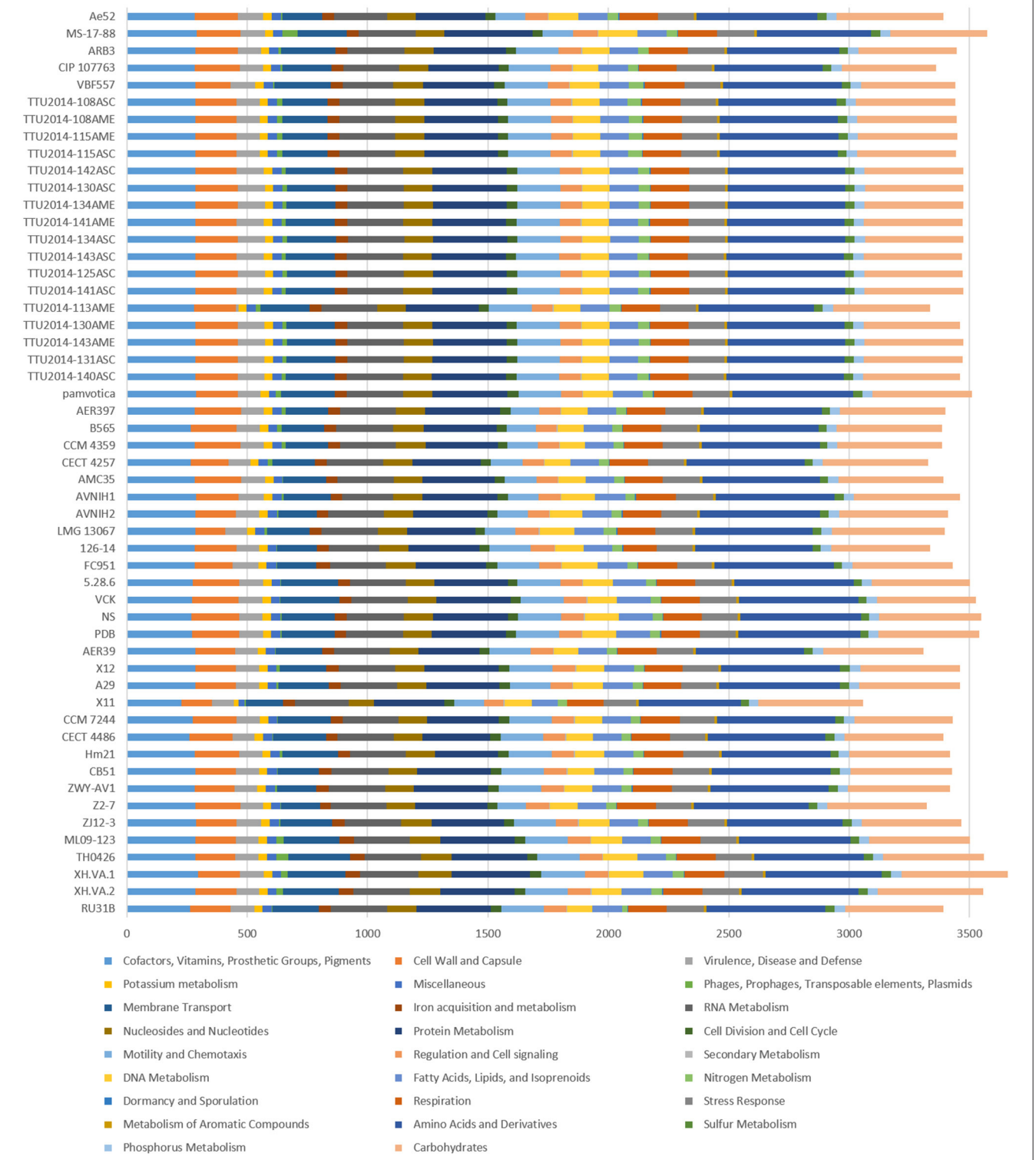

FIGURE 2 | Comparison of functional categories in 53 *A. veronii* genomes based on SEED. Functional categorization is based on roles of annotated and assigned genes. Each colored bar represents the number of genes assigned to each category.

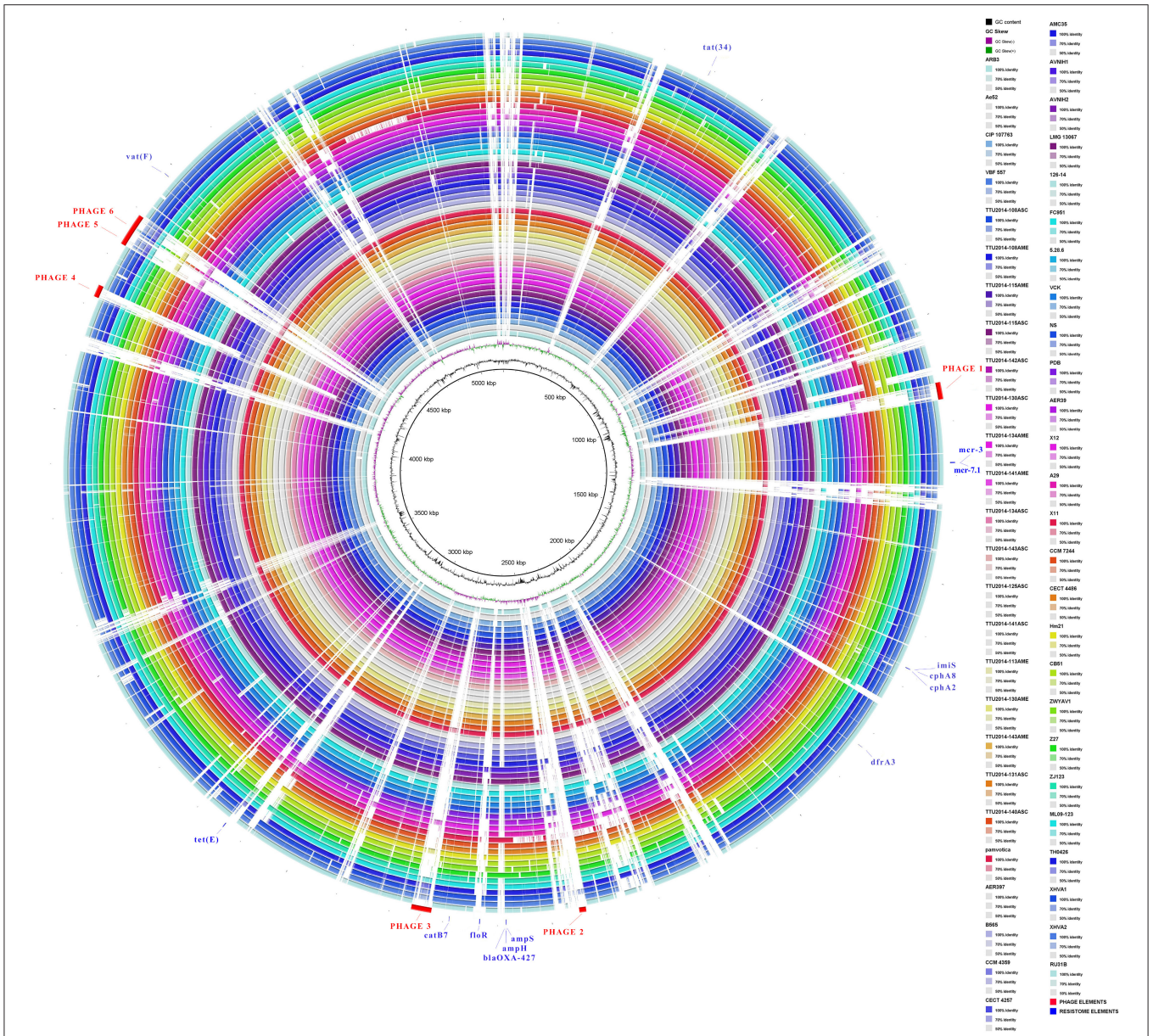

FIGURE 3 | Comparative circular map of the *A. veronii* MS-17-88 genome. Phage regions are highlighted with red color: phage region-1 encodes 41 proteins (31.8 Kb), phage region-2 encodes 12 proteins (12.6 Kb), phage region-3 encodes 39 proteins (37.7 Kb), phage region-4 encodes 31 proteins (22.9 Kb), phage region-5 encodes 45 proteins (48.6 Kb), and phage region-6 encodes 30 proteins (24.1 Kb).

among the 53 *A. veronii* strains. *A. veronii* MS-17-88 shared a common AMR gene composition with the other *A. veronii* genomes. **Figure 6** shows the distribution of antibiotic resistance genes in each strain. All the *A. veronii* genomes carry tetracycline [*tet(34)* and *tet(E)*], and trimethoprim (*dfrA3*) resistance genes. Oxytetracycline, tetracycline, and trimethoprim/sulfamethoxazole have been extensively used in human clinical, veterinary, and agricultural sectors for decades. The linkage between AM use and resistance has been demonstrated for other bacteria in aquaculture ecosystems and other animal husbandry facilities (Verner-Jeffreys et al., 2009; Lagana et al., 2011; Tamminen et al., 2011). In addition to *tet(34)*, *tet(E)*, and *dfrA3*, *A. veronii* MS-17-88 genome carries colistin resistance genes (*mcr-7.1* and *mcr-3*). There have been an increasing number of reports on the identification of *mcr* genes in many bacterial species globally (Stoesser et al., 2016; Elbediwi et al., 2019). A recent study reported that *mcr-3* variants are more common in Aeromonas than in other bacterial species but aeromonads do not inherently carry the *mcr-3* gene (Shen et al., 2018). However, it is speculated that Aeromonas isolates from the aquatic environment may be the major reservoir for the dissemination of *mcr-3* genes to other

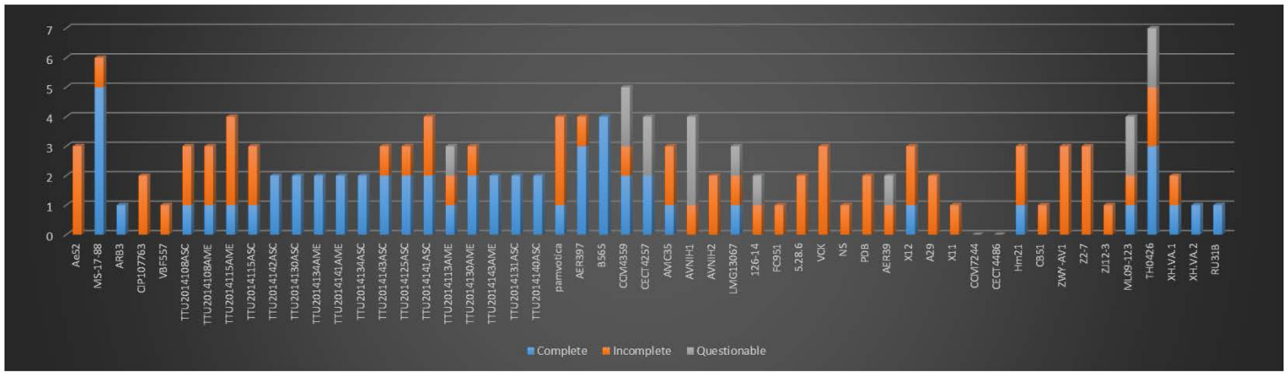

FIGURE 4 | Number of prophages with their completeness profiles in *A. veronii* genomes. Strains FC91, CCM7244, and CECT4486 did not have any prophage elements.

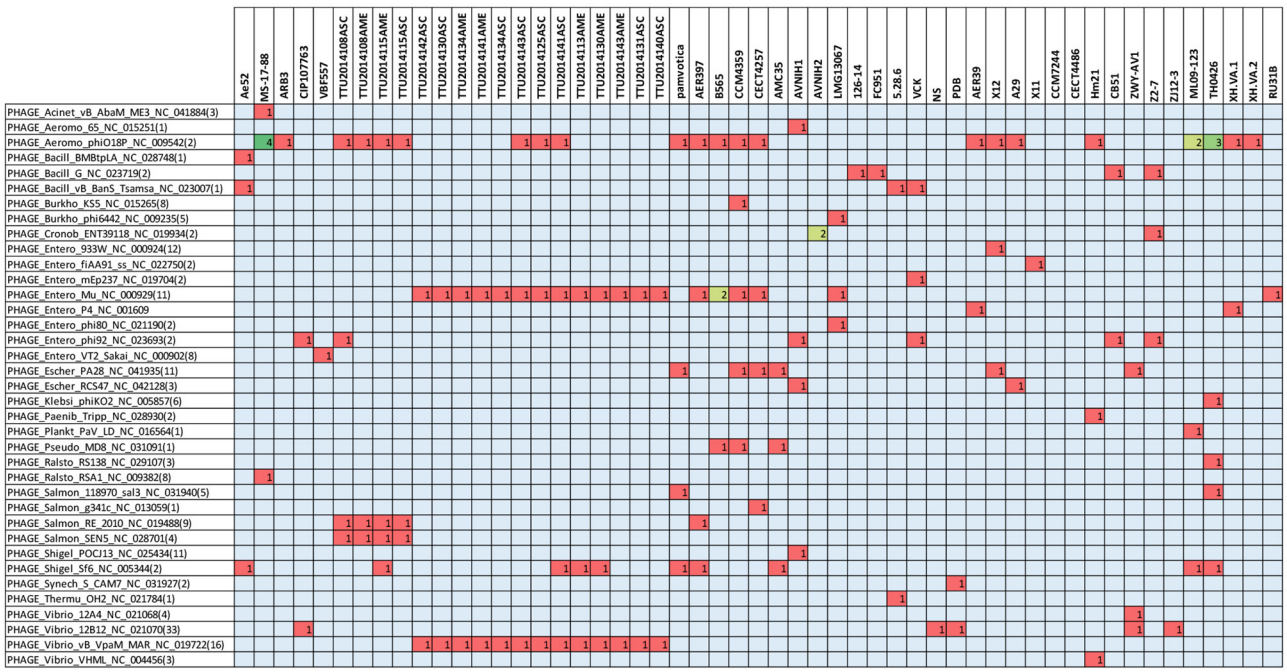

FIGURE 5 | Type of prophage elements present in the *A. veronii* genomes. Red color represents presence of the gene.

bacteria (Ling et al., 2017; Eichhorn et al., 2018). Furthermore, *A. veronii* MS-17-88 genome harbors a macrolide resistance gene *vat(F)* that encodes an acetyltransferase that acetylates class A streptogramins (Seoane and García Lobo, 2000). Six genes encoding resistance to β-lactamases were identified in *A. veronii* MS-17-88 genome including *ampH* and blaOXA-427 belong to class D beta-lactamase, ampS encoding a class 2d penicillinase and hydrolyzing mainly penicillins (Walsh et al., 1995), and *cphA2*, *cphA8*, and *imiS* encoding a class 3 metallo-β-lactamase and active mainly against carbapenems (Walsh et al., 1998).

Among the 53 *A. veronii* strains, AVNIH1 strain had resistance genes to almost all the antibiotic classes. This clinical strain was isolated from human stool, and the genome exhibits clear evidence of horizontal gene transfer (Hughes et al., 2016). In our analyses, we did not observe any pattern of antimicrobial resistance in specific bacterial host or sources. However, there was one exception: the highest number of AMR elements were observed in two human isolates (strain AVNIH from U.S.A; (Hughes et al., 2016) and ZJ12-3 from China; Shen et al., 2018), and one isolate from septicemic goldfish (strain Ae52 from Sri-Lanka; Jagoda et al., 2017). The use of antimicrobial agents in human medicine may be associated with these nosocomial trends (Hughes et al., 2016).

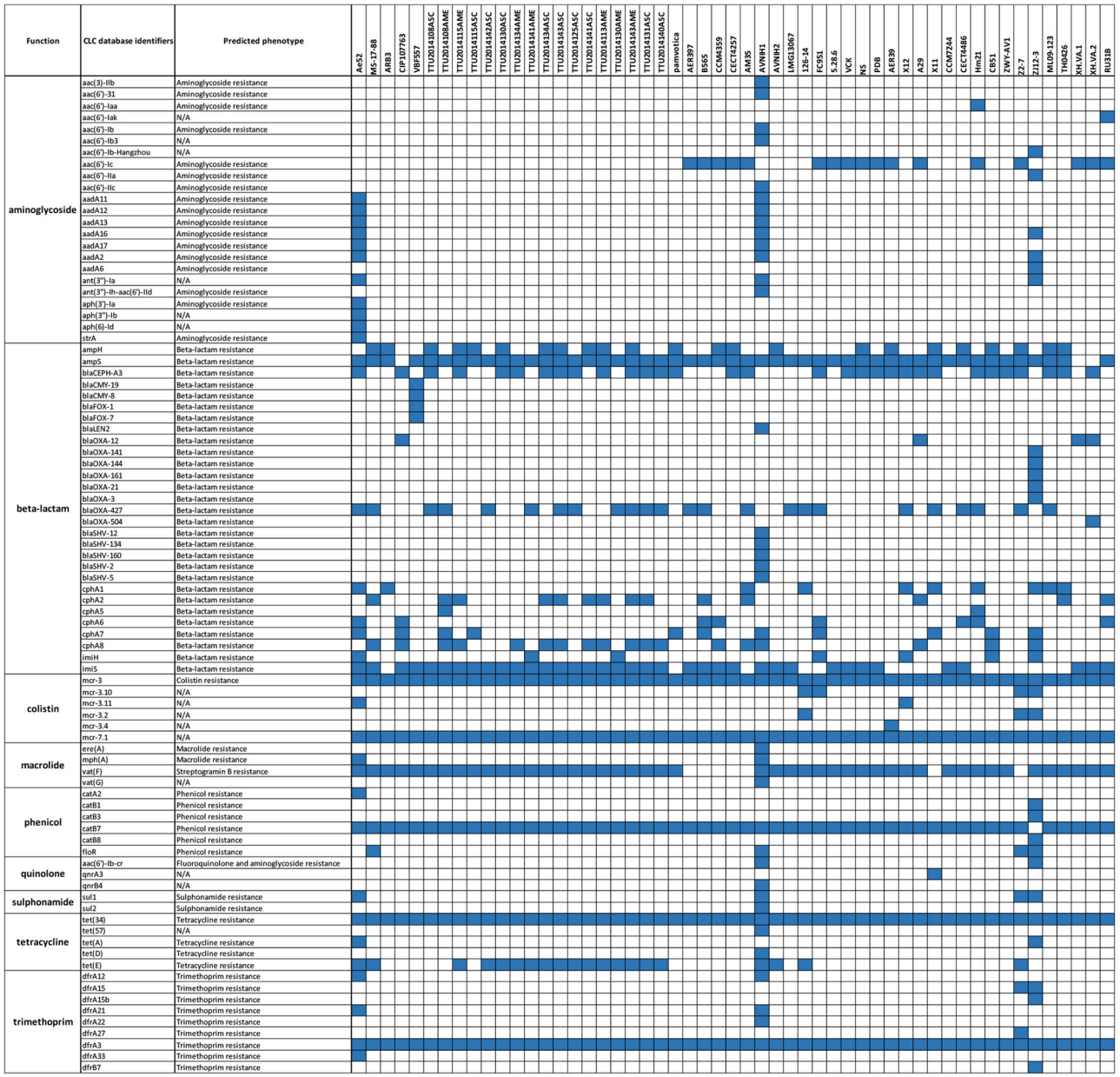

FIGURE 6 | AMR genes distribution across the 53 *A. veronii* genomes. Blue color represents presence of the gene.

In regard to sulphonamide resistance, *sul1* was detected in four strains (Ae52, ANIH1, Z2-7, and ZJ12-3) representing 7.5% of the *A. veronii* strains, and *sul2* was present in one strain (Z2-7) representing 1.8%. This suggests that *sul1* is the most frequent gene encoding sulfonamides resistance in *A. veronii*. Nearly all strains (100%) carried *tet(34)*, and a significant proportion of strains carried *tet(E)* (20 strains; 37%). In contrast, *tet(57)* and *tet(D)* were detected in only one strain (ANIH1) (1.8%), and *tet(A)* was detected in two strains (Ae52 and ZJ12-3) (3.8%). *floR* gene conferring resistance to florfenicol and chloramphenicol was present in only four strains (MS-17-88, AVNIH1, Z2-7, and ZJ12-3) (7.5%). The prevalence of beta-lactam resistance genes in the 53 *A. veronii* genomes was as follows: *ampH* was detected in 41.5% of the strains, *ampS* was detected in 92.4% of the strains, *imiH* was detected in 13.2% of the strains, *imiS* was detected in 71.7% of the strains, blaCEPH-A3 was detected in 56.6% of the strains, blaOXA-427 was detected in 45.3% of the strains, *cphA1* was detected in 17% of the strains, *cphA2* was detected in 26.41% of the strains, *cphA6* was detected in 13.2% of the strains, *cphA7* was detected in 20.7% of the

strains, and *cphA8* was detected in 44% of the strains. Of the aminoglycoside resistance genes, *aac(6′)-Ic* was the most prevalent (32%). Interestingly, *A. veronii* AVNIH1 and Ae52 strains carried multiple aminoglycoside-resistance genes. Several studies reported that the majority of *Aeromonas* species exhibit only a single aminoglycoside modifying gene (Dahanayake et al., 2019). However, *Pseudomonas aeruginosa* isolated from hospitals from Iran was reported to carry up to four aminoglycoside resistance genes (Perez-Vazquez et al., 2009).

In conclusion, we used genome sequencing to investigate genetic variation and AMR gene distribution in 53 *A. veronii* genomes. We found significant genetic differences and a high degree of genomic plasticity in the evaluated *A. veronii* genomes. Overall, the AMR gene frequency against sulfamethoxazole and florfenicol is low, while AMR genes against tetracycline are very high. Among tetracycline-resistant isolates, *tet(34)* and *tet(E)* were the most frequent AMR genes. Taken together, our results show that AMR genes are common and are distributed among *A. veronii* genomes; however, the frequency of most AMR genes in individual strains is still low. Identified phage elements may be useful for future development of an efficient and effective bio-treatment method to control bacterial diseases in aquaculture. The knowledge generated from this study can benefit our understanding of *A. veronii* evolution and provide insight into how *A. veronii* isolates are intrinsically resistant to multiple antimicrobials. In addition, *A. veronii* species are important considerations as potential sources for resistance determinants in the environment. Therefore, it is important to continue surveillance of resistance and genetic mechanisms of resistance in this species.

DATA AVAILABILITY STATEMENT

The datasets presented in this study can be found in online repositories. The names of the repository/repositories and accession number(s) can be found in the article.

AUTHOR CONTRIBUTIONS

HT, ML, and HA designed and conceived the analysis and experiments. HT, MA, C-YH, AT, JB, and HA performed the experiments and analyzed the data. HT, ML, and HA wrote the manuscript. All authors read and approved the final manuscript.

FUNDING

Salary support to HA was provided by the Center for Biomedical Research Excellence in Pathogen–Host Interactions, National Institute of General Medical Sciences, and National Institutes of Health awarded grant number P20GM103646-07. This work was supported by College of Veterinary Medicine and by USDA-ARS SCA no. 58-6066-7081 titled MS Center for Food Safety and Post-Harvest Technology, MS Agricultural and Forestry Experiment Station.

ACKNOWLEDGMENTS

The authors thank the Aquatic Diagnostic Laboratory at the College of Veterinary Medicine for providing *Aeromonas veronii* strain MS 17-88.

REFERENCES

Abdelhamed, H., Lawrence, M. L., and Waldbieser, G. (2019). Complete genome sequence data of multidrug-resistant *Aeromonas veronii* strain MS-18-37. *Data Brief* 23:103689. doi: 10.1016/j.dib.2019.01.037

Addy, H. S., Ahmad, A. A., and Huang, Q. (2019). Molecular and biological characterization of ralstonia phage RsoM1USA, a new species of P2virus, isolated in the United States. *Front. Microbiol.* 10:267. doi: 10.3389/fmicb.2019.00267

Alikhan, N. F., Petty, N. K., Ben Zakour, N. L., and Beatson, S. A. (2011). BLAST Ring Image Generator (BRIG): simple prokaryote genome comparisons. *BMC Genomics* 12:402. doi: 10.1186/1471-2164-12-402

Allen, H. K., Looft, T., Bayles, D. O., Humphrey, S., Levine, U. Y., Alt, D., et al. (2011). Antibiotics in feed induce prophages in swine fecal microbiomes. *MBio* 2. doi: 10.1128/mBio.00260-11

Arndt, D., Grant, J. R., Marcu, A., Sajed, T., Pon, A., Liang, Y., et al. (2016). PHASTER: a better, faster version of the PHAST phage search tool. *Nucleic Acids Res.* 44, W16–W21. doi: 10.1093/nar/gkw387

Arndt, D., Marcu, A., Liang, Y., and Wishart, D. S. (2019). PHAST, PHASTER and PHASTEST: tools for finding prophage in bacterial genomes. *Brief. Bioinform.* 20, 1560–1567. doi: 10.1093/bib/bbx121

Arslan, S., and Küçüksari, R. (2015). Phenotypic and genotypic virulence factors and antimicrobial resistance of motile *Aeromonas* spp. from Fish and Ground Beef. *J. Food Saf.* 35, 551–559. doi: 10.1111/jfs.12205

Awan, F., Dong, Y., Liu, J., Wang, N., Mushtaq, M. H., Lu, C., et al. (2018). Comparative genome analysis provides deep insights into *Aeromonas hydrophila* taxonomy and virulence-related factors. *BMC Genomics* 19:712. doi: 10.1186/s12864-018-5100-4

Aziz, R. K., Bartels, D., Best, A. A., DeJongh, M., Disz, T., Edwards, R. A., et al. (2008). The RAST Server: rapid annotations using subsystems technology. *BMC Genomics* 9:75. doi: 10.1186/1471-2164-9-75

Barony, G. M., Tavares, G. C., Assis, G. B., Luz, R. K., Figueiredo, H. C., and Leal, C. A. (2015). New hosts and genetic diversity of *Flavobacterium columnare* isolated from Brazilian native species and Nile tilapia. *Dis. Aquat. Org.* 117, 1–11. doi: 10.3354/dao02931

Bauer, A. W., Kirby, W. M., Sherris, J. C., and Turck, M. (1966). Antibiotic susceptibility testing by a standardized single disk method. *Am. J. Clin. Pathol.* 45, 493–496. doi: 10.1093/ajcp/45.4_ts.493

Beilstein, F., and Dreiseikelmann, B. (2008). Temperate bacteriophage *ΦO18P* from an *Aeromonas media* isolate: characterization and complete genome sequence. *Virology* 373, 25–29. doi: 10.1016/j.virol.2007.11.016

Bolger, A. M., Lohse, M., and Usadel, B. (2014). Trimmomatic: a flexible trimmer for Illumina sequence data. *Bioinformatics* 30, 2114–2120. doi: 10.1093/bioinformatics/btu170

Bomar, L., Stephens, W. Z., Nelson, M. C., Velle, K., Guillemin, K., and Graf, J. (2013). Draft genome sequence of *Aeromonas veronii* Hm21, a symbiotic isolate from the medicinal leech digestive tract. *Genome Announc.* 1:e00800-13. doi: 10.1128/genomeA.00800-13

Bowker, J. D., Ostland, V. E., Carty, D., and Bowman, M. P. (2010). Effectiveness of aquaflor (50% florfenicol) to control mortality associated with *Streptococcus iniae* in freshwater-reared subadult sunshine bass. *J. Aquat. Anim. Health* 22, 254–265. doi: 10.1577/H09-010.1

Brown-Jaque, M., Calero-Caceres, W., and Muniesa, M. (2015). Transfer of antibiotic-resistance genes via phage-related mobile elements. *Plasmid* 79, 1–7. doi: 10.1016/j.plasmid.2015.01.001

Buttimer, C., O'Sullivan, L., Elbreki, M., Neve, H., McAuliffe, O., Ross, R. P., et al. (2016). Genome sequence of jumbo phage vB_AbaM_ME3 of *Acinetobacter baumanni*. *Genome Announc.* 4:e00431-16. doi: 10.1128/genomeA.00431-16

Canchaya, C., Fournous, G., and Brussow, H. (2004). The impact of prophages on bacterial chromosomes. *Mol. Microbiol.* 53, 9–18. doi: 10.1111/j.1365-2958.2004.04113.x

Chen, F., Wang, K., Stewart, J., and Belas, R. (2006). Induction of multiple prophages from a marine bacterium: a genomic approach. *Appl. Environ. Microbiol.* 72, 4995–5001. doi: 10.1128/AEM.00056-06

Colomer-Lluch, M., Imamovic, L., Jofre, J., and Muniesa, M. (2011). Bacteriophages carrying antibiotic resistance genes in fecal waste from cattle, pigs, and poultry. *Antimicrob. Agents Chemother.* 55, 4908–4911. doi: 10.1128/AAC.00535-11

Colston, S. M., Fullmer, M. S., Beka, L., Lamy, B., Gogarten, J. P., and Graf, J. (2014). Bioinformatic genome comparisons for taxonomic and phylogenetic assignments using *Aeromonas* as a test case. *MBio* 5:e02136. doi: 10.1128/mBio.02136-14

Dahanayake, P. S., Hossain, S., Wickramanayake, M., and Heo, G. J. (2019). Antibiotic and heavy metal resistance genes in *Aeromonas* spp. isolated from marketed Manila Clam (*Ruditapes philippinarum*) in Korea. *J. Appl. Microbiol.* 127, 941–952. doi: 10.1111/jam.14355

Dang, H., Zhang, X., Song, L., Chang, Y., and Yang, G. (2007). Molecular determination of oxytetracycline-resistant bacteria and their resistance genes from mariculture environments of China. *J. Appl. Microbiol.* 103, 2580–2592. doi: 10.1111/j.1365-2672.2007.03494.x

Done, H. Y., Venkatesan, A. K., and Halden, R. U. (2015). Does the recent growth of aquaculture create antibiotic resistance threats different from those associated with land animal production in agriculture? *AAPS J.* 17, 513–524. doi: 10.1208/s12248-015-9722-z

Dziewit, L., and Radlinska, M. (2016). Two novel temperate bacteriophages co-existing in *Aeromonas* sp. ARM81 - characterization of their genomes, proteomes and DNA methyltransferases. *J. Gen. Virol.* 97, 2008–2022. doi: 10.1099/jgv.0.000504

Edgar, R. C. (2004). MUSCLE: multiple sequence alignment with high accuracy and high throughput. *Nucleic Acids Res.* 32, 1792–1797. doi: 10.1093/nar/gkh340

Eichhorn, I., Feudi, C., Wang, Y., Kaspar, H., Fessler, A. T., Lubke-Becker, A., et al. (2018). Identification of novel variants of the colistin resistance gene mcr-3 in *Aeromonas* spp. from the national resistance monitoring programme GERM-Vet and from diagnostic submissions. *J. Antimicrob. Chemother.* 73, 1217–1221. doi: 10.1093/jac/dkx538

Elbediwi, M., Li, Y., Paudyal, N., Pan, H., Li, X., Xie, S., et al. (2019). Global burden of colistin-resistant bacteria: mobilized colistin resistance genes study (1980-2018). *Microorganisms* 7:461. doi: 10.3390/microorganisms7100461

Enault, F., Briet, A., Bouteille, L., Roux, S., Sullivan, M. B., and Petit, M. A. (2017). Phages rarely encode antibiotic resistance genes: a cautionary tale for virome analyses. *ISME J.* 11, 237–247. doi: 10.1038/ismej.2016.90

Felsenstein, J. P. (1989). Phylogeny Inference Package (Version 3.2). *Cladistics* 5, 164–166.

Figueras, M. J. (2005). Clinical relevance of Aeromonas sM503. *Rev. Med. Microbiol.* 16, 145–153. doi: 10.1097/01.revmedmi.0000184410.98677.8a

Garriss, G., Waldor, M. K., and Burrus, V. (2009). Mobile antibiotic resistance encoding elements promote their own diversity. *PLoS Genet.* 5:e1000775. doi: 10.1371/journal.pgen.1000775

Goni-Urriza, M., Pineau, L., Capdepuy, M., Roques, C., Caumette, P., and Quentin, C. (2000). Antimicrobial resistance of mesophilic *Aeromonas* spp. isolated from two European rivers. *J. Antimicrob. Chemother.* 46, 297–301. doi: 10.1093/jac/46.2.297

Gordon, L., Cloeckaert, A., Doublet, B., Schwarz, S., Bouju-Albert, A., Ganiere, J. P., et al. (2008). Complete sequence of the floR-carrying multiresistance plasmid pAB5S9 from freshwater *Aeromonas bestiarum*. *J. Antimicrob. Chemother.* 62, 65–71. doi: 10.1093/jac/dkn166

Hassan, M. A., Noureldin, E. A., Mahmoud, M. A., and Fita, N. A. (2017). Molecular identification and epizootiology of *Aeromonas veronii* infection among farmed *Oreochromis niloticus* in Eastern Province, KSA. *Egyptian J. Aquat. Res.* 43, 161–167. doi: 10.1016/j.ejar.2017.06.001

Hossain, M. J., Sun, D., McGarey, D. J., Wrenn, S., Alexander, L. M., Martino, M. E., et al. (2014). An Asian origin of virulent *Aeromonas hydrophila* responsible for disease epidemics in United States-farmed catfish. *MBio* 5:e00848-14. doi: 10.1128/mBio.00848-14

Hossain, M. J., Waldbieser, G. C., Sun, D., Capps, N. K., Hemstreet, W. B., Carlisle, K., et al. (2013). Implication of lateral genetic transfer in the emergence of *Aeromonas hydrophila* isolates of epidemic outbreaks in channel catfish. *PLoS ONE* 8:e80943. doi: 10.1371/journal.pone.0080943

Hughes, H. Y., Conlan, S. P., Lau, A. F., Dekker, J. P., Michelin, A. V., Youn, J.-H., et al. (2016). Detection and whole-genome sequencing of carbapenemase-producing *Aeromonas hydrophila* isolates from routine perirectal surveillance culture. *J. Clin. Microbiol.* 54, 1167–1170. doi: 10.1128/JCM.03229-15

Igbinosa, I. H., Igumbor, E. U., Aghdasi, F., Tom, M., and Okoh, A. I. (2012). Emerging *Aeromonas* species infections and their significance in public health. *Sci. World J.* 2012:625023. doi: 10.1100/2012/625023

Jagoda, S. S. D. S., Honein, K., Arulkanthan, A., Ushio, H., and Asakawa, S. (2017). Genome sequencing and annotation of *Aeromonas veronii* strain Ae52, a multidrug-resistant isolate from septicaemic gold fish (*Carassius auratus*) in Sri Lanka. *Genom Data* 11, 46–48. doi: 10.1016/j.gdata.2016.11.011

Janda, J. M., and Abbott, S. L. (2010). The genus *Aeromonas*: taxonomy, pathogenicity, and infection. *Clin. Microbiol. Rev.* 23, 35–73. doi: 10.1128/CMR.00039-09

Kang, Y., Pan, X., Xu, Y., Siddiqui, S. A., Wang, C., Shan, X., et al. (2016). Complete genome sequence of the fish pathogen *Aeromonas veronii* TH0426 with potential application in biosynthesis of pullulanase and chitinase. *J. Biotechnol.* 227, 81–82. doi: 10.1016/j.jbiotec.2016.04.009

Kenzaka, T., Nakahara, M., Higuchi, S., Maeda, K., and Tani, K. (2014). Draft genome sequences of amoeba-resistant *Aeromonas* spp. isolated from aquatic environments. *Genome Announc.* 2:e01115-14. doi: 10.1128/genomeA.01115-14

Koren, S., Walenz, B. P., Berlin, K., Miller, J. R., Bergman, N. H., and Phillippy, A. M. (2017). Canu: scalable and accurate long-read assembly via adaptive k-mer weighting and repeat separation. *Genome Res.* 27, 722–736. doi: 10.1101/gr.215087.116

Kropinski, A. M., Prangishvili, D., and Lavigne, R. (2009). Position paper: the creation of a rational scheme for the nomenclature of viruses of Bacteria and Archaea. *Environ. Microbiol.* 11, 2775–2777. doi: 10.1111/j.1462-2920.2009.01970.x

Lagana, P., Caruso, G., Minutoli, E., Zaccone, R., and Santi, D. (2011). Susceptibility to antibiotics of *Vibrio* spp. and *Photobacterium damsela* ssp. piscicida strains isolated from Italian aquaculture farms. *New Microbiol.* 34, 53–63.

Li, Y., Liu, Y., Zhou, Z., Huang, H., Ren, Y., Zhang, Y., et al. (2011). Complete genome sequence of *Aeromonas veronii* strain B565. *J. Bacteriol.* 193, 3389–3390. doi: 10.1128/JB.00347-11

Liang, C. Y., Yang, C. H., Lai, C. H., Huang, Y. H., and Lin, J. N. (2019). Genomic features, comparative genomic analysis, and antimicrobial susceptibility patterns of *Chryseobacterium arthrosphaerae* strain ED882-96 isolated in Taiwan. *Genes* 10:309. doi: 10.3390/genes10040309

Ling, Z., Yin, W., Li, H., Zhang, Q., Wang, X., Wang, Z., et al. (2017). Chromosome-mediated mcr-3 variants in *Aeromonas veronii* from chicken meat. *Antimicrob. Agents Chemother.* 61:e01272-17. doi: 10.1128/AAC.01272-17

Liu, D., Geng, Y., Wang, K., Chen, D., Huang, X. L., Ou, Y., et al. (2016). *Aeromonas veronii* infection in cultured channel catfish, *ictalurus punctatus*, in Southwest China. *Israeli J. Aquacult.* 68.

Liu, W., Yang, M., Xu, Z., Zheng, H., Liang, W., Zhou, R., et al. (2012). Complete genome sequence of *Pasteurella multocida* HN06, a toxigenic strain of serogroup D. *J. Bacteriol.* 194, 3292–3293. doi: 10.1128/JB.00215-12

Loch, T. P., and Faisal, M. (2010). Infection of lake whitefish (*Coregonus clupeaformis*) with motile *Aeromonas* spp. in the Laurentian great lakes. *J. Great Lakes Res.* 36, 6–12. doi: 10.1016/j.jglr.2009.07.001

Marshall, B. M., and Levy, S. B. (2011). Food animals and antimicrobials: impacts on human health. *Clin. Microbiol. Rev.* 24, 718–733. doi: 10.1128/CMR.00002-11

Okocha, R. C., Olatoye, I. O., and Adedeji, O. B. (2018). Food safety impacts of antimicrobial use and their residues in aquaculture. *Public Health Rev.* 39:21. doi: 10.1186/s40985-018-0099-2

Perez-Vazquez, M., Vindel, A., Marcos, C., Oteo, J., Cuevas, O., Trincado, P., et al. (2009). Spread of invasive Spanish *Staphylococcus aureus* spa-type

t067 associated with a high prevalence of the aminoglycoside-modifying enzyme gene ant(4')-Ia and the efflux pump genes msrA/msrB. *J. Antimicrob. Chemother.* 63, 21–31. doi: 10.1093/jac/dkn430

Piotrowska, M., and Popowska, M. (2015). Insight into the mobilome of *Aeromonas* strains. *Front. Microbiol.* 6:494. doi: 10.3389/fmicb.2015.00494

Richter, M., and Rossello-Mora, R. (2009). Shifting the genomic gold standard for the prokaryotic species definition. *Proc. Natl. Acad. Sci. U.S.A.* 106, 19126–19131. doi: 10.1073/pnas.0906412106

Sanchez-Cespedes, J., Blasco, M. D., Marti, S., Alba, V., Alcalde, E., Esteve, C., et al. (2008). Plasmid-mediated QnrS2 determinant from a clinical *Aeromonas veronii* isolate. *Antimicrob. Agents Chemother.* 52, 2990–2991. doi: 10.1128/AAC.00287-08

Schwarz, S., Kehrenberg, C., Doublet, B., and Cloeckaert, A. (2004). Molecular basis of bacterial resistance to chloramphenicol and florfenicol. *FEMS Microbiol. Rev.* 28, 519–542. doi: 10.1016/j.femsre.2004.04.001

Seoane, A., and García Lobo, J. M. (2000). Identification of a streptogramin A acetyltransferase gene in the chromosome of *Yersinia enterocolitica*. *Antimicrobial Agents Chemother.* 44, 905–909. doi: 10.1128/AAC.44.4.905-909.2000

Serrano, P. H. (2005). *Responsible Use of Antibiotics in Aquaculture*. Rome: Food and Agriculture Organization.

Shen, Y., Xu, C., Sun, Q., Schwarz, S., Ou, Y., Yang, L., et al. (2018). Prevalence and genetic analysis of mcr-3-positive *Aeromonas* species from humans, retail meat, and environmental water samples. *Antimicrob. Agents Chemother.* 62:e00404-18. doi: 10.1128/AAC.00404-18

Stoesser, N., Mathers, A. J., Moore, C. E., Day, N. P., and Crook, D. W. (2016). Colistin resistance gene mcr-1 and pHNSHP45 plasmid in human isolates of *Escherichia coli* and *Klebsiella pneumoniae*. *Lancet Infect. Dis.* 16, 285–286. doi: 10.1016/S1473-3099(16)00010-4

Sun, J., Zhang, X., Gao, X., Jiang, Q., Wen, Y., and Lin, L. (2016). Characterization of virulence properties of *Aeromonas veronii* isolated from diseased gibel carp (*Carassius gibelio*). *Int. J. Mol. Sci.* 17:496. doi: 10.3390/ijms17040496

Tamminen, M., Karkman, A., Lõhmus, A., Muziasari, W. I., Takasu, H., Wada, S., et al. (2011). Tetracycline resistance genes persist at aquaculture farms in the absence of selection pressure. *Environ. Sci. Technol.* 45, 386–391. doi: 10.1021/es102725n

Tekedar, H. C., Kumru, S., Blom, J., Perkins, A. D., Griffin, M. J., Abdelhamed, H., et al. (2019). Comparative genomics of *Aeromonas veronii*: identification of a pathotype impacting aquaculture globally. *PLoS ONE* 14:e0221018. doi: 10.1371/journal.pone.0221018

Tinsley, C. R., Bille, E., and Nassif, X. (2006). Bacteriophages and pathogenicity: more than just providing a toxin? *Microbes Infect.* 8, 1365–1371. doi: 10.1016/j.micinf.2005.12.013

Verner-Jeffreys, D. W., Welch, T. J., Schwarz, T., Pond, M. J., Woodward, M. J., Haig, S. J., et al. (2009). High prevalence of multidrug-tolerant bacteria and associated antimicrobial resistance genes isolated from ornamental fish and their carriage water. *PLoS ONE* 4:e8388. doi: 10.1371/journal.pone.0008388

Vincent, A. T., Paquet, V. E., Bernatchez, A., Tremblay, D. M., Moineau, S., and Charette, S. J. (2017). Characterization and diversity of phages infecting *Aeromonas salmonicida* subsp. salmonicida. *Sci Rep* 7:7054. doi: 10.1038/s41598-017-07401-7

Walker, B. J., Abeel, T., Shea, T., Priest, M., Abouelliel, A., Sakthikumar, S., et al. (2014). Pilon: an integrated tool for comprehensive microbial variant detection and genome assembly improvement. *PLoS ONE* 9:e112963. doi: 10.1371/journal.pone.0112963

Walsh, T. R., Hall, L., MacGowan, A. P., and Bennett, P. M. (1995). Sequence analysis of two chromosomally mediated inducible beta-lactamases from *Aeromonas sobria*, strain 163a, one a class D penicillinase, the other an AmpC cephalosporinase. *J. Antimicrob. Chemother.* 36, 41–52. doi: 10.1093/jac/36.1.41

Walsh, T. R., Neville, W. A., Haran, M. H., Tolson, D., Payne, D. J., Bateson, J. H., et al. (1998). Nucleotide and amino acid sequences of the metallo-beta-lactamase, ImiS, from *Aeromonas veronii* bv. *sobria*. *Antimicrob. Agents Chemother.* 42, 436–439. doi: 10.1128/AAC.42.2.436

Webb, H. E., Bugarel, M., den Bakker, H. C., Nightingale, K. K., Granier, S. A., Scott, H. M., et al. (2016). Carbapenem-resistant bacteria recovered from faeces of dairy cattle in the high plains region of the USA. *PLoS ONE* 11:e0147363. doi: 10.1371/journal.pone.0147363

Wu, C-J., Chen, P.-L., Wu, J.-J., Yan, J.-J., Lee, C.-C., Lee, H.-C., et al. (2012). Distribution and phenotypic and genotypic detection of a metallo-β-lactamase, CphA, among bacteraemic aeromonas isolates. *J Med Microbiol.* 61, 712–719. doi: 10.1099/jmm.0.038323-0

Yamada, T., Kawasaki, T., Nagata, S., Fujiwara, A., Usami, S., and Fujie, M. (2007). New bacteriophages that infect the phytopathogen *Ralstonia solanacearum*. *Microbiology* 153, 2630–2639. doi: 10.1099/mic.0.2006/001453-0

Yang, Q., Zhao, M., Wang, K. Y., Wang, J., He, Y., Wang, E. L., et al. (2017). Multidrug-Resistant *Aeromonas veronii* recovered from channel catfish (*Ictalurus punctatus*) in China: prevalence and mechanisms of fluoroquinolone resistance. *Microbial Drug Resist.* 23, 473–479. doi: 10.1089/mdr.2015.0296

Zankari, E., Hasman, H., Cosentino, S., Vestergaard, M., Rasmussen, S., Lund, O., et al. (2012). Identification of acquired antimicrobial resistance genes. *J. Antimicrob. Chemother.* 67, 2640–2644. doi: 10.1093/jac/dks261

Zimin, A. V., Marcais, G., Puiu, D., Roberts, M., Salzberg, S. L., and Yorke, J. A. (2013). The MaSuRCA genome assembler. *Bioinformatics* 29, 2669–2677. doi: 10.1093/bioinformatics/btt476

Conflict of Interest: The authors declare that the research was conducted in the absence of any commercial or financial relationships that could be construed as a potential conflict of interest.

Advantages of publishing in Frontiers

OPEN ACCESS
Articles are free to read for greatest visibility and readership

FAST PUBLICATION
Around 90 days from submission to decision

HIGH QUALITY PEER-REVIEW
Rigorous, collaborative, and constructive peer-review

TRANSPARENT PEER-REVIEW
Editors and reviewers acknowledged by name on published articles

Frontiers
Avenue du Tribunal-Fédéral 34
1005 Lausanne | Switzerland

Visit us: www.frontiersin.org
Contact us: info@frontiersin.org | +41 21 510 17 00

REPRODUCIBILITY OF RESEARCH
Support open data and methods to enhance research reproducibility

DIGITAL PUBLISHING
Articles designed for optimal readership across devices

FOLLOW US
@frontiersin

IMPACT METRICS
Advanced article metrics track visibility across digital media

EXTENSIVE PROMOTION
Marketing and promotion of impactful research

LOOP RESEARCH NETWORK
Our network increases your article's readership